



University of Nevada, Reno



Nevada Bureau of Mines and Geology Report 56

Geology and Geophysics of White Pine and Lincoln Counties, Nevada, and Adjacent Parts of Nevada and Utah: The Geologic Framework of Regional Groundwater Flow Systems



**Peter D. Rowley, Gary L. Dixon, Edward A. Mankinen, Keith T. Pari,
Darcy K. McPhee, Edwin H. McKee, Andrew G. Burns, James M. Watrus,
E. Bartlett Ekren, William G. Patrick, and Judith M. Brandt**

NEVADA BUREAU OF MINES AND GEOLOGY
REPORT 56

Geology and Geophysics of White Pine and Lincoln Counties, Nevada, and Adjacent Parts of Nevada and Utah: The Geologic Framework of Regional Groundwater Flow Systems

Peter D. Rowley¹, Gary L. Dixon², Edward A. Mankinen³, Keith T. Pari⁴, Darcy K. McPhee³, Edwin H. McKee³, Andrew G. Burns⁴, James M. Watrus⁴, E. Bartlett Ekren⁵, William G. Patrick⁴, and Judith M. Brandt⁴

¹Geologic Mapping, Inc., New Harmony, Utah

²Southwest Geology LLC, Blackfoot, Idaho

³U.S. Geological Survey, Menlo Park, California

⁴Southern Nevada Water Authority, Las Vegas, Nevada

⁵Private consultant, White Sulphur Springs, Montana

2017

SOUTHERN NEVADA WATER AUTHORITY
Resources & Facilities Department
Water Resources Division
◆ snwa.com

© Copyright 2017 The University of Nevada, Reno. All Rights Reserved.



SOUTHERN NEVADA
WATER AUTHORITY

This report is dedicated to Gary L. Dixon, who died at age 73 from cancer on January 14, 2017 as the manuscript was being reviewed and edited. Gary, a great field geologist, led the 20-year study presented here through the strength of his competence and personality. He began the study when he was a Geologist with the U.S. Geological Survey. After retirement, he continued with it as a consulting geologist. Perhaps more important to his coauthors and many others, we loved Gary and can attribute major parts of our careers to mentorship by him and to collaboration with him. To his wife, Wendy Dixon, and his children, Chris Dixon and Natalie Dixon Pique, he was a loving husband and father and a loyal friend to them and most others he met. His passions were geology, golf, and supporting Wendy's equally extraordinary career with the U.S. Department of Energy. All of us miss him.

CONTENTS

| | |
|---|-----|
| CONTENTS | iii |
| FIGURES..... | v |
| PLATES..... | vi |
| ABSTRACT | 7 |
| INTRODUCTION | 8 |
| Background..... | 8 |
| Study Area | 9 |
| Fracture Flow..... | 11 |
| Technical Approach | 13 |
| Preparation of Geologic Maps and Sections..... | 15 |
| GEOLOGY..... | 19 |
| Overview | 19 |
| Stratigraphy | 19 |
| Precambrian Rocks | 20 |
| Paleozoic Rocks | 21 |
| Mesozoic Rocks..... | 30 |
| Cenozoic Rocks | 31 |
| Structural Geology..... | 35 |
| Antler Orogeny | 35 |
| Sevier Orogeny | 36 |
| Middle Cenozoic Volcanism..... | 37 |
| East-Trending Transverse Zones | 39 |
| Basin and Range Extension | 39 |
| GEOPHYSICS..... | 44 |
| Overview | 44 |
| Gravity, Aeromagnetic, and Ground Magnetic Studies | 44 |
| Collection of Data..... | 44 |
| Processing of Data | 46 |
| Interpretation | 54 |
| Audiomagnetotelluric Studies..... | 61 |
| Collection and Processing of Data..... | 61 |
| Interpretation | 61 |
| DESCRIPTIONS OF BASINS AND RANGES | 88 |
| Ruby Mountains, Bald Mountain, and Buck Mountain | 88 |
| Maverick Springs Range..... | 88 |
| Butte Mountains and White Pine Range | 89 |
| Horse, Grant, and Quinn Canyon Ranges..... | 89 |
| Worthington Mountains and Timpahute Range | 91 |
| Golden Gate Range, Mount Irish, and Pahrnagat Range | 91 |
| Sheep Range, Las Vegas Range, and Elbow Range..... | 92 |
| Cherry Creek Range | 93 |
| Northern Egan Range | 93 |
| Southern Egan Range..... | 94 |
| Seaman Range | 95 |
| North Pahroc, South Pahroc, and Hiko Ranges | 95 |

| | |
|---|-----|
| Schell Creek Range..... | 97 |
| Fairview, Bristol, West, Ely Springs, Highland, Black Canyon, Burnt Spring, and Chief Ranges, and Pioche Hills..... | 97 |
| Delamar Mountains | 98 |
| Meadow Valley Mountains..... | 99 |
| Arrow Canyon Range | 99 |
| Fortification Range, Wilson Creek Range, and White Rock Mountains | 100 |
| Clover Mountains and Bull Valley Mountains | 101 |
| Mormon Mountains | 102 |
| North Muddy Mountains, Muddy Mountains, and Dry Lake Range | 103 |
| Antelope Range | 104 |
| Deep Creek Range | 104 |
| Kern Mountains and Adjacent Small Ranges | 105 |
| Snake Range and Limestone Hills | 105 |
| Confusion Range, Conger Range, Burbank Hills, and Tunnel Spring Mountains..... | 109 |
| Needle Range and Wah Wah Mountains | 110 |
| Fish Springs and House Ranges..... | 111 |
| CONCLUSIONS | 113 |
| Geologic Framework | 113 |
| Hydrogeologic Implications | 115 |
| ACKNOWLEDGMENTS | 117 |
| DESCRIPTION OF MAP UNITS..... | 118 |
| REFERENCES | 123 |

FIGURES

| | |
|---|----|
| Figure 1. Location of project basins and other hydrographic areas..... | 10 |
| Figure 2. Hydrographic areas, ranges, and flow systems in the study area..... | 12 |
| Figure 3. Conceptualization of fault components and factors controlling permeability and groundwater flow (after Caine et al., 2010)..... | 14 |
| Figure 4. Previous large-scale mapping used to evaluate geology and to create the geologic and hydrogeologic maps of plates 1 and 2. | 16 |
| Figure 5. Geologic time scale, including rock type and tectonic events (after Walker et al., 2013).. | 21 |
| Figure 6. Geologic units of Lincoln County, Nevada (from Tschanz and Pampeyan, 1970).. | 22 |
| Figure 7. Geologic Units of White Pine County, Nevada (from Hose and Blake, 1976)..... | 23 |
| Figure 8. Geologic units of Clark County, Nevada (from Longwell et al., 1965)..... | 24 |
| Figure 9. Geologic units of western Utah (after Hintze and Kowallis, 2009, Charts 45 and 46)..... | 25 |
| Figure 10. Schematic diagram of Sevier thrust sheets, illustrating the movement of Paleozoic carbonates over cratonic sediments. | 37 |
| Figure 11. Paleozoic carbonates thrust over Jurassic Aztec Sandstone in the Muddy Mountains near Muddy Peak. | 38 |
| Figure 12. Shaded-relief map of eastern Nevada and western Utah..... | 45 |
| Figure 13. Isostatic-gravity field in eastern Nevada and western Utah. | 47 |
| Figure 14. Aeromagnetic map of eastern Nevada and western Utah. | 48 |
| Figure 15. Isostatic gravity anomalies upward-continued by 3 km..... | 50 |
| Figure 16. Aeromagnetic data transformed to their magnetic potential (“pseudogravity”).. | 51 |
| Figure 17. Constraints for the gravity inversion method..... | 52 |
| Figure 18. Depth to pre-Cenozoic basement in eastern Nevada and western Utah..... | 53 |
| Figure 19. Shaded relief map of the Spring and Snake valley region. | 57 |
| Figure 20. Isostatic gravity (A) and reduced-to-pole aeromagnetic (B) anomalies in the Spring and Snake valley area. | 58 |
| Figure 21. Map of Spring Valley area showing locations of AMT profiles..... | 62 |
| Figure 22. Geologic map and 2D model of AMT profile SVN13..... | 64 |
| Figure 23. Geologic map and 2D model of AMT profile of area of POD54010. | 65 |
| Figure 24. Geologic map and 2D model of AMT profile SVN10 West..... | 66 |
| Figure 25. Geologic map and 2D model of AMT profile SVN10 East..... | 67 |
| Figure 26. Geologic map and 2D model of AMT profile SVN9..... | 69 |
| Figure 27. Geologic map and 2D model of AMT profile SVN9..... | 70 |
| Figure 28. Geologic map and 2D model of AMT profile SVNA..... | 71 |
| Figure 29. Geologic map and 2D model of AMT profile SVNL. | 72 |
| Figure 30. Geologic map and 2D model of AMT profile SVNP..... | 73 |
| Figure 31. Map of Snake Valley area showing locations of AMT profiles..... | 75 |
| Figure 32. 2D model of AMT profile SNK1. | 76 |
| Figure 33. 2D model of AMT profile SNK4. | 76 |
| Figure 34. Map of Cave, Dry Lake, and Delamar valleys, showing locations of AMT profiles. | 77 |
| Figure 35. Geologic map and 2D model of AMT profile CVE..... | 78 |
| Figure 36. Geologic map and 2D model of AMT profile DLV50..... | 80 |
| Figure 37. Geologic map and 2D model of AMT profile DLV3..... | 81 |
| Figure 38. Geologic map and 2D model of AMT profile DLV24..... | 82 |
| Figure 39. Geologic map and 2D model of AMT profile DLV4..... | 83 |
| Figure 40. Geologic map and 2D model of AMT profile DLV8..... | 85 |

| | |
|--|----|
| Figure 41. Geologic map and 2D model of AMT profile DELA5. | 86 |
| Figure 42. Geologic map and 2D model of AMT profile DELA1. | 87 |

PLATES

| | |
|---------|--|
| Plate 1 | Geologic map of the northern part of the study area, Nevada and Utah |
| Plate 2 | Geologic map of the southern part of the study area, Nevada and Arizona |
| Plate 3 | Geologic cross sections of the northern part of the study area, Nevada and Utah |
| Plate 4 | Geologic cross sections of the southern part of the study area, Nevada and Arizona |

ABSTRACT

This report describes the geologic framework of a >65,000 km² area that straddles the Nevada-Utah border. The studied region includes most of White Pine and Lincoln counties and adjacent counties in eastern Nevada, as well as parts of Tooele, Juab, Millard, Beaver, and Iron counties in western Utah. This study represents more than a 20-year effort by the Southern Nevada Water Authority (SNWA) to understand the groundwater resources of this part of the Great Basin. This first step, which includes a compilation of all the information on the geologic and geophysical setting, was necessary for hydrological and biological investigations. To understand the geologic framework, we compiled all known geologic mapping at a scale of 1:250,000, and constructed 25 geologic cross sections at the same scale. We also present new geophysical data, consisting of gravity surveys and audiomagnetotelluric (AMT) profiles, plus assembly of available aeromagnetic data, contracted from the U.S. Geological Survey (USGS), as well as additional AMT profiles by the SNWA. This report focuses on two large regional groundwater flow systems: the White River and Great Salt Lake Desert systems. Although the map boundaries presented here bound these aforementioned flow systems, the maps, cross sections, and text are intended to serve as a modern multidisciplinary regional geological and geophysical review, comparable to many old county reports in Nevada and Utah.

Many of the oldest exposed rocks are thick marine quartzites and other clastic rocks deposited in Neoproterozoic and Early Cambrian time. In the Middle Cambrian through late Permian time, there was a shift in sedimentation to ~10 km thick marine carbonates that represent the great carbonate aquifer. In Late Devonian to late Mississippian time, east-verging thrust faults and folds of the Antler orogeny affected the area just northwest of the study area, resulting in clastic sedimentation, including the Chainman Shale that was deposited in a foreland basin east of the Antler Highland.

These clastic confining rocks are intertongued with the carbonates. Mesozoic to lower Cenozoic rocks consist mostly of continental clastic deposits, now significantly removed by erosion except in the southern part of the study area. These rocks were deposited, in part, during east-verging thrusting and folding of the Sevier orogeny of Middle Jurassic through early Paleocene. Large frontal thrusts formed in the extreme south as well as east of the study area, but most of the area is referred to as the orogenic hinterland (highland) of small thrusts that was the source of clastic sedimentation eastward.

Eocene to lower Miocene, subduction-related, calc-alkaline volcanic rocks, mostly ash-flow tuffs, were erupted from east-trending igneous belts that young to the south. These deposits are locally thick in the south but are older in the north and therefore have been mostly removed by erosion. The igneous belts are prominent on aeromagnetic maps. From lower Miocene to the present, east-west regional Basin and Range extension affected most of the study area. The Great Basin formed as large, north-striking, high-angle normal faults resulted in alternating ranges and basins. Thick clastic, continental basin-fill deposits were deposited in the basins from erosion of the ranges, and relatively small-volume bimodal (basalt and high-silica rhyolite) volcanic rocks were simultaneously deposited. Gravity-inversion data show that the basin-fill deposits are in many places 3 km thick, and they are the most important aquifer in the area. The east-west extension led to less extensive northeast- or northwest-striking transfer faults and east-striking transverse zones. Also secondary to the north-striking high-angle faults are low-angle, non-rooted, normal attenuation/denudation faults that formed as the tops of the ranges slid into adjacent basins during uplift of the ranges along the large high-angle normal faults. The present topography formed from ~10 Ma to the present, during the most active part of Basin and Range extension.

INTRODUCTION

This report describes the geology and geophysics of a >65,000 km² area in east-central to southeastern Nevada and adjacent parts of western Utah. We compiled geologic maps at a scale of 1:250,000 from all available published and unpublished maps, supplemented by site studies and local new geologic mapping in all parts of the area, especially in the south. Based on these compiled maps, we constructed 25 new geologic cross sections at the same scale. We also compiled and interpreted new geophysical data from the U.S. Geological Survey (USGS), including primarily gravity readings and audiomagnetotelluric (AMT) profiles, and available but re-gridded aeromagnetic data.

This report is an update of the many valuable geologic reports originally done in the 1960s through 1980s for all counties in Nevada. Such geologic reports, authored by geologists of the USGS in cooperation with geologists of the Nevada Bureau of Mines and Geology (NBMG), contained 1:250,000-scale geologic maps. At about the same time, the USGS published a series of 1x2-degree (1:250,000 scale) geologic-map sheets, but only two of these reached as far west as western Utah and none were done in Nevada. The Utah Geological Survey (UGS) also had a program at the same time of scattered county reports that included reconnaissance geologic maps. With few exceptions, all these older maps and reports lacked geophysics and cross sections, and most are now partly obsolete. In the last two decades, however, the UGS has issued modern 0.5- x 1-degree geologic-map sheets (1:100,000-scale), with cross sections, that span most of the state, including some of the Utah part of the study area.

BACKGROUND

In the early 1990s, the Southern Nevada Water Authority (SNWA), which is the research arm that supplies culinary water to the city of Las Vegas through Las Vegas Valley Water District, became interested in the availability and amounts of groundwater resources in upstate Nevada. Las Vegas at the time was the fastest growing city in the U.S., and its culinary water came primarily

from the surface water in Lake Mead, with some supplementary groundwater from Las Vegas basin. By then they had secured groundwater rights and applications for additional rights in selected upstate groundwater basins. The basins of interest are, from north to south, Snake Valley, Spring Valley, Cave Valley, Dry Lake Valley, Delamar Valley, and Coyote Spring Valley. SNWA recognized that understanding the hydrology and the water resources of these basins required a three-dimensional geologic framework of these basins and adjacent basins that may or may not be hydraulically connected. They eventually selected the large study area outlined in red on [figure 1](#).

The SNWA contracted with USGS geologists from the Las Vegas office to develop geologic maps across the study area. These geologists included some of the authors of this report. Detailed (1:24,000 scale) geologic maps were prepared of problem areas and parts of the southern basins, concentrating on likely groundwater flow paths as well as boundaries between basins so as to test their hydraulic connections with each other. The sheer size of the area required that the scale be at 1:250,000. Geologic maps commonly include geologic cross sections at the same scale that are constructed based on surface observations. However, geologic maps that focus on mineral or groundwater resources need more accurate assessments of the subsurface geology via geophysical methods and well data. The SNWA contracted for new gravity surveys, new AMT profiles, and analysis of available aeromagnetic data with the USGS office in Menlo Park, California. These data were used to prepare the geologic cross sections of this report.

The southern part of the White River regional groundwater flow system ([figure 2](#)) was compiled first. The geologic map and some hydrogeologic implications of this area, about 22,000 km² in size and almost entirely in Nevada, were published at 1:250,000 scale by Page et al. (2005a). Related geophysical studies, primarily gravity data, were reported by Phelps et al. (2000) and Scheirer (2005).

More recently we extended the study area northward to encompass the entire White River

flow system and adjacent parts of other flow systems. The White River system extends about 430 km from north to south. Dixon et al. (2007a) released the first summary of the geology, geophysics, and hydrogeology of the flow systems, including parts of the adjacent Great Salt Lake Desert regional groundwater flow system ([figure 2](#)) in Nevada and Utah. This is the same scale (1:250,000) and area as that of the present report. Dixon et al. (2007a) included summaries and analysis of the USGS gravity and AMT studies. This regional framework study, along with hydrology reports by SNWA and analyses of all springs in the study area (Southern Nevada Water Authority, 2006), were presented at hearings of the Nevada State Engineer. The full geophysical reports were published by Mankinen et al. (2006, 2007, 2008), McPhee et al. (2005, 2006a and b, 2007, 2008), Scheirer et al. (2006), and Scheirer and Andreason (2008).

We next extended studies of similar scope farther northeast, concentrating in Snake and Hamlin valleys but also in more eastern Utah parts of the Great Salt Lake Desert flow system ([figure 2](#)). This flow system is about 240 km from north to south. The published topics consisted of water chemistry (Acheampong et al., 2009), surface water and springs (Kistinger et al., 2009), gravity and aeromagnetic studies (Mankinen and McKee, 2009, 2011), AMT profiles (McPhee et al., 2009), and geology and limited hydrology (Rowley et al. 2009). The geologic map and profiles of the study area covered almost 16,000 km² (plate 1 of Rowley et al., 2009) at 1:250,000 scale, most of it northeast of the present study area.

This northeastward expansion of the study allowed greater understanding of the Great Salt Lake Desert flow system. It was followed by further updating of the geology, geophysics, and hydrogeology of the primary study area, with an emphasis on the project basins of Spring, Cave, Dry Lake, and Delamar valleys. The result was the geologic and geophysical framework analysis of Rowley et al. (2011), of the same area as that of Dixon et al. (2007a). This unpublished analysis was presented at new (late 2011) hearings of the Nevada State Engineer. Other primary components of the hearings testimony included the hydrologic analysis (Burns and Drici, 2011) and all AMT

profiles (Pari and Baird, 2011). We also incorporated the results of the various geological, geophysical, hydrogeological, and hydrological investigations into an Environmental Impact Statement (Southern Nevada Water Authority, 2011; Bureau of Land Management, 2012), which included an updated analysis of all significant springs in the study area. The current report covers the same study area of both Dixon et al (2007a) and Rowley et al. (2011). Although updated by new data and interpretations, the current report stresses the geology and geophysics but limits the discussion of hydrologic conclusions. Mankinen et al. (2016) and Rowley et al. (2016) provided early summaries of the current report. We suggest that this overall multi-year effort is how a modern groundwater analysis should be fashioned.

STUDY AREA

The study area is within the Great Basin physiographic province, primarily characterized by north-trending basins and ranges that formed by north-striking normal faults. This topography consists of a number of closed and partially closed basins, typical of the Great Basin region, where surface-water flow is generally restricted to each individual basin. Exceptions to closed surface-water basins occur near the Great Basin boundary, where a few basins have surface water exiting to the Colorado River. These exceptions include basins containing the Virgin River, Muddy River, and Las Vegas Wash ([figure 1](#)), as well as basins containing the ancestral White River and Meadow Valley Wash.

During wetter periods of Pleistocene time, the latest of which was about 10,000 to 15,000 years before the present (Reheis et al., 2014), ancestral lakes formed and grew in many closed basins. Some of these lakes filled and overtopped individual basins, one by one, and thus integrated multiple basins. For instance, the White River and its tributaries integrated several basins and eventually flowed southward through much of the southwestern part of the map area (Tschanz and Pampeyan, 1970). During this time, the White River joined other streams that flowed southward to join the Colorado River near present-day Lake Mead, at the southern edge of the study area.

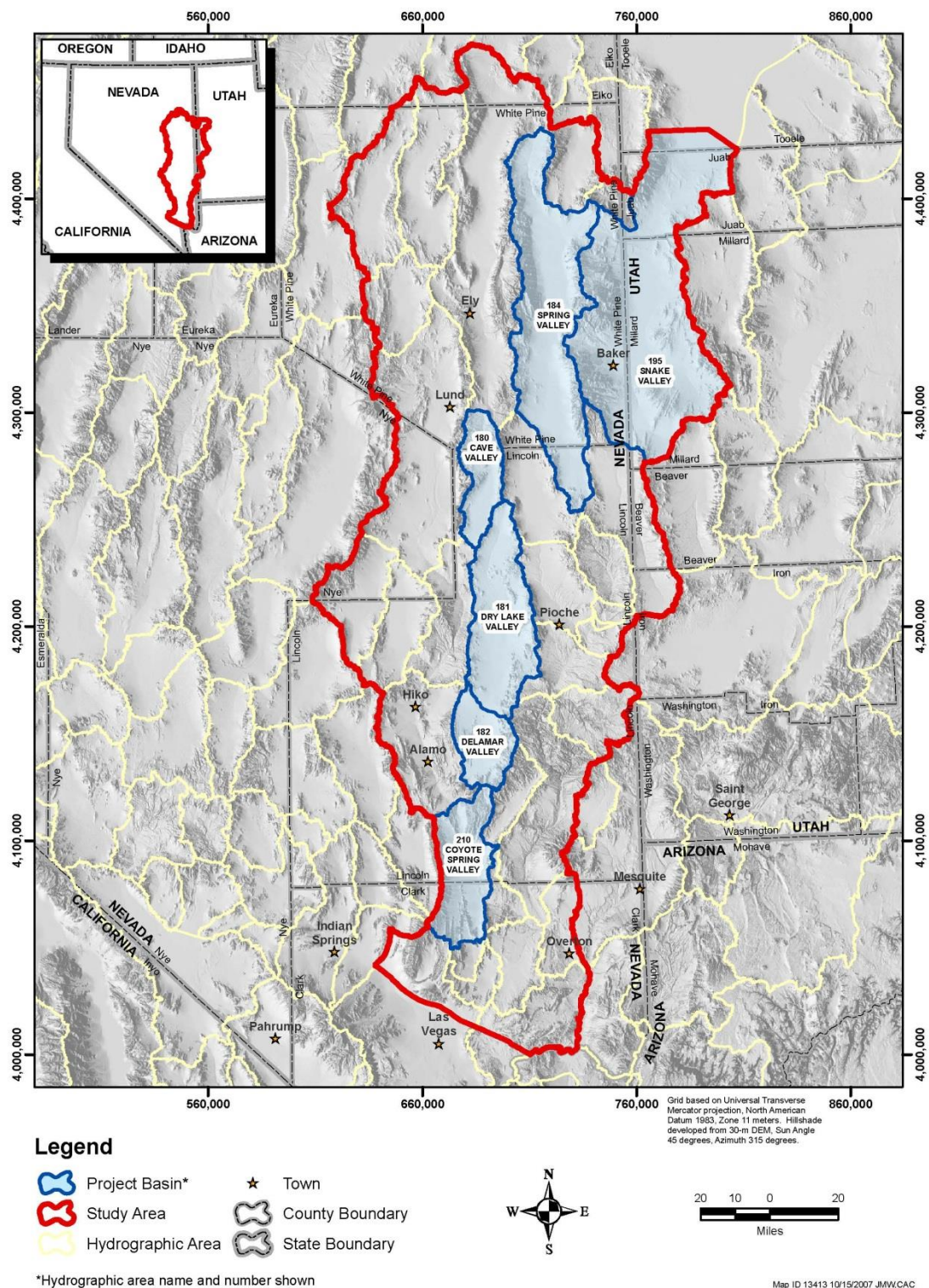


Figure 1. Location of project basins and other hydrographic areas.

Presently, the descendant drainages of the White River are discontinuously dispersed and intermittent over most of its course and as far south as Moapa, Nevada.

Despite the intermittent nature of surface water, groundwater occurs at different depths beneath all of the map area. The groundwater exists in aquifers within and between a number of groundwater basins, and it flows through these aquifers in a large number of defined regional groundwater flow systems. These flow systems may include a dozen or more closed or integrated topographic basins that are interconnected in the subsurface. These regional flow systems are defined by evidence that their groundwater flow paths pass beneath topographic divides and continue beneath some adjacent basins and ranges (Eakin, 1966; Winograd and Thordarson, 1975; Harrill et al., 1988; Harrill and Prudic, 1998).

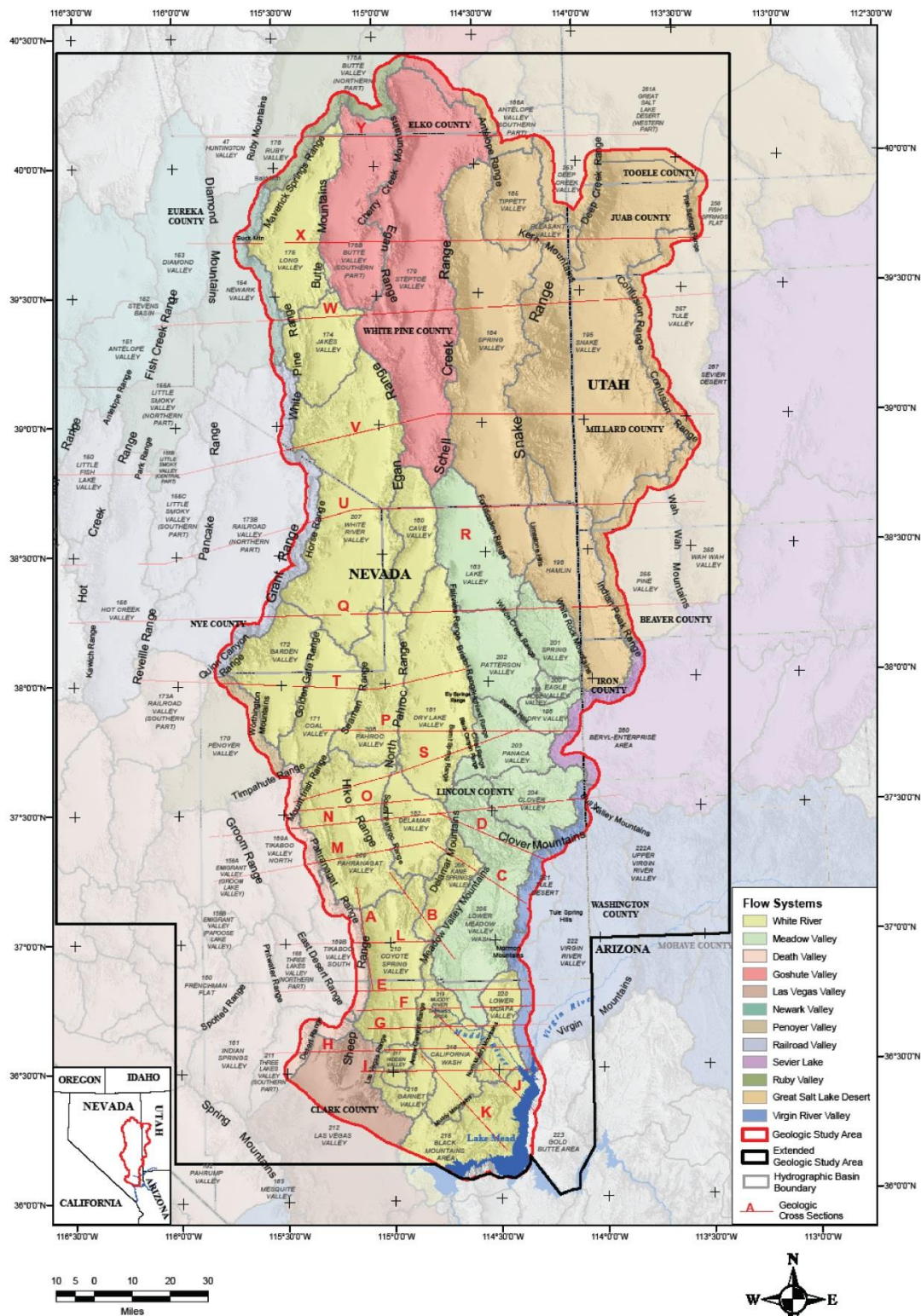
The White River and part of the Great Salt Lake Desert regional groundwater flow systems are shown with respect to the study area, which is portrayed by the red line in [figure 2](#). The White River flow system (Eakin, 1966), as referred to here, was called the Colorado flow system by Harrill and Prudic (1998) and Heilweil and Brooks (2011) (see also Belcher, 2004). The Meadow Valley flow system was considered a subset of the Colorado flow system, and therefore can be considered part of the White River system ([figure 2](#)). The various flow systems were defined by Eakin (1966), Harrill et al. (1988), and Harrill and Prudic (1998). Groundwater flow in the White River flow system is southward to the Colorado River, whereas flow in the Great Salt Lake Desert flow system is northward to the Great Salt Lake Desert. Parts of adjacent flow systems are included within this study because their basins may be in hydraulic connection with those of the White River and Great Salt Lake Desert systems. In other words, the entire broader region ([figure 1](#)) needed study because of the potential hydraulic continuity or discontinuity between basins due to geologic influences. In addition, we compiled the regional geology and made cross sections at a constant scale (1:250,000) over an even larger area, whose limits are demarcated by the thick black line outside the edge of the study area in

[figure 2](#). This was done to assess the broader geologic framework in order to determine the best model area and to provide additional data should the boundaries of the model area later change. Later the sections, map, and discussion were revised to an area that was trimmed to the current size.

The primary regional aquifers in the flow systems consist of Paleozoic carbonate rocks, volcanic rocks (notably Tertiary ash-flow tuffs), and Miocene to Holocene basin-fill sediments. The primary regional aquitards within the flow systems are Proterozoic to Cambrian schist, quartzite, slate, and shale, Mississippian shale, Mesozoic clastic sedimentary rocks, and Jurassic to Tertiary plutonic rocks.

FRACTURE FLOW

In addition to influencing the present topography, Basin and Range extension controls groundwater flow. This is because the direction of groundwater flow is generally enhanced along (parallel to), and the direction guided by, high-angle normal faults. More specifically, groundwater flows along and through rock fractures associated with these high-angle faults (Rowley et al., 2012; see discussion below). Conversely, groundwater flow across faults is commonly retarded. Extensional (normal) faults are more important than contractional (reverse) faults in allowing flow along them, because normal faults tend to stay open. This concept is especially important in understanding the groundwater hydrology of the study area in the Great Basin region because normal faults are abundant. Therefore, geologic mapping and identification of faults provides a first approximation of groundwater flow in the study area. This manner of groundwater movement is known as "fracture flow" or "fracture-dominated flow" (Caine et al., 1996). Knowledge about fracture flow has accumulated for many decades, because it plays an important role in the study of isolation of radioactive waste in underground repositories, groundwater transport of radionuclides, cleanup of toxic waste, exploitation of geothermal and petroleum reservoirs, and of course movement of groundwater (e.g., Rowley and Dixon, 2004).



Note: Geologic cross sections are presented in Plates 4 and 5.

Figure 2. Hydrographic areas, ranges, and flow systems in the study area.

Much of what we know about fracture flow began with U.S. Department of Energy-funded studies, primarily by the USGS, on the Nevada Test Site (NTS), to trace movement of contaminated groundwater resulting from hundreds of above- and below-ground nuclear tests (Winograd and Thordarson, 1968, 1975; Lacznia et al., 1996; Leahy and Lyttle, 1998; Rowley and Dixon, 2004). These studies began in the 1950s and resulted in publications on the geology, detailed geologic mapping of the entire NTS, and conclusions from well tests and other hydrologic data. The studies resulted in the discovery of the large (north-south length about 300 km) Death Valley regional groundwater flow system (Harrill et al., 1988; Dettinger, 1992; Dettinger et al., 1995; Burbey, 1997; Lacznia et al., 1996; Harrill and Prudic, 1998; Slate et al., 1999; D'Agnese et al., 2002; Workman et al., 2002a and b; Belcher, 2004). In this flow system, recharge originated in the broad, high mountains of central Nevada, and flow terminated as spring discharge in Ash Meadows, Oasis Valley, and Death Valley. Among the numerous reports that resulted, the words structural "barriers" and "conduits" were introduced (Winograd and Thordarson, 1968, p. 35) to describe faults and other fractures that respectively create dams to groundwater flow across them and exhibit high transmissivities along them.

A greater understanding of the role of faults in groundwater flow came from the studies of Caine et al. (1996), Sibson (1996), and Caine and Forster (1999). In particular, Caine et al. (1996) proposed that a central "core zone" of a fault commonly contains fine-grained gouge that inhibits flow across it, whereas on either side of the core zone, a "damage zone" consists of fractures parallel to the core zone that provide increased secondary permeability along them ([figure 3](#)). Where the damage zones are in carbonate rocks, solution of the carbonate rocks along the fractures can create still larger groundwater flow paths.

All known springs of significance, whether cold or hot, in the study area rise along faults (Kistinger et al., 2009; Southern Nevada Water Authority, 2011; Bureau of Land Management, 2012). Many of the active springs have active spring mounds, generally of calcium carbonate.

Pleistocene spring mounds for springs that are no longer active occur locally, as in the Ute railroad stop in the California Wash area. Feeders for ancient springs and for spring mounds that have been eroded away are locally expressed as calcite veins or dikes, as in the Wildcat Wash area of the southeastern Meadow Valley Mountains (Page and Pampeyan, 1996) and in other areas (Schmidt, 1994; Schmidt and Dixon, 1995).

Because of its importance in understanding movement of groundwater in the study area, expanded discussions of fracture flow were given in Rowley and Dixon (2004), Page et al. (2005a), and Rowley et al. (2009, 2011). The concept is also used to site production water wells along faults, as documented in the Mesquite basin of southeastern Nevada (Dixon and Katzer, 2002; Johnson et al., 2002) and in the Sand Hollow well field east of St. George of southwestern Utah (Rowley et al., 2004). Bhark et al. (2006) demonstrated conduit flow when they injected tracers down wells in a fault zone on the NTS, then detected those tracers 69 hours later in a pumped (1900 lpm) well 180 m down gradient (south) on the same fault. Pumping this well also lowered the water level in a well 9.6 km north of it on the same fault, yet pumping had no effect (barrier flow) on wells east and west of the fault. In a study of interference (drawdown of water levels) in springs and monitoring wells by pumping wells 0.8 and 1.3 km away on the same fault zone south of New Harmony, Utah, Rowley et al. (2012) documented conduit flow, and on wells east and west of that fault, a lack of interference indicated barrier flow.

TECHNICAL APPROACH

In this investigation we combined and reviewed published and unpublished geologic information from dozens of references, which was supplemental with geologic fieldwork by the authors. In addition, we evaluated borehole information from oil and gas test wells, monitor wells such as those drilled during the U.S. Air Force's MX missile-siting program of the early 1980s, and borehole information from exploratory test wells and monitor wells constructed by SNWA in support of the project. Geophysical studies concentrated on gravity surveys and AMT profiles

performed by the USGS under contract from SNWA and on AMT profiles by SNWA. These geophysical studies provided many of the details on the geometry and location of many normal faults and on thickness of basin fill.

Based on the evaluation of the compiled and new data, we compiled the geologic maps (plates 1

and 2) and constructed new geologic cross sections (plates 3 and 4). Because of the complexity of the geology of the study area, the maps and cross sections represented works in progress, and we periodically updated them as new data became available.

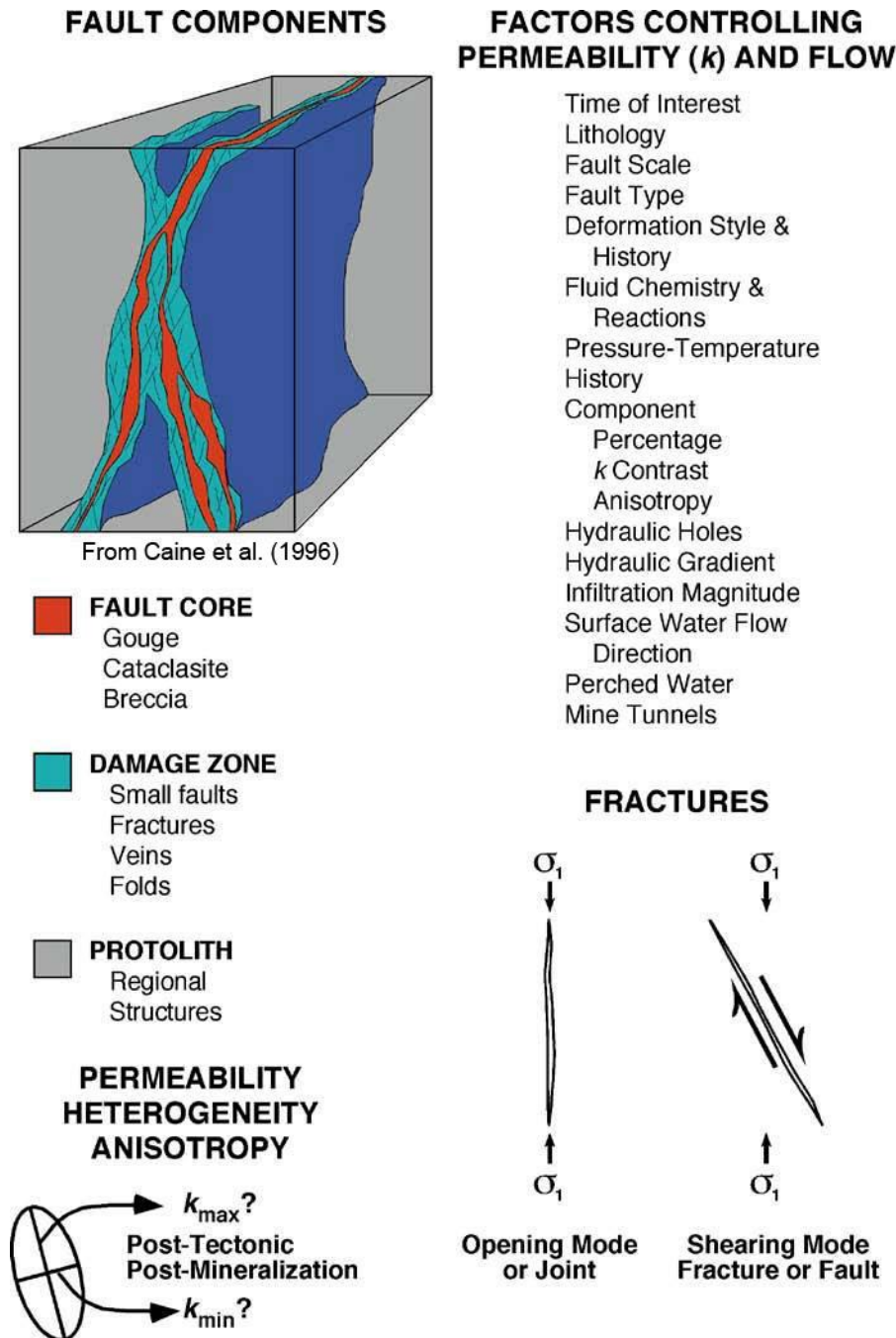


Figure 3. Conceptualization of fault components and factors controlling permeability and groundwater flow (after Caine et al., 2010).

PREPARATION OF GEOLOGIC MAPS AND SECTIONS

The geology of the southern part of the study area ([figure 4](#)) has been discussed by Page et al. (2005a). In their report, the geology for this area was compiled as a digital map at 1:250,000 scale; most of their map is included in [plate 2](#). To the west of this area, digital geologic and tectonic maps were also published at 1:250,000 scale (Workman et al., 2002a and b), and some of this mapping was included in southwestern parts of plates [1](#) and [2](#). These previous geologic maps included significant new and unpublished geologic mapping. The geology of the northeastern part of the study area, and of some adjacent basins east of this northeastern area were compiled at 1:250,000 scale and discussed by Rowley et al. (2009, plate 1).

For the geologic maps (plates [1](#) and [2](#)) and the [Description of Map Units](#), much of the Nevada geology was compiled from county 1:250,000-scale geologic maps and the Nevada 1:500,000-scale state geologic map (Stewart and Carlson, 1978). From west to east and north to south, the Nevada counties covered by these maps are southern Elko County (Roberts et al., 1967), eastern Nye County (Cornwall, 1972; Kleinhampl and Ziony, 1985), White Pine County (Hose and Blake, 1976), Lincoln County (Tschanz and Pampeyan, 1970), and Clark County (Longwell et al., 1965). Most of the Utah geology was compiled from four 1:100,000-scale maps (Hintze and Davis, 2002a and b; Rowley et al., 2006 and 2008; Biek et al., 2009), two 1:250,000-scale maps (Morris, 1987; Steven et al., 1990), and the Utah 1:500,000-scale state geologic map (Hintze, 1980a). Summary reports on the geology of Millard County (Hintze and Davis, 2003) and the geology of Utah (Hintze, 1988 and 2005; Hintze and Kowallis, 2009) were also valuable. Both the Nevada and Utah state geologic maps were digitized and re-released as digital files, but not updated with respect to maps and reports published since their original release dates of 1978 and 1980, respectively. These new 1:500,000-scale digital files were compiled by Hess and Johnson (1997), Raines et al. (2003), and Crafford (2007) for Nevada and by Hintze et al. (2000) for Utah.

Most of the regional geologic maps ([figure 4](#)) were published decades ago. A significant part of the entire study area was compiled by Terrascan Group, Inc. (Howard, 1978), but in most places this compilation included the same county maps without updating them. As part of the USGS Basin and Range Carbonate-Rock Aquifer System study (BARCAS; Welch et al., 2007; Sweetkind et al., 2007b), Sweetkind et al. (2007a) compiled a 1:500,000-scale, digital geologic map of a large area that includes all but the eastern edge of the area of [plate 1](#). However, their map was compiled from Stewart and Carlson (1978), Hintze (1980a), Hintze et al. (2000), and Raines et al. (2003), from which all faults were removed. To that file, Sweetkind et al. (2007a) added some gravity interpretations, dotted "geophysically determined faults," and some sketched faults. Two diagrammatic cross sections accompanied this map, but neither matched the topography, geology, or geophysics of their map. As part of the BARCAS study, Watt and Ponce (2007) and Wallace et al. (2007) provided geophysical data for east-central Nevada and west-central Utah, but their maps were at 1:750,000 scale.

Hurlow (2014) published a major Utah Geological Survey summary report on the hydrology and hydrogeology of a large area of Utah that focused on Snake Valley, Hamlin Valley, Tule Valley, and Fish Springs Flat and also included adjacent areas in Utah and Nevada. It followed several years of drilling, geochemistry, and monitoring of the groundwater resources of the Utah part of their study area. They found that water levels in Snake Valley have been falling since 1980, due largely to increasing irrigation pumping in Utah and partly to decreases in annual precipitation (see also Hurlow and Inkenbrandt, 2016). The report of Hurlow (2014) included a geologic map and cross sections at 1:250,000 scale that cover most of the northeastern part of our [plate 1](#) area. It also included a study of the geophysics, primarily the collection of new gravity stations in the area and the analysis of these data to determine depth to basement in the valleys. The maps, cross sections, and geophysics provided an important framework for their hydrogeologic conclusions.

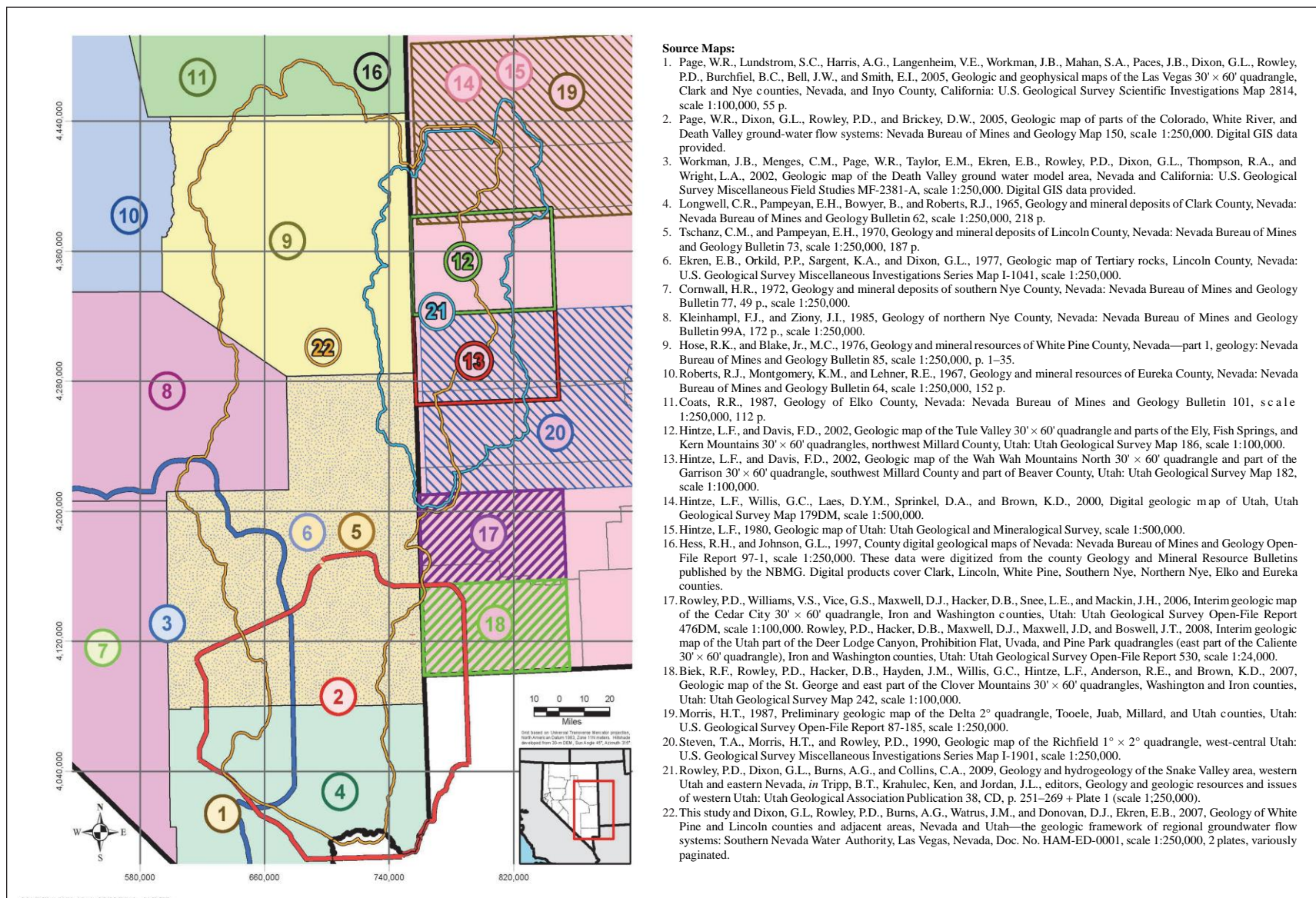


Figure 4. Previous large-scale mapping used to evaluate geology and to create the geologic and hydrogeologic maps of plates 1 and 2.

The plates and text of our report incorporate all known revisions and reinterpretations of previously published reports and geologic maps that were deemed necessary. Large-scale (less detailed) geologic maps used in the creation of plates [1](#) and [2](#) are indexed in [figure 4](#). Many more small-scale (more detailed) maps were used in the creation of plates 1 and 2. These are cited in the text. In addition, plates 1 and 2 include some new, unpublished geologic mapping and field observations.

The compilation of the geology in this 65,000 km² area required many name changes to specific geologic units throughout this large study area. Map scale required some lumping of units with others. New names or new correlations required other changes. In many places, facies changes resulted in major changes in the lithology of a specific unit, and in other places, different formation names were used essentially for the same unit. In some instances, a specific unit thinned in certain areas and was included as a member of another unit or as an inconsequential bed within another unit. An example is the Mississippian Chainman Shale, which is a major shale confining unit in the north, as in White Pine County (Hose and Blake, 1976), but a generally inconsequential shale bed included within other units in the southern map area, as in Clark County (Longwell et al., 1965). During compilation of the geologic map, separate stratigraphic columns were used for different counties, along with a stratigraphic column for units in western Utah. Correlations between specific geologic units are commonly given in the literature, and these correlations were generally used to associate units of the same or similar age in different parts of the map area. An example is the correlation of the Devonian Guilmette Formation with the Devils Gate Limestone (Hose and Blake, 1976).

During map compilation, a hard copy of the available digital file—generally the county map—was modified by hand, then digitized. Before this compilation, all available new geologic data about the area were accumulated, assimilated, and evaluated. The new data included reports, different concepts, detailed or regional maps, geophysics, and well logs. Several new interpretations conflicted with older interpretations, some

resulting from more accurate placement of contacts or faults. Decisions on the final linework were based on what appeared to be scientifically the most reasonable alternative and depended primarily on the judgment and experience of the authors.

The geologic maps (plates [1](#) and [2](#)) includes many new geologic cross sections (plates [3](#) and [4](#)) that trend mostly east-west so as to be perpendicular to most structures. In addition, geologic cross sections were drawn through many springs in the study area (Volume 3 of Southern Nevada Water Authority, 2008). The cross sections on plates [3](#) and [4](#) are roughly evenly spaced across the study area, at the same scale as the map, and at locations chosen to best show specific geologic and structural relationships important to the interpretation of the hydrogeology. Few of the reports and maps used to compile the geologic maps had associated geologic cross sections, so the cross sections in our report are based on our interpretations of the county geologic maps along with all other available maps and reports of the study area. The geologic map by Terrascan Group, Inc. (Howard, 1978), however, presented associated cross sections that were used to help interpret some of the cross sections in our report. In addition, the geologic map of Elko County (Coats, 1987) was used to help interpret cross section Y–Y' ([plate 3](#)), along the northern edge of the study area. The cross sections of Page et al. (2006) aided in constructing the cross sections in the southern part of the study area. The cross section of Smith et al. (1991) was useful in constructing cross section X–X' ([plate 3](#)) near the northern margin of the study area.

Unlike our compiled geologic maps, most of the cross sections are newly authored for this report. The first step in the construction of cross sections is to satisfy the three-dimensional geometry of the rocks at depth based on the types, attitudes, and thicknesses of rocks and structures on the surface. Without additional data, subsurface geometries are relatively unconstrained in cross sections constructed from the surface geology alone. Therefore, geophysics and well logs, when located near the line of sections, are valuable. Aeromagnetic and gravity geophysical data were widely available for much of the area, but well

logs, AMT profiles, and publicly available seismic reflection profiles are rare. When subsurface data is unavailable, analogies are made with areas in other parts of the Great Basin, where seismic and drill-log data provide insight to the geometries of rocks and structures at depth. As with the compilation of geologic maps, the judgment and experience of the authors is also important.

All cross sections incorporated lithologic information from available oil- and water-well logs. Oil-well logs in Nevada are available online from the Nevada Bureau of Mines and Geology (NBMG) (data from 1907 to 2011) and related publications (Garside et al., 1988; Hess, 2001, 2004; Hess et al., 2011). Oil-well logs in Utah were obtained from the Utah Division of Oil, Gas, and Mining website (2006, 2011). Water-well logs in Utah were obtained from the Utah Division of Water Rights website (2006).

Geophysical studies, notably gravity maps (Saltus, 1988a and b; Cook et al., 1989; Ponce, 1992; Saltus and Jachens, 1995; Ponce et al., 1996), aeromagnetic maps (Hildenbrand and Kucks, 1988a and b), and seismic reflection sections (Allmendinger et al., 1983; Hauser et al., 1987; Alam, 1990; Alam and Pilger, 1991) were used to aid in the interpretation of geologic cross sections. Gravity maps and AMT profiles were completed by the USGS as part of USGS/SNWA joint funding agreements (Mankinen et al., 2006, 2007, 2008, and 2016; McPhee et al., 2005, 2006a and b, 2007, 2008, and 2009; Mankinen and McKee, 2009 and 2011; Scheirer, 2005; Scheirer et al., 2006; Scheirer and Andreason, 2008). The gravity data were converted to depth-to-basement data and were used to aid in constructing the cross sections.

GEOLOGY

OVERVIEW

The study area ([figure 2](#)) is in the Great Basin subprovince of the Basin and Range physiographic province (Fenneman, 1931). The Basin and Range Province is made up of mostly parallel north-trending mountain ranges separated by parallel northerly trending alluvial basins (valleys). The ranges and basins formed because the region was affected by regional extension since the Miocene (e.g., Hamilton and Myers, 1966; Stewart, 1971, 1980a and b; Christiansen and Yeats, 1992). This ongoing east-west extension has resulted in north-striking normal faulting and the development of the north-trending basins and ranges.

Defining regional flow systems and determining directions and amounts of groundwater flow requires an understanding of the stratigraphy and structural geology of the study area. The study area (plates [1](#) and [2](#)) is characterized by a thick stratigraphic sequence of Proterozoic to Holocene rocks that have been structurally deformed during several tectonic episodes. The thick sequence includes three major assemblages that are important aquifers:

- Carbonate aquifer of Paleozoic age
- Volcanic rocks of Tertiary age
- Basin-fill sediments of Tertiary to Quaternary age.

Along with the aquifers are moderate to thick confining units or low-permeability units, including:

- Archean to Proterozoic metamorphic and igneous rocks
 - Neoproterozoic to Lower Cambrian quartzite and shale
 - Shale, sandstone, and conglomerate of Mississippian age
 - Triassic to Cretaceous shale, siltstone, and sandstone
- Mesozoic and Cenozoic plutons.

Three tectonic episodes, plus an intervening episode of extensive volcanism, have affected the

hydrogeology of the region. The oldest tectonic episode is the Antler deformation (Late Devonian to Late Mississippian). This episode included east-verging thrust sheets. The second tectonic episode was the Sevier deformation (Jurassic through early Cenozoic) that resulted in east-verging thrust sheets in which Paleozoic carbonate rocks were placed over younger rocks.

In Eocene to early Miocene time, volcanism resulted in the development of thick deposits of ash-flow tuff and related lava flows, including many scattered calderas that were the sources of the tuffs. The caldera margins formed new groundwater flow paths and barriers.

The third tectonic episode is the Miocene to Holocene Basin and Range deformation that shaped the current topography of the Great Basin. Basin and Range extensional faulting produced graben and horst topography, resulting in deep basins and relatively high mountain ranges, generally oriented north-south. The mountain ranges provided areas of groundwater recharge, and accumulations of alluvial fill within the basins provided areas of aquifer storage and avenues of groundwater flow. Normal faults may provide hydrogeologic barriers to groundwater flow (Caine et al., 1996; Caine and Forster, 1999). But more commonly, these normal faults provide conduits to groundwater flow, especially north or south directed flow. These north-south conduits may act as barriers to east or west flow (Caine, et al., 1996).

STRATIGRAPHY

The age of the rocks in the study area is summarized in a geologic time scale chart ([figure 5](#)). The oldest rocks are Paleoproterozoic (early Proterozoic) and Neoproterozoic (late Proterozoic) metamorphic and igneous units. These rocks are overlain by thick sequences of Neoproterozoic quartzite and subordinate shale, which are locally metamorphosed to slate and schist. The Neoproterozoic rocks transition conformably upward into rocks of similar type and thickness, though less metamorphosed, that are Neoproterozoic to Early Cambrian. During Middle

Cambrian time, carbonate deposition initiated, and thick sequences of marine limestone and dolomite were deposited until the Permian. These rocks make up the carbonate aquifer of Nevada and adjacent parts of Utah and range in thickness between 1500 and 9000 m throughout this area (Harrill and Prudic, 1998).

Locally, marine sandstone and shale interfinger with the carbonates. These units generally do not form significant impediments to regional groundwater flow, with the exception of the Late Mississippian Chainman Shale and related shale and sandstone. This unit locally exceeds 600 m in thickness, and in all but the southern part of the study area, this unit divides the carbonate aquifer into two distinct aquifers, the lower and upper carbonate aquifers. The Chainman Shale and related clastic units were derived from erosion of a structural highland, the Antler Highland, in and northwest of the study area. The highland, made up in large part of the Roberts Mountain allochthon, was produced by the Antler orogeny.

Mesozoic rocks in the study area consist of generally thin (mostly <600 m except in the extreme southern part of the area) deposits of nonmarine clastic rocks that have mostly been removed by erosion. Mesozoic and older rocks were deformed during the Sevier deformational event (DeCelles, 2004). At this time, the study area was a highland as part of the hinterland of the Sevier thrust belt, and regional erosion removed most Mesozoic rocks.

Plutons of Late Jurassic to Paleocene age were intruded during Sevier deformation. These plutons were likely associated with extrusive volcanic units that have since been eroded. Mesozoic plutons commonly led to significant mineralization in the study area.

Middle Tertiary (Eocene to lower Miocene) time marked the continuation of calc-alkaline intrusion and resulting volcanism, the terminal product of relatively rapid subduction beneath western North America that began in the Triassic (Lipman et al., 1972; Hamilton, 1995; Dickinson, 2009; Humphreys, 2009; Schellart et al., 2010). Above individual source plutons, vent deposits included andesitic and dacitic lava flows and volcanic mudflow breccia that locally exceeded several hundred meters of thickness. Caldera

deposits consist of dacitic to rhyolitic ash-flow tuffs, which are at least several hundred meters thick within individual calderas. Farther outward from the vents above the plutons, lava flows are sparse because they do not flow more than a few kilometers from their source vents; outflow ash-flow tuffs, on the other hand, traveled as far as 160 km from their source caldera, so accumulated to aggregate thicknesses exceeding 300 m in most of the study area (e.g., Cook, 1965).

Starting at about 20 Ma (lower Miocene), subduction ceased or slowed and extensional deformation increased in the Great Basin (Christiansen and Lipman, 1972; Christiansen and Yeats, 1992; Rowley and Dixon, 2001; Schellart et al., 2010). Basin and Range deformation, characterized by steeply dipping normal faulting, began to form alternating mountain ranges and valley basins. The main pulse of this basin and range faulting began about 10 Ma, during which time the present topography formed. As valleys formed, they were filled by debris eroded from the adjacent mountain ranges, creating basin-fill deposits.

Individual rock units, structures, basins, and ranges are described in the following sections. Thicknesses of most units are from the county reports. The relationships between geologic units in the different areas of the map can be determined from figures 6 to 9. These figures illustrate geologic columns for Lincoln ([figure 6](#)), White Pine ([figure 7](#)), and Clark counties ([figure 8](#)), Nevada, and western Utah ([figure 9](#)). The Utah area consists of western Iron, Beaver, Millard, and Juab counties and the southwestern corner of Tooele County.

Precambrian Rocks

Proterozoic Rocks

The oldest rocks are in and adjacent to the southern part of the study area in the Beaver Dam Mountains, Mormon Mountains, Virgin Mountains, northeastern Spring Mountains, and the Desert Range ([plate 2](#)) (Tschanz and Pampeyan, 1970; Longwell et al., 1965). These rocks are Paleoproterozoic crystalline

| | EON | ERA | PERIOD | EPOCH | TIME | PROCESSES AND ROCK TYPES |
|-------------|-------------|-----------|------------|---------------|---------|---|
| | Phanerozoic | Cenozoic | Quaternary | Holocene | Present | Valley-fill alluvium |
| | | | | Pleistocene | 2.8 Ma | |
| | | | Neogene | Pliocene | 5.3 Ma | |
| | | | | Miocene | 23 Ma | Start of regional extension (20 Ma) Volcanics and older sediments Emplacement of calderas |
| | | Tertiary | Paleogene | Oligocene | 33.9 Ma | |
| | | | | Eocene | 56 Ma | |
| | | Mesozoic | Cretaceous | Jurassic | 66 Ma | Sevier orogeny, intrusions Continental sediments |
| | | | | | 252 Ma | |
| | | Paleozoic | Permian | Pennsylvanian | | Antler orogeny, intrusions Chinaman Shale, carbonates |
| | | | | | | |
| | | | | | | |
| | | | | | | |
| Precambrian | Proterozoic | | | | 541 Ma | Quartzite and shale |
| | Archaen | | | | 2.5 Ga | |
| | Hadean | | | | 4.0 Ga | |

Figure 5. Geologic time scale, including rock type and tectonic events. (after Walker et al., 2013)

metamorphic rocks (Page et al., 2005a) that have been mapped in this report as Precambrian rocks (pC). Over most of the study area, however, the oldest rocks are Neoproterozoic to Lower Cambrian quartzite. These Neoproterozoic to Cambrian units appear to be the initial deposits of the Cordilleran miogeocline, a western belt of offshore carbonate-shelf and intertidal deposits (Page et al., 2005a). These units were deposited in shallow marine waters along a passive continental margin of western North America (Stewart and Poole, 1974; Stewart, 1976). No Mesoproterozoic rocks or pre-Proterozoic rocks are exposed in the study area.

In White Pine County and adjacent Utah, the principal Neoproterozoic unit is the McCoy Creek Group (figure 7). The assemblage consists of well-bedded, resistant feldspathic quartzite and subordinate slate and argillite more than 2700 m thick in the Schell Creek Range (plate 1) and about 2300 m thick in the Deep Creek Range, Utah. The metamorphic grade of these units is low to moderate, locally producing schist. The unit is

mapped in the Deep Creek Range with the underlying Trout Creek group (figure 9), also of Neoproterozoic age and similar in appearance. The Trout Creek group is estimated at 3500 m thick (Hintze and Kowallis, 2009) and of higher metamorphic grade. Link et al. (1993) concluded that, based on fossils, both of these sequences range in age from 780 to 560 Ma and that the upper part of the McCoy Creek Group may correlate with the Johnnie Formation of southern Nevada, which is as much as 1200 m thick. In Lincoln County and at least in parts of White Pine County, the basal units of the overlying Prospect Mountain Quartzite are considered to be partly Neoproterozoic. The McCoy Creek and Trout Creek units are mapped in the study area as Precambrian rocks (pC).

Paleozoic Rocks

Cambrian Rocks

The Prospect Mountain Quartzite (Cambrian to Precambrian sedimentary rocks, CpCs) overlies

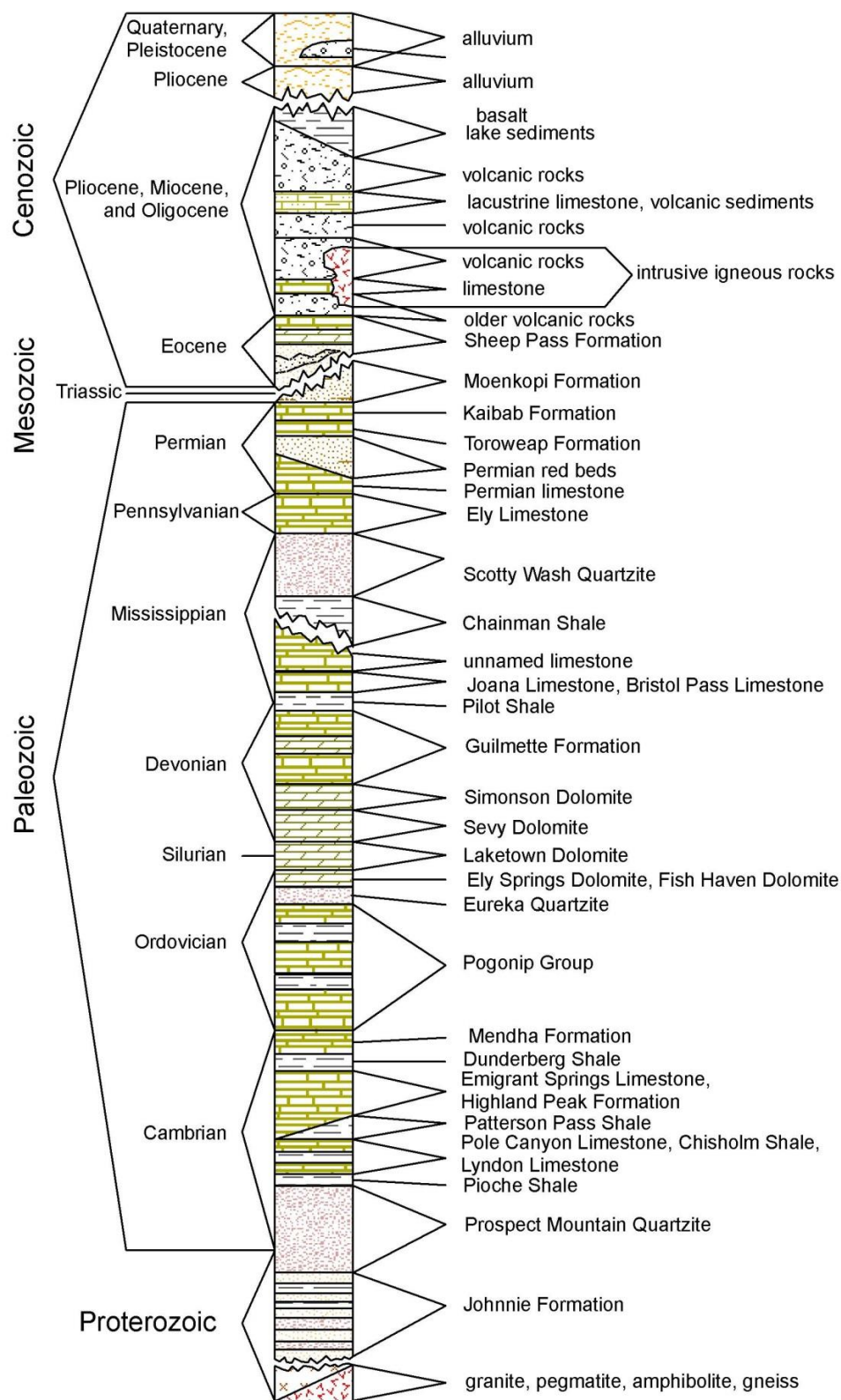


Figure 6. Geologic units of Lincoln County, Nevada (from Tschanz and Pampeyan, 1970). Vertical scale shows relative thickness of units.

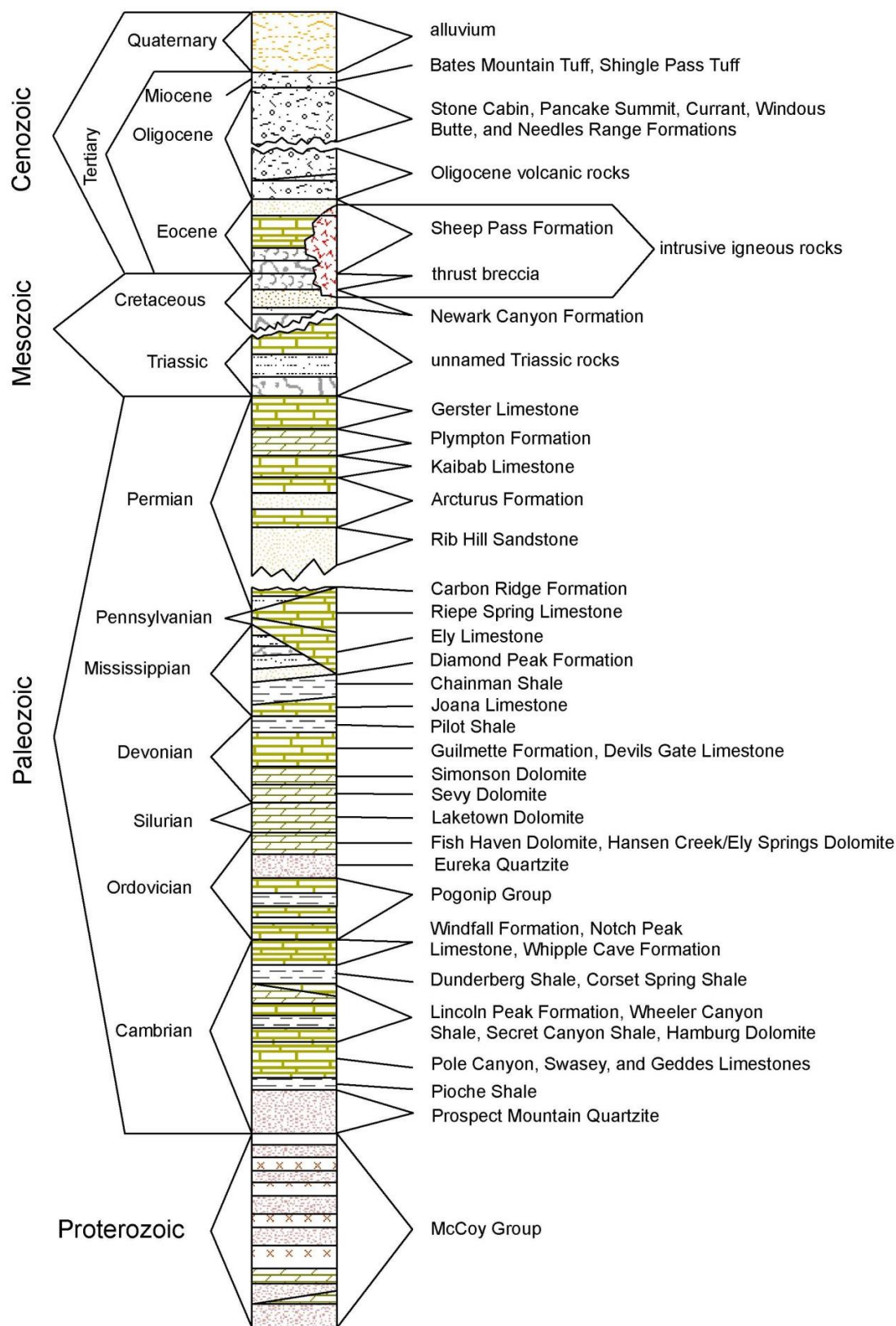


Figure 7. Geologic Units of White Pine County, Nevada (from Hose and Blake, 1976).
Vertical scale shows relative thickness of units.

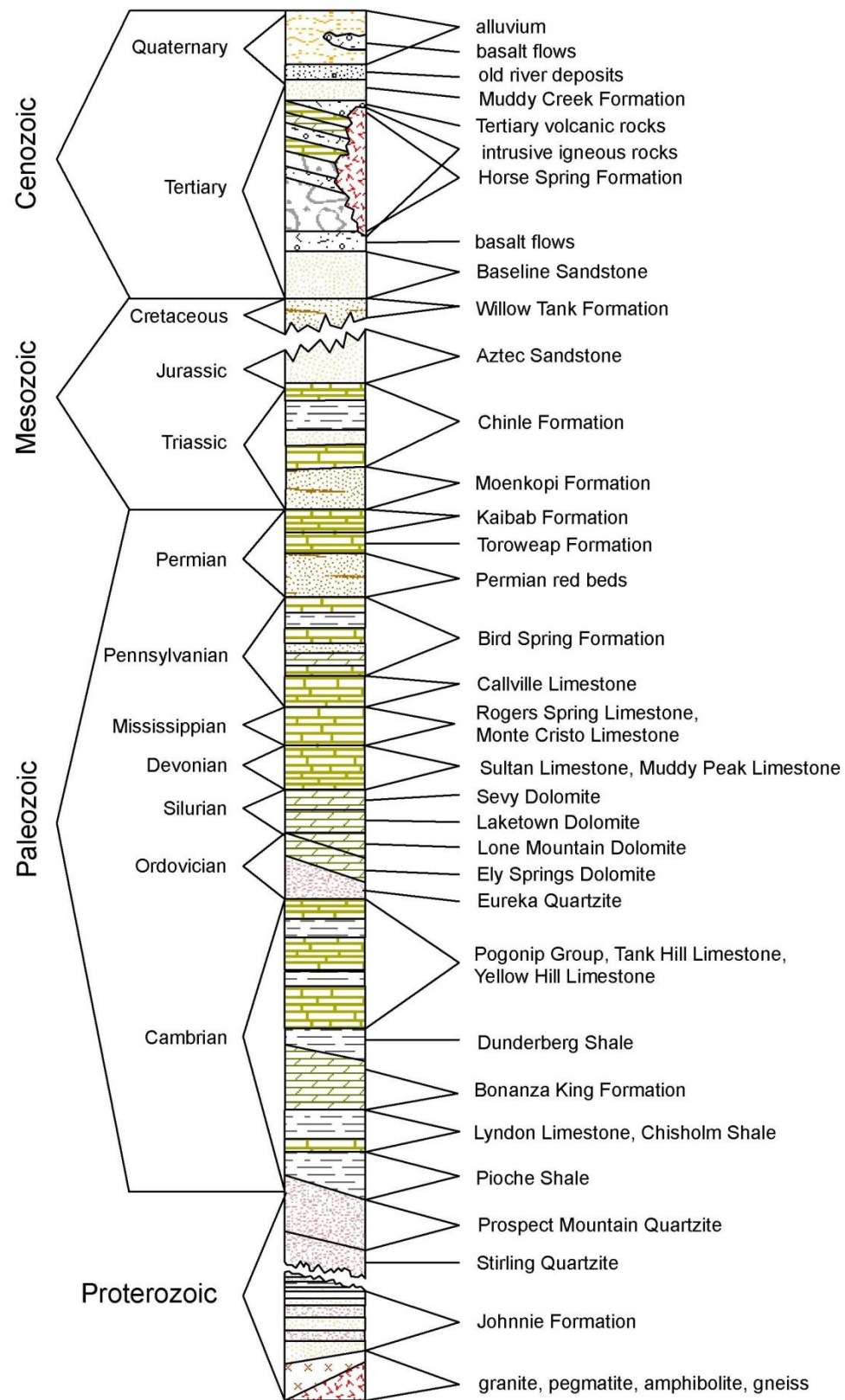


Figure 8. Geologic units of Clark County, Nevada (from Longwell et al., 1965). Vertical scale shows relative thickness of units.

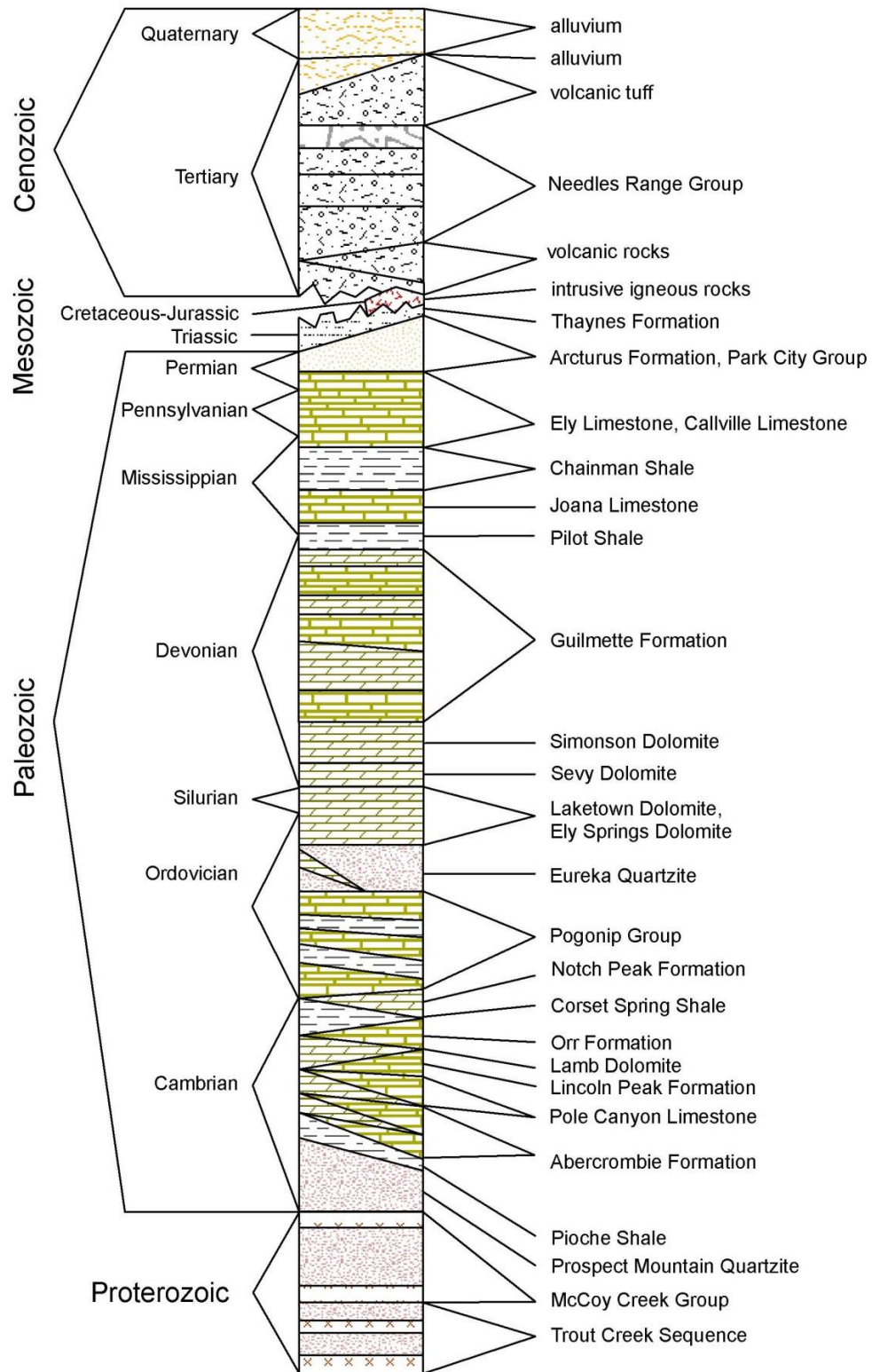


Figure 9. Geologic units of western Utah (after Hintze and Kowallis, 2009, Charts 45 and 46). Vertical scale shows relative thickness of units.

the McCoy Creek Group in White Pine County (figure 7). The Prospect Mountain Quartzite consists of well-bedded, resistant quartzite and subordinate shale, commonly weakly metamorphosed. It has been generally considered to be Early Cambrian, although it is not well characterized by age or correlation from place to place, and at least in the southern part of the study area is partly Neoproterozoic. In the study area, complete sections are uncommon, but the unit ranges from 900 to about 2400 m thick (Tschanz and Pampeyan, 1970). Thickness decreases southward to just 100 m in the Mormon Mountains. The Prospect Mountain Quartzite in the southern half of the study area is correlated with three units mapped in and west of the southern part of the study area: the Stirling Quartzite (Neoproterozoic and Early Cambrian), the Wood Canyon Formation (Early Cambrian), and the Zabriskie Quartzite (Early Cambrian) (Stewart, 1970, 1974, and 1984; Rowley et al., 1994).

In the southern part of the study area, the Stirling Quartzite is at least 600 m thick and the base is not exposed. Link et al. (1993) considered the Stirling Quartzite to postdate the Neoproterozoic McCoy Creek Group. In the Desert Range and above the Gass Peak thrust in the Las Vegas Range, the Wood Canyon Formation, a quartzite, is 300 to 900 m thick.

Above the Prospect Mountain Quartzite are, from base to top, the Pioche Shale (Lower and Middle Cambrian, 60 to 300 m thick), Lyndon Limestone (Middle Cambrian, 45 to 120 m thick), and Chisholm Shale (Middle Cambrian, 30 to 100 m thick) are present. These three units are combined in many places with the Prospect Mountain Quartzite, as $\epsilon p \epsilon s$ in White Pine County. These rocks are partly correlative with the Carrara Formation at the NTS and in portions of Clark County.

Cambrian carbonate rocks range in thickness from almost 1500 m over most of the study area to about 2300 m just southwest of the study area. The map unit is mostly middle Cambrian labeled ϵm . In the southern half of the study area, the most widespread and best studied of the Cambrian carbonate rocks is the Highland Peak Formation, consisting of Middle and Late Cambrian, well-bedded limestone and dolomite about 1400 m thick

(Tschanz and Pampeyan, 1970). To the west, in the Groom mining district, it is 1645 m thick.

In the northern part of the study area, the Cambrian carbonate rocks consist of many named units of generally similar lithology, total thickness, and age (Hose and Blake, 1976). Just to the northwest, in the Eureka area, these were originally named, from base to top, the Eldorado dolomite, the Geddes Limestone, the Secret Canyon Shale, and the Hamburg dolomite (Roberts et al., 1967). In the Snake Range, these are, from base to top, the Pole Canyon Limestone, the Lincoln Peak Formation, and the Johns Wash Limestone. These latter names are now preferred in the northwestern part of the study area and areas to the west. In the Cherry Creek Range and extending into western Utah, the units making up the entire sequence of Middle Cambrian carbonate rocks are, from base to top, the Dome Formation, Swasey Limestone, Wheeler Shale, Marjum Limestone, Weeks Limestone, Trippe Limestone, Wah Wah Summit Formation, Orr Formation, and others (Hose and Blake, 1976; Hintze and Davis, 2003). The overall Middle Cambrian carbonate sequence is roughly equivalent to the Bonanza King Formation to the south (Longwell et al., 1965). See figures 6 to 9 for geologic sections in different areas of the maps.

Above the Middle Cambrian carbonate section in Nevada is an Upper Cambrian to Lower Ordovician(?) sequence that includes a lower unit, the Dunderberg Shale, and an unnamed upper unit of limestone and dolomite (Tschanz and Pampeyan, 1970). The rocks are mapped as an upper part of the Cambrian section (ϵu); in some cross sections, the map unit is combined with ϵm as Cambrian carbonate rocks, undivided (ϵc). In White Pine County and in Utah, the ϵu limestone unit has been variously referred to as the Windfall Formation, Orr Formation, Notch Peak Limestone, and Whipple Cave Formation. In the southern part of the study area, the ϵu limestone unit is the Nopah limestone. See figures 6 to 9 for geologic sections. The Dunderberg Shale generally is about 90 m thick over most of the study area, but it is as much as 420 m thick in the southern Ruby Mountains (Hose and Blake, 1976). The overlying limestone ranges in thickness from 120 to 1200 m, generally thickest on the western side of the study area (Tschanz and Pampeyan, 1970).

Ordovician to Devonian Rocks

Ordovician to Silurian rocks in the study area are shown as a lower unit (Middle and Lower Ordovician, symbol Ol) and an upper unit (Silurian and Upper Ordovician, symbol SOu). The lower unit consists in ascending order of the Pogonip Group and the Eureka Quartzite. The Pogonip Group consists of interbedded thick-bedded limestone, sandy to silty limestone, conglomerate, and shale, generally about 600 to 1070 m thick in the study area. The Eureka Quartzite is a distinctive white, resistant, brittle, vitreous, fine- to medium-grained quartzite that thins southward from 180 to 240 m thick in the Confusion Range to 60 m in southern Lincoln County (Hose and Blake, 1976; Tschanz and Pampeyan, 1970). The Eureka Quartzite is a major marker bed throughout most of the study area (plates [1](#) and [2](#)). Just northwest of the study area, the lower unit includes the Vinini and Valmy Formations.

The upper unit (SOu) is comprised of, in ascending order, the Hanson Creek Formation, Ely Springs Dolomite, Fish Haven Dolomite, and Laketown Dolomite. The Ely Springs Dolomite is a poorly resistant, gray to dark-gray carbonate unit that occurs over most of the area of [plate 1](#) in Lincoln County (Tschanz and Pampeyan, 1970). The Ely Springs Dolomite in Lincoln County overlaps into northern Nye and Eureka counties, where it is locally called the Hanson Creek Formation, a dark dolomite and/or limestone unit that thins southward from 150 to 30 m (Tschanz and Pampeyan, 1970; Kleinhampl and Ziony, 1985). In White Pine County, the Ely Springs Dolomite is called the Fish Haven Dolomite and ranges between 60 and 260 m thick. The Silurian Laketown Dolomite is lithologically similar to the Ely Springs Dolomite and Fish Haven Dolomite and ranges between 180 and 560 m thick. Where the Ely Springs Dolomite and Laketown Dolomite are thin in Lincoln and Clark counties, they are included with unit Ol.

In Eureka and Nye counties, the Laketown Dolomite is underlain by, and partly equivalent in age to, the Lone Mountain formation. This unit consists of reef limestone and dolomite that is not present farther east in Lincoln and White Pine counties (Kleinhampl and Ziony, 1985). In Nye

County, these units, particularly the Lone Mountain formation, overlie and interfinger with the Roberts Mountain Formation. The Roberts Mountain Formation is a western facies of deep-water sediments and is comprised of shaley limestone, dolomite, and shale with a thickness of 150 to 580 m (Kleinhampl and Ziony, 1985).

Devonian carbonate rocks in eastern Nevada formed on a shallow-water marine carbonate platform. These rocks have been mapped as, in ascending order, the Sevy Dolomite, Simonson Dolomite, and Guilmette Formation. Where combined, they are mapped as undivided Devonian rocks (Du) or, when local Silurian rocks are included, as undivided Devonian and Silurian sedimentary rocks (DS). In the southern part of the study area, the DS map unit includes the Muddy Peak Limestone (Upper and Middle(?) Devonian). However, in most places the two mapped formations are the Sevy and Simonson Dolomites (Ds) and Guilmette Formation (Dg). Sandberg et al. (1997) redefined the upper part of the Simonson Dolomite in Nevada, or the lower part of the Guilmette Formation in Utah (Hintze and Kowallis, 2009), as the Fox Mountain formation. The Sevy Dolomite is a resistant, gray dolomite, commonly argillaceous and with a sandstone unit near the top. This dolomite increases in thickness southward across the study area from about 140 m in the Snake Range to 400 m in the Limestone Hills and southward (Tschanz and Pampeyan, 1970). This thickness decreases south of the Pahrangat Range, and the unit disappears south of the Delamar Mountains. The Simonson Dolomite is resistant, dark- and light-gray dolomite about 270 to 370 m thick over most of the study area, but it thins to less than 210 m in the southeastern part of the study area, continuing to decrease in thickness farther south. The Simonson Dolomite is about 150 m thick in the Snake Range (Tschanz and Pampeyan, 1970), although both the Simonson and Sevy Dolomites were locally reduced in thickness by faulting. The Fox Mountain formation consists of thin (generally 30 to 45 m), gray limestone except for dolomite in its upper part.

The Guilmette Formation (Dg) is a mostly resistant, fossiliferous limestone and dolomite, with biostromes and bioherms, and commonly

sandy with minor sandstone layers. The unit ranges in thickness from about 300 to 1070 m and appears to decrease in thickness in all directions from its thickest occurrences in north-central Lincoln County (Tschanz and Pampeyan, 1970; Hose and Blake, 1976). The middle part of the Guilmette Formation consists of the Alamo Breccia Member, which is as thick as 90 m northwest of Alamo, Nevada. It was formed by the cataclysmic Alamo bolide impact event (Warne et al., 2008). In Clark County, the Guilmette map unit includes the Sultan Limestone, which is made up of a lower dolomite unit and an upper limestone unit with a thickness of 550 m (Longwell et al., 1965). The Sultan Limestone is equivalent to the Muddy Peak Limestone in the Muddy Mountains.

In Eureka County and northern Nye County, the rocks of the Sevy, Simonson, and lower Guilmette units are called the Nevada formation (Dn), which is about 750 m thick. This map unit locally includes the Cockalorum Wash formation. In Eureka and northern Nye counties, the upper Guilmette Formation is called the Devils Gate Limestone (Dd), which is about 600 m thick (Roberts et al., 1967; Hose and Blake, 1976; Kleinhampl and Ziony, 1985).

Mississippian to Lower Permian Rocks

In White Pine County, a distinctive sequence of clastic rocks consists, in ascending order, of the Pilot Shale, Joana Limestone, Chainman Shale (Mc), and Diamond Peak Formation (Md). In Lincoln County, only the Pilot Shale is recognized (Tschanz and Pampeyan, 1970). These map units represent products of the Antler deformation, which took place in Late Devonian to Late Mississippian time and resulted in the Antler Highland located along the western side and northwest of the study area (Roberts et al., 1967; Kleinhampl and Ziony, 1985). The basin of deposition of these units was to the east of the highland (Poole and Sandberg, 1977 and 1991; Larson and Langenheim, 1979, figures 7 and 8). Where these four units are thin, they are categorized on the maps as Mississippian to Devonian rocks (MDd). But in most places, Chainman Shale and Diamond Peak Formation are mapped separately

and Pilot Shale and Joana Limestone are combined as unit MD. The Late Devonian to Early Mississippian Pilot Shale is a poorly resistant, gray, thin-bedded dolomitic siltstone and limestone containing little shale. This unit is generally 30 to 120 m thick, but locally, in northern White Pine County and western Utah, it is 150 to 270 m thick (Hose and Blake, 1976; Tschanz and Pampeyan, 1970; Hintze and Davis, 2002a and b). The Joana Limestone (Lower Mississippian) is a mostly resistant, bluish-gray limestone, and is 30 to 300 m thick.

The Monte Cristo Group of southern Nevada, which is Upper and Lower Mississippian, is considered equivalent to the Joana Limestone. The Monte Cristo Group overlies the Sultan Limestone. The Monte Cristo Group is a dark-gray to light-gray limestone containing abundant chert and is about 230 m thick. In the Muddy Mountains, the Mississippian Rogers Spring Limestone has a similar lithology and is considered to be equivalent in age to the Monte Cristo Group (Longwell et al., 1965). The general equivalent of the Chainman Shale southwest of the study area is the Eleana Formation (Mississippian and Upper Devonian), which is at least 1000 m thick (Workman et al., 2002a). The Monte Cristo Group, Rogers Spring Limestone, and Eleana Formation are included with the MD map unit. The map unit also includes local units Mercury Limestone and Bristol Pass Limestone (both mostly in White Pine County), Webb Formation (Elko County), Ochre Mountain Limestone (Utah), and West Range Limestone (Upper Devonian) in northern Lincoln County, Nevada.

The Upper Mississippian Chainman Shale is a soft, black, impermeable shale that is between 60 and 600 m thick. This unit is mapped as unit Mc over the northern part of the study area, but the Chainman is thin to the south, where it is included within a sequence of more permeable carbonate rocks. It is a regional confining unit (called the “upper aquitard”) separating the lower carbonate aquifer from the upper carbonate aquifer over all except the southern part of the study area. Paleotopography during deposition and post-depositional erosion resulted in substantial variations in Chainman thickness. The unit was mapped (Hintze and Davis, 2002a) in the

Confusion Range with a thicknesses greater than 600 m. A similar thickness is reported from an oil-well log in Lake Valley (Hess, 2004). Although these two locations are distal from the source area, they represent localized depositional basins.

In the northwestern part of the study area, the Upper Mississippian Diamond Peak Formation is mapped as unit **Md** above the Chainman Shale. The Diamond Peak Formation is a poorly resistant, gray siltstone, claystone, sandstone, and conglomerate that ranges in thickness from 180 to 760 m (Hose and Blake, 1976; Kleinhampl and Ziony, 1985). The unit thins and pinches out eastward in north-central White Pine County. The Diamond Peak Formation is derived from erosion of the Antler Highland and is generally included in the upper aquitard with the Chainman Shale. The Diamond Peak Formation is generally equivalent to the Scotty Wash Quartzite in the southern part of the study area. The Scotty Wash Quartzite is made up of interbedded sandstone, shale, and local limestone of limited extent. The Scotty Wash Quartzite is included with the **Md** map unit.

The Mississippian to Permian Ely Limestone, which is predominately Pennsylvanian in age, underlies much of the study area. Here it is mapped as Pennsylvanian rocks (**P**). In the Utah part of the study area, the Ely Limestone is 560 to 600 m thick (Hintze and Davis, 2002a and b). The map unit is called the Wildcat Peak Formation in the northwestern part of the study area and the Callville Limestone in the southern and eastern part of the study area. The Ely Limestone is overlain by a Lower Permian limestone of similar lithology in northern White Pine County (Hose and Blake, 1976). All units are resistant, gray limestone sequences that collectively range in thickness from 600 to 900 m thick. The overlying Lower Permian limestone is called the Riepe Spring Limestone. Where both the Ely and Riepe Spring Limestones are mapped together in the northern part of the study area, they are shown as Permian and Pennsylvanian rocks, undivided (**PIP**). The rocks in the **PIP** unit are unnamed in Lincoln County and range from 1100 to more than 1500 m thick (Tschanz and Pampeyan, 1970). The Ely and Riepe Spring Limestones are overlain by, and partly equivalent to, the Carbon Ridge

Formation, a Lower Permian, nonresistant, thin-bedded limestone and shale that is 420 to 700 m thick. The Carbon Ridge Formation is locally mapped separately in the northwestern part of the study area as **Pc**, or where thinner is included within the **PIP** map unit.

The Bird Spring Formation is an Upper Mississippian to Lower Permian limestone in the southern part of the study area that is roughly equivalent in age to the combined Ely Limestone, Riepe Spring Limestone, and Carbon Ridge Formation of White Pine County (Longwell et al., 1965; Tschanz and Pampeyan, 1970). The Bird Spring is a sequence of limestone beds with sandstone and dolomitic limestone layers. The formation is as much as 2400 m thick in the Spring Mountains and Las Vegas Range (Page et al., 2005b) and at least 1650 m thick in the Meadow Valley Mountains (Pampeyan, 1993). The Bird Spring Formation is included in the **PIP** map unit, as is the Brock Canyon Formation in the northwestern part of the study area and the Oquirrh Group (Lower Permian and Pennsylvanian) in the northeastern part of the study area.

The Lower Permian Rib Hill Sandstone (**Pr**) overlies the Carbon Ridge Formation in the northwestern part of the study area (Hose and Blake, 1976). The Rib Hill Sandstone is a nonresistant sandstone and dolomite 150 to 420 m thick. In northern White Pine County and adjacent parts of Utah, the Lower Permian Arcturus Formation (**Pa**) is the name for a sequence of poorly resistant, gray limestone, sandstone, and siltstone that is 820 to 1040 m thick (Hose and Blake, 1976). In the northwestern part of the study area, the Arcturus Formation overlies the Rib Hill Sandstone. Where the two are combined in the mapping, they are shown as unit **Par**. In Elko County, this map unit includes the Pequop Formation, a fusulinid-bearing limestone as much as 1160 m thick (Coats, 1987). In the southern part of the study area, the **Par** map unit is about 400 m thick (Longwell et al., 1965) and includes a redbed sequence, and in the southeastern part of the study area, the map unit includes the Queantoweap Sandstone.

Park City Group

The Park City Group (Pp) is a distinctive, resistant, light-gray Lower Permian limestone and dolomite sequence that is exposed only locally. The scattered nature of the outcrops suggests that the unit was originally fairly extensive in the study area but has been partly removed by erosion over most of its original extent. In White Pine County and adjacent western Utah, the group is made up, from base to top, of the Kaibab Limestone, Plympton Formation, and Gerster Limestone. The Kaibab Limestone is 15 to 180 m thick, the Plympton Formation is 210 to 275 m thick, and the Gerster Limestone is as thick as 335 m (Hose and Blake, 1976). These rocks are not observed in Eureka or Nye counties.

In Lincoln County and east of the study area in Utah, the east platform part of the sequence consists of the Toroweap Formation, the Kaibab Limestone, and locally the Plympton Formation (Tschanz and Pampeyan, 1970). In Lincoln County, these units have a combined thickness of between 75 and 140 m. The Toroweap Formation is a cherty, thin-bedded, shaley limestone, and the Kaibab Limestone is a cherty, sandy, light-gray limestone. The Kaibab Limestone and Toroweap Formation in Clark County have a maximum combined thickness of 400 m in the Muddy Mountains (Bohannon, 1983). In Clark County, their lithology is dominated by cherty limestone, sandstone, and red shale, with local gypsum beds (Bohannon, 1983; Page et al., 2005b).

Mesozoic Rocks

Mesozoic rocks in eastern Nevada and western Nevada were deposited locally or have been largely removed by erosion (e.g., Long, 2012). However, they are exposed in some ranges and are widespread east and south of the study area. Most of these rocks are continental clastic rocks deposited in fluvial, lacustrine, eolian, and marginal marine environments (Hintze and Davis, 2003; Long, 2012). The Thaynes Formation (Lower Triassic) is a nonresistant, gray, thin-bedded claystone and limestone that is locally about 580 m thick in western Utah in the northeastern part of the study area (Hintze and

Davis, 2002a). The overlying Moenkopi Formation (Lower Triassic) is a mostly nonresistant, red and gray, thin-bedded siltstone, limestone, sandstone, and shale, commonly gypsiferous, and locally about 600 m thick in western Utah. The Thaynes and Moenkopi Formations are mostly thin in the Nevada portion of [plate 1](#) and are not separated on this map. In White Pine County, these thin rocks are considered to be the Thaynes Formation. In Clark and southeast Lincoln counties, however, the Moenkopi Formation is about 600 m thick and of similar lithology to that in Utah, with gypsum beds in the upper part of the Formation (Page et al., 2005b); the Thaynes Formation is not present here.

The Upper Triassic Chinle Formation includes a basal unit, the Shinarump Conglomerate Member, which is a resistant gray sandstone and conglomerate that ranges from 3 to 75 m thick. The balance of the formation is of soft, variegated mudstone and siltstone that is widely exposed above the Moenkopi Formation in the southern part of the study area (Bohannon, 1983; Page et al., 2005b). This mudstone and siltstone have been measured to be about 300 to 1000 m thick within the study area. The Luning Formation (Upper Triassic) is locally exposed northwest of the area. All Triassic rocks have been combined as Triassic sedimentary rocks (**TRs**).

Jurassic sedimentary rocks (Js) are exposed in the southern part of the study area ([plate 2](#)). These rocks are dominated by the Lower Jurassic Aztec Sandstone, a brick-red, buff, and light-gray, fine- to medium-grained eolian sandstone containing large-scale (10+ m) cross beds. The Aztec Sandstone is 180 to 1100 m thick. The equivalent Navajo Sandstone is about 600 m thick in the southeastern part of the study area. It is here underlain by the Moenave (lower) and Kayenta (upper) Formations, both of Early Jurassic age and mostly made up of fine-grained sandstone and siltstone of eolian and fluvial origin, with a combined thickness of 150 to 900 m. The Navajo Sandstone is here overlain by the Temple Cap (lower) and Carmel (upper) Formations, both of Middle Jurassic age and made up of sandstone, limestone, siltstone, and shale of mostly marginal marine origin and with a combined thickness of

about 280 m. The map unit also includes the Dunlap Formation (Lower Jurassic) in the northwestern part of the study area.

Cretaceous synorogenic sedimentary rocks (Ks) are present but uncommon in the study area. Most of this area was a highland undergoing erosion at that time (Hintze and Davis, 2003). The Lower Cretaceous Newark Canyon Formation occurs in the northwestern part of the study area as a poorly exposed, reddish-brown to gray, fresh-water limestone, siltstone, conglomerate, and sandstone from 430 to 550 m thick (Hose and Blake, 1976). Upper Cretaceous sedimentary rocks, shed east from erosion of Sevier highlands in and north of the study area, are thin and patchy in the map area but extensive and thick to the east and south. Upper Cretaceous through Paleocene fault breccias, primarily from thrust faults related to Sevier deformation, are locally exposed in the study area.

In Clark County, Cretaceous sedimentary units include from older to younger the Willow Tank Formation (Lower Cretaceous) and the Baseline Sandstone. The Willow Tank Formation is 90 to 140 m thick and consists of a basal conglomerate and overlying fine-grained sediments, including bentonitic clay, and is primarily restricted to the Muddy Mountains. The Baseline Sandstone consists of about 900 to 1500 m of gray and red, well-bedded sandstone and conglomerate. In the southeastern (Utah) part of the study area, the Upper Cretaceous Cedar Mountain Formation and overlying Iron Springs Formation consist of mudstone, shale, sandstone, and conglomerate about 900 m thick.

Plutonic rocks related to the Middle Jurassic through Paleocene Sevier deformational event are exposed locally throughout the study area (Maldonado et al., 1988). Much of the southern Snake Range is intruded by a Middle and Upper Jurassic batholith (Miller et al., 1999a), and Jurassic quartz monzonite and diabase have been identified in the House Range and in the Burbank Hills, respectively, both in Utah near the eastern edge of the study area (Hintze and Davis, 2002a and b, and 2003). Other quartz monzonite to granodiorite plutons, mostly of Middle Jurassic age, form a north-trending belt along the eastern edge of White Pine County, Nevada, extending

from the southern Snake Range to the Clifton Hills of western Utah. A north-trending plutonic belt of Cretaceous age is exposed in eastern White Pine County, Nevada, extending into the Deep Creek Range of western Utah and including the main mass of the large Kern Mountains granite batholith of apparent Cretaceous and Eocene age (Best et al., 1974; Miller et al., 1999a). On the geologic maps, these plutonic rocks are shown as Jurassic (Ji), Cretaceous (Ki), Tertiary to Cretaceous (TKi), or Tertiary (Ti) intrusive rocks. Geophysical data show that the batholith extends eastward, downthrown beneath Snake Valley and buried by basin-fill sediments (Mankinen and McKee, 2009). East trending strings of small Lower Cretaceous plutons are present in the Eureka and Ely areas ([plate 1](#)).

Cenozoic Rocks

Cenozoic rocks in the study area belong to three main sequences: (1) locally exposed, mostly thin, older continental sedimentary rocks; (2) generally voluminous, calc-alkaline volcanic rocks and their source plutons; and (3) rocks that formed during regional extension, namely thin bimodal-composition (basalt and high-silica rhyolite) lava flows and locally thick basin-fill sediments. On the geologic maps, most of these rocks are separated into several rock types based on age, following the mapping strategy of Ekren et al. (1977). Basalts are mapped as Quaternary to late Tertiary basaltic rocks (QTb). Basin-fill sedimentary rocks and surficial sediments are mapped as Quaternary to late Tertiary alluvium (QTa). Locally thin basalts intertongued with basin-fill sediments are included in QTa.

Latest Cretaceous (?) to Miocene Sedimentary Rocks

The oldest Cenozoic sedimentary rocks (Ts₁) are thin and poorly exposed in the study area but are more common in eastern Clark County and southwestern Utah. These units were deposited with, or unconformably deposited on, rocks deposited and deformed during the Sevier orogeny. In eastern Nevada, the principal Ts₁ unit is the Sheep Pass Formation of Eocene to Oligocene age

(Hose and Blake, 1976; Druschke et al., 2009). The Sheep Pass Formation occupies a 40,000 km² basin extending south from Ely and Eureka, Nevada, to Penoyer and northern Pahrnagat valleys (Vandervoort and Schmitt, 1990; Fouch et al., 1991; Druschke et al., 2009). The unit is mostly nonresistant, gray conglomerate, sandstone, mudstone, and limestone, with a thickness of 180 to 900 m.

In Utah, just southeast of the study area, the mostly resistant Grapevine Wash Formation and overlying Claron Formation are included within the Ts₁ map unit. The Grapevine Wash Formation, poorly constrained in age as Late Cretaceous to early Tertiary but considered by Hintze et al. (1994a) to postdate Sevier deformation, consists of as much as 600 m of gray, tan, and red conglomerate and sandstone. The Claron Formation, also poorly constrained in age but likely Eocene and Paleocene (Biek et al., 2015), is sandstone, limestone, and conglomerate as much as 600 m thick.

Similar sedimentary rocks (Ts₂, Ts₃, and Ts₄) of various names and ages, from Oligocene to Miocene, are exposed in the study area. These include the Gilmore Gulch Formation of about 30 Ma (Ts₂), exposed in the northwestern part of the area. The Horse Spring Formation, about 12 to 20 Ma, and the red sandstone unit, 11 to 12 Ma, that overlies it are mapped as Ts₄ in the southern part of the study area (Bohannon, 1983 and 1984). The Horse Spring Formation consists of conglomerate, sandstone, siltstone, claystone, limestone, dolomite, tuff, and gypsum as much as 3000 m thick.

Tertiary Volcanic Rocks

Volcanic rocks make up the primary Cenozoic rock type in the study area. The older (Eocene to lower Miocene) sequence of calc-alkaline arc rocks consists of andesite to low-silica rhyolite that are mapped as different units separated by rock type and age. Tertiary plutonic rocks, which are the sources for the volcanic rocks, are mapped as unit Ti whether of calc-alkaline or bimodal origin. The calc-alkaline sequence is made up largely of regional ash-flow tuff sheets derived from widely scattered calderas. The oldest tuffs are mapped as

Tt₁ (Eocene and Oligocene) that predate the Needles Range Group (about 32 Ma). The next younger group of tuffs, consisting mostly of the Needles Range Group, is mapped as Tt₂ (Oligocene), from about 32 Ma to 27 Ma. The younger aged tuffs are part of the Isom Formation. The next younger tuffs are mapped as Tt₃ (Oligocene and Miocene), ranging in age from that of the Shingle Pass Tuff (about 27 Ma) to the youngest calc-alkaline tuffs (about 18 Ma). Individual calderas are filled with thick intracaldera ash-flow tuffs that are at least several hundred meters thick. Their outflow sheets are typically thin; generally less than 300 m, but the aggregate thickness of all of these tuffs is at least 1000 m in the southern half of the study area. Isopach (thickness) maps of most tuffs in the study area were given by Sweetkind and du Bray (2008).

The outflow tuffs are interspersed with locally distributed but thick central stratovolcano deposits made up of lava flows and volcanic mudflow breccia generally deposited above their source plutons. Where these calc-alkaline flows and breccia are largely andesite, they are mapped as Ta₁, Ta₂, Ta₃, and Ta₄ based on ages that correspond to those of the related ash-flow tuffs. Unit Ta₄ is made up of post-18 Ma andesitic (calc-alkaline) flows that are exposed in the southern part of the study area. Where calc-alkaline flows and breccia are predominately low-silica rhyolite, they are mapped as Tr₁, Tr₂, and Tr₃ based on ages that correspond to those of the tuffs (e.g., Tr₁: >32 Ma, Tr₂: 32–27 Ma, and Tr₃: 27–18 Ma).

In the Great Basin, vents—notably calderas—for Tertiary calc-alkaline arc volcanic rocks comprise a generally east-trending igneous belt that youngs from north to south (Ekren et al., 1976 and 1977; Stewart and Carlson, 1976; Stewart et al., 1977; Rowley, 1998; Rowley and Dixon, 2001). These magmatic belts, as well as other belts in the southern Basin and Range that become young to the north, represent removal (Humphreys, 1995, 2009) or rollback (Dickinson, 2006, 2009, 2013) of parts of the subducted Farallon slab beneath the Great Basin. The igneous belts are partly controlled by transverse zones and are underlain by batholiths whose cupolas provide the vents for the volcanic rocks. The oldest volcanic rocks in the study area

belong to the Ely-Tintic igneous belt (belt names from Rowley, 1998) in the northern part of the study area. The ages of vents in this belt are ~38 Ma and locally older (Eocene) along the northern margin of the area, and 36 Ma farther south (Rowley, 1998). An east-trending gap in vent areas, with a 50–100 km north-south width, occurs south of Ely and Preston, Nevada, and a volcanic plain of thin outflow tuffs underlies the gap (Gans et al., 1989). The axis of the next igneous belt to the south, the Pioche-Marysville igneous belt, is south of Pioche, Nevada. The volcanic centers here are 32–31 Ma on the northern side of the belt and 28–27 Ma along the southern part. About 20 km south of the Pioche-Marysville belt is the Delamar-Iron Springs igneous belt, of ~24 Ma along its northern side and 16 Ma along its southern side. Its southern edge is just south of the latitude of Pahrangat Valley, Nevada.

In the Ely-Tintic igneous belt, the 35 Ma Kalamazoo ash-flow tuff is the most voluminous volcanic unit, which was deposited as an east-trending 145-km-long and 40-km-wide elongate tuff sequence (Gans et al., 1989). Its caldera source has not been found but Gans et al. (1989) suggested that it may be buried beneath northern Spring Valley, which is near the center of the area of deposition of the Kalamazoo tuff. Gravity data ([Gravity Data section](#), Geophysics chapter) do not support this hypothesis but rather suggest that the caldera may be buried beneath southern Tippet Valley. Other ash-flow tuffs and lava flows underlie and overlie the Kalamazoo tuff, and the overall thickness of the volcanic rocks in the igneous belt is about 150 to 450 m. Plutons ranging in age from 45 to 30 Ma, are scattered throughout the belt; most of these represent source areas of volcanic rocks that have since been removed by erosion. One of these plutons (Best et al., 1974) is the composite-age Kern Mountains pluton. This and other Eocene to Oligocene plutons and batholiths in the northern Snake Range, Kern Mountains, and Deep Creek Range represent initial calc-alkaline magmatism beneath these ranges (Miller et al., 1999a) that later were uplifted during Basin and Range extension.

In the Pioche-Marysville belt, volcanic rocks are thicker and more widespread than in the Ely-Tintic belt: calderas are more abundant and larger,

and the volcanic rocks are somewhat younger and thus less eroded. Most volcanic rocks are regional ash-flow tuffs from calderas, but lava flows and mudflow breccia erupted from volcanoes in and along the margins of calderas or from isolated volcanoes such as the Seaman Range volcanic center. The largest vent area in the belt is the Indian Peak caldera complex (Best et al., 1989a and 2013a) in the southeastern part of the study area. It erupted ash-flow tuffs and related rocks of the Needles Range Group (Oligocene, about 32 to 27 Ma) and the Isom Formation (27 to 26 Ma). This may be the largest caldera complex in the world; ash-flow tuffs from this complex are spread over an area of about 320 km east-west by 240 km north-south.

Intracaldera megabreccia deposits result from landsliding of the outside wall of a caldera margin into a caldera following rapid eruption of huge ash-flow tuff sheets and the resulting collapse of the caldera floor to fill the erupted parts of the underlying magma chamber (Rowley et al., 1995, 2001; Best et al., 2013a). These megabreccia deposits (Tmb) are mapped only in the Indian Peak caldera complex ([plate 1](#)) and cross section Q–Q' ([plate 3](#)). Megabreccia deposits (Tmb) are also mapped in and west of the southern Sheep Range ([plate 2](#), [plate 4](#) - cross section H–H'); however, these deposits do not include significant volcanic rocks but instead result from large gravity slides off the Sheep Range.

A cluster of smaller calderas west of the Indian Peak caldera complex also belongs to the Pioche-Marysville igneous belt (e.g., Dixon et al., 1972, Ekren et al., 1972, 1973a and b, and 1974; Snyder et al., 1972; Quinlivan et al., 1974; Sargent and Roggensack, 1984). Some of these calderas produced regional ash-flow tuffs, from oldest to youngest and generally from north to south respectively, known as the Stone Cabin Tuff (35.3 Ma), Pancake Summit Tuff (34.8 Ma), Windous Butte Formation (31.3 Ma), tuff of Hot Creek Canyon (29.7 Ma), Monotony Tuff (27.3 Ma), tuff of Orange Lichen Creek (26.8 Ma), Shingle Pass Tuff (26.7 to 26 Ma), tuff of Lunar Cuesta (25.4 Ma), tuff of Goblin Knobs (25.4 Ma), tuff of Big Ten Peak (25 Ma), Pahrangat tuff (22.6 Ma), and Fraction Tuff (18.3 Ma) (Best et al., 1989b, 1993, and 2013b; Ekren et al., 2012). This cluster of

calderas has been referred to as the “central Nevada caldera complex” (Best et al., 1993 and 2013b; Scott et al., 1995a). However, we note that this feature is not a classic caldera complex because it has not all subsided following tuff eruptions but instead consists of individual calderas separated by Phanerozoic sedimentary rocks. Within calderas in the study area, intracaldera ash-flow tuffs and subordinate lava flows and mudflow breccia are several hundred meters thick and are underlain by intracaldera source plutons. Outside the calderas, the thickness of volcanic rocks in the belt in the area is about 450 to 900 m, but locally more. A few plutons of the same age range, likely representing sources for volcanic rocks that have been removed by erosion, occur in the Grant Range and many other parts of the study area.

In the Delamar-Iron Springs igneous belt, at the southern edge of the study area, the largest igneous centers are the Caliente and Kane Springs Wash caldera complexes ([plate 2](#)). The Caliente caldera complex erupted ash-flow tuffs that were deposited over an area extending 240 km by 160 km in the east-west and north-south directions, respectively. The complex was active for at least ~10 myr. (Rowley et al., 1995). The regional ash-flow tuffs derived from it include the Swett (23.7 Ma) and Bauers (22.8 Ma) Tuff Members of the Condor Canyon Formation, Racer Canyon Tuff (18.7 Ma), Hiko Tuff (18.3 Ma), tuff of Tepee Rocks (17.8 Ma), tuff of Dow Mountain (17.4 Ma), tuff of Acklin Canyon (17.1 Ma), tuff of Rainbow Canyon (15.6 Ma), Ox Valley Tuff (13.5 Ma), and probably the Leach Canyon Formation (23.8 Ma) (Hintze et al., 1994a; Rowley et al., 1995; Scott and Swadley, 1995; Snee and Rowley, 2000; Best et al., 2013a). The Kane Springs Wash caldera complex, just to the south, erupted the tuff of Narrow Canyon (15.8 Ma), tuff of Boulder Canyon (15.1 Ma), and Kane Wash Tuff (14.7 to 14.4 Ma) (Scott et al., 1995a and 1996; Scott and Swadley, 1995). The total thickness of volcanic rocks in the igneous belt generally does not exceed 300 m outside the caldera complexes.

The middle Miocene to Quaternary bimodal sequence, which postdates the calc-alkaline sequence, is made up of small basalt lava flows and cinder cones as well as small high-silica rhyolite

volcanic domes, lava flows, ash-flow tuffs, and ash-fall tuffs. The basalts are categorized on the geologic maps as unit QTb, rhyolite domes and flows as Tr₄, and tuffs as Tt₄. All the volcanic rocks derived from the Kane Springs Wash caldera complex, and those that postdate the tuff of Tepee Rocks (Rowley et al., 1995) from the Caliente caldera complex, are included within the bimodal assemblage. The tectonic environment during bimodal magmatism was severe east-west extension, with the direction of principal maximum compressive stress generally oriented vertically, creating an environment of north-south normal faults. Bimodal magmatism coincided with Basin and Range extension, in which the present topography was created and previous tectonic features and topography were deformed and obscured.

Miocene to Holocene Sediments

With the start of Basin and Range deformation at ~20 Ma, north-striking normal faults created the present ranges and basins. Erosion of the uplifted ranges resulted in basin-fill sediments that accumulated to thicknesses of locally more than 3000 m in down-faulted basins. In most places, the basin-fill sediments are unnamed. These units are referred to here as middle Miocene to Holocene alluvium (QTa) and are mostly aquifers, especially where fractured by faulting.

Coeval bimodal volcanic rocks were either high-silica rhyolite or basalt lava flows and tuffs. Their distribution is sporadic ([plates 1 and 2](#)) and their thickness is rarely more than a kilometer, except for their source volcanic domes or cinder cones. Where thin (roughly 10 m), they may be combined in the cross sections with the older, much thicker calc-alkaline volcanic rocks or with thick interbedded basin-fill sediments.

The basin-fill sediments (QTa) were largely deposited by streams in closed basins. In general, coarse-grained materials accumulated around the edges of the mountain fronts, whereas finer materials accumulated toward the center of the basins. In some basin interiors, fine-grained sediments accumulated in ephemeral playa lakes. The largest lakes were pluvial lakes of Pleistocene age, including the latest Pleistocene Bonneville

and Lahontan lakes that had water depths of as much as 300 m, resulting in deposition of clay and saline sediments in many basins (Mifflin and Wheat, 1979; Currey, 1982; Currey et al., 1984; Reheis et al., 2014). These lakes, however, were short lived and produced fine-grained materials that rarely exceeded 10 m in thickness. The Bonneville lake left behind spectacular shorelines in some northeast parts of the study area, including the high Bonneville shoreline that formed about 18,000 years ago and the lower Provo shoreline that formed between 16,500 and 15,000 years ago (Reheis et al., 2014). Quaternary basin-fill deposits are mostly thin (a couple hundred meters) and overlie Pliocene and Miocene basin-fill sediments that may be thousands of meters thick, depending on the throw of the normal faults that produced the basins. Data from boreholes in Snake Valley indicate at least 100 m of Tertiary evaporites within the deepest part of the basin.

The concept that extensional basins contain coarse-grained sediments on their margins and fine-grained sediments in their interiors may be valid for periods of time that are geologically short (thousands of years) but is invalid for longer periods (tens of thousands of years) because of the vagaries of the sizes of storms that deposit sediments, of climate changes, of integration of some basins, and of timing of the deformation of basin-bounding versus intra-basin faults. Basin margins may become basin centers and vice versa, over 10 myr. Therefore, in practice, the stratigraphy of basin-fill sediments is characterized by a complex intertonguing of beds of all lithologies. Intra-basin faults commonly produced horsts of soft basin-fill sediments that were then eroded away by streams and redeposited as younger basin-fill sediments. [Plate 1](#) includes thin surficial deposits in and on the flanks of the ranges, including stream deposits, landslides, and spring deposits. However, these deposits are not individually separated in this report or on the maps because of their limited extent.

In some places the basin-fill sediments have local names that were categorized as QTa on the geologic maps, for example, the 11–5 Ma Muddy Creek Formation (Bohannon, 1984) in southern Lincoln and Clark counties (southeastern part of [plate 2](#)). The Muddy Creek Formation consists of

locally gypsiferous shale, siltstone, and fine-grained sandstone. Another named unit is the ~10–2 Ma Panaca Formation, located in the central part of the study area (Meadow Valley, southeastern part of [plate 1](#)), which consists of sandstone, siltstone, shale, and conglomerate (Rowley and Shroba, 1991). Other units of similar lithology to the Panaca Formation are the Horse Camp Formation in the northwestern part of the area (Brown and Schmitt, 1991) and the Salt Lake Formation northeast of the area. All these units are generally more than 300 m thick and locally more than 1500 m thick.

STRUCTURAL GEOLOGY

Three Phanerozoic tectonic events affected the study area: (1) Late Devonian to Late Mississippian Antler orogeny, (2) Late Jurassic to early Tertiary Sevier orogeny, and (3) late Cenozoic Basin and Range extension. Between the Sevier and Basin and Range deformation during the middle Cenozoic, eastern Nevada was characterized by mild extension (Hamilton, 1995; Rowley, 1998; Miller et al., 1999a; Rowley and Dixon, 2001), voluminous calc-alkaline volcanism, and initiation of east-trending transverse zones. These events profoundly affected the topography of the study area.

Antler Orogeny

The Late Devonian to Late Mississippian Antler orogeny affected the northwestern part of the study area, generating a north-trending highland (Larson and Langenheim, 1979; Carpenter et al., 1994; Poole and Sandberg, 1977, 1991; Dickinson, 2006). This event formed folds and thrusts of the Roberts Mountain allochthon, which was at least 2500 m thick and passed through Eureka, Nevada (Carpenter et al., 1994; Saucier, 1997), just northwest of the study area. The thrusts transported deeper-water sedimentary rocks eastward as much as 160 km. The effect to the study area consisted of coarse synorogenic siliceous clastic detritus shed from the highland into the foreland basin to the east, transitioning to shale farther east. The main synorogenic rock units that resulted were the Chainman Shale and

Diamond Peak Formation, and farther south the Scotty Wash Quartzite.

Sevier Orogeny

The second structural event in the Phanerozoic, the Middle Jurassic to early Tertiary Sevier orogeny, resulted in generally north- to north-northeast-striking, east-verging folds and thrust faults. Scattered Middle Jurassic to lower Tertiary plutons were emplaced in many mountain ranges of the study area. Eastward-directed overthrusts emplaced Neoproterozoic to middle Paleozoic rocks over Paleozoic to Jurassic rocks (Armstrong, 1968). At least six frontal thrusts are exposed in the Las Vegas area, each with displacements ranging from several to 30 km (Page et al., 2005b). Minimum shortening estimates in southern Nevada are at least 35 to 72 km (Stewart, 1980b; Burchfiel et al., 1974). East of the study area, at least four major frontal thrust systems are well exposed, with total shortening of at least 210 km (DeCelles, 2004; DeCelles and Coogan, 2006). Except for the southern part of the study area, most of the study area is considered to be the hinterland of the deformation. In other words, Sevier deformation thickened the crust and created Late Cretaceous to early Tertiary highlands (hinterlands) that in turn shed most clastic debris to the east (Vandervoort and Schmitt, 1990; Druschke et al., 2009; DeCelles, 2004; DeCelles and Coogan, 2006; Long, 2012; Long et al., 2014 and 2015). However, some of the Las Vegas area thrusts, including the Gass Peak thrust, have been projected northward into the hinterland in the central and northern part of the study area, including the Timpahute Range, Worthington Mountains, Golden Gate Range, Grant Range, Pancake Range, and Newark Valley (Vandervoort and Schmitt, 1990; Dobbs et al., 1994; Taylor et al., 1991 and 2000). Taylor et al. (1993 and 2000), Long (2012), and Greene (2014) referred to this region as the central Nevada thrust belt, and considered it to be a fold-thrust belt of relatively small displacement within the overall hinterland. In contrast to the small east-verging thrusts in the hinterland, Lewis et al. (1999) and Gebelin et al. (2015) suggested some west-verging Sevier thrusts in the northern Snake Range and the Deep Creek Range.

East of the central Nevada thrust belt, a north-trending belt of high-grade metamorphic rocks is exposed, with its axis passing along the Snake Range. The rocks contain Jurassic, Cretaceous, and lower Tertiary components and notably yield Late Cretaceous cooling ages. The belt is interpreted to represent a crustal welt of tectonic shortening that spawned the frontal Sevier thrusts to the east (Coney and Harms, 1984; Miller and Gans, 1989, DeCelles, 2004).

Small east-verging thrusts have been mapped in the Confusion Range (e.g., Hintze and Davis, 2002a and b). Most workers, including us, consider these thrusts to represent mostly minor movement along bedding planes in weak beds during tight folding of Sevier age (e.g., Hintze and Davis, 2003). Anderson (1983), however, interpreted the faults to have formed by gravity sliding into the axis of a synclinalorium. A broad uplifted area east of the Confusion Range, in the House Range and Sevier Desert, known as the Sevier arch or Sevier culmination, was similarly considered to be an area of minor thrusting (Hintze and Davis, 2003). Therefore, the Confusion Range and Sevier arch make up the eastern part of the hinterland. DeCelles (2004) and DeCelles and Coogan (2006), in an extensive, long-term review of Sevier-age thrusts in the west, projected some of their major thrusts beneath the Sevier arch. More recently, Greene and Herring (2013) have taken this theme significantly further by drawing cross sections through the Confusion Range that show significant thrusts in the subsurface. Although they agree with the previous mapping in the Confusion Range that indicates only minor thrusts, they concluded on the basis of their analysis and cross sections that the Confusion Range may be a western part of the Sevier frontal thrust belt yet exposed well east of the Sevier arch. Any proof of major thrusts beneath the Confusion Range must await future seismic studies or deep drilling. Some of their inferred thrusts are beneath the level of our cross sections. Greene (2014) expanded on these interpretations to give the regional implications of the thrusts in and beneath the Confusion Range. He named these thrusts and folds the western Utah thrust belt, comparable to the central Nevada thrust belt, and both containing relatively small-displacement thrusts and folds within the hinterland. These two

small belts were suggested to each have roughly 10 km of horizontal shortening (Greene, 2014). Sevier-type deformation is shown schematically on [figure 10](#), and the Sevier-age Glendale/Muddy Mountain thrust in the Muddy Mountains of the southern part of the study area is shown on [figure 11](#).

Middle Cenozoic Volcanism

Middle Cenozoic time was characterized by voluminous calc-alkaline arc magmatism (Rowley,

1998; Miller et al., 1999a; Rowley and Dixon, 2001). This was the terminal product of subduction beneath western North America that began in the Triassic (Lipman et al., 1972; Hamilton, 1995; Dickinson, 2009; Humphreys, 2009). This last episode of subduction was low angle, so the subducted slab extended as far east beneath western North America as Colorado, generating arc magmas along the way. The tectonic environment during calc-alkaline magmatism was generally one of mild east-west extension in the

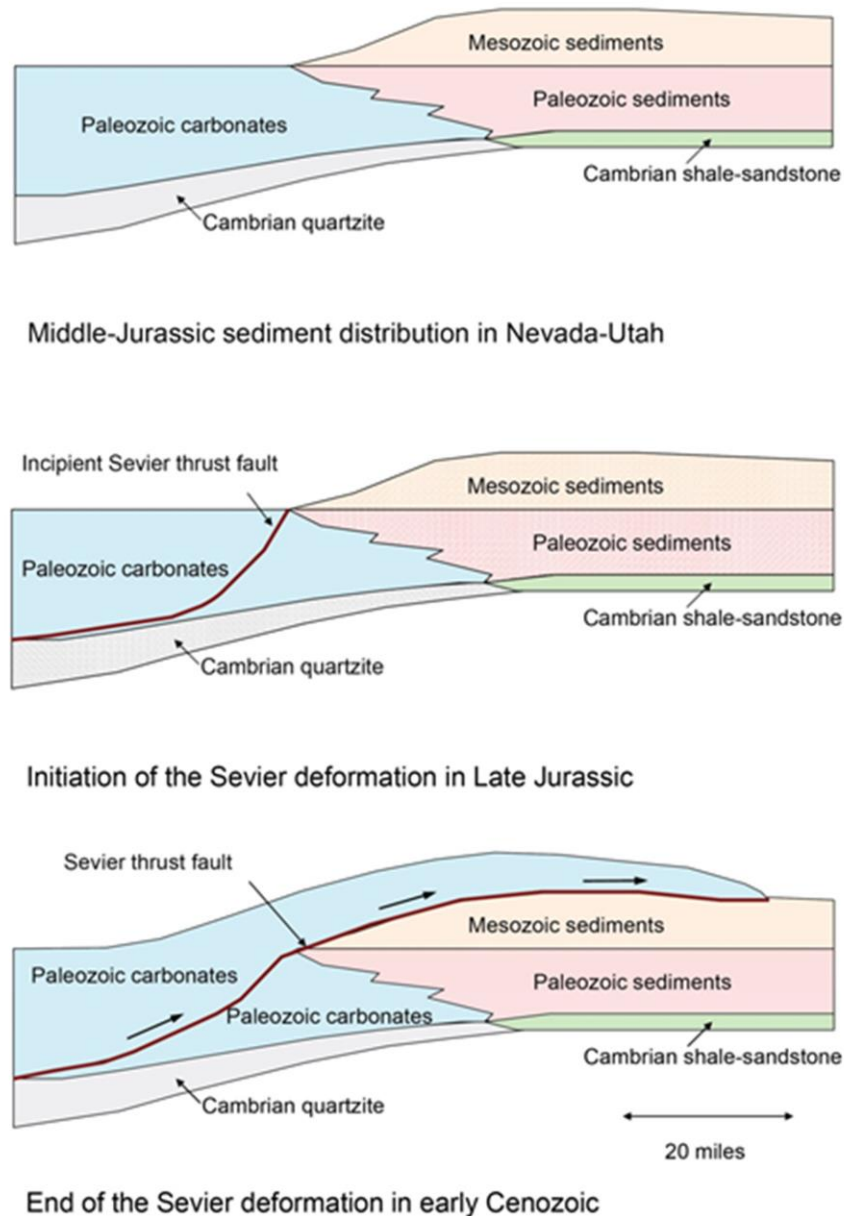


Figure 10. Schematic diagram of Sevier thrust sheets, illustrating the movement of Paleozoic carbonates over cratonic sediments.

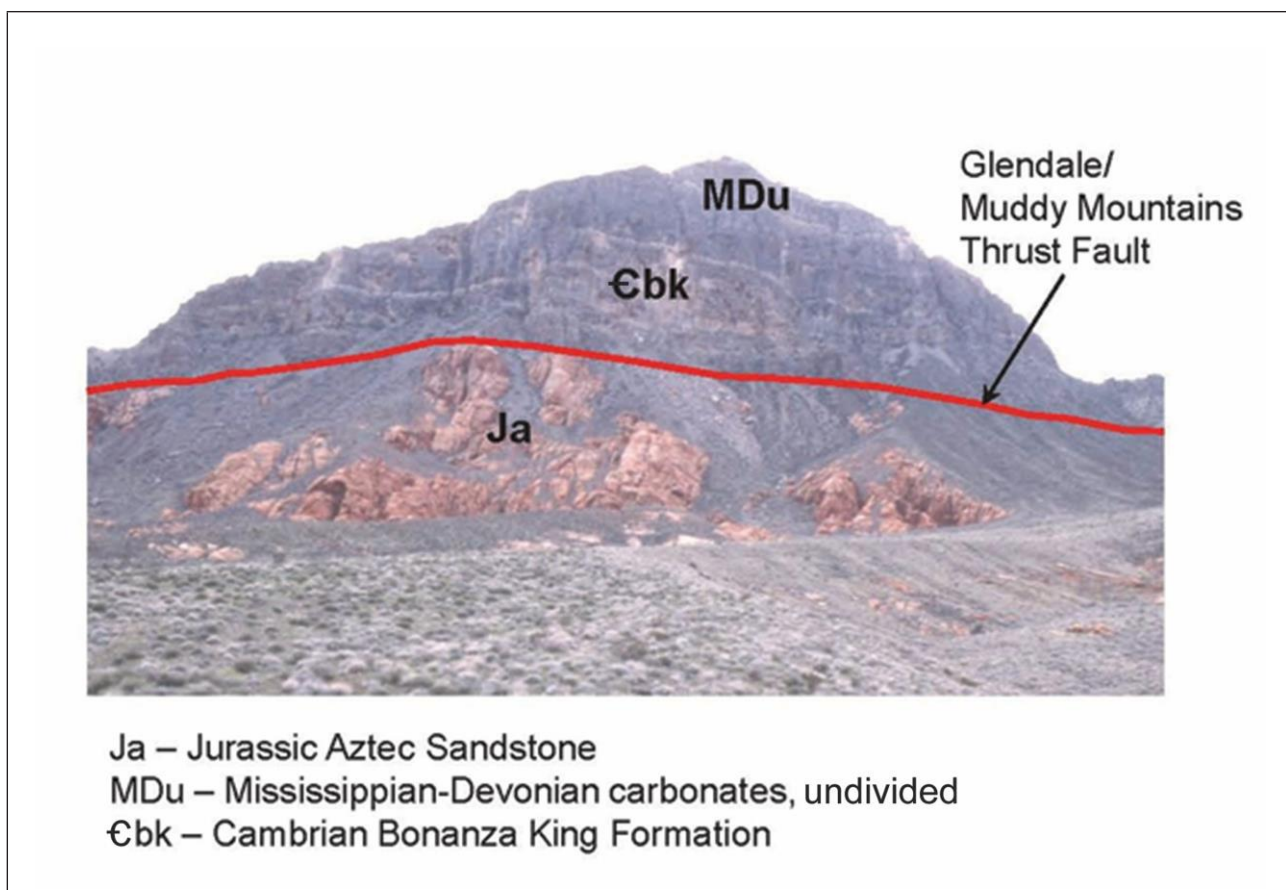


Figure 11. Paleozoic carbonates thrust over Jurassic Aztec Sandstone in the Muddy Mountains near Muddy Peak.

Great Basin. The direction of principal maximum compressive stress was generally north-south, creating an environment of strike-slip and oblique-slip faults (Anderson, 1981, 1983, 1989, 2013; Anderson and Barnhard, 1993; Anderson et al, 2013; Rowley, 1998).

In the Great Basin, the mostly east-trending igneous belts are made up of volcanic vents, including calderas, and underlying source batholiths, resulting in a topography almost 90 degrees different from the present topography, with generally east-trending highlands that resulted from thermal expansion by the underlying batholith and from near-vent volcanism. These highlands presumably alternated with plains north and south of the highland, where outflow tuffs accumulated after erupting from calderas in the highlands. Lava flows, unlike ash-flow tuffs, are not deposited far from their vents so they accumulated to great thicknesses in the higher axes

of the belts. Nonetheless, at that time most of the Great Basin was a high upland (Vandervoort and Schmitt, 1990; Dilek and Moores, 1999; Henry, 2008; Henry et al., 2012; Best et al., 2009; Long, 2012), analogous to the Altiplano of the modern Andes and thus termed by DeCelles (2004) as the Nevadaplano. The upland was a holdover from crustal thickening caused by Sevier crustal shortening in the hinterland west of the frontal thrusts of the Sevier deformational event. The Nevadaplano extended from the eastern part of what is now the Sierra Nevada to the frontal Sevier thrust faults that surfaced along the eastern edge of the Great Basin. The Nevadaplano had a north-trending east-west drainage divide in eastern to central Nevada (Henry, 2008; Henry et al., 2012; Long, 2012).

East-Trending Transverse Zones

East-striking folds and faults and alignments of plutons, volcanic vents, geophysical anomalies, hot springs, hydrothermally altered rocks, mineral deposits, and local basins and ranges have been noted in the Great Basin for years, primarily by geologists of the mining industry. Ekren et al. (1976, 1977), Rowley et al. (1978), and Stewart et al. (1977) called these alignments “lineaments” with an origin similar to transform faults in the ocean basins. Ekren et al. (1976) suggested that the lineaments began to form in the Cretaceous, if not earlier, and continued to be active throughout both Tertiary calc-alkaline magmatism and Basin and Range deformation. Like transform faults, these lineaments seem to represent boundaries between areas to the north and south that had different amounts, rates, and types of structural deformation. Rowley (1998) and Rowley and Dixon (2001) referred to them as transverse zones, and we follow their terminology here. They are poorly known and have been mapped in detail only locally, so they are projected with limited evidence between the areas where they are known. Therefore, transverse zones are delineated as speculative zones of potential disruption on plates [1](#) and [2](#).

Transverse zones bound parts of most igneous belts in the Great Basin. They also define the northern and southern sides of the Caliente caldera complex, representing structures by which this caldera spread east and west to a degree much more profound than most other caldera complexes in the Great Basin. Some transverse zones seem to be discontinuous along strike. The Sand Pass transverse zone (Rowley, 1998; Rowley and Dixon, 2001), which bounds the northern and southern side of the Kern Mountains, is buried beneath surficial sediments in Snake Valley, absent through the carbonate bedrock of the northern Confusion Range and western Middle Range ([plate 1](#)), and exposed again in the carbonate bedrock and basin-fill sediments of the central and eastern Middle Range and of Sand Pass (Rowley et al., 2009, plate 1). Farther east, east-trending features are absent in the Drum Mountains and Thomas Range (Rowley et al., 2009, plate 1), but they are prominent east of the Thomas Range most of the

way to and east of the Wasatch front in central Utah (Stoeser, 1993; Rowley, 1998; Rowley and Dixon, 2001).

Basin and Range Extension

Ongoing Basin and Range extension began at ~20 Ma. It is characterized by east-west extension accommodated primarily by north-striking normal faults. Early phases of this deformation locally produced north-striking basins and ranges due partly to broad warping (Rowley et al., 1981; Liberty et al., 1994), but these basins and ranges were not necessarily in the same locations as they are today. The present topography was produced later, during the main pulse of extension that began after 10 Ma for most parts of the Great Basin. The north-south orientation of axes of some basins and ranges, which formed during main-phase (post-10 Ma) extension, may be 10 km or more east or west of axes produced during early (20 to 10 Ma) extension (Rowley et al., 1981; Liberty et al., 1994; Rowley, 1998). Some parts of the older basins were uplifted as part of the new ranges and some parts of the older ranges were downthrown as part of the new basins. An example is the presence of Miocene lacustrine limestones and associated clastics in the North Pahroc and Pahrnagat ranges (Tschanz and Pampeyan, 1970) that were originally deposited in one or more older extensional basins.

Most structures shown on plates [1](#) and [2](#) formed during Basin and Range extension. Therefore, the maps illustrate many types of structures that have combined over mostly the last 20 Ma to produce a dynamic and continuing regional pattern of extensional deformation. Such deformation, in the experience of the authors, is typical of most other parts of the Great Basin but is not commonly portrayed at such a regional scale in a single report. Although faults exposed in basin fill and bedrock were faithfully reproduced from previously published maps, we applied geophysics and well logs to show buried (dotted) faults in the basins, thereby adding to the overall framework by showing structures not previously published. The resulting complex pattern thus consists of (1) the primary, mostly north-striking high-angle normal faults, (2) low-angle normal attenuation/denudation or detachment faults, (3)

northwest- or northeast-striking oblique-slip transfer faults, and (4) east-striking transverse zones. All are the result of east-west extension. We interpret that most of the total deformation was produced by fault type #1 (i.e., the steeply dipping normal faults) some of which had dip-slip movement of more than 3000 m; only some of the other fault types locally included such large displacements. We present the larger faults that are responsible for large-magnitude displacement, most of which bound the ranges, on plates [1](#) and [2](#) as regional faults, whereas lesser faults are shown as subsidiary faults. Movement on the high-angle normal faults caused the dominant topography of alternating north-trending ranges and valleys, which are mostly made up respectively of complex horsts and grabens (Stewart, 1971, 1980).

Of the four types of normal faults, the attenuation/denudation faults (fault type #2) shown on plates [1](#) and [2](#) are non-rooted faults that represent failure by gravity as the ranges went up along the large high-angle normal faults and the rising tops of these ranges failed along weak beds. Some of these attenuation/denudation faults may be considered gravity slides, as in the southwestern Sheep Range/Desert Range (Guth, 1980) and in the Mormon Mountains (Carpenter and Carpenter, 1994a). The Snake Range décollement is a regional fault in the Pioche Shale that is covered below in greater detail because of its controversial nature; we consider it to be an attenuation/denudation fault.

Fault type #3, transfer faults, are those that transfer east-west strain into both normal and strike-slip movement because the faults strike mostly northeast or northwest. A synonym for transfer faults that we have previously applied (e.g., Rowley et al., 2016) are “accommodation” faults. However, Faulds and Varga (1998) have defined this fault more narrowly as a belt of intermeshing, oppositely-dipping normal faults. The northwest-striking transfer faults tend to have right-lateral movement under east-west extension, in addition to some component of vertical movement, whereas the northeasterly-striking transfer zones tend to have left-lateral movement in addition to some component of vertical movement. Examples of transfer zones include the northeast-striking, left-lateral Pahrnatat shear

zone (PSZ) at the southern end of Pahrnatat and Delamar valleys (Ekren et al., 1977). The eastern and western ends of some of these northeast-striking faults merge with north-striking dip-slip normal faults. Another transfer zone is the north-northeast-striking, left-lateral Kane Spring fault zone that separates the Delamar Range from the Meadow Valley Mountains. Others are the west-northwest-striking, right-lateral Las Vegas Valley shear zone, which passes eastward into the east-northeast-striking, left-lateral Lake Mead fault zone (e.g., Anderson and Beard, 2010).

Fault type #4, the east-striking transverse zones, separate broad masses of rock, both north and south of the zone, that were pulled apart in east and west directions at different rates or amounts, or by different expressions of deformation—including folding—north and south of the transverse zone (Ekren, et al., 1976, 1977; Rowley et al., 1978; Rowley, 1998; Rowley and Dixon, 2001). Transverse zones are long lived (probably several million years) and deep seated, so along strike they may pass beneath rocks that appear to exhibit no surface expression, although such an absence of structures may reflect older mapping that we compiled. Most faults in transverse zones tend to be strike-slip or oblique-slip. Compilation of transverse zones in the Great Basin (Rowley, 1998; Rowley and Dixon, 2001) suggests that their strike-slip component most commonly is left lateral but it seems likely, given their long-lived nature and their origin as transform structures, that both right-lateral and left-lateral motions may be present on the same fault or on different strands of the same transverse zone. Examples of transverse zones, from north to south, include the Sand Pass transverse zone, which is clearly present at Sand Pass, separating the Fish Springs Range on the north from the House Range on the south (see Rowley et al., 2009, Plate 1), as well as many but not all areas along strike extending well to the east (Stoeser, 1993). West of Sand Pass, its presence across the Middle Range and northern Confusion Range is expressed only by several easterly-striking faults, but its expression is much more profound farther west in the Kern Mountains, where it bounds both sides of this unusual east-trending range. The Blue Ribbon transverse zone farther south is well expressed east

of the study area (Rowley et al., 1978), not expressed by published mapping across the Indian Peak caldera complex, well expressed between the Fairview Range and Bristol Range (Ekren and Page, 1995; Page and Ekren, 1995), and moderately to well-expressed to the western edge of the study area, and, indeed, to the western edge of the Great Basin, where Ekren et al. (1976) called it the Warm Springs lineament (Rowley, 1998; Rowley and Dixon, 2001). The Timpahute transverse zone farther south is well expressed across the entire map area, as well as far to the east and west (Ekren et al., 1976, 1977; Rowley, 1998; Rowley and Dixon, 2001). Transverse zones are not well known, and few persons besides the authors have mapped any parts of them in detail. Most of the transfer faults and transverse zones may represent activation of older structures.

The main (post-10 Ma) episode of Basin and Range deformation continued from the late Miocene through the Pliocene and Quaternary. Except for the attenuation/denudation faults, all the different types of faults that were active during this regional extension had some Pleistocene and/or Holocene movement. Age relationships of faults shown on plates [1](#) and [2](#) suggest that Pleistocene and Holocene motion can be considered the latest tectonic adjustment to east-west extension that is now at the same or a greater level of deformation as earlier, throughout the study area. In other words, the primary current deformation regime is regional extension—with ranges going up and the basins moving down along normal faults—along with many domains involving strike-slip and oblique-slip motion.

In northern parts of the study area, many low-angle faults previously mapped as thrust faults (e.g., Hazzard and Turner, 1957; Misch, 1960; Nelson, 1966; Drewes, 1967) have since been interpreted as Cenozoic low-angle normal faults. The workers who mapped them as thrusts correctly noted that most of them partly followed weak shale beds and placed younger rocks on top of older rocks, in contrast to Sevier thrust faults that are exposed to the east. The first workers to publish on the significance of the younger on older relationships were Scott (1965) and Moores et al. (1968) from detailed geologic mapping in the Grant and White Pine ranges, as well as Armstrong

(1963, 1972) from regional studies over much of the study area. They and other geologists also recognized that the rocks above these faults were not thickened and compressed, as above thrust faults, but instead were stretched and attenuated. Therefore, they must represent Cenozoic expressions of structural extension. Although most rocks deformed by the faults are of Paleozoic age, the mapping and regional studies confirmed that the faults postdated Sevier deformation and most likely represented Basin and Range deformation. These geologists suggested that the low-angle faults formed during and after rapid Basin and Range uplift of the ranges, in which the tops of the uplifted blocks were structurally stripped (or attenuated or denuded) by low-angle faults that verged into the adjacent low areas, much like large gravity slides. They called them attenuation or denudation faults. Most formed during the Basin and Range deformation. Nonetheless, compilation of the county maps of the area (Hose and Blake, 1976; Kleinhampl and Ziony, 1985) showed the low-angle faults as thrusts, even though these authors (especially Kleinhampl and Ziony) had misgivings and clearly recognized that at least some of these faults were due to Cenozoic extension. Later, Lund et al. (1991), Lund and Beard (1992), Francis and Walker (2002), Walker and Francis (2002), Long (2014), and Long and Walker (2015) remapped part of the northern Grant Range, confirming that most of the low-angle faults are brittle attenuation faults that continue beneath parts of Railroad Valley to the west, and whose interpretation has implications for finding oil occurrences in the large Railroad Valley oil field. The faults here largely follow weak beds of the Chainman Shale.

Low-angle normal faults in the Schell Creek and Snake Ranges have been studied in great detail, and are generally correlated with each other and referred to as the Snake Range décollement (Misch, 1960). This assumed single fault horizon, which largely follows weak beds of the Pioche Shale, juxtaposed Middle Cambrian carbonates and some younger rocks over Lower and Middle Cambrian and older rocks. The oldest of these rocks are in the Hendrys Creek area on the eastern flank of the northern Snake Range, where metamorphosed muscovite-bearing quartzite and

schist of the Neoproterozoic McCoy Creek Group are exposed (Lewis et al., 1999; Gebelin et al., 2015). Drewes (1967) mapped the décollement east of the crest of the Schell Creek Range. Whitebread (1969) mapped it in detail over a large part of the southern Snake Range that includes Great Basin National Park (GBNP). Hose and Blake (1976) extended the décollement (shown as a thrust) in reconnaissance over the Snake, Schell Creek, Egan, Cherry Creek, Antelope, and southwestern Deep Creek ranges. These workers emphasized that younger rocks were emplaced over older rocks, which is opposite of the thrust-fault geometry. Misch (1960) and Drewes (1967) considered the structure to be a thrust anyway, whereas Whitebread (1969) and Hose and Blake (1976) were equivocal on the age or origin of the faults.

An important advance was made by Coney (1974), who studied small-scale structures in the hanging wall of the décollement in the Snake and Schell Creek ranges and found that upper-plate rocks on the eastern side of the Schell Creek Range and both the eastern and western sides of the Snake Range moved down the flanks of the ranges, whether to the east or the west; he considered the faults to be Tertiary denudation faults comparable to gravity slides that moved downslope along much the same (Lower Cambrian) planes of weakness. Therefore these large faults were not necessarily all the same fault, whose hanging wall moved eastward, as many others suggested. Gebelin et al. (2015) appeared to have confirmed Coney's conclusions by a study of samples collected from the footwall metamorphic rocks of the décollement from both the western side of the northern Snake Range (north of the latitude of Sacramento Pass) and 16 km to the east from the eastern side (Hendrys Creek) of the Snake Range. Gebelin et al. found that footwall rocks on the western flank indicated movement of the hanging wall to the west, whereas footwall rocks on the eastern flank indicated movement of the hanging wall to the east. Yet despite his remark (p. 154) that "quartzite from the two areas did not experience the same type of deformation," Gebelin et al. (2015) seemed to have discarded his own relative-movement data from the western side, preferring instead to join

most previous workers in advocating that the décollement was a single large structure whose upper plate moved east. Following a comprehensive study of the décollement, Miller et al. (1983) and Gans et al. (1985, 1989) reinterpreted the fault as an Eocene to Miocene low-angle surface in which the rocks above it were extended by brittle mechanisms, whereas the rocks below were extended a similar amount by ductile mechanisms, then later the surface was exhumed during uplift of the area as a metamorphic core complex. They suggested that relative movement along the décollement was minor because the surface represented a ductile-brittle transition zone that originally formed at about 6 km depth.

Bartley and Wernicke (1984) interpreted the Snake Range décollement differently, using a model based on work by Wernicke et al. (1985) from a study of the Mormon Mountains of southern Nevada. Bartley and Wernicke (1984, p. 652) suggested that the décollement was a major low-angle detachment fault with 60 km of eastward displacement of the upper plate relative to its underlying footwall. A detachment fault is a low-angle normal fault whose use may be applied in such a non-genetic way, but more commonly the term is used for a low-angle normal fault due to extension above a rising metamorphic core complex. This hypothesis was later accepted by numerous other geologists (Allmendinger et al., 1983; Lee, 1995; Lewis et al., 1999; Kirby and Hurlow, 2005; Sweetkind et al., 2007a and b; Wallace et al., 2007). In contrast, Gans and Miller (1985, p. 411; Gebelin et al., 2015) pointed out that the fault plane occupies the same stratigraphic position (top of the Pioche Shale) and does not "cut downsection to the east," so they therefore proposed that it could not have "a large amount of translation" and more likely represents "decoupling along the stratigraphic horizon in the Pioche Shale."

After more field work, Miller et al. (1999a) concluded that, whereas the décollement had an older (late Eocene and early Oligocene) history, most displacement on it was early Miocene and younger, coinciding with Basin and Range deformation. Gebelin et al. (2015) also emphasized the possibility of early (Eocene)

deformation on the décollement based on $^{40}\text{Ar}/^{39}\text{Ar}$ ages (49–45 Ma) in footwall rocks from the eastern flank of the northern Snake Range, yet plutonism and volcanism of this same age occurs throughout the Ely-Tintic igneous belt, and such magmatism has no bearing on low-angle faults elsewhere. Ruksznis and Miller (2014) re-emphasized that most uplift and deroofing of the northern Snake Range and Kern Mountains was post-21 Ma, synchronous with Basin and Range deformation. Yet Norman and Gans (2014) noted $^{40}\text{Ar}/^{39}\text{Ar}$ ages of 40–35 Ma for two low-angle normal faults in the central Schell Creek Range. In their summary report of all field work on the origin of the décollement, Miller et al. (1999a) recanted some of their earlier theories and presented several alternative origins. Among them was adoption of a rolling-hinge model (Lee, 1995) for a metamorphic core complex, by which the hanging wall of the décollement had been translated primarily eastward about 11 to 14 km, although they acknowledged that movement on the décollement on the western side of the Snake Range was westward, as had been recognized by Coney (1974). Their core complex consisted only of the Deep Creek Range, Kern Mountains, and Snake Range. Then, in their final concluding paragraph, Miller et al. (1999a, p. 902) also proposed that the décollement may not be a normal fault at all but instead a "highly complex structural boundary developed above a rising and extending mass of hot crystalline rocks."

Most regional summaries of the geology of the Great Basin list the Snake Range as a metamorphic core complex (e.g., Dickinson,

2006), following the conclusions of Miller et al. (1983). In a summary of world-wide core complexes, Whitney et al. (2013, p. 277, figures 2 and 3) was one of the latest to make this conclusion. Among such advocates, Greene (2014, p. 163–165) in particular had difficulty reconciling thrusting in the Confusion Range with a detachment dipping eastward beneath Snake Valley and the Confusion Range and presumably carrying the Confusion Range in its hanging wall, as most workers have suggested. In the eastern Great Basin, not all high mountain ranges that contain flat faults (e.g., Deep Creek, Antelope, Cherry Creek, Snake, Egan, Schell Creek, and Grant ranges and Mineral, Tushar, Pine Valley, and Mormon mountains) are core complexes. In other words, it is likely that most large ranges in the Basin and Range Province contain low-angle normal faults, whether as detachments related to core complexes or as non-rooted (gravity driven) denudation/attenuation faults related to structural uplift along large, high-angle range-front normal faults. In fact, in places where these high mountain ranges consist mostly of Tertiary volcanic rocks, huge gravity slides of the same or greater areal extent as the so-called Snake Range décollement may form as sector collapses of volcanic fields prior to basin and range deformation, as in the Pine Valley Mountains of southwestern Utah (Hacker, 1998; Hacker et al., 2002) and the Tushar Mountains/Markagunt Plateau of south-central Utah (Biek et al., 2014, 2015; Hacker et al., 2014). Most such denudation/attenuation faults and giant gravity slides fail along weak shale beds.

GEOPHYSICS

OVERVIEW

To interpret the subsurface of the study area, SNWA contracted with the USGS Geophysical Unit at Menlo Park, California, to collect and analyze geophysical data in the area. This was done in a series of cooperative agreements between SNWA and USGS between 2003 and 2010. The primary studies used gravity, aeromagnetic, ground magnetic, and audiomagnetotelluric (AMT) methods. Particular attention was given to a series of basins that covered an area of about 60,000 km² in eastern Nevada and western Utah. These data were combined with those previously obtained, mostly by the USGS, in adjacent ranges over an area of about 155,000 km² ([figure 12](#)). The analysis defined the overall shape and thickness of basins, identified buried faults that may be either barriers or conduits to groundwater flow, speculated on interbasin flow, helped characterize aquifers, and allowed us to better understand the overall geology. Discussions below will concentrate on both the larger region as well as selected areas for more detailed study.

GRAVITY, AEROMAGNETIC, AND GROUND MAGNETIC STUDIES

Collection of Data

Gravity Data

Gravity data for the region were obtained from Ponce (1997), Bankey et al. (1998), Scheirer (2005), Kucks et al. (2006), Mankinen et al. (2006, 2007, 2008), Scheirer and Andreasen (2008), and Mankinen and McKee (2007, 2009, 2011). These were supplemented with unpublished USGS data obtained from the Basin and Range Carbonate Aquifer Study (BARCAS) project (Sweetkind et al., 2007a and b; Watt and Ponce, 2007). All data were reduced using standard gravity corrections (Blakely, 1995) and were referenced to the International Gravity Standardization Net 1971

(ISGN 71) gravity datum (Morelli, 1974) to produce the complete Bouguer anomaly. A regional isostatic field was calculated using an Airy-Heiskanen (Heiskanen and Vening Meinesz, 1958) model for local compensation of topographic loads (Jachens and Roberts, 1981; Simpson et al., 1986). This model assumes a crustal thickness of 25 km, a crustal density of 2670 kg/m³, and a 400 kg/m³ density contrast between the crust and mantle. This regional isostatic field was subtracted from the Bouguer anomaly, thus removing long-wavelength variations in the gravity field that are inversely related to topography. The resulting isostatic residual gravity anomaly, therefore, is a reflection of local density distributions within middle to upper crustal levels.

Because gravity data for the study area were obtained by many different observers at different times, we examined the composite dataset to remove duplicate and inconsistent entries. To test for possible errors, we first compared reported station elevations with elevations interpolated from 10 and 30 m DEMs, using the procedure of D. Plouff (written commun., 2005). Large elevation differences indicate possible errors in station location or elevation, and each station identified was examined individually to determine the cause of the discrepancy. Some errors occurred because of imprecise locations (e.g., lack of significant digits in published reports) and could be corrected with a high degree of confidence. If the source of the discrepancy could not be determined and corrected, the station was omitted from the data set. The revised data set was gridded at a spacing of 0.5 km using a minimum curvature algorithm of Webring (1981), resulting in the isostatic gravity map shown in [figure 13](#). Anomalies reflect local density variations in the middle and upper crust. Gravity lows (cool colors) generally indicate sedimentary material within valleys; gravity highs (warm colors) generally reflect denser basement rocks in mountain ranges.

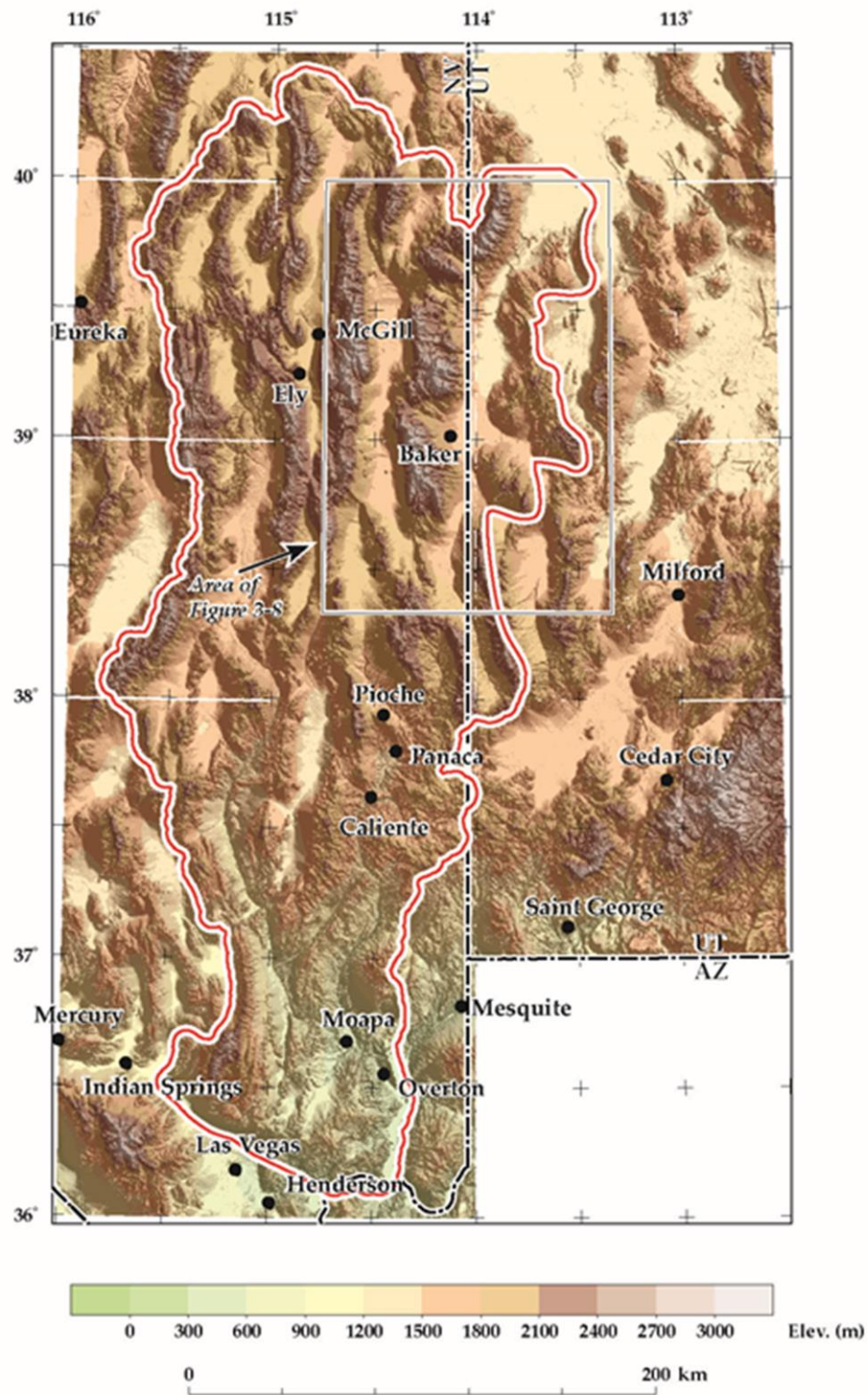


Figure 12. Shaded-relief map of eastern Nevada and western Utah. Red line bounds study area.

Aeromagnetic Data

Aeromagnetic surveys of the Great Basin were presented by Zietz et al. (1976, 1978), Mabey et al. (1978), Hildenbrand et al. (1983), Hildenbrand and Kucks (1988a and b), and Bankey et al. (1998). Flight-line spacing ranged between 3.2 and 1.6 km in Utah, and between 8 and 1.6 km over most of Nevada. Because aeromagnetic survey specifications are often widely disparate for a variety of reasons, a collaborative effort was undertaken by the Geological Survey of Canada, the Consejo de Recursos Minerales de Mexico, and the USGS to upgrade all available data from Canada, Mexico, and the United States. The data were reprocessed, gridded at a spacing of 1 km, converted from level to drape, and merged into a coherent representation of the data as if they had all been flown at a constant 305 m above terrain. Results are available as a digital magnetic anomaly database and map for North America (North American Magnetic Anomaly Group [NAMAG], 2002). Aeromagnetic data shown in [figure 14](#) were extracted from this map and re-gridded to a 0.5 km spacing. A recent compilation of aeromagnetic data for Nevada also is available from Kucks et al. (2006).

Ground Magnetic Data

Ground magnetic data were obtained from selected traverses using a portable cesium-vapor magnetometer integrated with a differential GPS receiver. The GPS receiver has an accuracy of less than 1 m horizontally and 1–2 m vertically. The magnetometer was mounted on a non-magnetic aluminum frame and towed behind a vehicle at speeds of as much as 60 km/hr. (Tilden et al., 2006). Measurements were taken at one-second intervals while operating the instrument in continuous mode. A stationary base-station magnetometer to record diurnal variations was not employed because of the short duration of the traverses.

Processing of Data

Geophysical data can be enhanced in a number of ways to better characterize causative sources of their anomalies (e.g., Blakely, 1995). Derivative gravity and magnetic maps used here are intended to de-emphasize surface and near-surface features. The deep-seated crustal structures thus identified reveal major tectonic domains that form the structural underpinnings of the region. Boundaries between these crustal blocks may represent zones of weakness that could later influence the emplacement of intrusions or potentially localized mineral deposits, regional groundwater flow, hydrothermal activity, and young tectonic activity.

Upward Continuation

The gravity anomalies shown in [figure 13](#) were analytically upward-continued by 3 km (Hildenbrand, 1983) to de-emphasize surface and near-surface features and to enhance the contribution from deeper sources, resulting in [figure 15](#). This figure also shows "maxspots," which are discussed below in Horizontal Gradients.

Magnetic Potential

The aeromagnetic data of the study area were analyzed by transforming them to their magnetic potential (the "pseudogravity" transform of Baranov, 1957; Blakely, 1995), shown in [figure 16](#). This procedure generally helps to isolate broad magnetic features that may be masked by high-amplitude shallow magnetic sources, reduces anomaly asymmetry, and roughly centers the anomalies over their sources. Because the pseudogravity transform converts a magnetic anomaly into one that would be observed if the magnetic distribution of the body were replaced by an identical density distribution, interpretation of their sources is simplified by allowing the use of gravity techniques, as described below.

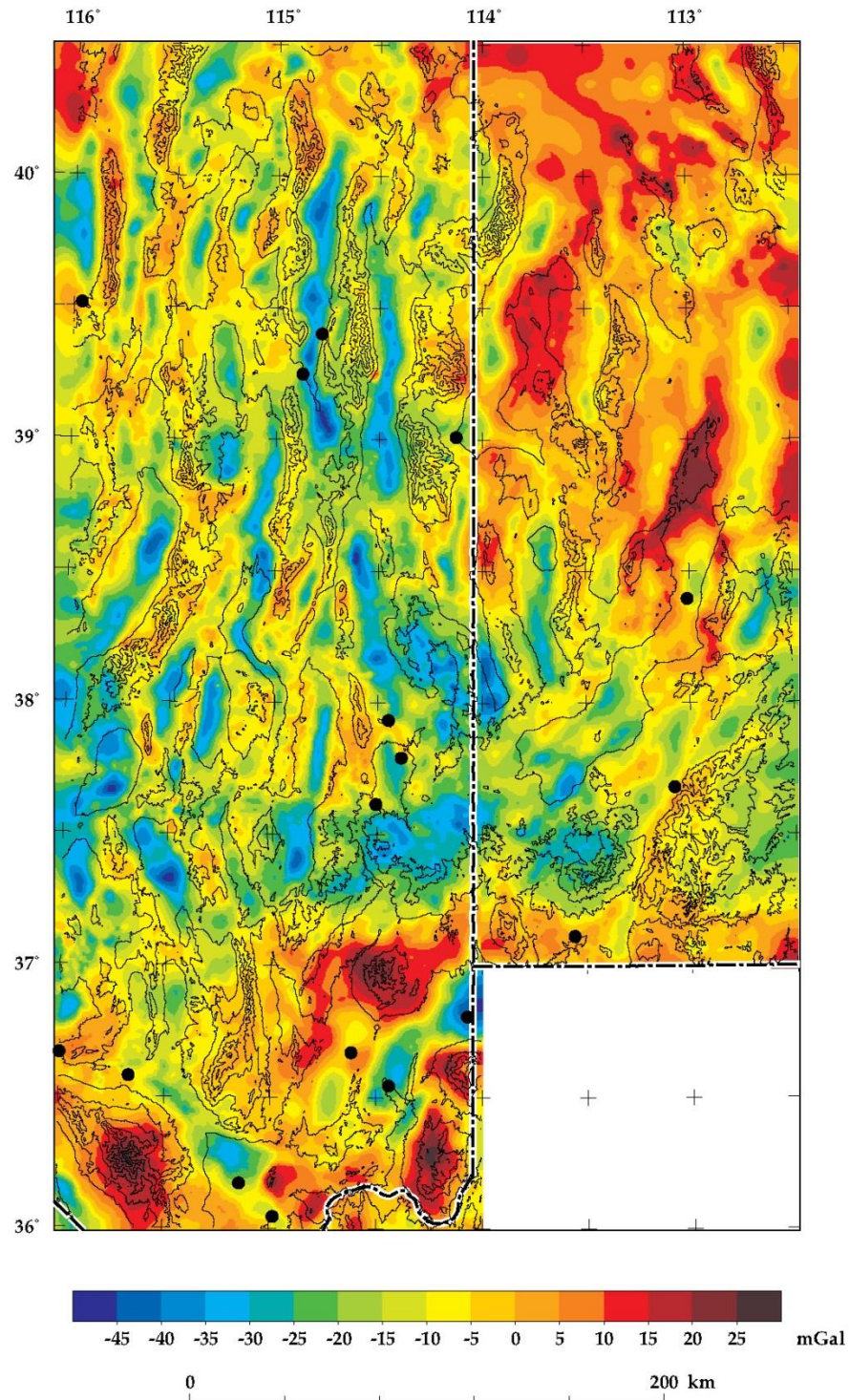


Figure 13. Isostatic-gravity field in eastern Nevada and western Utah. Black dots are towns. Topographic contour interval is 400 m.

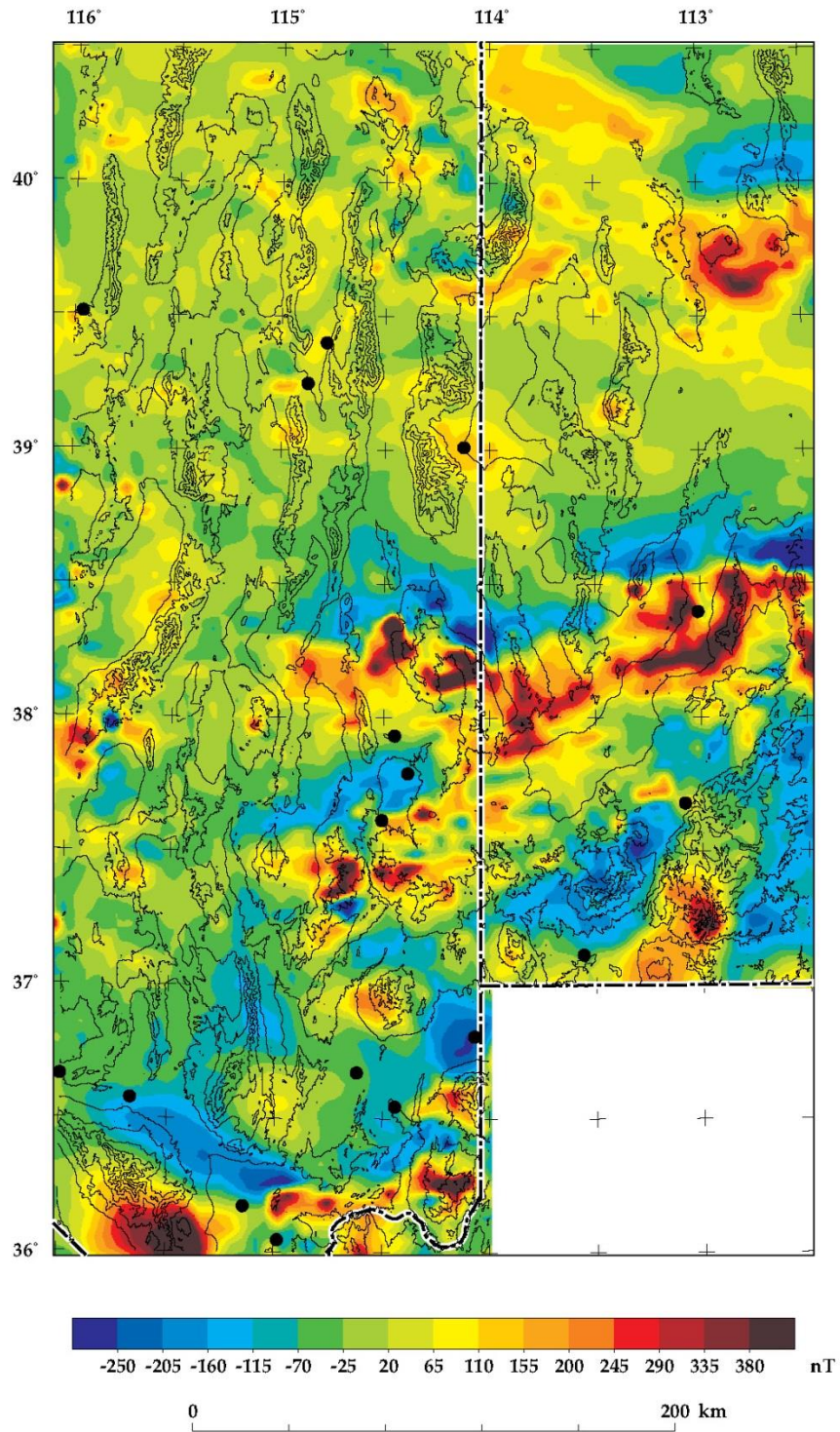


Figure 14. Aeromagnetic map of eastern Nevada and western Utah. Black dots are towns. Topographic contour interval is 400 m.

Horizontal Gradients

Horizontal gradients can be calculated for the long-wavelength gravity anomalies identified by the upward-continued data (e.g., Cordell, 1979; Blakely, 1995) and by the magnetic potential (Cordell and Grauch, 1985). When calculated for two-dimensional data grids, horizontal gradients will place narrow ridges over significant contrasts in gravity ([figure 15](#)) and magnetic potential ([figure 16](#)). The method of Blakely and Simpson (1986) was used to calculate the maximum values of these horizontal gradients of the upward-continued data or "maxspots," the locations of which tend to overlie the edges of causative bodies with abrupt, near-vertical contacts. These maxima identify contrasts that can help delineate deep-seated crustal structures, primarily faults that separate major tectonic domains. Figures 15 and 16 show the results of upward continuation, with calculation of maxima (small dots or maxspots) that in most places shown are faults but in some places could be caldera margins or intrusive contacts. For non-vertical contacts between geologic units of contrasting properties, maximum values of the horizontal gradients will be displaced down-dip and away from the edges of the body.

Gravity Inversion

The isostatic gravity field ([figure 13](#)) generally reflects a pronounced contrast between dense pre-Cenozoic rocks and significantly less dense overlying volcanic and sedimentary rocks. Because of this relationship, the gravity inversion method derived by Jachens and Moring (1990) can be used to separate the isostatic residual anomaly into pre-Cenozoic basement and young basin fill, and thereby provide an estimate of the thickness of Cenozoic volcanic rocks and sedimentary basin fill. Subvolcanic Cenozoic intrusions are included here as part of the basement because their physical properties are similar to most of the older rocks and differ greatly from those of the volcanic and basin-fill sequences. The method first separates gravity observations on pre-Cenozoic

rocks from those on Cenozoic deposits. A modified version of the method (B.A. Chuchel, USGS, unpublished data, 2005) allows basement gravity values to be approximated by correcting the isostatic gravity anomaly at sites where depth to basement is known from deep boreholes or inferred from seismic data (e.g., Gans et al., 1985). At locations where wells did not penetrate the full thickness of the basin-fill, the maximum depths reached were used as minimum constraints in an iterative process. Constraints on the inversion process, shown in [figure 17](#), are gravity measurements on pre-Cenozoic rocks and available well data. Information on oil and gas wells for Nevada and Utah is available at Hess (2004) and <http://ogm.utah.gov/oilgas/>, respectively. Additional data were obtained from Utah geothermal wells (Hintze and Davis, 2003), selected USGS test wells (Berger et al., 1987; Schaefer et al., 1989), test-well data from the MX-missile siting study in Utah (Mason et al., 1985), and SNWA test wells.

The accuracy of thickness estimates derived by the gravity inversion technique depends on the assumed density-depth relation of the Cenozoic volcanic and sedimentary rocks and on the initial density assigned to the basement rocks. Density of basement rocks is assumed to be 2670 kg/m^3 , and density-depth values are from Jachens and Moring (1990). These values have been shown to be widely applicable throughout the Great Basin (Saltus and Jachens, 1995; Blakely et al., 1998, 2000; Mankinen et al., 2003). Isostatic gravity ([figure 13](#)) and the digital geology of Nevada and Utah were converted to a 2-km grid before performing the inversion. Results were then re-gridded at a spacing of 0.5 km. The result, as given in [figure 18](#), is the depth to pre-Cenozoic basement. Deepest blue colors denote all depths greater than 3 km. The basin-thickness estimates calculated by Hurlow (2014) from gravity are somewhat greater than the more conservative estimates given here, because of slightly different assumptions.

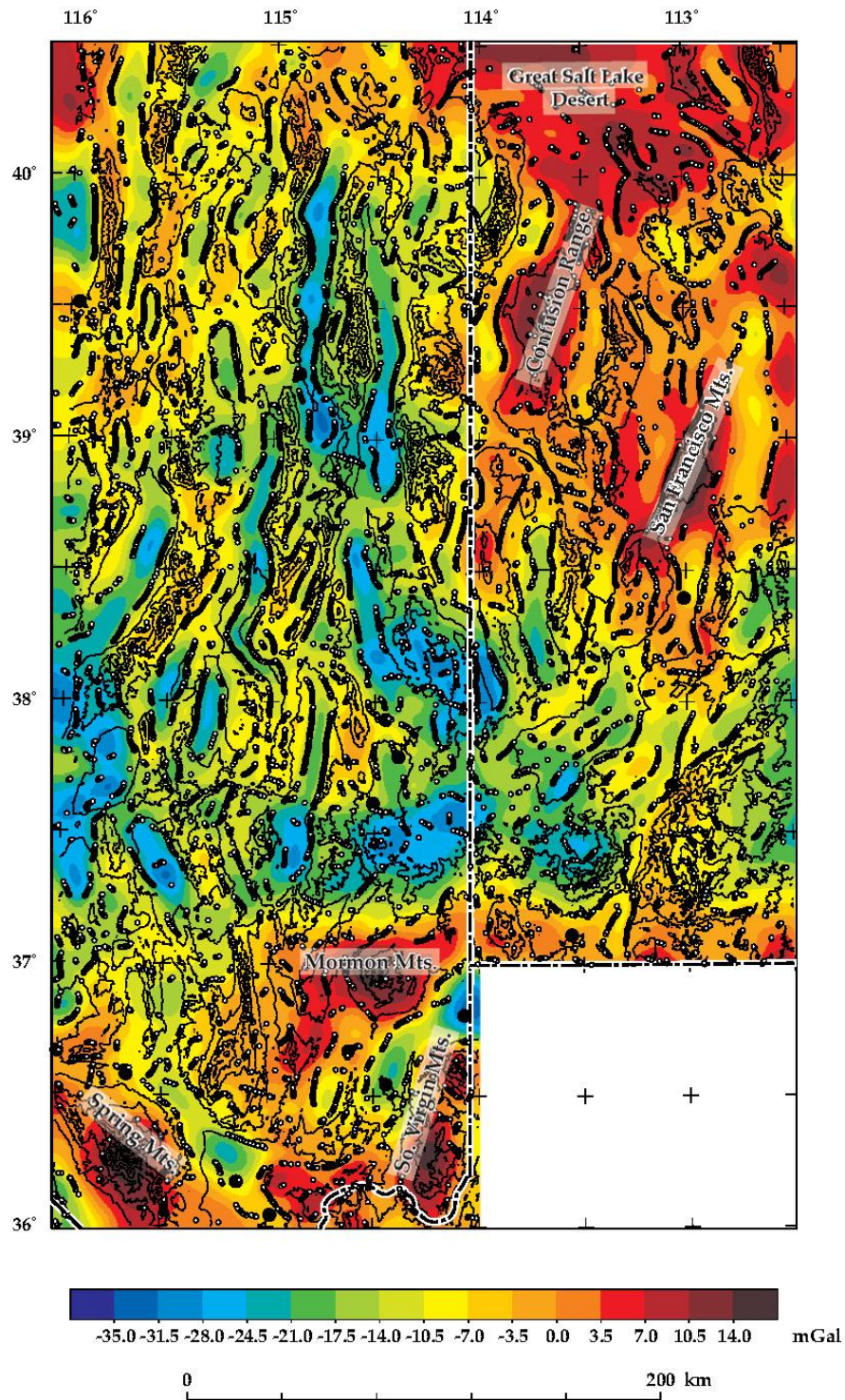


Figure 15. Isostatic gravity anomalies upward-continued by 3 km. Small dots are maxima in the horizontal gradient.

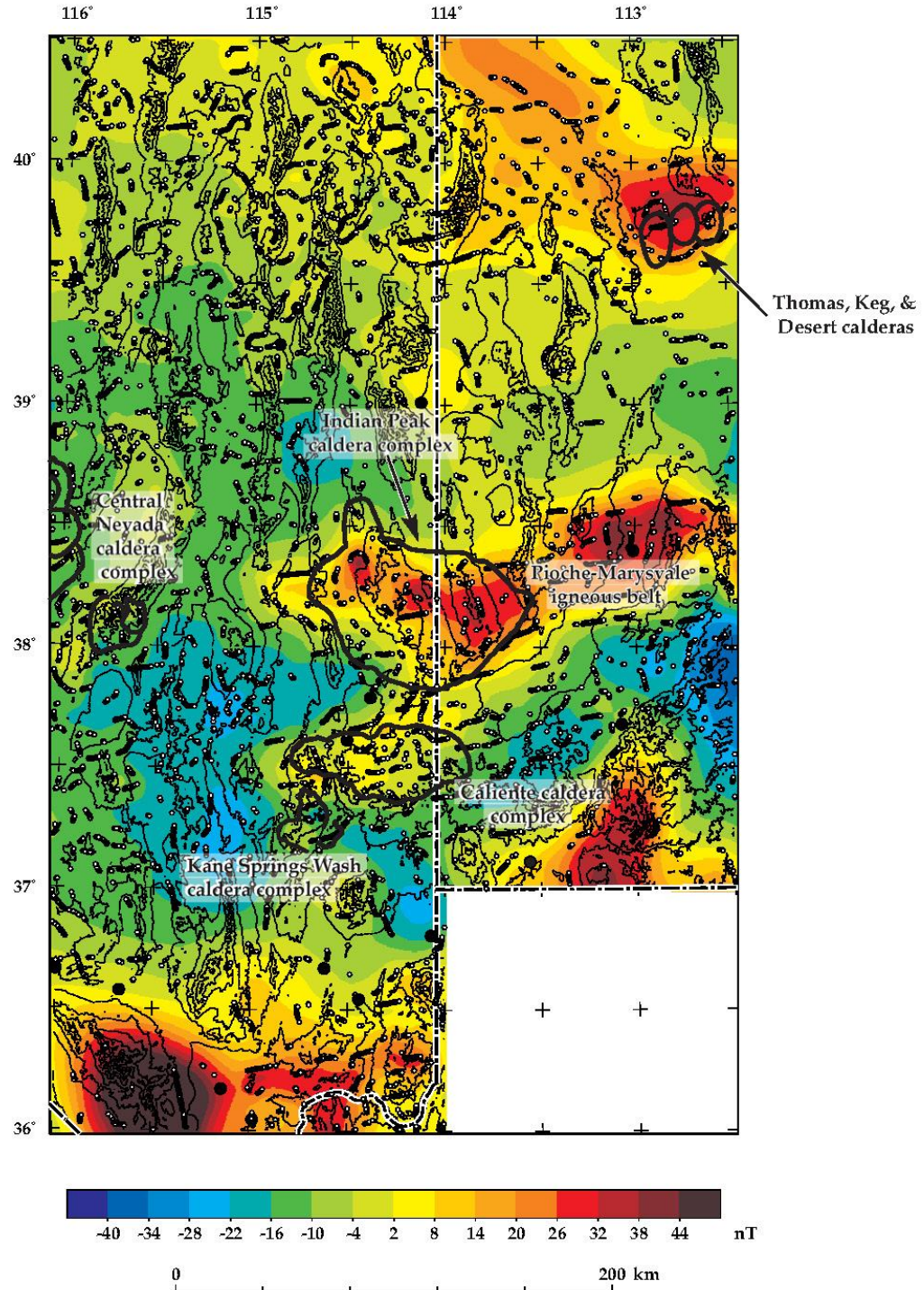


Figure 16. Aeromagnetic data transformed to their magnetic potential (“pseudogravity”). Small dots are maxima in the horizontal gradient. Heavy lines are calderas.

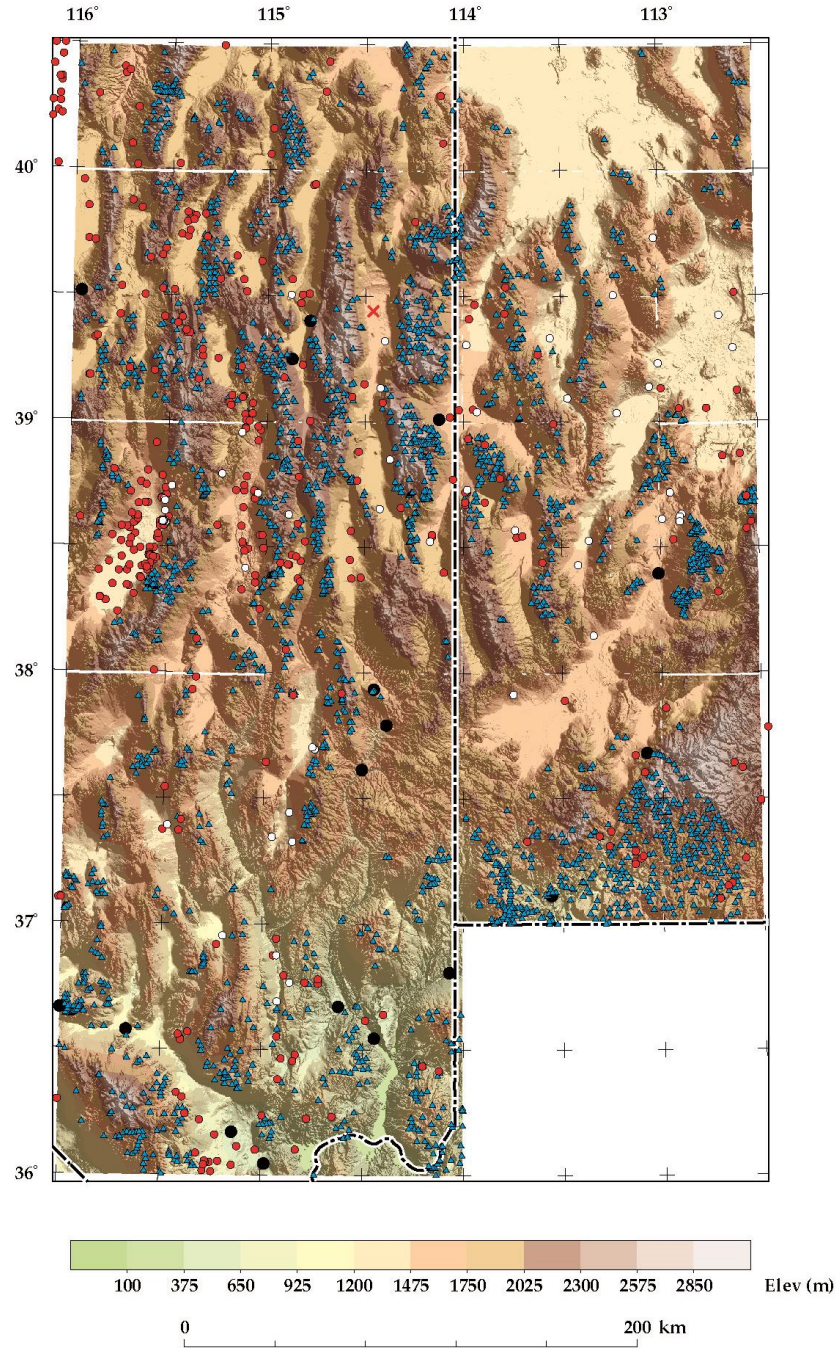


Figure 17. Constraints for the gravity inversion method. Red dots are wells spudded into or reaching pre-Cenozoic basement; white dots are wells providing minimum depth constraints; triangles are gravity observations on pre-Cenozoic basement rocks; red “x” is a pre-Cenozoic basement pick from a seismic survey (Gans et al., 1985).

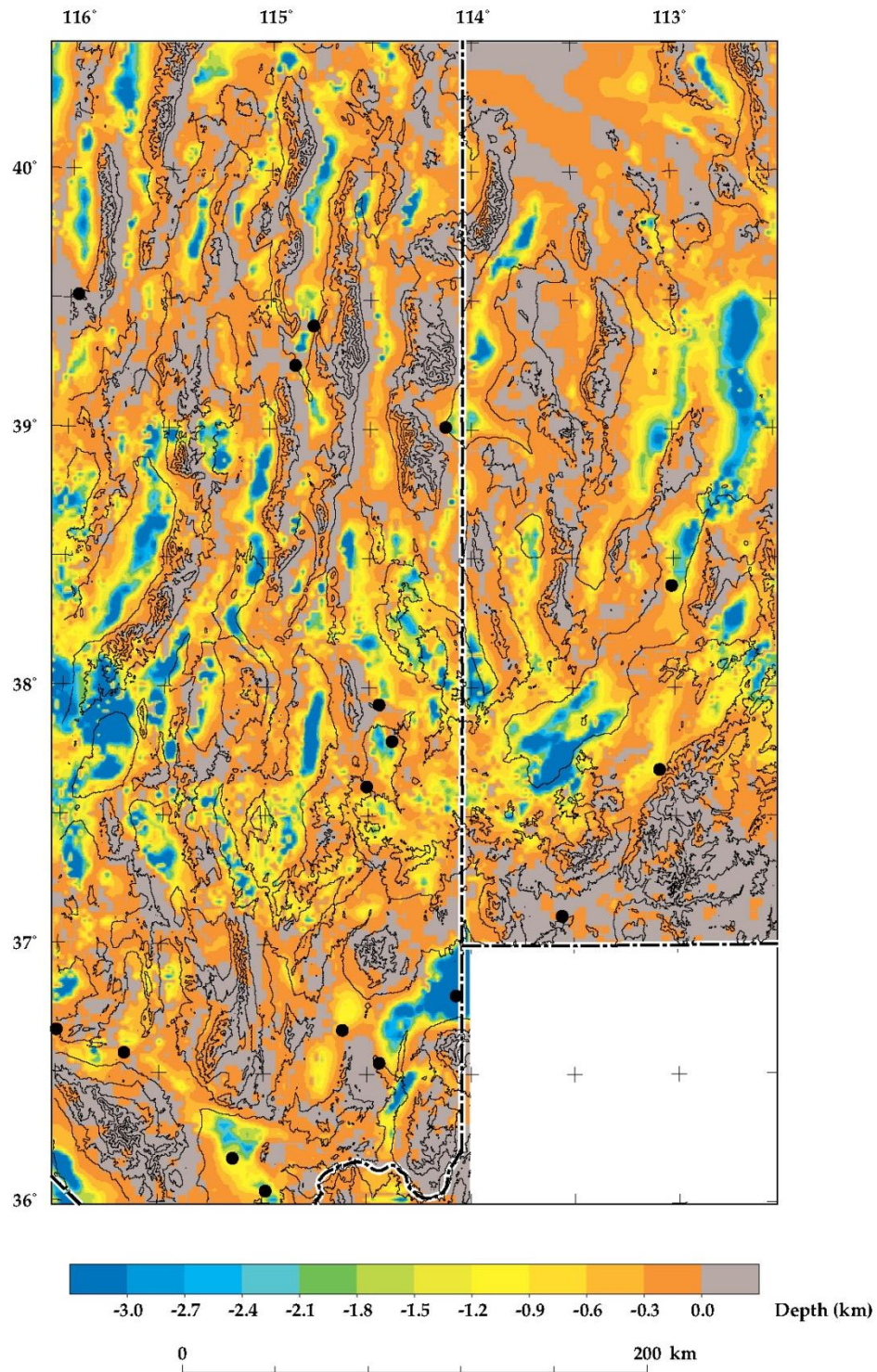


Figure 18. Depth to pre-Cenozoic basement in eastern Nevada and western Utah.

Interpretation

Regional Geophysics

Figures 13 through 18 provide geophysical data for the area shown in [figure 12](#). The following section discusses geophysical observations, and interpretations, from across this region. [Figure 13](#) displays the pronounced contrast between dense pre-Cenozoic rocks and significantly less dense overlying strata. Most gravity geophysicists refer to pre-Cenozoic rocks as "basement," even though that is not to mean that they are Precambrian. The Cenozoic rocks above such "basement" consist of calc-alkaline and high-silica rhyolite (bimodal) volcanic rocks and overlying basin-fill and surficial sedimentary rocks and sediments. In most cases, volcanic rocks and these sedimentary rocks cannot be distinguished by gravity data. However, Cenozoic basaltic rocks are dense and have the same higher anomalies as pre-Cenozoic rocks, but basalts are rare or thin in the general area except along the eastern edge of [figure 13](#) south of 40°N, in the Sevier and Black Rock deserts. The pre-Cenozoic rocks underlie most ranges, which therefore are shown in shades of red, orange, and yellow (warm colors), whereas Cenozoic volcanic rocks and basin-fill sedimentary rocks most commonly underlie the valleys and basins, which are shown in blue and green (cool colors). [Figure 13](#) has an obvious north-south linear pattern, reflecting Basin and Range deformation that produced alternating basins (grabens) and ranges (horsts). Deep basins, in dark blue, are particularly noticeable as Steptoe Valley, containing McGill and Ely ([figure 12](#)), and Spring Valley to the east. In some places, however, the Cenozoic volcanic rocks make up volcanic fields that are commonly exposed in the ranges or in calderas that typically span north-south basins and ranges. Examples of calderas (subcircular and blue) that show up particularly well are the Indian Peak caldera complex north and east of Pioche, and the Caliente caldera complex south and southeast of Caliente ([figure 12](#)). East of the Caliente caldera complex in Utah, another subcircular area in blue and green consists of calc-alkaline volcanic rocks and laccoliths exposed in the Bull Valley Mountains and Pine Valley Mountains.

There is a marked contrast in the magnitude of gravity anomalies between eastern Nevada and western Utah. This is especially true in the northern half of the area of [figure 13](#), where ranges and even most parts of the Great Salt Lake Desert show up as strong positive anomalies, in red. These anomalies include the large red anomaly northeast of Baker ([figure 12](#)) that underlies the Confusion and Conger ranges, narrow parts that extend northward and northeastward of these ranges that underlie the Fish Springs, Thomas, and Dugway ranges, and narrow parts that extend from them southeast of Baker that underlie the Burbank Hills and Mountain Home Range. Most of these positive anomalies are caused by carbonate rocks, especially dolomite with a density of 2.8 g/cm³, which constitutes about 80 percent of the Middle Cambrian through Permian stratigraphic sequence in these areas (Mankinen et al., 2016). Ranges with Pennsylvanian to Permian outcrops have a greater thickness of carbonate rocks than those that have only the lower part (e.g., Silurian, Ordovician, and Cambrian) of the carbonate rock sequence at the surface. We would therefore expect that ranges that have the most complete, and hence thickest, section of carbonate strata would produce the highest gravity anomalies. This interpretation is supported by the observations in figures 13 and 15, where gravity anomalies are much stronger over the Confusion Range (~7 km of carbonate rock) than over the northern House Range (~3.5 km of carbonate rock) to the east and the southern Snake Range (southeast of Baker) to the west. About a 1 to 2 km thick sequence of quartzose rocks (densities about 2.6 g/cm³) of the Neoproterozoic to Lower Cambrian McCoy Creek Group and Prospect Mountain Quartzite underlies much of the carbonate rock. The northern and central Snake Range, as well as the Kern Mountains and southern Deep Creek Range farther north, are cored by this quartzite and intruded by granite plutons, so here the anomalies are of much smaller amplitude (yellow).

The ranges north of Milford, Utah ([figure 12](#), shown in bright red on [figure 13](#)) represents the San Francisco and Cricket mountains, to the south and north respectively. The San Francisco Mountains are underlain by Tertiary volcanic rocks and Neoproterozoic quartzite, whereas the Cricket

Mountains are underlain by ~2 km of Cambrian carbonate rocks. These rocks in both ranges, however, are interpreted to be underlain by large frontal Sevier thrusts that likely contain repeated sections of Paleozoic carbonates (DeCelles and Coogan, 2006), resulting in significant positive anomalies. Similar explanations are applied in the southwestern part of [figure 13](#), where strong positive anomalies underlie the Mormon Mountains, the Meadow Valley Mountains and Arrow Canyon Range (west of Moapa, red finger on [figure 13](#)), and the Spring Mountains (far to the southwest). Here, the exposed rocks are middle and upper Paleozoic, but these areas are underlain by the large frontal Sevier thrusts of the Las Vegas area (Page et al., 2005a). The two red bullseyes south of Mesquite and southeast of Overton, however, are interpreted to be due to denser high-grade metamorphic Paleoproterozoic rocks (Page et al., 2005b; Beard et al., 2007).

The aeromagnetic map ([figure 14](#)) shows areas of high magnetization with warm colors and areas of low magnetization with cool colors. Unlike the gravity map ([figure 13](#)), a lack of north-south texture indicates that the main causes of magnetic anomalies are unrelated to the episode of Basin and Range deformation. Instead, most high (red) anomalies are due to calc-alkaline and lesser bimodal intrusions, most of which are arranged in three east- to east-northeast-trending igneous belts that span all or parts of the study area. These belts represent the main eruptive centers in the area. High magnetic anomalies in the southern part of the area (mostly southern Nevada), however, appear to be caused by Paleoproterozoic high-grade metamorphic or igneous rocks (Page et al., 2005b; Langenheim et al., 2010). Anderson (1981) and Anderson and Barnhard (1993) formerly called this same southern area an "amagmatic corridor" because of its lack of Cenozoic igneous rocks.

The three igneous belts become younger from north to south (Stewart et al., 1977; Christiansen and Yeats, 1992; Rowley, 1998; Rowley and Dixon, 2001), and in the southern Basin and Range, igneous belts are younger from south to north (Anderson, 1989; Humphreys, 2009). The igneous belts, from north to south, are the (1) Ely-Tintic igneous belt (39° to 40° N latitude) that extends at

least as far west as Ely; (2) Pioche-Marysville igneous belt that extends 100 km into Nevada (mostly south of 38° 30' N at the eastern end but both north and south of 38° N at the western end); and (3) the Delamar-Iron Springs igneous belt that also extends well into Nevada (north and south of 38° N at the eastern end but north of 37° N at the western end) (Rowley, 1998; Rowley and Dixon, 2001). The Ely-Tintic belt is less pronounced than the Pioche-Marysville belt probably because it is older and more eroded. The Delamar-Iron Springs belt is less pronounced than the Pioche-Marysville belt probably because many of the source plutons are high-silica granite (bimodal). The margins of some of these igneous belts are bounded by transverse zones that were active both during and subsequent to the calc-alkaline magmatism (Rowley, 1998; Rowley and Dixon, 2001). Between these belts, cool colors show basins with the same trend that contain the eruptive and sedimentary products of these centers. One such area, in the southwestern part of [figure 14](#) north of Las Vegas, trends west-northwest; it is a basin controlled by the Las Vegas Valley shear zone, which is a transfer fault created by oblique-slip (right-lateral and normal) motion during Basin and Range deformation.

[Figure 15](#) presents upward-continued gravity data, which provide emphasis on deeper causes of the anomalies. When compared with the anomalies of [figure 13](#), the positive anomalies are larger. This supports the interpretation that most range-front fault contacts between the carbonate rocks that probably cause the anomalies and the basin fill on either side must be dipping toward the basin. The lines of maxspots that are the most continuous are ones where confidence is greatest that these are maxima. The locations of the maxspots suggest that most of these contacts are faults. For example, the maxspots on both sides of Steptoe and Spring Valleys agree with reconnaissance mapping of these valleys that faults bound the valley margins. Therefore, we infer that the maxspots define grabens. Similarly, the maxspots along the western side of the Confusion Range support our conclusion that this is a good fault zone that separates the range from eastern Snake Valley, although some workers have argued

otherwise. We are also confident that the western side of Snake Valley is a large fault zone, yet here the maxspots are not as continuous, probably because the gravity contrast across the fault is not as large as that on the eastern side of Snake Valley.

[Figure 16](#) shows aeromagnetic data that have been transformed to pseudogravity in order to emphasize sources of magnetism, after which maxspots were drawn. In comparison with [figure 14](#), the anomalies are broader and more diffuse, probably reflecting more accurately the intrusive sources of many of the anomalies, some of which are batholiths. Many of the maxspots may reflect intrusive contacts. As in [figure 14](#), three main areas dominate the magnetic potential of the region. In the northeast part of the overall area, ash-flow tuffs and intrusions are associated with the Thomas, Keg, and Desert calderas (Shawe, 1972) in the Ely-Tintic igneous belt. The central area contains the ash-flow tuffs and intrusive rocks of the Indian Peak caldera complex (Best et al., 1989a). This complex makes up the western part of the east-trending Pioche-Marysville igneous belt (Rowley, 1998; Rowley and Dixon, 2001), which continues eastward to the Marysville volcanic field (Steven et al., 1984, 1990). The southern area contains thick intracaldera ash-flow tuffs of the Caliente and Kane Springs Wash caldera complexes (Rowley et al., 1995; Scott et al., 1995a), which are the western part of the east-trending Delamar-Iron Springs igneous belt.

For purposes of hydrology, an important type of geophysical data is the calculation of gravity inversion. This allows determinations of thickness of Cenozoic volcanic and sedimentary rocks above the geophysical "basement." [Figure 17](#) gives the constraints used for this calculation. In general, in areas where there is good basement depth control from outcrops and drill holes that encountered pre-Cenozoic rocks, the inversion uncertainties are approximately 300 m (e.g., Jachens and Moring, 1990; Hildenbrand et al., 2006). [Figure 18](#) presents the map of the results, from which depth to basement data were used directly to draw our cross sections. This determination is especially useful in estimating thickness of basin-fill deposits within structural basins, which are the primary aquifers in the area. Volcanic rocks, whose densities are similar to sedimentary basin-fill deposits, cannot be

distinguished from the sedimentary rocks. Unlike the sedimentary deposits, which were deposited during or after structural development of the basins, most of the volcanic rocks predate the development of basins related to regional extension, so they are commonly exposed in the adjacent ranges. Therefore, this exposed volcanic thickness can be subtracted from the depth-to-basement thickness to determine the sedimentary basin-fill component.

[Figure 18](#) shows that most of the major valleys have basin-fill (including the volcanic rocks) ranging from 1 to 3 km thick. Deeper (thicker) areas extend to about 6 km in Cave Valley (see also Scheirer, 2005) south-southwest of Ely, to 7 km beneath the Sevier Desert near the eastern edge of the [figure 18](#), and to 7 km beneath Railroad Valley and Sand Spring Valley near the western edge of the figure, where several of the central Nevada calderas contribute to the thickness. The deepest basins are beneath the Escalante Desert (i.e., a depth of 9 km) west of Cedar City and the Virgin River depression/Mesquite basin (i.e., a depth of 8 km). Part of the Virgin River depression in Arizona may be as deep as 10 km (Langenheim et al., 2000).

Geophysics of Spring and Snake Valleys

The Spring and Snake valley areas ([figure 19](#)) were investigated in greater detail to better understand the aquifers as well as their interconnection, recharge, and groundwater flow. [Figure 20](#) presents their isostatic gravity and aeromagnetic anomalies, with maxspots (small dots) added for each so as to utilize fully the horizontal gradients of the data. Solid lines in the figure are interpreted as major gravity and magnetic lineaments, whereas light blue lines are locations of ground-magnetic traverses. Maxspots are calculated for only vertical or nearly vertical density or magnetic contrasts, so low-angle faults, including thrusts, that have been suggested for the area will not be visible by this method. Some parts of the analysis were given by Mankinen et al. (2006 and 2007), Mankinen and McKee (2009), and Rowley et al. (2009) for not only the area of [figure 19](#) but also areas in Utah farther east and south.

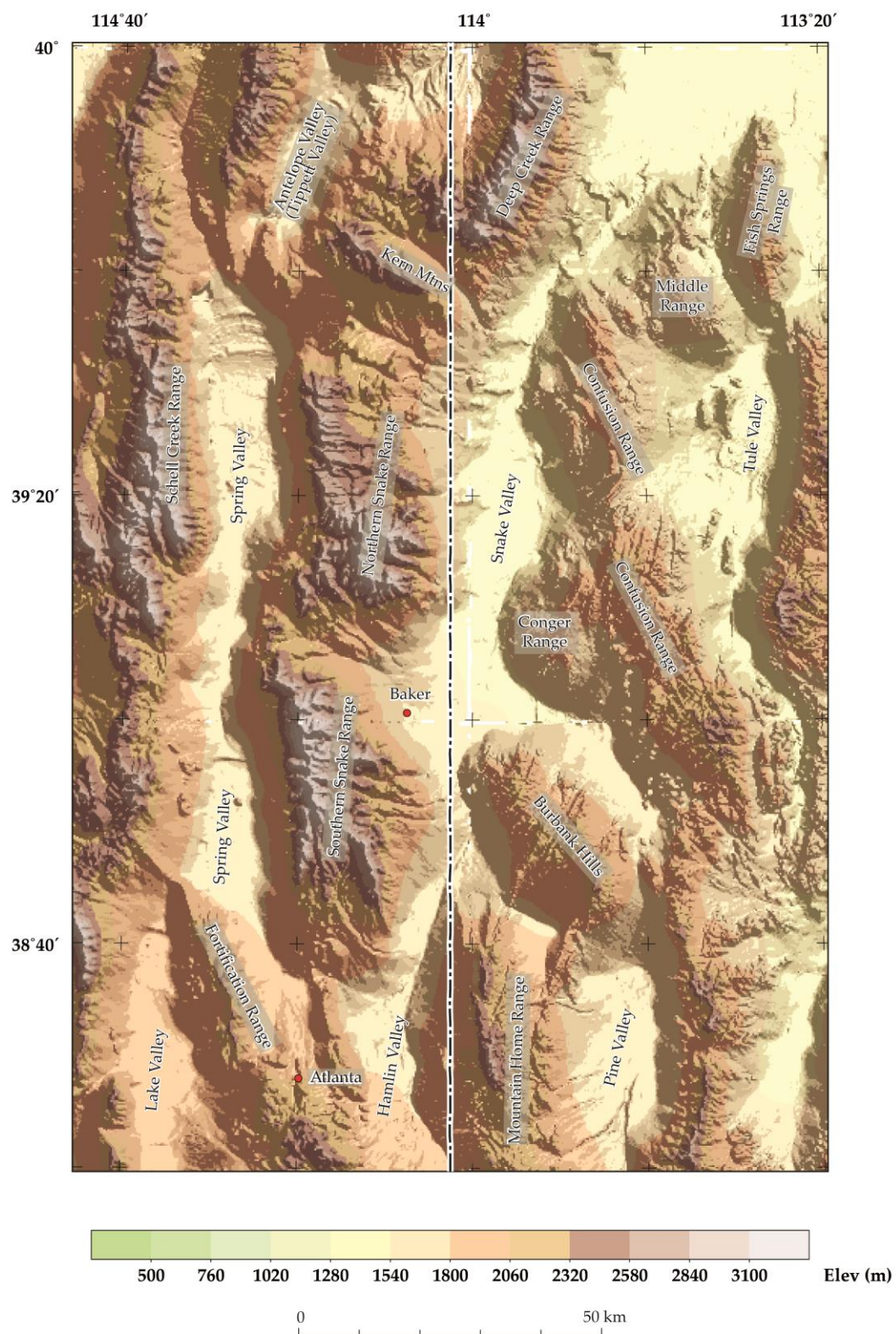


Figure 19. Shaded relief map of the Spring and Snake valley region.

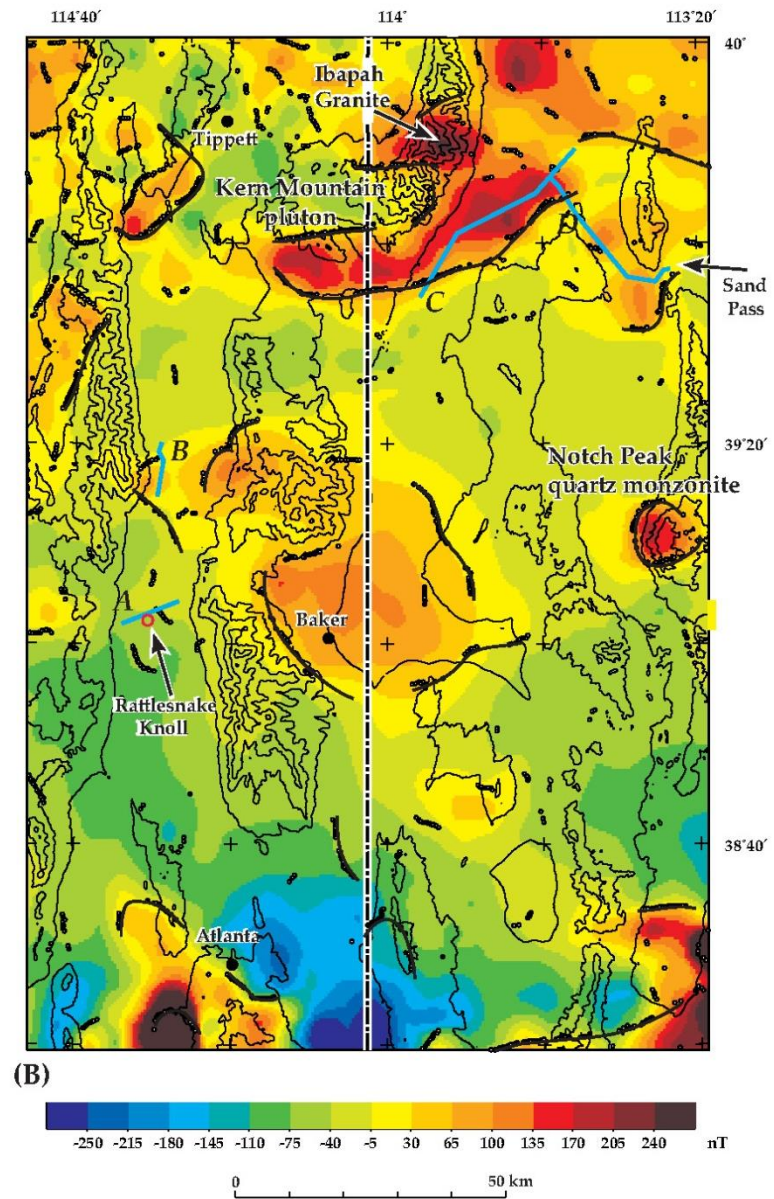
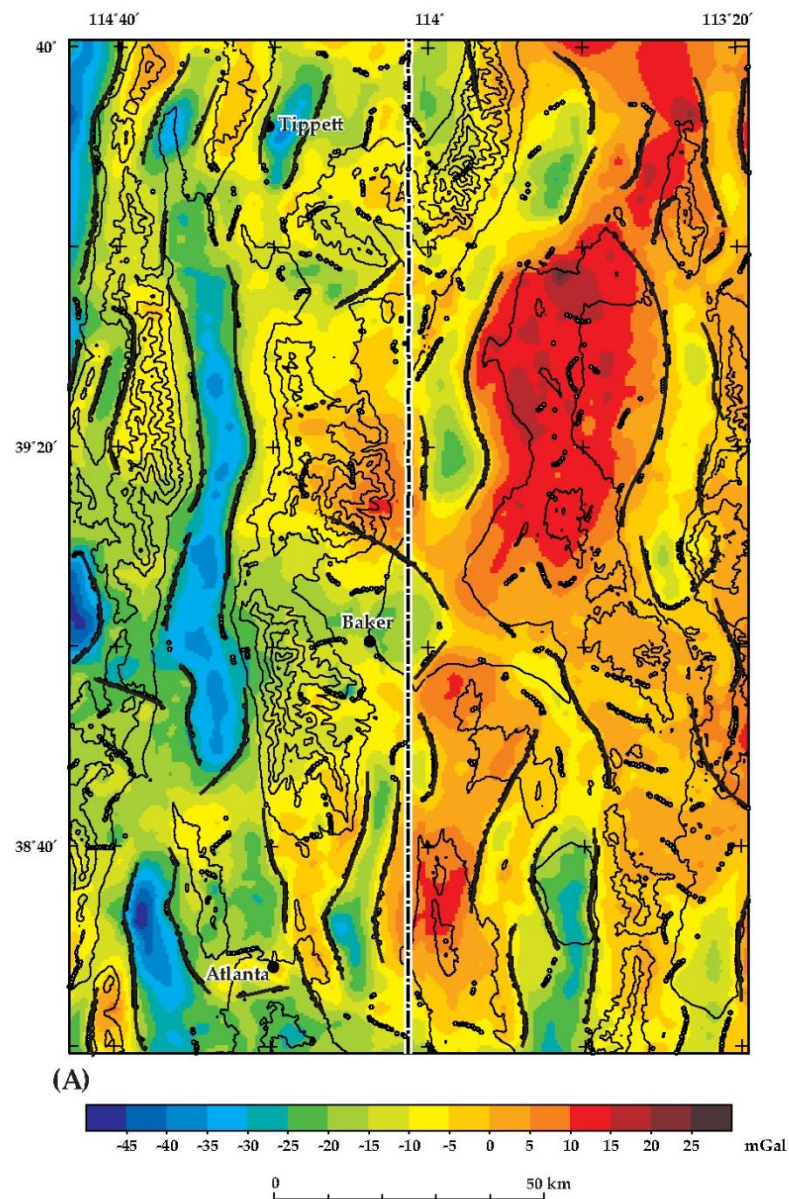


Figure 20. Isostatic gravity (A) and reduced-to-pole aeromagnetic (B) anomalies in the Spring and Snake valley area.

[Figure 20a](#) provides isostatic gravity data that delineate alternating basins and ranges by their different densities. The deepest basins ([figure 18](#)) are Spring Valley, northern Lake Valley, and—at the western edge of the figure—Steptoe Valley. Although the Snake and Hamlin valleys appear continuous and uninterrupted on the ground, Hamlin Valley is of lesser depth. Tule Valley, which separates the Confusion Range from the House Range to the east, is shallow, generally less than 1 km. All basins have deeper interior parts, or holes, reflecting local areas of deeper subsidence, largely due to concealed interior grabens.

Specifics on basin depth in Spring Valley comes from depth-to-pre-Cenozoic-basement analyses reported by Mankinen et al. (2006 and 2007) that were more detailed than given in [figure 18](#). They showed that the volcanic rocks and basin-fill sediments in Spring Valley have a maximum thickness of almost 4 km in the northern part (west of the Antelope Range) but elsewhere are generally 1.5 to 2 km thick, and locally 3 km thick. Two geophysical sub-basins in Spring Valley are separated by an intra-valley bedrock ridge that is entirely buried to a depth of about 0.4 km by basin-fill alluvium, extending between the northern Fortification Range and the southwestern Snake Range. The southern sub-basin, west of the Limestone Hills, has a maximum depth of 1.6 km. Tippet Valley, east of the Antelope Range, has a general depth of more than 3 km but locally is 5 to 5.5 km depth. Steptoe and Hamlin valleys have a maximum depth of 3 to 3.5 km except that Steptoe Valley gets to about 4 km at its northern end. The deepest part of Snake Valley is at a depth of about 4 km, but the rest of the valley is considerably less.

South of the area of [figure 19](#), detailed depth-to-pre-Cenozoic-basement analyses of the Cave, Dry Lake, and Delamar valleys were summarized by Mankinen et al. (2008). They found that southern Cave Valley extends down to 3 to 5 km, northern Dry Lake Valley has a maximum depth of 2 km, southern Dry Lake Valley has a maximum depth of 3 to 5 km and perhaps locally to 6.5 km, and southern Delamar Valley has a maximum depth of 2 to 3 km ([figure 18, plate 1](#)). Still farther south, Coyote Spring Valley northwest of Moapa was

studied by Phelps et al. (2000), who found two deeper parts of the basin, at about 1 km deep each, just west of the Meadow Valley Mountains and north and northeast of the Arrow Canyon Range (Dixon et al., 2007a; [figure 18, plate 2](#)).

Most maxspots in [figure 20a](#) represent high-angle normal faults that have been verified by geologic mapping or are concealed and inferred by mapping. The faults shown by maxspots should be considered but a small expression of the faults in the area, for many faults juxtapose rocks of similar densities so would not be shown. The maxspots demonstrate, as also indicated by mapping, that most basins are grabens and most ranges are horsts. In the center of [figure 20a](#), maxspots show a northwest-striking fault that crosses the state border. This is the Sacramento Pass fault, which cuts across the Snake Range closely following the highway. This fault, which is mapped on [plate 1](#), has Pleistocene or younger displacement at its southeastern end. The maxspots do not continue northwest all the way to Spring Valley, but the gravity anomaly continues farther northwest, and northeast-trending audiomagnetotelluric (AMT) profile SNV13 farther northwest images that fault (see [AMT Profile SVN13](#)).

Greene and Herring (2013) and Greene (2014) proposed that the Confusion Range is part of an east-vergent Sevier fold-thrust system with about 10 km of horizontal shortening. They acknowledged that this area is part of the hinterland of the Sevier and Black Rock frontal thrust systems, which accommodated a minimum of ~220 km shortening (DeCelles and Coogan, 2006). Yet the interpretation of Greene and Herring (2013) and Greene (2014) suggests much greater thrust deformation than previously proposed (e.g., Hintze and Davis, 2002a and b, 2003) and is not supported by any drilling or seismic work. In other words, their new thrusts are not exposed and are hypothesized to be at great depth in the subsurface. If valid, their proposal would entail significant thickening of the stratigraphic sequence. The gravity data of [figure 20a](#) are unable to support such thickening. The gravity anomalies given in figures 13 and 20a can be accounted for by the geology as previously mapped and interpreted, and they argue against the

deep thrusts proposed by Greene and Herring (2013) and Greene (2014).

Aeromagnetic data from the Spring and Snake valley region were extracted from [figure 14](#), reduced to the magnetic pole, and shown as [figure 20b](#). The reduced-to-pole technique eliminates asymmetry of most anomalies and shifts their positions laterally so that they are more nearly centered over the bodies that cause them. Although one of the largest plutons in the region forms the core of the Kern Mountains, it is expressed by a weak magnetic anomaly (green). The main part of this composite pluton (the two-mica Tungstonia Granite of Best et al., 1974) is atypical of Great Basin plutons in that it has a weak magnetic signature and apparently lacks a coherent remanent magnetization (Hudson and Geissman, 1982). More clearly expressed (yellow and red) is an east-trending belt of volcanic rocks and intrusions that extend from the southern edge of the Kern Mountains into Snake Valley. Hagstrum and Gans (1989) described one of these intrusions as a Tertiary hornblende dacite pluton, containing significant Fe-Ti oxides and thus presumably more typical of Great Basin plutons. Other small plutons, mapped as Tertiary or Cretaceous in the northernmost Snake Range could be larger at depth. These plutons could also have caused the red east-trending anomaly that continues into Snake Valley, beneath basin-fill sediments. Maxspots on the northern and southern sides of the red anomaly may be intrusive contacts. The Ibapah granite (Miller et al., 1999a) of the southern Deep Creek Range clearly has a magnetic signature (red) that is typical of Great Basin plutons and also resembles the anomalies beneath Snake Valley basin fill, suggesting that the Snake Valley anomalies are down faulted Ibapah granite.

Other plutons are apparent in [figure 20b](#). The sharp positive anomaly beneath the Notch Peak quartz monzonite (Hintze and Davis, 2003) is obvious in the southern House Range, and its maxspots are probably intrusive contacts. Even stronger positive anomalies apparent at the southern edge of the figure represent intracaldera intrusions in the Indian Peak caldera complex. The western of these anomalies may have led to the mineral deposits in the Atlanta mining district ([figure 19](#)). A large subdued anomaly in the

middle of [figure 20b](#) doubtless represents one or more plutons that are exposed in the area and mapped as Jurassic to Tertiary (Grauch et al., 1988). The largest of these exposed plutons is just north of Sacramento Pass, near the center of the strongest part of the anomaly. The overall anomaly is ringed by maxima (maxspots) that are suggestive of intrusive contacts except for the southern part of the southwesternmost one, which may be due to the Sacramento Pass fault. Subdued anomalies on either side of the northern Fish Springs Range represent a buried pluton that has been intersected during drilling in the adjacent Fish Springs mining district (Staargaard, 2009; Rowley et al., 2009). The western of these anomalies continues northwest to the edge of the area covered by the figure.

Four ground magnetic traverses, shown by blue lines in [figure 20b](#), were done in Spring and Snake valleys. Profile A is along U.S. Highway 50 adjacent to Rattlesnake Knoll, which consists of bedded volcanic breccia that has been mined for fluorspar. Rattlesnake Knoll protrudes into the middle of Spring Valley and is interpreted to represent a buried east-trending bedrock ridge (see also [AMT profile POD 54010](#),) at about 600 m depth that crosses the graben (Mankinen et al 2007). Profile B, farther north, was designed to investigate a subdued magnetic high in Spring Valley, which we conclude is caused by calc-alkaline volcanic rocks within the fill at a depth of 400 m (Mankinen et al., 2007).

Profile C crossed Snake Valley to investigate the origin and depth of the strong anomalies, probably plutons. Mankinen and McKee (2009) interpreted the source to be at a depth of about 800 m near the southwestern end of the traverse, and at a depth of 200–500 m near the northeast end of the traverse. Profile D traversed from Snake Valley at the northwest along a road between the Middle Range and Fish Springs Range to Sand Pass (Mankinen and McKee, 2009). From the northwest end, it passed along basaltic rocks at the surface and depth, then crossed a sharper positive anomaly interpreted to be a buried pluton at the northern end of Tule Valley, and then crossed a small positive anomaly at Sand Pass interpreted to be a buried part of a pluton found by Chidsey (1978).

AUDIOMAGNETOTELLURIC STUDIES

Collection and Processing of Data

Audiomagnetotelluric (AMT) technology detects variations in shallow (<300 m) subsurface electrical resistivity. The results are presented as a two-dimensional cross section model along a linear profile perpendicular to geologic structures. The technology is a valuable tool to map subsurface faults and the lithology of shallow parts of basins (McPhee et al., 2006a, b, 2007, 2008, 2009; Pari and Baird, 2011).

AMT uses the magnetotelluric (MT) method, a technique that applies the earth's natural electromagnetic fields as an energy source to investigate the electrical resistivity structure of the subsurface (Telford et al., 1990; Vozoff, 1991). Within the earth's upper crust, the resistivity of geologic units is largely dependent on their fluid content, porosity, density, fractures, and conductive mineral content (Keller, 1987). Saline fluids within pore spaces and fracture openings can reduce bulk resistivity by several orders of magnitude relative to dry rock. Resistivity can also be lowered by the presence of conductive clay minerals, graphite, and metallic sulfide minerals. Tables of electrical resistivity for a variety of rocks, minerals, and geologic environments may be found in Keller (1987) and Palacky (1987). For example, marine shale, mudstone, Pleistocene lake beds, and clay-rich alluvium are normally conductive, with values of a few tens of ohm-m (ohm-meters). Fault zones can appear as low-resistivity (i.e., high conductivity) units of less than 100 ohm-m when they are composed of rocks fractured enough to host fluids and clay alteration minerals (Eberhart-Phillips et al., 1995). Carbonate and clastic rocks are moderately to highly resistive, having values of hundreds to thousands of ohm-m depending on their fluid content, porosity, fractures, and impurities. Unaltered, metamorphic, and nongraphitic rocks are moderately to highly resistive. Unaltered, unfractured igneous rocks normally are resistive and have values greater than 500 ohm-m.

Using the same principles as the MT method, the AMT method estimates the electrical resistivity of the earth over depth ranges of a few meters to

about one kilometer, depending upon site conditions, using a high-frequency range (Zonge and Hughes, 1991; MCPhee et al., 2006a), whereas MT typically uses a lower frequency range. In areas where the resistivity distribution does not change rapidly from station to station, resistivity soundings provide a good estimate of the resistivity layering beneath the site.

Interpretation

AMT profiling was done in the Spring, Snake, Cave, Dry Lake, and Delamar valleys to define the faults, interpret the stratigraphy, and aid in siting drill-hole locations. Most profiles were oriented east-west, perpendicular to mapped and inferred faults. Initially, the data in the profiles were collected by the USGS through a cooperative agreement with SNWA and largely interpreted by SNWA. Later profiles were collected by Layne Geosciences (2009), working for SNWA, and interpreted by SNWA. More recent profiles were entirely collected and interpreted by SNWA. Except for the profiles in Snake Valley, we show the location of each profile plotted on a geologic map, below which is the 2D inversion model with its interpretation. The vertical scale to the right of the model gives resistivity, in ohm-m. We use the words resistivity and conductivity to describe the anomalies, but the reader should remember that they have opposite meanings: low resistivity is the same as high conductivity, and high resistivity is the same as low conductivity. All except the profiles in Snake Valley and one in Spring Valley are described in greater detail by Pari and Baird (2011). Those profiles that were collected and first published by the USGS are noted. The profiles within each valley are described from north to south.

Spring Valley

The most AMT profiles (i.e., 26) were done in Spring Valley. All profiles were interpreted by SNWA and all but one are discussed by Pari and Baird (2011). Only nine of the analyzed profiles are presented here, from north to south, as shown in [figure 21](#). Four of these were collected and first published by the USGS, as noted below. Of the rest,

profile SVN13 was collected and interpreted by SNWA, whereas the rest were collected by Layne Geosciences (2009) and interpreted by SNWA.

AMT Profile SVN13

Profile SVN13 ([figure 22](#)) was designed to extend northeastward for 2.3 km so as to cross and confirm a large concealed, northwest-striking oblique-slip fault mapped through Sacramento Pass at the eastern edge of Spring Valley (plate 1; also Dixon et al., 2007a, and Rowley et al., 2009). The fault shows up as a large resistivity contrast at about the 0.6 to 0.7 km mark in the profile; this clear, broad anomaly is characteristic of large oblique-slip or strike-slip faults, such as in parts of Dry Lake Valley ([AMT Profile DLV50](#)) and the Pahrnagat shear zone in southern Delamar Valley ([AMT Profile DELA5](#) and [AMT Profile DELA1](#)), which strikes northeast and has left-lateral offset. Such faults are heavily fractured and commonly carry groundwater, and other parts of the high-conductivity anomaly may owe to hydrothermal clays and gouge in the fault zone. The strike of the fault suggests that the strike-slip component is right lateral, as is commonly the case with northwest-striking faults subject to east-west Basin and Range extension in the Great Basin. The fault entirely crosses the pass and the Snake Range, from Spring Valley to Snake Valley. It passes into or cuts down-to-the-east normal faults that displace Snake Valley downward, relative to the Snake Range, near Baker. Smaller faults are apparent in the profile: (1) a concealed relatively small down-to-the-southwest fault near the left edge of the profile, and (2) a concealed fault that crosses the profile southwest of Rock Spring and results in a significant resistivity contrast near the right side of the profile. This latter fault may be the same one that is exposed eastward on the geologic map and that separates Ordovician from Precambrian bedrock. It was considered by Hose and Blake (1976) to be relatively low angle, although the profile suggests that this fault is relatively high angle, and it is shown as such in the profile interpretation.

AMT Profile POD 54010

Profile POD 54010 ([figure 23](#)) was completed near the center of Spring Valley, just south of U.S. Highway 6/U.S. Highway 50 and north and east of Rattlesnake Knoll, a small hill of volcanic breccia that protrudes from the basin fill (see also the ground magnetic profile described in [Geophysics of Spring and Snake Valleys](#)). The profile is about 2.0 km long and passes through the location of a Point of Diversion (POD) application of SNWA. Station S5 was not used in the modeling process due to poor data quality from an unknown noise source. The profile defines a deep graben east of Rattlesnake Knoll. The fault block at and just east of Rattlesnake Knoll is relatively shallow, for it is underlain by high-resistivity bedrock. The high-conductivity basin-fill rocks in the upper part of this shallower block and in the graben to the east are probably playa lake beds and/or beds containing significant groundwater.

AMT Profile SVN10 West

Profile SVN10 West ([figure 24](#)) was completed in western Spring Valley, about 10 km south of U.S. Highway 6/U.S. Highway 50 and mostly west of U.S. Highway 93, on the northern side of a horst block of carbonate rocks protruding from the basin fill. The profile, about 3.2 km long, was sited to identify faults in the large normal fault zone that defines the eastern side of the Schell Creek Range. Shallow and deep resistivity contrasts are interpreted as faults. The carbonates show high resistivity, and the eastern faults bound high conductivity rocks that probably are lake beds and/or large amounts of groundwater.

AMT Profile SVN10 East

Profile SVN10 East ([figure 25](#)) extends for 8.5 km east of U.S. Highway 93 across the main graben of Spring Valley, now occupied by a playa and formerly occupied by Pleistocene Lake Bonneville. In conjunction with Profile SVN10 West, the profile gives a good overview of the fault complexity of the basin in the vicinity of SNWA's Point of Diversion (POD). Stations S5, S6, S13, and S15 through S19 were not used in the

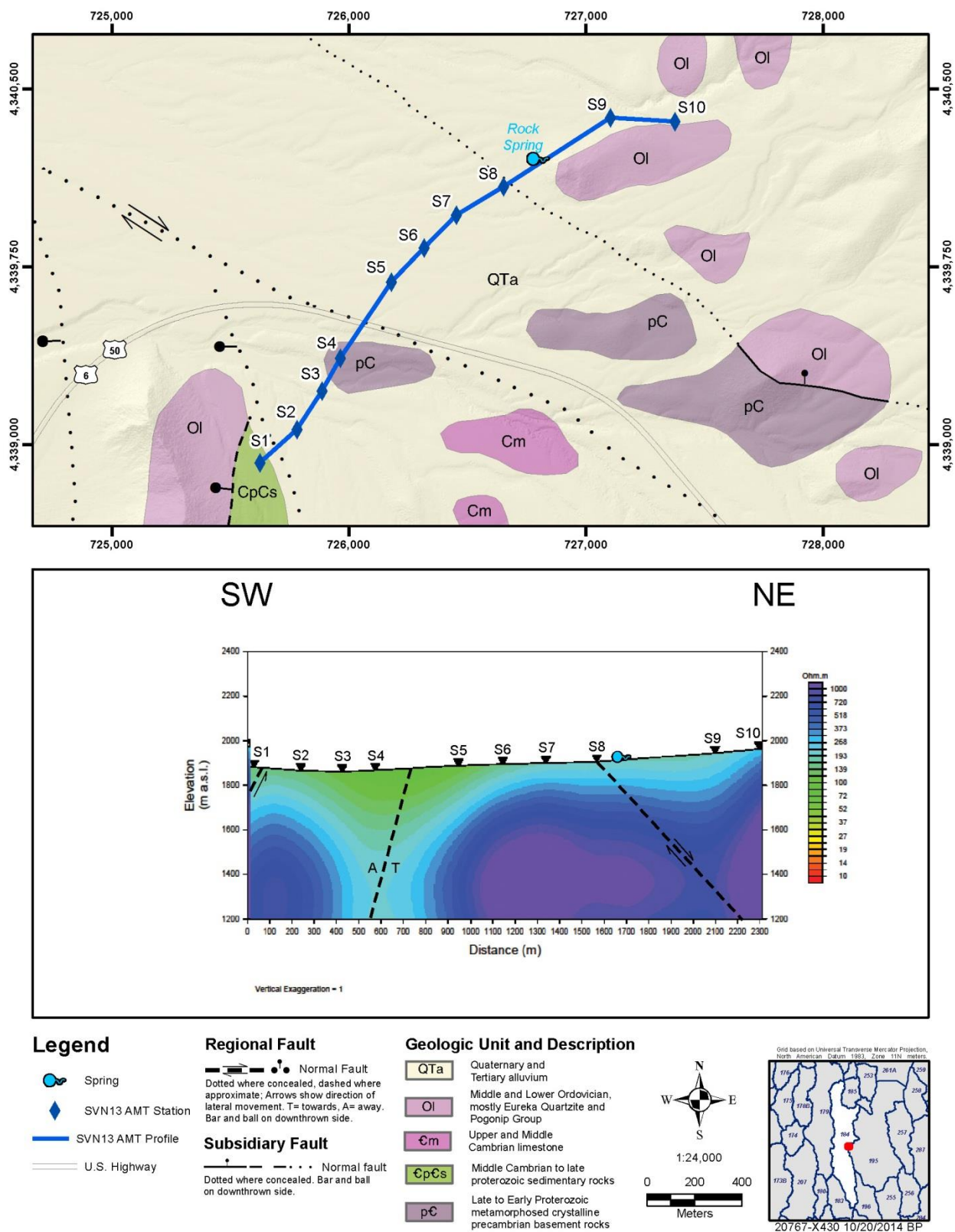


Figure 22. Geologic map and 2D model of AMT profile SVN13.

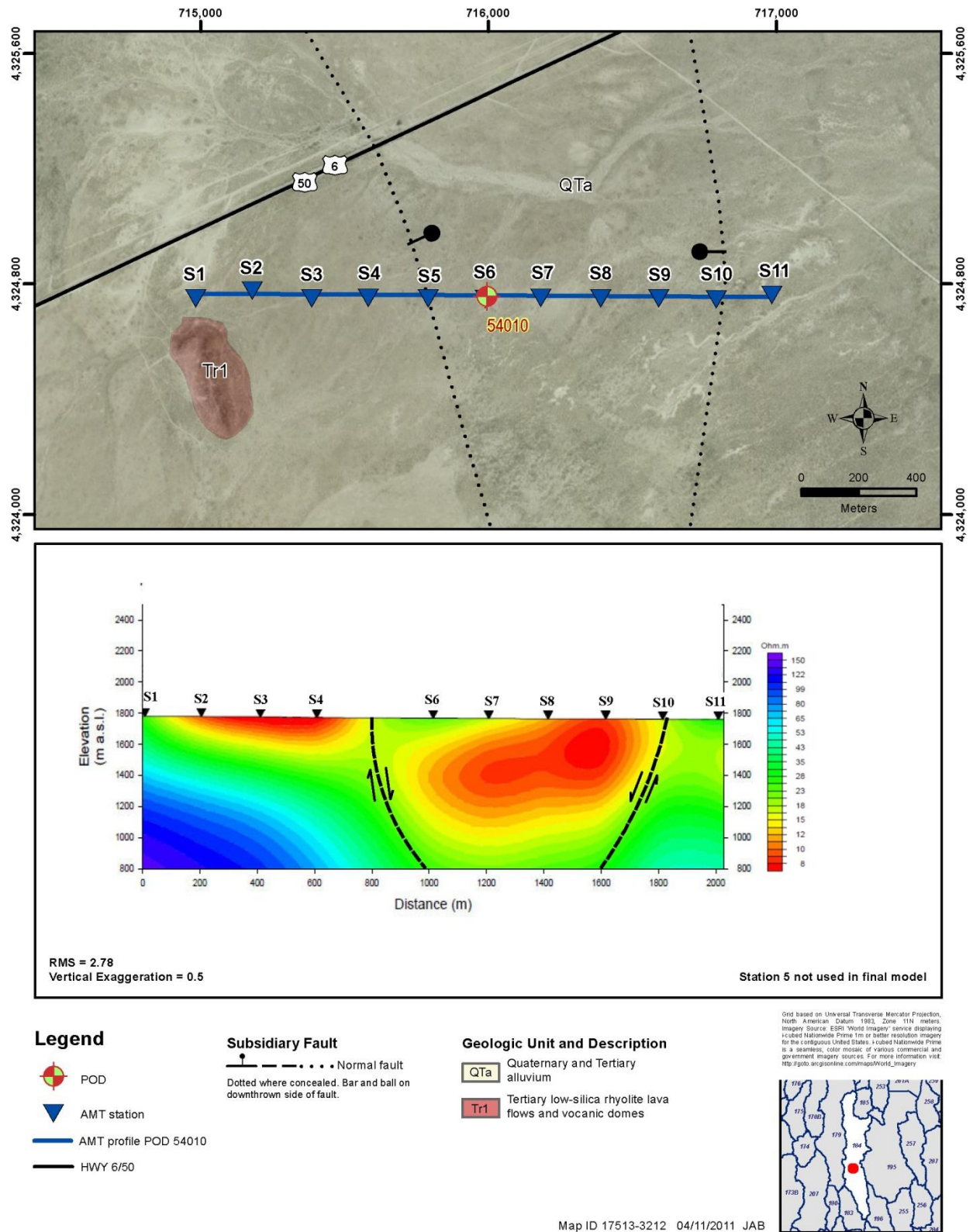


Figure 23. Geologic map and 2D model of AMT profile of area of POD54010.

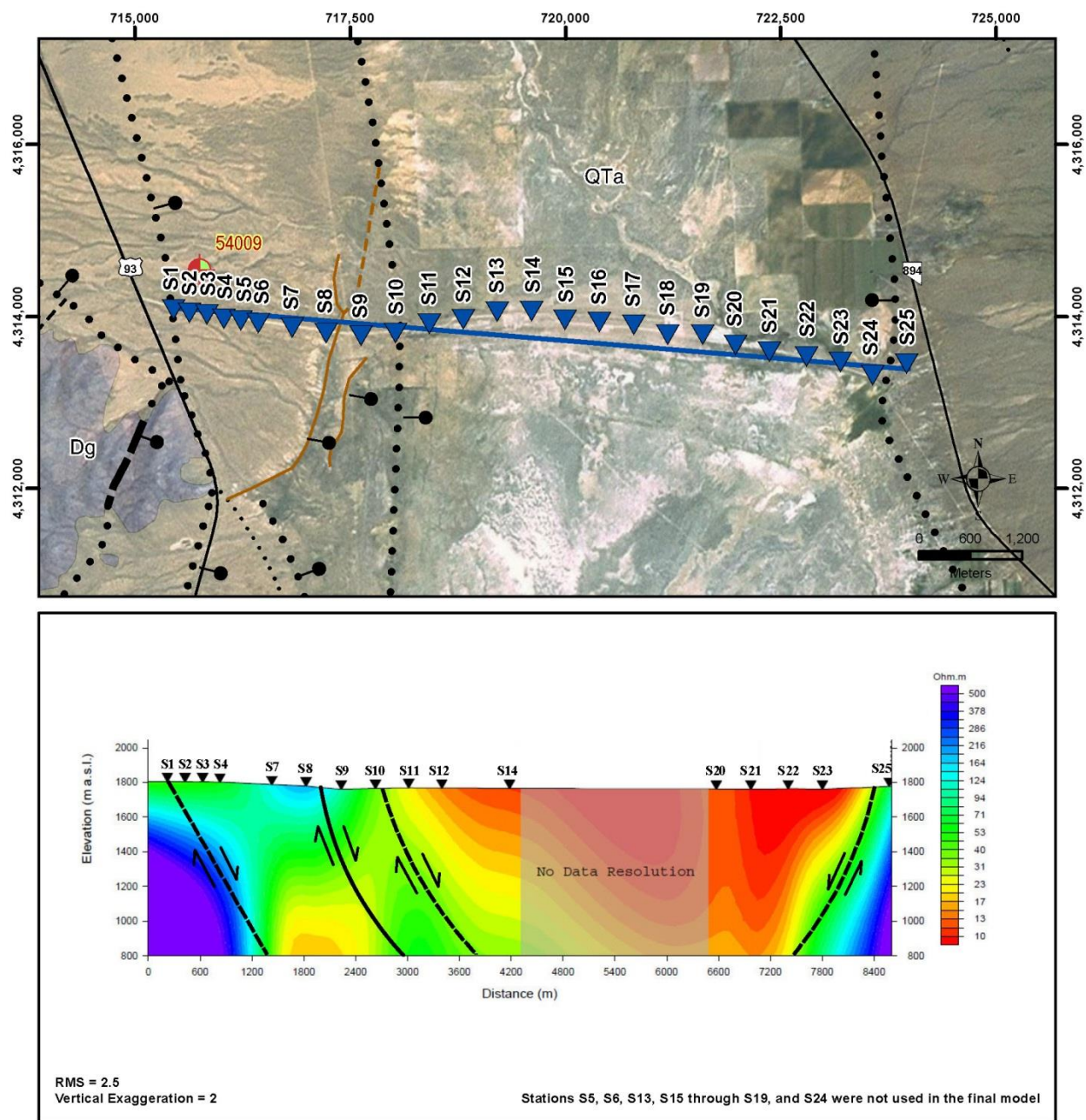


Figure 25. Geologic map and 2D model of AMT profile SVN10 East.

modeling process due to poor data quality from an unknown noise source. The fault near station S8 is a mapped fault that has Quaternary displacement. This fault, the fault east of it, and the fault at station S25 control several springs. The high-conductivity rocks between stations S10 and S25 are probably saline playa-lake deposits with significant groundwater, as are being deposited today.

AMT Profile SVN9

Profile SVN9 ([figure 26](#)) extends for 4.8 km, in western Spring Valley across the fault zone that raised the Schell Creek Range to the west. Stations S19, S21, and S24 were not included in the model due to poor data quality caused by an unknown noise source. At station S23, a large down-to-the-east fault is well displayed by the resistivity data, and its displacement is confirmed by several mapped Quaternary faults that control several springs. Lake beds and/or a low groundwater level are suggested by the anomalies east of station S14.

AMT Profile SVN N

Profile SVN N ([figure 27](#)) was completed for 2.5 km across down-to-the-west normal faults on the eastern side of Spring Valley that accommodated uplift the western Snake Range (McPhee et al., 2008). The main range-front fault passes through station S12, with highly resistive bedrock in the footwall (eastern side), and the smaller fault at station S3 is interpreted to be an intra-basin fault. Swallow Spring, near station S10, may be the cause of the higher conductivity anomaly there. The spring is perhaps controlled by a fracture or small fault related to the main fault at station S12. Alternatively, the more conductive rocks here represent finer grained beds within the basin-fill sediments. Test well SPR7007X, near station S6, was drilled by SNWA to a depth of 317 m, entirely in Quaternary and Tertiary basin-fill sediments, which here consist of coarse sand and gravel of quartzite clasts derived from erosion of the adjacent Snake Range.

AMT Profile SVNA

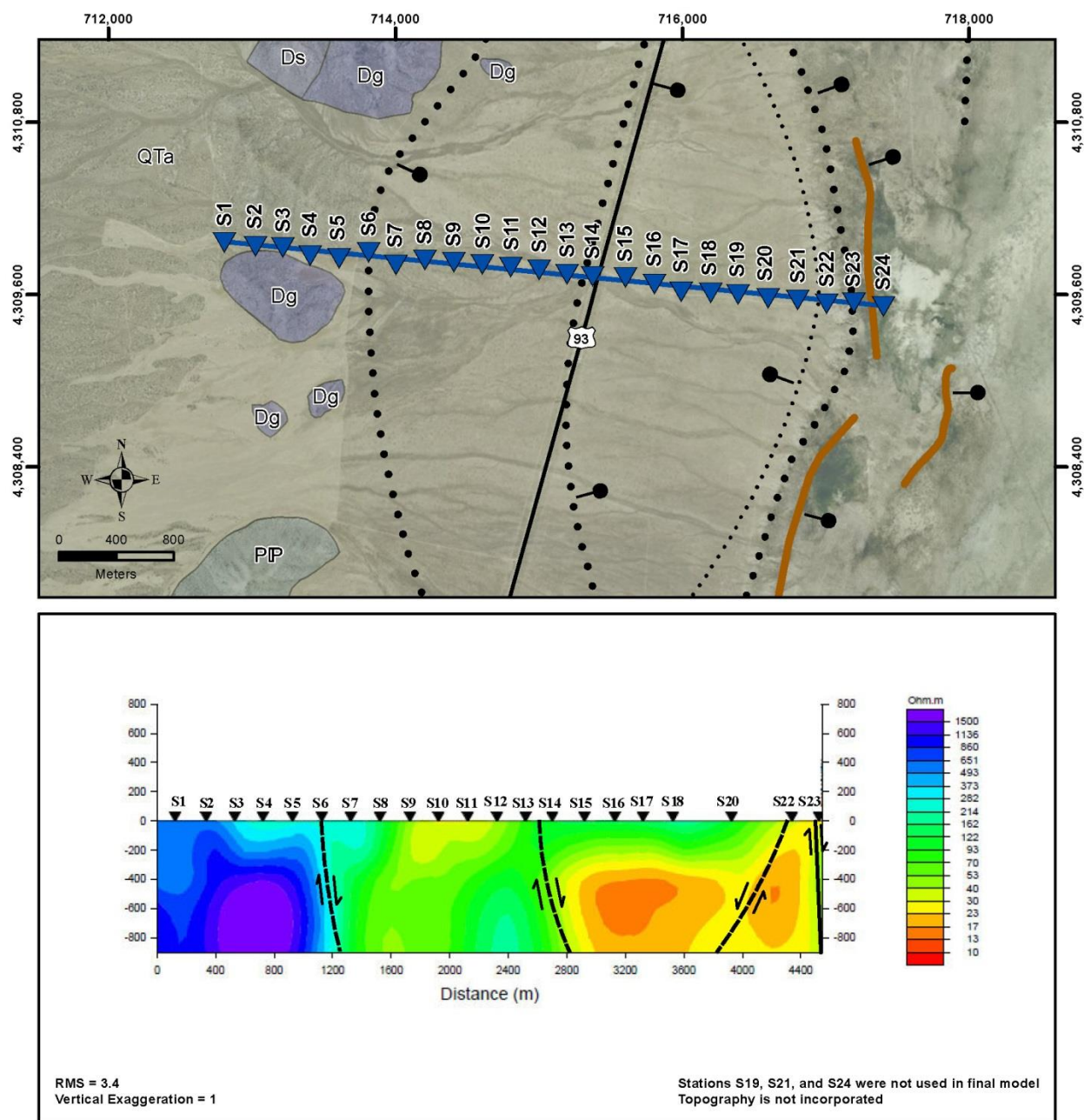
Profile SVNA ([figure 28](#)) extends for 12.7 km, entirely across the southern sub-basin of Spring Valley, from the Fortification Range on the west to the Limestone Hills on the east (McPhee et al., 2005, 2006a and b). The profile identified 14 faults, providing a typical example of the fault complexity of the various basins studied in the study area. Monitor well 184W508M, near station S11, was drilled by SNWA to a depth of 360 m, encountering only 27 m of basin-fill alluvium, then 332 m of nonwelded to moderately welded ash-flow tuff, which makes up the adjacent part of the Fortification Range. The higher-conductivity anomalies in the basin fill may represent groundwater and/or lake beds.

AMT Profile SVN L

Profile SVN L ([figure 29](#)) is 2.0 km long, located just south of the eastern part of Profile SVNA (McPhee et al., 2007). It was sited to identify faults between volcanic and carbonate rocks and to help interpret SNWA Test Well 184W101, which was drilled to a depth of 536 m, entirely in carbonates. At depth, beneath stations S5 to S6, the large resistivity contrast of the bedrock units juxtaposed by the fault are typical of ash-flow tuff versus carbonate rocks, with the high-conductivity bed west of the fault interpreted to be a permeable ash-fall tuff interbedded within the ash-flow tuff.

AMT Profile SVN P

Profile SVN P ([figure 30](#)) extends for 2.8 km through The Troughs, a cattle tank in a low pass through the Limestone Hills (McPhee et al., 2008). The profile was sited to provide more information on mapped faults in the area, which might provide eastward groundwater flow through the pass, from Spring Valley to Snake Valley. The high conductivity rocks beneath station S10 may be the fault itself. The basin-fill sediments farther west have higher conductivity at depth, probably reflecting



Legend

- ▲ AMT station
- AMT profile SVN9
- HWY 93

Regional Faults

- Normal fault
- Quaternary normal fault
- Solid where known; dotted where concealed.
- Bar and ball on downthrown side of fault.

Subsidiary Fault

- Normal fault
- Dotted where concealed. Bar and ball on downthrown side of fault.

Geologic Unit and Description

- QTa Quaternary and Tertiary Alluvium
- PP Permian and Pennsylvanian Riepe Spring Limestone and Ely Limestone
- Dg Upper and Middle Devonian Guilmette Formation
- Ds Middle and Lower Devonian Simonson and Sevy Dolomites

Map ID 17522-3212 04/11/2011 JAB

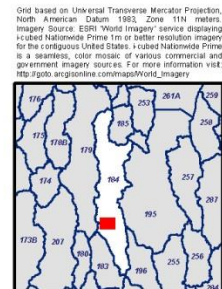


Figure 26. Geologic map and 2D model of AMT profile SVN9.

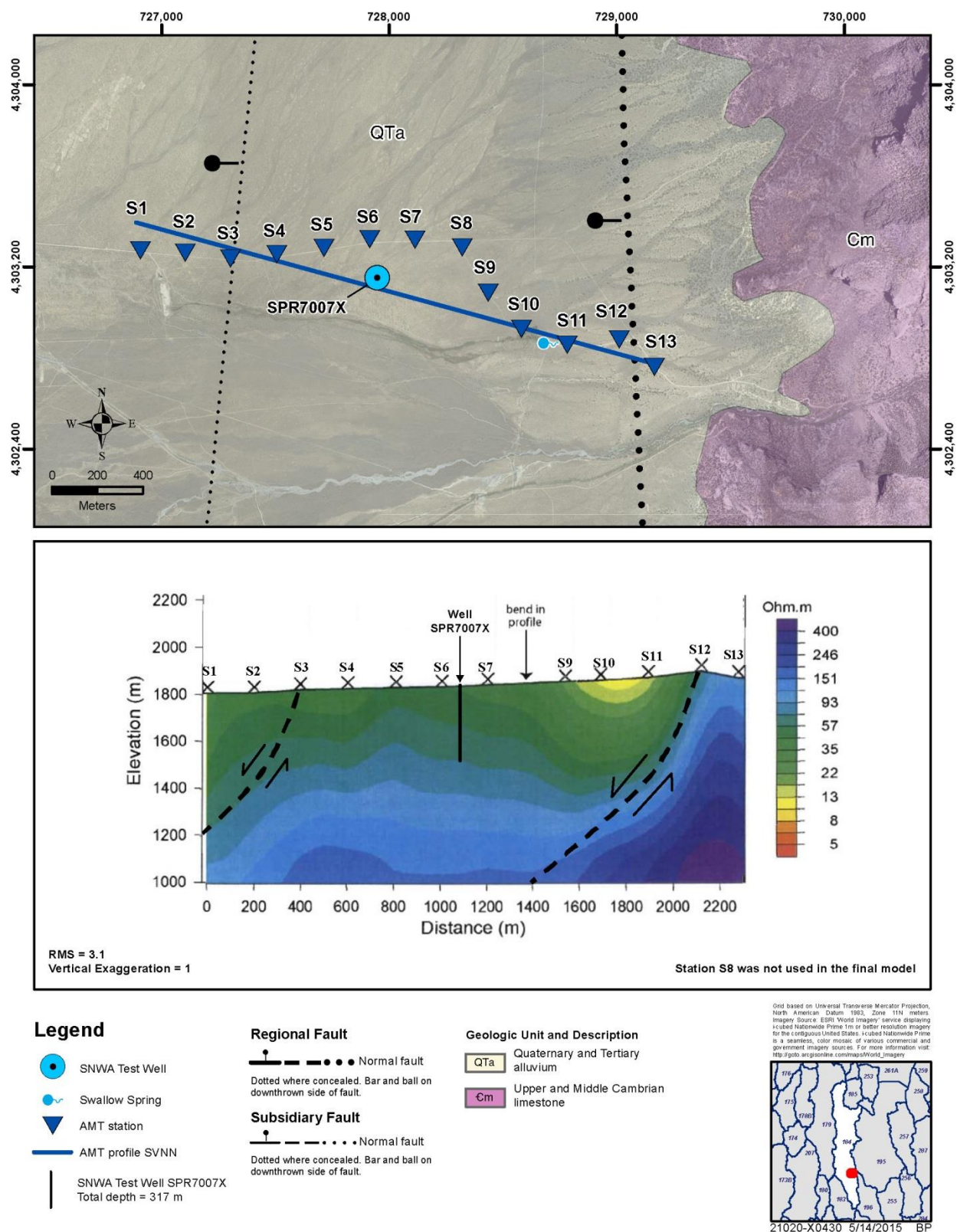


Figure 27. Geologic map and 2D model of AMT profile SVNN.

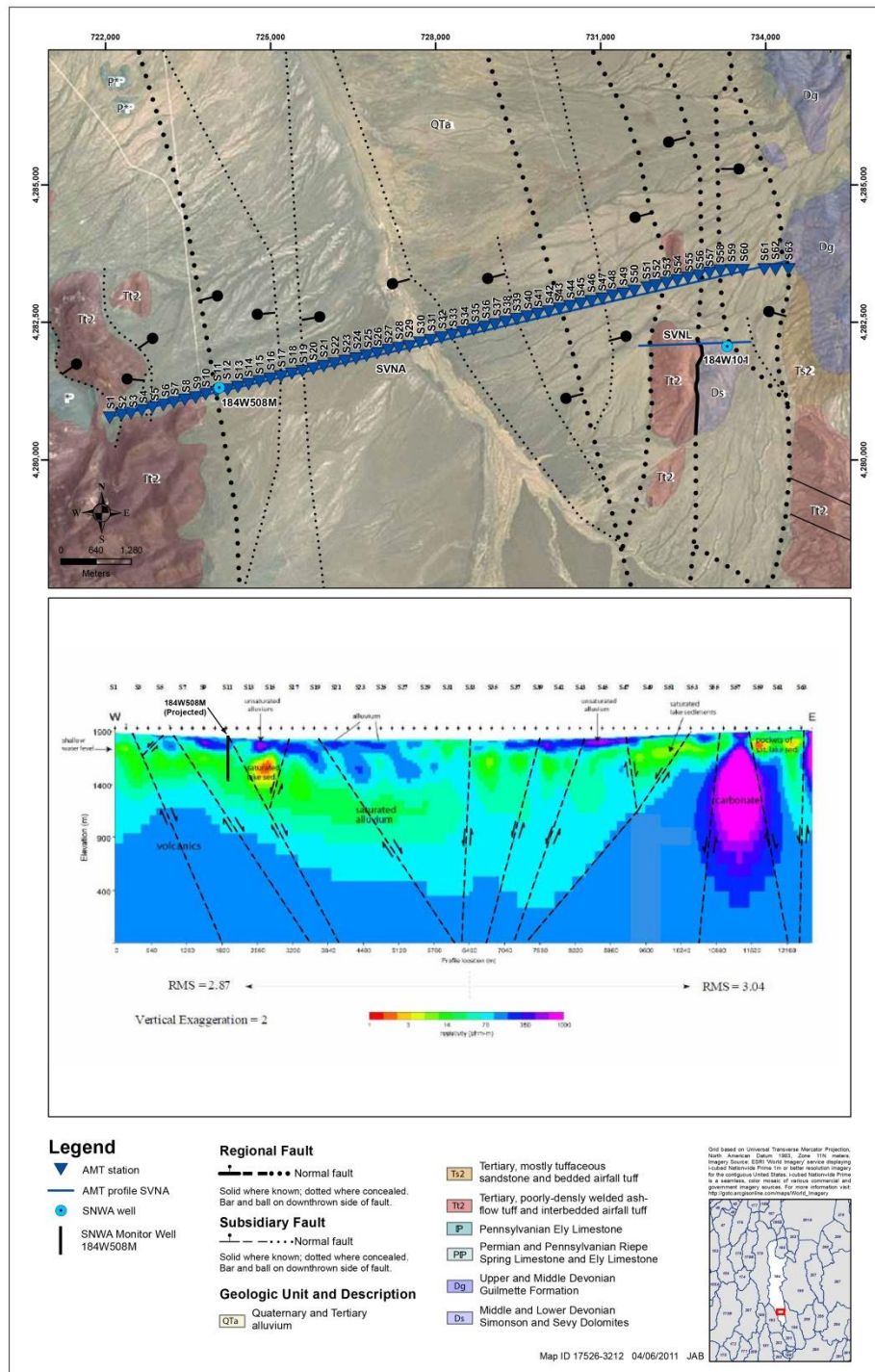


Figure 28. Geologic map and 2D model of AMT profile SVNA.

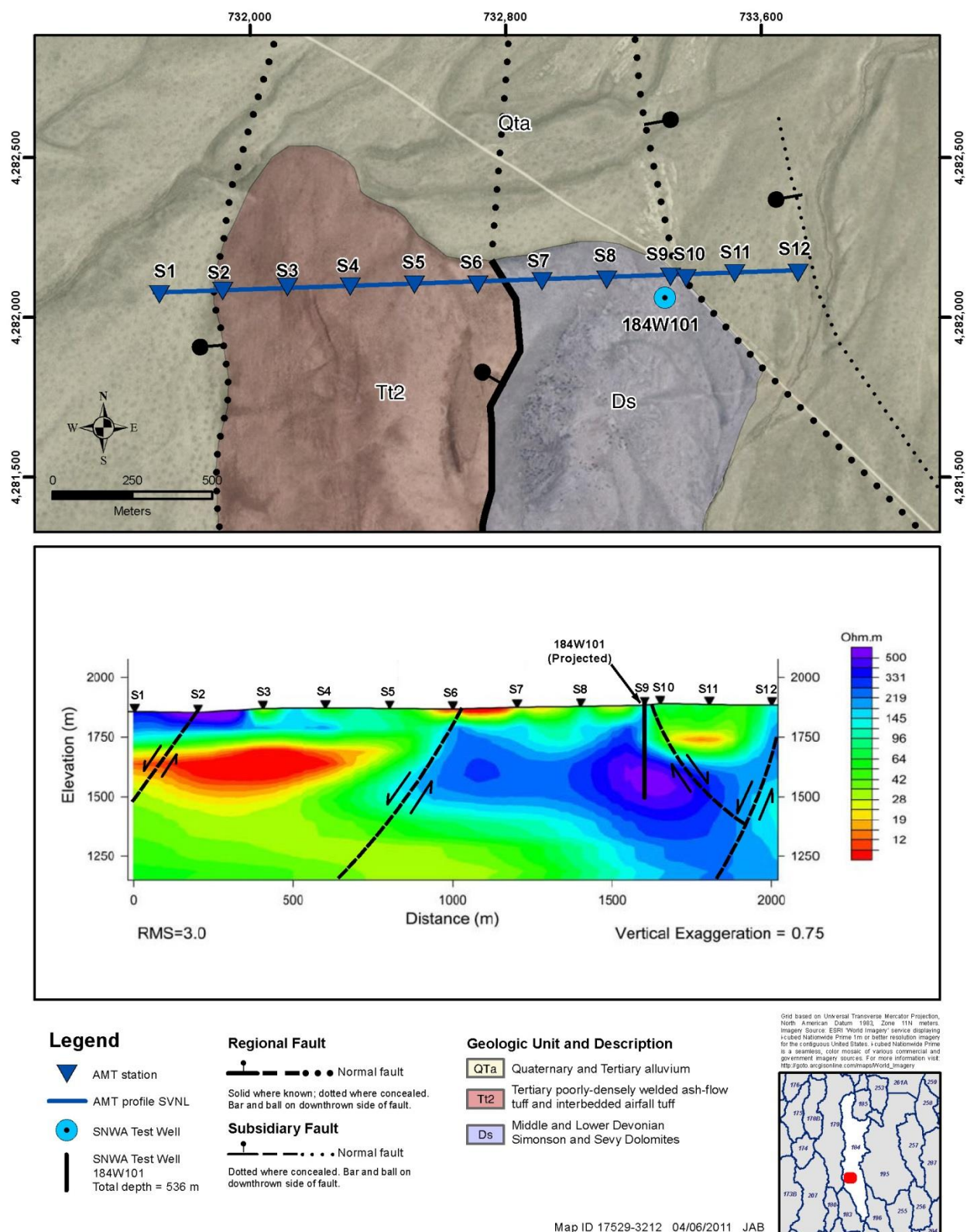
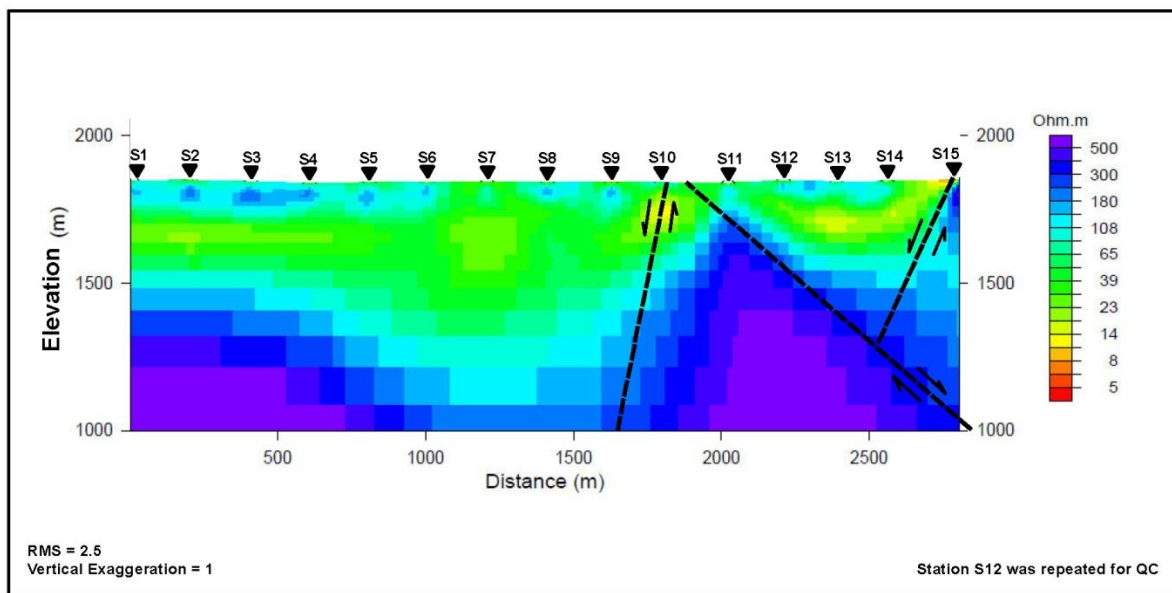
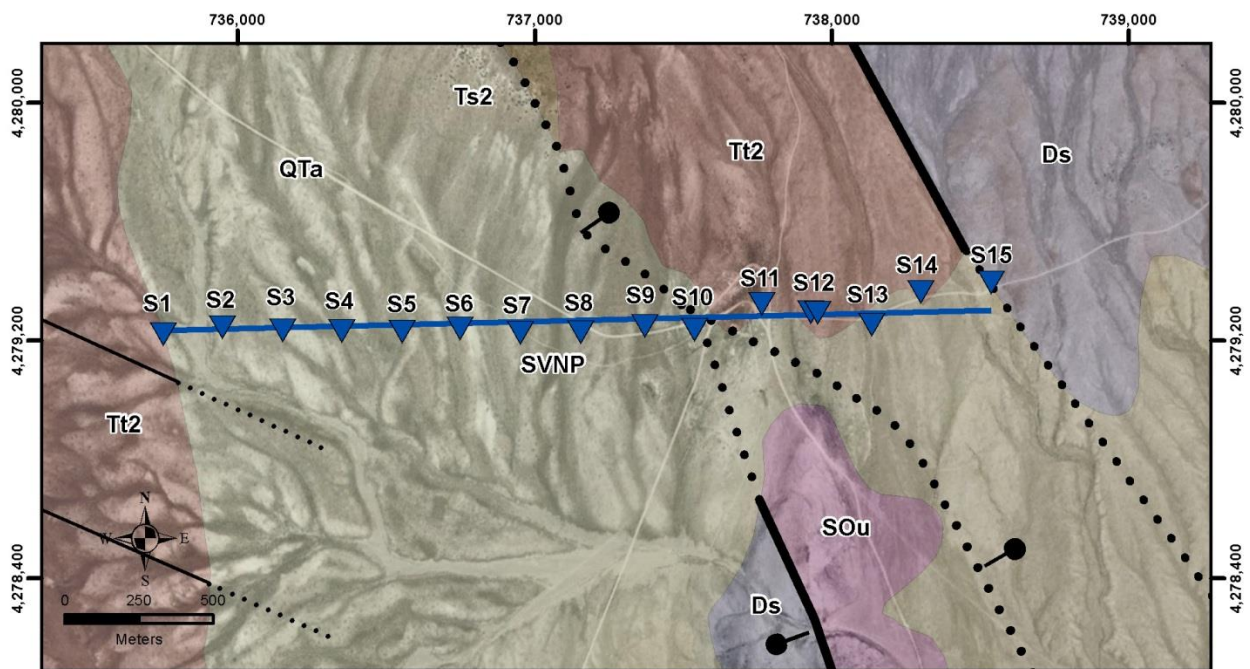


Figure 29. Geologic map and 2D model of AMT profile SVNL.



Legend

- ▲ AMT station
- AMT profile SVNP

Regional Fault

- Normal fault
- Solid where known; dotted where concealed.
- Bar and ball on downthrown side of fault.

Subsidiary Fault

- Normal fault
- Solid where known; dotted where concealed.
- Bar and ball on downthrown side of fault.

Geologic Unit and Description

- QTa Quaternary and Tertiary alluvium
- Ts2 Tertiary, mostly fluvial tuffaceous sandstone and bedded airfall tuff
- Tt2 Tertiary poorly-densely welded ash-flow tuff and interbedded airfall tuff
- Ds Middle and Lower Devonian Simonson and Sevy Dolomites
- SOu Silurian and Upper Ordovician dolomite, undivided

Map ID 17585-3212 04/06/2011 JAB

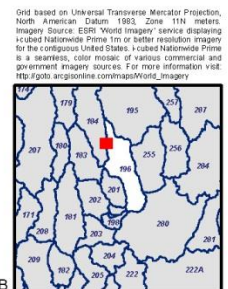


Figure 30. Geologic map and 2D model of AMT profile SVNP.

groundwater beneath a water table. The higher conductivity rocks east of S10 may represent a permeable bed within the volcanic section, perhaps ash-fall tuff.

Snake Valley

Four AMT profiles were done on the Nevada (western) side of Snake Valley. All were completed by the USGS (McPhee et al., 2007) and in part interpreted by SNWA and republished (McPhee et al., 2009). Locations and geologic setting of all of them are given on [figure 31](#), from MCPhee et al. (2009, figure 1). The profiles were intended to identify the location of the main range-front faults that raise the eastern Snake Range with respect to Snake Valley. Two of these profiles are given below.

AMT Profile SNK1

Profile SNK1 ([figure 32](#)) extends for 4.6 km from limestone bedrock at the range front, just east of which is a large range-front fault (McPhee et al., 2009, figure 3A). Farther east, the profile crosses a broad graben. A small north-south power line crosses the middle of the graben, resulting in minor model resolution in this part of the profile. Farther east, the profile continues across the eastern part of the graben, then past a narrow horst of limestone, the eastern bounding fault of which is the main range-front fault that separates the Snake Range from Snake Valley. High-conductivity rocks in the basin fill just east of this fault probably are saline playa lake beds at depth in the valley.

AMT Profile SNK4

Profile SNK4 ([figure 33](#)) extends for nearly 5.0 km from limestone bedrock at the range front eastward across basin-fill sediments to determine the fault control for springs at and near Big Springs (McPhee et al., 2009, figure 6A). Some of these faults have Pleistocene, or possibly Holocene, displacement that may be traced for kilometers as low scarps in Pleistocene alluvial fans. At the western end of the profile, basin-fill sediments are thin, then at about station 12, the large range-front

fault is crossed, and higher conductivity basin-fill deposits are present to the east. Yet low-conductivity sediments occur at the surface, probably representing sediments above the water table. The basin fill is hardly uniform in appearance along the profile, requiring an interpretation of at least four more faults. The fault shown between stations 21 and 22 is interpreted to be the concealed southern part of the exposed Pleistocene fault scarp that controls Big Spring itself, about 2 km to the north. The most highly conductive rocks east of this fault is likely fine-grained lake sediments, charged with groundwater. The faults interpreted at stations 38 and 45 are considered to be the controls for, respectively, North Little Springs and South Little Springs, about 1 km north of the profile.

Cave Valley

Only one AMT profile was completed in Cave Valley. It is on the eastern side of southern Cave Valley, starting at the western part of Sidehill Pass at the edge of the Schell Creek Range ([figure 34](#)).

AMT Profile CVE

Profile CVE ([figure 35](#)) has a length of 3.4 km, as collected and interpreted by MCPhee et al. (2005, 2006a and b). It is also discussed by Dixon et al. (2007a) and Pari and Baird (2011). The profile images the western range-front fault of the Schell Creek Range and shows conductive basin-fill sediments west of this fault. The lower conductivity beds at the surface are above the water table. A case could be made for several small faults west of the big fault, but the evidence is not clear. SNWA well 180W504M, drilled south of the profile and east of the main fault, penetrated basin-fill sediments to a depth of 150 m, then passed into carbonate rocks to a total depth of 272 m. Sidehill Pass Federal No. 18-13, drilled just north of the map of [figure 35](#) and west of the big fault, penetrated 1550 m of basin-fill sediments before passing into the Mississippian Joana Limestone, then continued to a total depth of 2000 m (Hess, 2004).

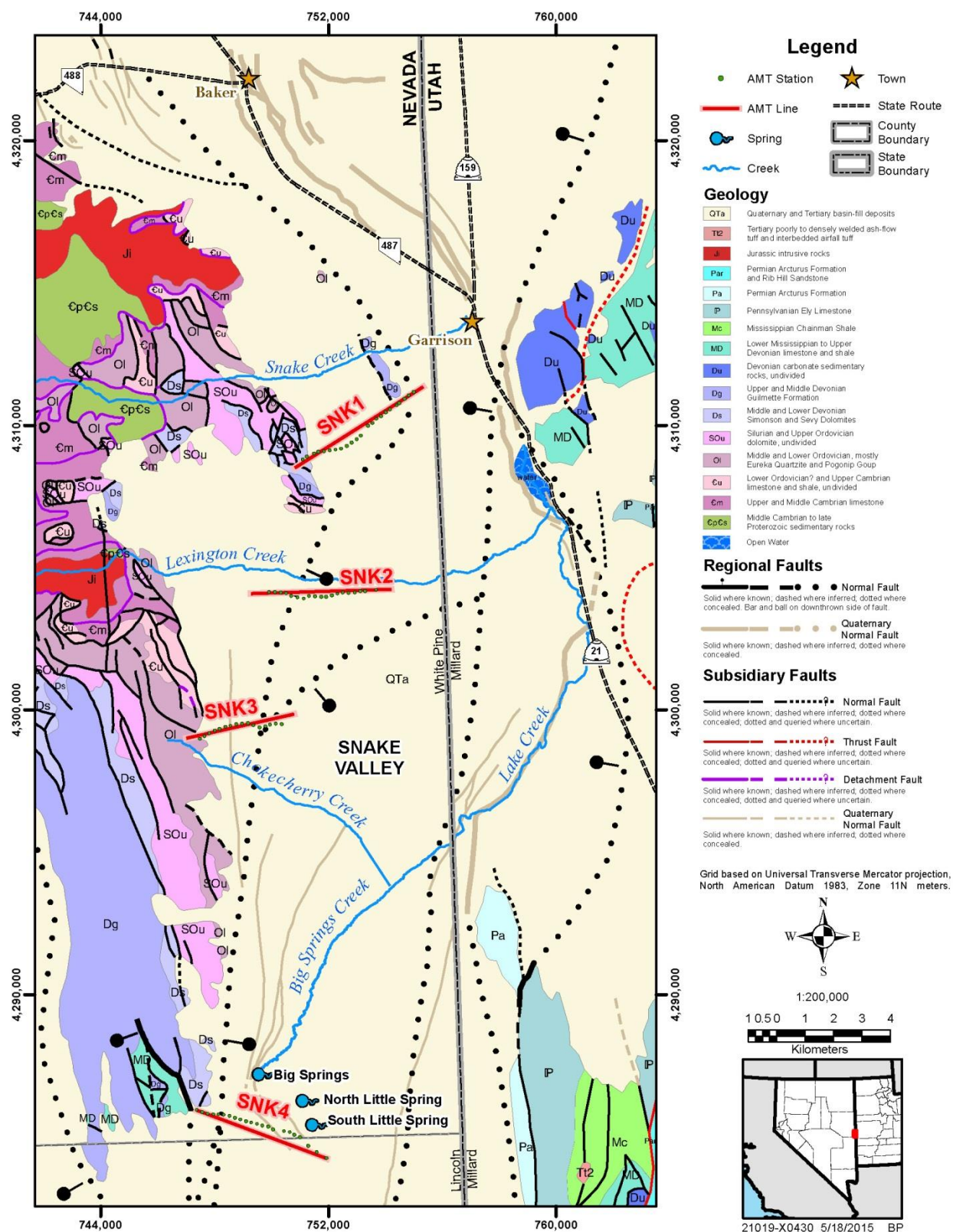


Figure 31. Map of Snake Valley area showing locations of AMT profiles.

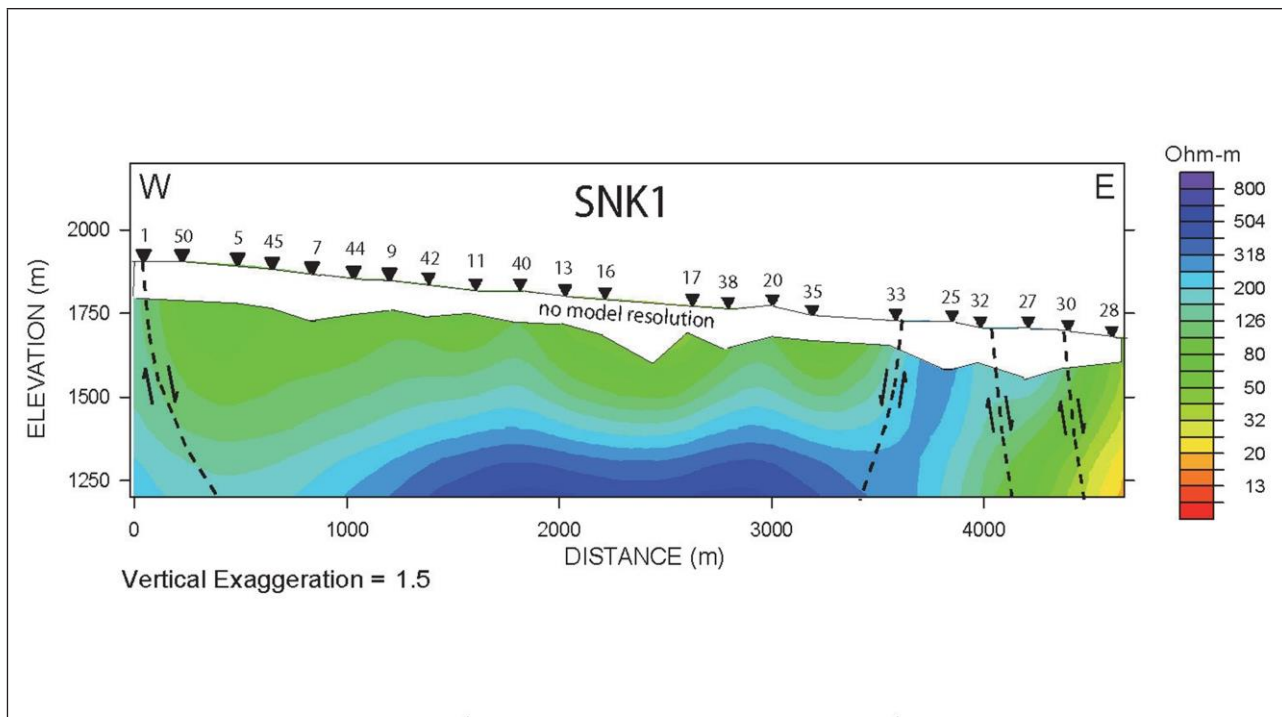


Figure 32. 2D model of AMT profile SNK1.

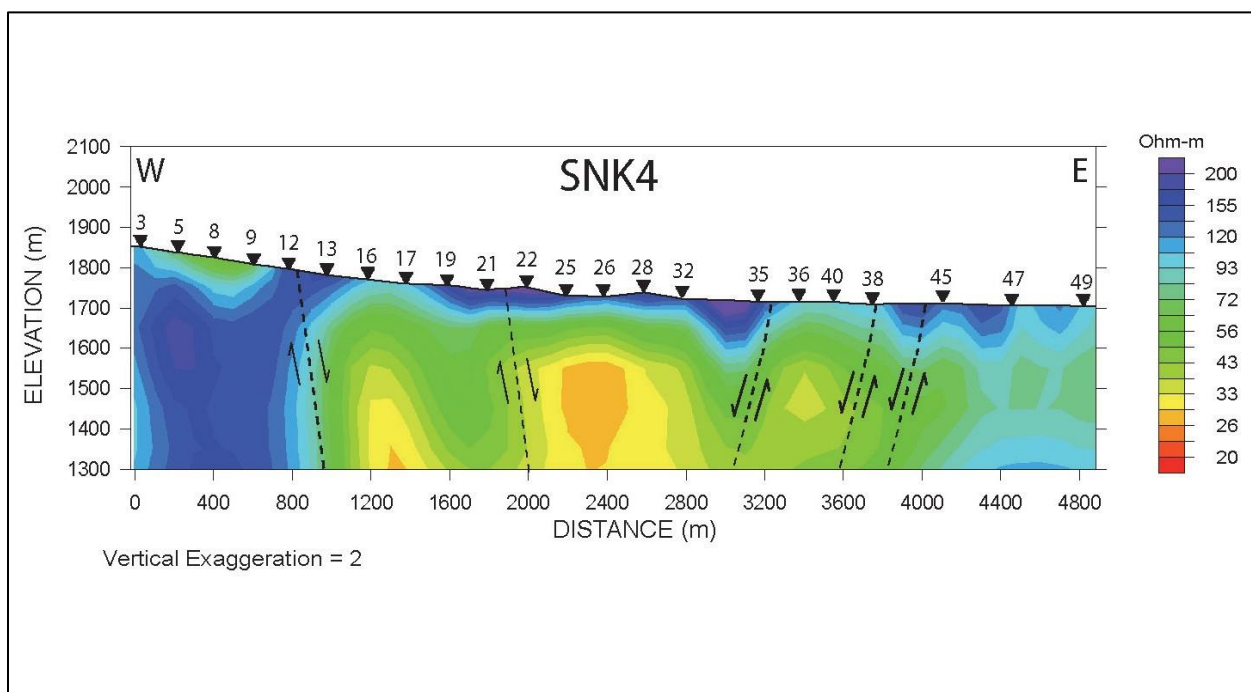


Figure 33. 2D model of AMT profile SNK4.

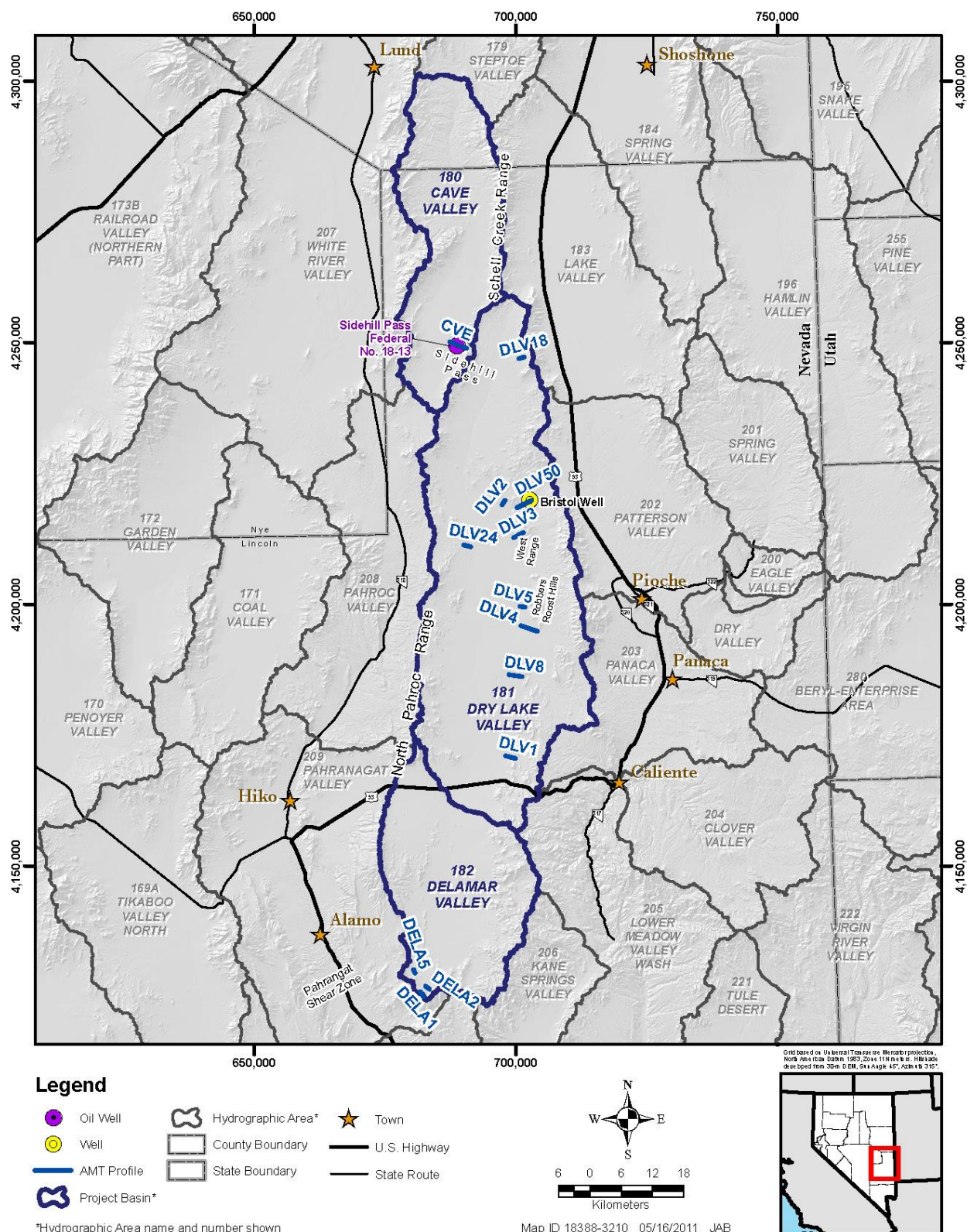


Figure 34. Map of Cave, Dry Lake, and Delamar valleys, showing locations of AMT profiles.

Dry Lake Valley

Dry Lake Valley, whose northern end is locally called Muleshoe Valley and is east of southern Cave Valley, continues south to where it appears to pass uninterrupted into Delamar Valley. Northern Dry Lake (Muleshoe) Valley is relatively shallow and is separated from the southern, deeper, main part of Dry Lake Valley by a series of uplifted fault blocks that span much of the valley and formed along the generally east-striking Blue Ribbon transverse zone (Rowley, 1998; Rowley and Dixon, 2001). The southern end of Dry Lake Valley is separated from northern Delamar Valley by a similar series of uplifted fault blocks of the generally east-striking Timpahute transverse zone, but these blocks are not exposed and are covered by thin basin-fill sediments. Dry Lake Valley was the focus of nine AMT profiles, seven by the USGS (McPhee et al., 2008) and two by SNWA. All profiles are described by Pari and Baird (2011). Only five of them are discussed here ([figure 34](#)).

AMT Profile DLV50

Profile DLV50 ([figure 36](#)) extends for 3.2 km along a northeast trend so as to cross several faults along the eastern side of the West Range and west of Bristol Well. Bristol Well served the traveler along an east-west wagon trail and road that allowed access from Lake Valley on the east, across Dry Lake Valley, to White River Valley on the west. The West Range is a structurally complex area in the northeastern part of the main part of Dry Lake Valley just west of the northern Bristol Range. These areas were mapped in detail by Page and Ekren (1995). The profile was collected and interpreted by SNWA; stations S1 through S3 were omitted from the profile due to poor data quality. Three faults were imaged by the remaining part of the profile, all interpreted to be oblique-slip faults with right-lateral and normal displacement. As with other faults in the Great Basin that have a significant component of strike slip, the faults are broad and their resistivity contrasts are large. The high conductivity that marks the faults is probably a function of large amounts of groundwater flow, plus fault gouge and hydrothermal clay, along the faults. The higher conductivity beds between S8

and S14 probably are lake beds and/or high groundwater.

AMT Profile DLV3

Profile DLV3 ([figure 37](#)) extends for 2.1 km from the western side of the West Range into the main part of Dry Lake Valley. The data were collected by MCPhee et al. (2008) and interpreted by SNWA. Three down-to-the-west normal faults that accommodated development of Dry Lake Valley are imaged. The western of these cuts Pleistocene and Holocene basin-fill sediments. Interpretation of the AMT data indicates that the eastern of these is relatively small, the middle fault is the main fault, and the western fault has significant displacement, only the latest of which is demonstrated by the mapped fault scarp. Inner-basin lake deposits, probably containing groundwater, are indicated at depth beneath stations S3 and S7.

AMT Profile DLV24

Profile DLV24 ([figure 38](#)), which has a length of 1.4 km, was collected by MCPhee et al. (2008) and interpreted by SNWA. The profile extends basinward from the eastern part of the North Pahroc Range (Ekren and Page, 1995). Three buried faults are imaged, the western of which Ekren and Page (1995) interpreted to be an oblique-slip fault based on their mapping. The two faults farther east form a graben containing probable high-conductivity lake beds and/or permeable sediments containing groundwater. The low-conductivity material at the eastern end of the profile suggests that a block of Paleozoic carbonates has been brought up from depth, although this is based only on station S8, one data point.

AMT Profile DLV4

Profile DLV4 ([figure 39](#)) extends westward 3.2 km from the western edge of the Burnt Springs Range so as to look at the concealed normal faults in this part of eastern Dry Lake Valley. The data were collected by MCPhee et al. (2008) and interpreted by SNWA. The profile

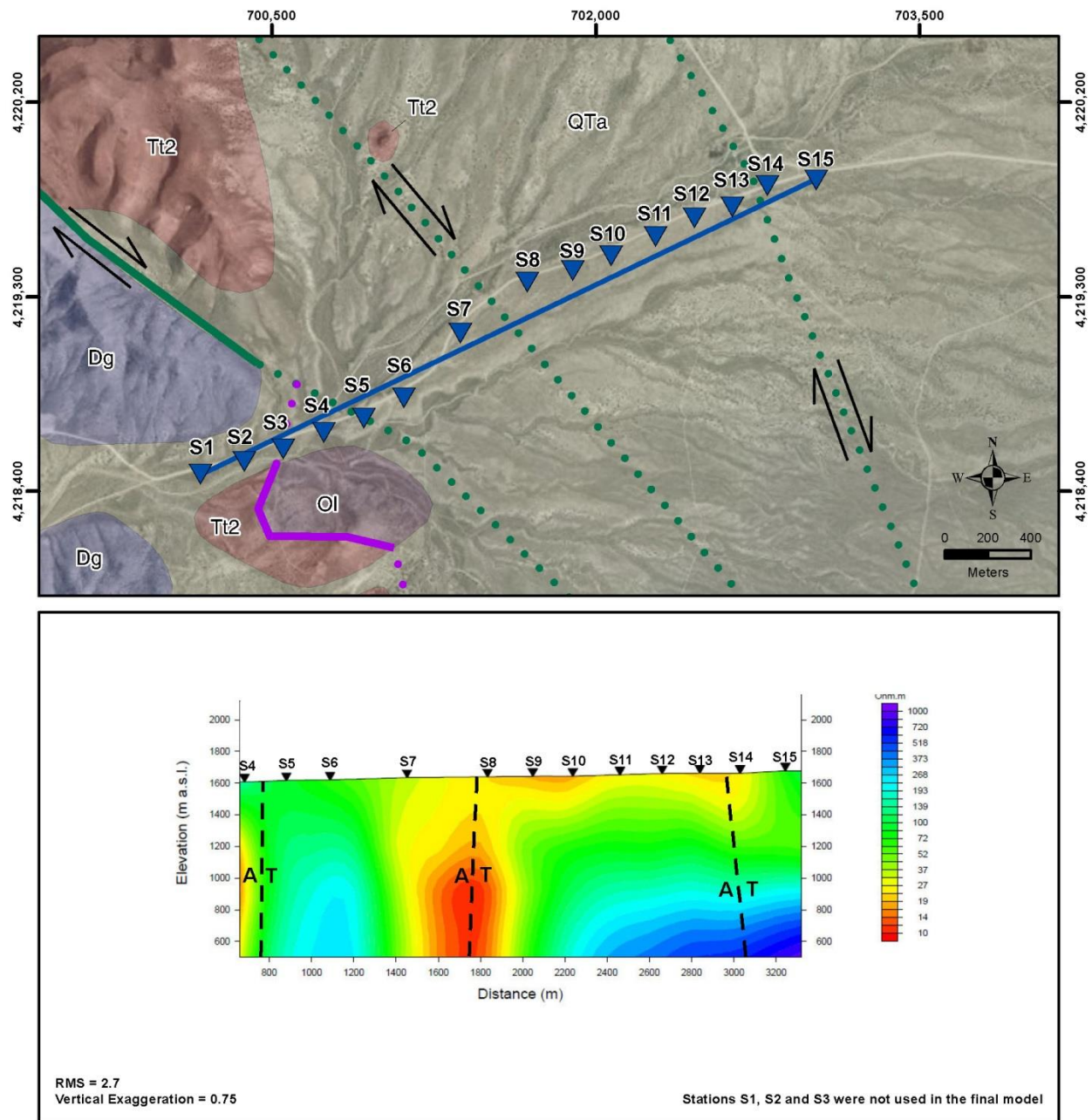


Figure 36. Geologic map and 2D model of AMT profile DLV50.

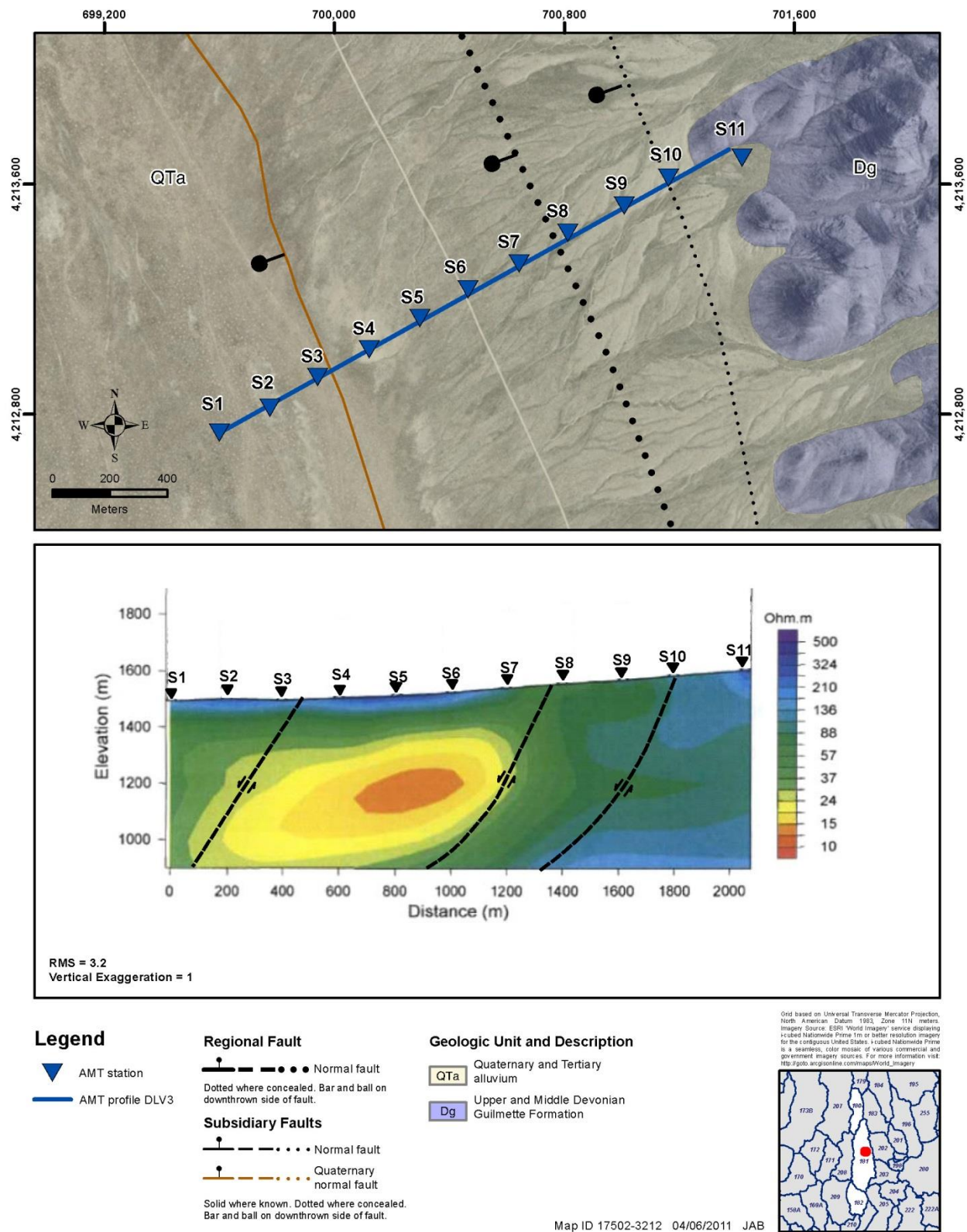


Figure 37. Geologic map and 2D model of AMT profile DLV3.

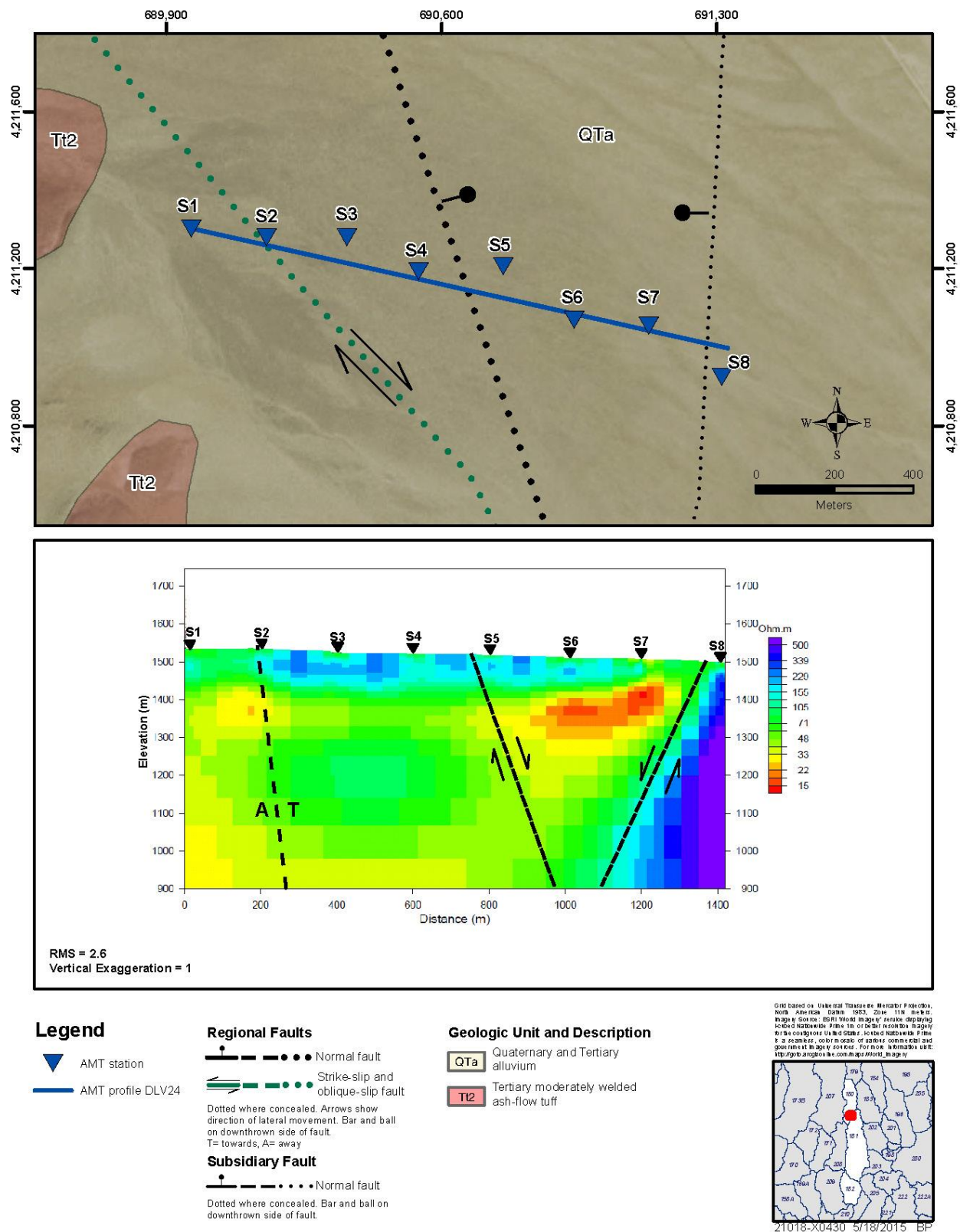


Figure 38. Geologic map and 2D model of AMT profile DLV24.

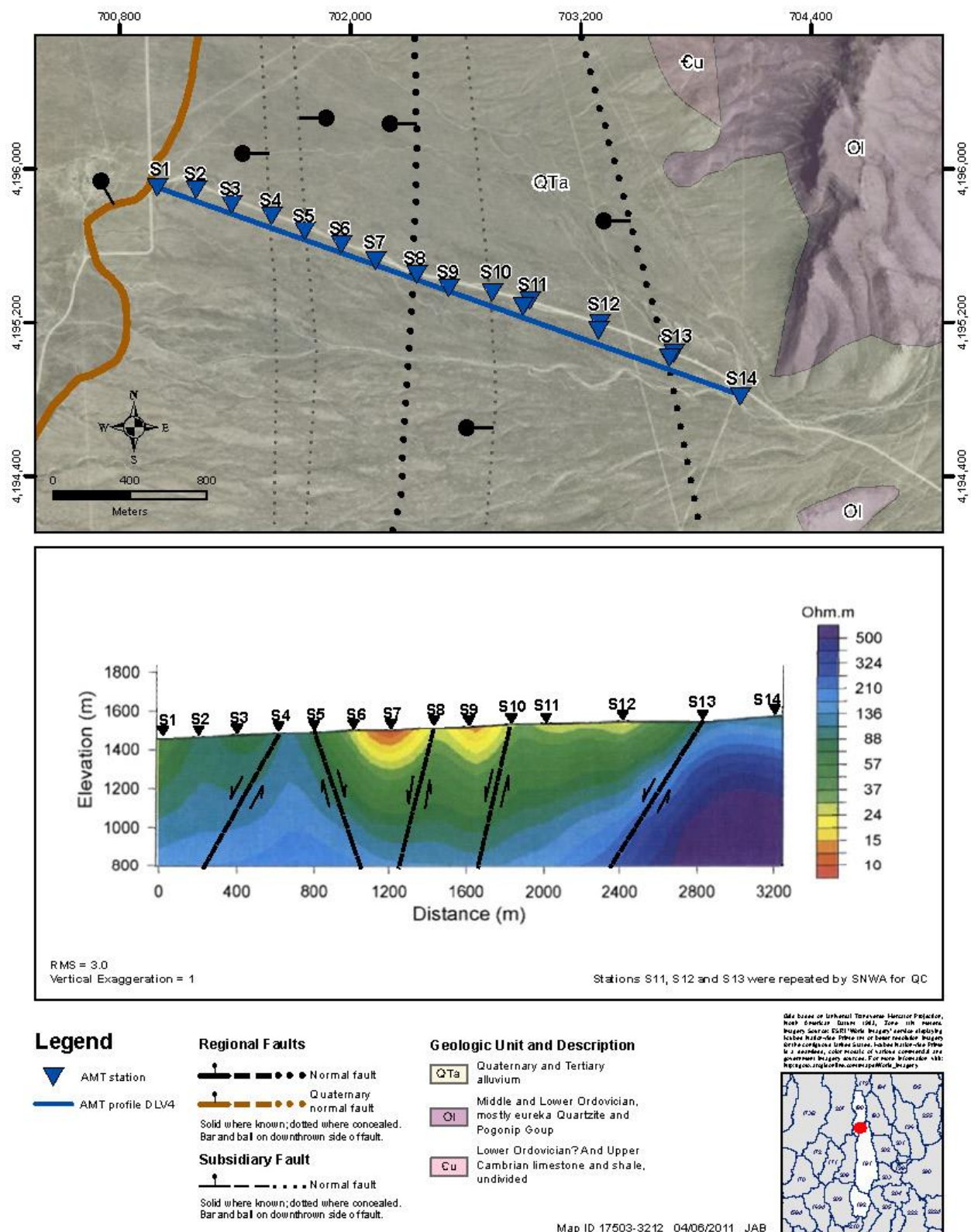


Figure 39. Geologic map and 2D model of AMT profile DLV4.

reveals the complexity of concealed normal faults in Dry Lake Valley. Only the westernmost of these faults was mapped, displacing Quaternary deposits, although the profile did not cross it. The profile allows interpretation of the buried faults and the most likely locations of high-conductivity lake beds. These AMT data demonstrate a horst block in the western part of the profile and show that the eastern fault is the main fault.

AMT Profile DLV8

Profile DLV8 ([figure 40](#)), farther south from the western edge of the Burnt Springs Range into eastern Dry Lake Valley, has a length of 2.5 km. The data were collected by McPhee et al. (2008) and interpreted by SNWA. They show that the mapped fault, which has Quaternary displacement, has significant older displacement. About 10 km north of the profile, large historic open fissures (Swadley, 1995) formed by movement along this Quaternary fault, and surface water pours into these cracks during each rainstorm. The main fault, however, is the eastern buried one. The highly conductive material probably represents gouge and groundwater in the Quaternary fault and its fissures as well as groundwater and lake clays in the basin-fill sediments.

Delamar Valley

Three northwest-trending AMT profiles were done in southwestern Delamar Valley to look at two large northeast-striking, oblique-slip (left lateral and normal) faults of the Pahrnagat shear zone (Ekren et al., 1977; Scott et al., 1993). These faults pass into north-striking normal faults at both of their ends, so the Pahrnagat shear zone can be considered a transfer fault that allowed east, west, northeast, and southwest movement during east-west extension. In other words, the slip in this

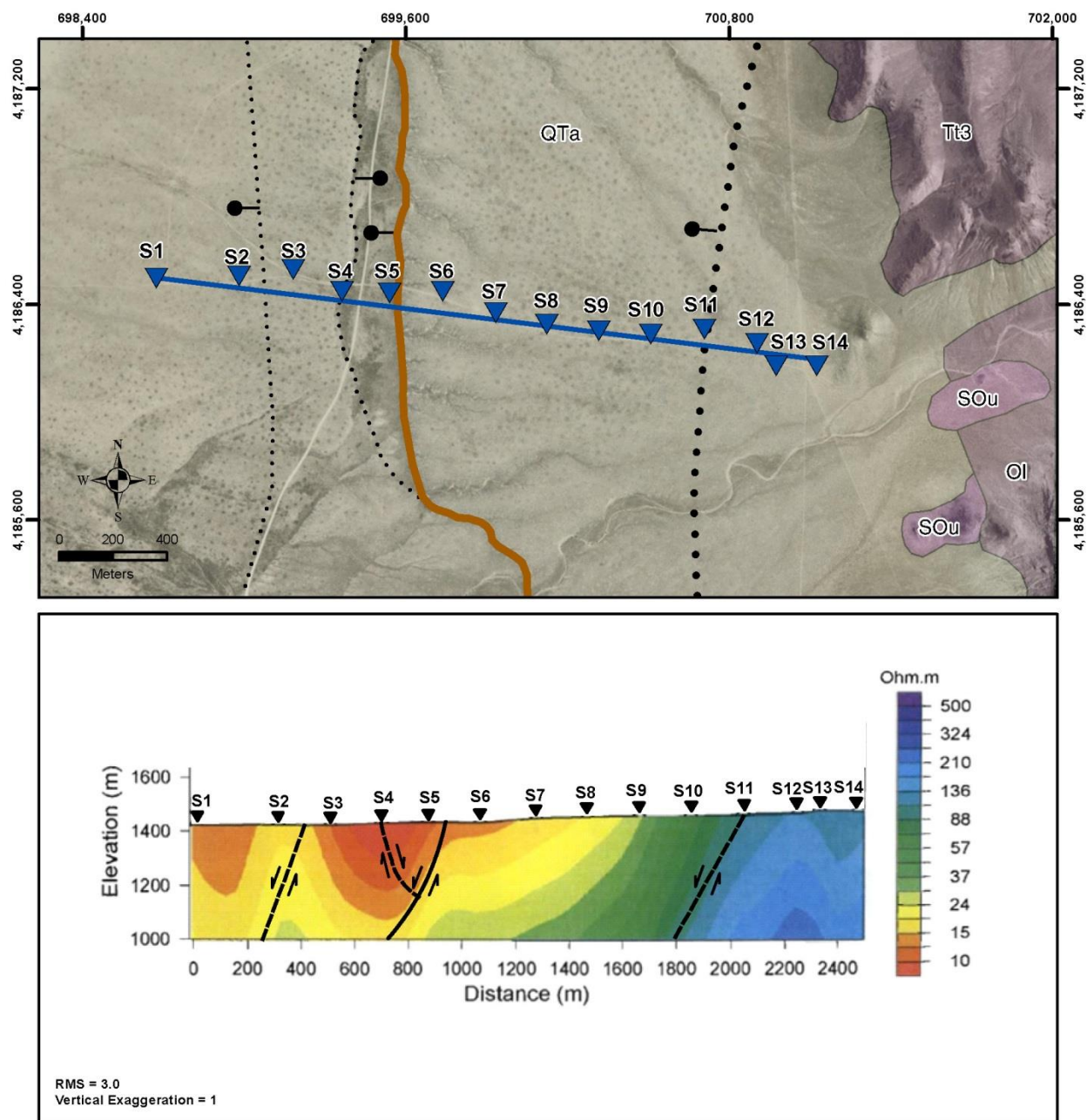
overall arrangement of faults is largely strike-slip along the northeast-striking faults and is largely dip-slip along the north-striking faults. It is likely that considerable groundwater is moving southwestward along these two faults. All profiles were collected by McPhee et al. (2008) and interpreted by SNWA; all are discussed by Pari and Beard (2011). Only two of the profiles are described here ([figure 34](#)).

AMT Profile DELA5

Profile DELA5 ([figure 41](#)) has a length of 0.7 km so as to cross the Delamar Lake fault of the Pahrnagat shear zone. The map shows that the profile runs along the southwestern side of Delamar Lake, a playa lake that is generally dry except after rain. The profile shows a wide, steeply southeast-dipping fault zone marked by highly conductive material that likely represents hydrothermal clay, fault gouge, and groundwater. South of the fault zone, lake clays are the more highly conductive material at depth; lower conductivity rocks at the surface are sediments above the water table.

AMT Profile DELA1

Profile DELA1 ([figure 42](#)) has a length of 1.2 km, extending northwestward from the southern Delamar Mountains to cross the Maynard Lake fault, the largest of the faults of the Pahrnagat shear zone. The spectacular resistivity contrasts clearly demonstrate a large subvertical strike-slip fault carrying a great deal of groundwater southwestward. Interestingly, the axis of the fault has less conductivity than the rocks on either side. This axis probably represents fault gouge in the central core zone of the fault, which has less permeability than the fractures on either side of the axis in the outer damage zones of the fault.



Legend

- ▲ AMT station
- AMT profile DLV8

Regional Faults

- Normal fault
- Quaternary normal fault
- Solid where known; dotted where concealed. Bar and ball on downthrown side of fault.

Subsidiary Fault

- Normal fault
- Dotted where concealed. Bar and ball on downthrown side of fault.

Geologic Unit and Description

- QTa Quaternary and Tertiary alluvium
- Tt3 Tertiary poorly-densely welded ash-flow tuff and interbedded airfall tuff
- SOu Silurian and Upper Ordovician dolomite, undivided
- Ol Middle and Lower Ordovician, mostly eureka Quartzite and Pogonip Goup

Map ID 17505-3212 04/06/2011 JAB

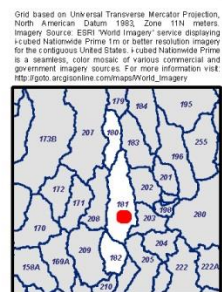


Figure 40. Geologic map and 2D model of AMT profile DLV8.

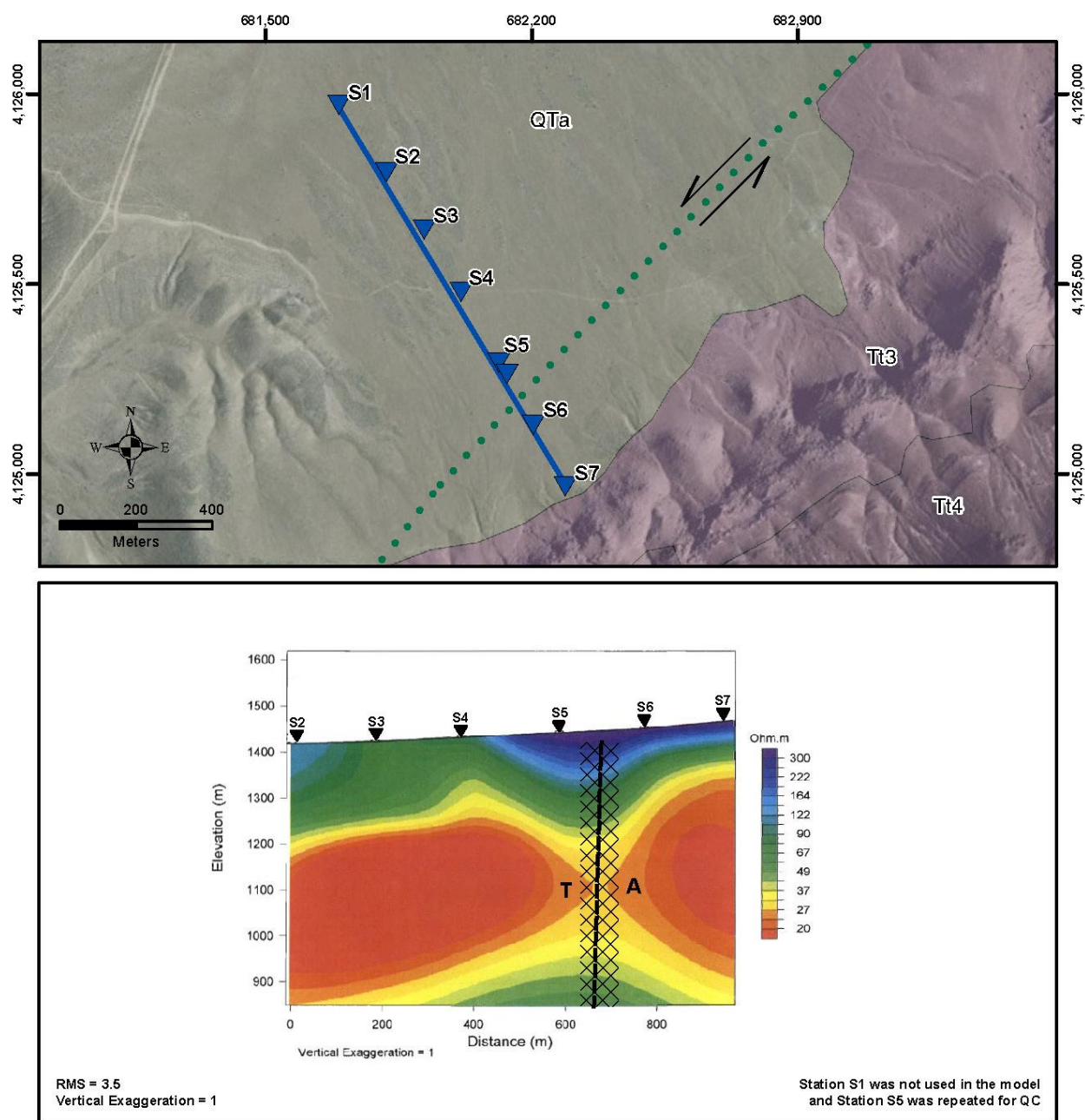


Figure 42. Geologic map and 2D model of AMT profile DELA1.

DESCRIPTIONS OF BASINS AND RANGES

Knowledge of the structure, stratigraphy, and geometry of individual basins and ranges in the study area ([figure 2](#)) was needed in order to understand the potential for interbasin groundwater flow. Specific flow pathways are controlled by topographic and geologic features, whose accurate geologic mapping and analysis are critical to interpreting flow routes between basins. This section also updates the discussion of individual basins and ranges provided by the old county reports. Mountain ranges adjacent to the basins are described in more detail than the valleys due to their greater exposure of pre-Quaternary geologic units. Because of this, the discussion below is organized by ranges, and the adjacent basins are discussed within these sections going from north to south and west to east, starting in the northwestern part of the study area.

RUBY MOUNTAINS, BALD MOUNTAIN, AND BUCK MOUNTAIN

The Ruby Mountains, just west of the study area, form a horst in which large amounts of vertical uplift resulted in detachment or attenuation faults along the margins. The range is considered a metamorphic core complex formed during major uplift (Howard et al., 1979; Wright and Snoke, 1993; Howard et al., 2011). Most rocks in the range dip east and are early Paleozoic in age. The Ruby Mountains is cored by a Jurassic to Miocene batholith and Precambrian to Lower Cambrian rocks.

Bald Mountain consists of east-dipping lower Paleozoic rocks cored by Jurassic intrusions that formed major deposits of gold, silver, and other metals (Hitchborn et al., 1996). Bald Mountain joins Buck Mountain, a horst of subhorizontal middle Paleozoic rocks. Low-angle Tertiary attenuation faults separate Paleozoic units in many places, from Bald Mountain to Buck Mountain, and several Sevier thrust faults of small displacement were also noted (Nutt, 2000; Nutt and Hart, 2004).

Ruby Valley is a deep graben bounded by the Ruby Mountains to the west, Maverick Springs Range (see [Maverick Springs Range](#) below) to the

east, and Bald Mountain to the south ([figure 2](#)). This graben is locally ~1500 m deep. On the western side of the Ruby Mountains and Bald Mountain is Huntington Valley, a graben that is several hundred meters deep. This valley is bounded on the west by the Diamond Mountains. Newark Valley is bounded by the Diamond Mountains to the west and by Bald and Buck mountains to the east. This valley is another graben with locally more than 1500 m of valley fill ([plate 3](#), cross section X–X'); it is further described in [Butte Mountains and White Pine Range](#). Seismic profiles reveal Sevier thrusts beneath the basin-fill deposits (Dobbs et al., 1994). These thrusts, which are well exposed just to the west, south of the town of Eureka, are part of the east-verging thrusts and folds of the central Nevada thrust belt, within the Sevier hinterland (Greene, 2014).

MAVERICK SPRINGS RANGE

The Maverick Springs Range of northern White Pine County, Nevada, is a low, northeast-trending range of mostly east-dipping upper Paleozoic rocks uplifted along a normal fault on the western side. The range bounds the southeastern edge of Ruby Valley. The eastern side of the Maverick Springs Range is bounded by a normal fault, down to the east, that separates it from Long Valley to the east. The northern end of the Maverick Springs Range is cored by a Tertiary pluton ([plate 3](#), cross section Y–Y') that continues north into Elko County, Nevada, as a broad series of hills, floored by cupolas of a Tertiary stock or batholith. The southern half of the Maverick Springs Range becomes Alligator Ridge, which joins Buck Mountain to the south, although geologically separated from Buck Mountain by a down-to-the-west normal fault. Alligator Ridge is the site of a major gold deposit (Nutt, 2000). Tertiary attenuation faults and a small Sevier thrust fault have been mapped on Alligator Ridge (Nutt, 2000; Nutt and Hart, 2004).

Long Valley, at the northwestern part of the study area, is narrow and shallow (i.e., thin basin-fill sediments) at its northern end but it widens and

deepens to at least 1000 m of basin-fill sediments to the south. The fault zone that bounds the western side of the Maverick Springs Range in Ruby Valley passes south through Mooney Basin (between the southern Maverick Springs Range and the Bald Mountain-Buck Mountain ridge).

BUTTE MOUNTAINS AND WHITE PINE RANGE

The Butte Mountains are located east of Long Valley, to the west of central and southern Butte Valley. The Butte Mountains are a 60-km-long, north-trending horst of east-dipping to anticlinally folded, upper Paleozoic sedimentary rocks (Hose and Blake, 1976; Otto, 2008; Douglass, 1960; Pekarek, 1988). Several Sevier thrust faults of small displacement were mapped by Howard (1978) and Otto (2008). The small thrusts are due to tight harmonic folding (Otto, 2008). Southward, the Butte Mountains joins the eastern side of the north-trending, 80-km-long White Pine Range across a low range of hills of upper Paleozoic carbonate rocks and Tertiary volcanic rocks. The southern end of the Butte Mountains also joins with several repeated fault ridges of the Egan Range (see [Northern Egan Range](#)) to the east across a similarly low range of volcanic hills that forms the southern end of Butte Valley.

The northern White Pine Range is comprised of a low, broad series of horsts and grabens (Gans, 2000a). One of the grabens becomes Long Valley to the north, and the eastern horst becomes the Butte Mountains to the north. The northern White Pine Range is underlain largely by upper Paleozoic rocks, but middle Paleozoic rocks underlie some of the horsts (Lumsden et al., 2002) and Tertiary volcanic rocks underlie some of the grabens ([plate 3](#), cross section W–W'). The middle Paleozoic rocks include repeated fault blocks containing the Chainman Shale. The southern end of the White Pine Range has considerable elevation (up to 3500 m) and is made up mostly of east-dipping, lower to middle Paleozoic rocks. The range here has a large eastward bulge, the White River caldera, which includes an underlying resurgent dome that undoubtedly is responsible for the high relief of the range ([plate 3](#), cross section V–V'). The north-trending axis of the caldera contains a narrow,

north-striking graben. West of the caldera, the rocks include Cambrian to Precambrian siliciclastic rocks intruded by a Tertiary pluton. Locally the Paleozoic rocks are cut by late Cenozoic attenuation/denudation faults (Moores et al., 1968; Francis and Walker, 2002; Walker and Francis, 2002), and Gans (2000a) mapped one small east-verging Sevier thrust.

Butte Valley, east of the Butte Mountains, is a graben similar to Long Valley. Butte Valley contains upper Paleozoic rocks at a shallow depth, with overlying Tertiary volcanic rocks in the southern part of the valley. The valley fill is a maximum of about 1200 m thick, in turn overlying less than 300 m of Tertiary volcanic rocks. A narrow horst is within the northern end of Butte Valley ([plate 3](#), cross section Y–Y').

Jakes Valley, south of the Butte Mountains, may be as deep as 2000 m ([plate 3](#), cross section W–W'), with Tertiary volcanic rocks and upper Paleozoic carbonate rocks beneath about 1500 m of basin-fill sediments. West of the White Pine Range, Newark Valley is a shallow graben, narrowing and becoming shallower to the south, as described in [Ruby Mountains, Bald Mountain, and Buck Mountain](#). West of the southern end of the White Pine Range, Newark Valley opens out southward into Railroad Valley, a broad deep graben. East of the axis of the White River caldera, the White Pine Range is dropped down along many down-to-the-east normal faults that also accommodated development of White River Valley to the east. Although relatively shallow at this latitude, near Preston and Lund, Nevada, White River Valley widens and becomes a deep, broad graben to the south, with a depth of more than 1500 m (see next section).

HORSE, GRANT, AND QUINN CANYON RANGES

At the southern side of the White River caldera in northern Nye County, Nevada, the east-striking, oblique-slip (left lateral and normal) Currant Summit fault zone (Moores et al., 1968; Williams and Taylor, 2002), part of the Pritchards Station transverse zone (Ekren et al., 1976; Rowley, 1998; Rowley and Dixon, 2001), structurally separates the White Pine Range to the north from

the small, 30-km-long, north-trending Horse Range to the south. Another east-striking, oblique-slip (left-lateral and normal) fault zone, called the Stone Cabin fault zone by Moores et al. (1968), passes through the Horse Range about 15 km south of the Pritchards Station transverse zone and continues west to terminate the northern end of the Grant Range; this is the eastern part of the Pancake Range transverse zone (Ekren et al., 1976; Rowley, 1998; Rowley and Dixon, 2001). The Horse Range (Moores et al., 1968) consists of east-dipping, lower to middle Paleozoic sedimentary rocks ([plate 3](#), cross section U–U'). The Horse Range is uplifted on its western side against thick, east-dipping volcanic rocks and basin-fill sediments to the west. The basin-fill sediments fill Horse Camp Basin (Moores et al., 1968; Brown and Schmitt, 1991), and the volcanic rocks form the eastern flank of the northern Grant Range and underlie the basin.

The Grant Range is 60-km-long, increasing in width southward. It, in turn, passes into the high, broad Quinn Canyon Range to the south, which is 24 km north-south by 32 km east-west. These ranges are bounded on the west by the deep graben of Railroad Valley, whereas the Horse and Grant ranges are bounded on the east by the large, deep graben of White River Valley. The Grant Range is underlain mostly by east-dipping Cambrian through Permian carbonate rocks (Lumsden et al., 2002), with Tertiary ash-flow tuffs on the eastern flank (Scott, 1965). In addition to the large north-striking, high-angle normal faults that control the range, the northern part of the range is cut by many late Cenozoic, low-angle attenuation/denudation faults (Scott, 1965; Moores et al., 1968; Lund et al., 1991; Lund and Beard, 1992; Francis and Walker, 2002; Walker and Francis, 2002). These low-angle faults continue south into the northern Quinn Canyon Range, north into the White Pine Range, and west into Railroad Valley. They also have been mapped as far east as the Schell Creek Range. Commonly the faults follow the Chainman Shale (Francis and Walker, 2002; Walker and Francis, 2002). In the Grant Range, the attenuation faults were preceded by east-verging Sevier thrust faults of the central Nevada thrust belt (Bartley et al., 1988; Fryxell, 1988; Bartley and Gleason, 1990; Taylor et al.,

1993, 2000; Ekren et al., 2012). Composite Upper Cretaceous and Tertiary plutons, including the Troy Peak granite, were intruded into the Paleozoic rocks in the southwestern part of the Grant Range (Armstrong, 1970; Fryxell, 1988) ([plate 3](#), cross section Q–Q'). Low-angle Tertiary attenuation/denudation faults dip into Railroad Valley from both sides, especially from the Grant Range on the east (Lund et al., 1991). Many subsurface attenuation/denudation faults were detected during widespread exploration for oil in Railroad Valley (Lund et al., 1991; Blank, 1993; Schalla and Johnson, 1994; French and Schalla, 1998; Ehni and Faulds, 2002). The carbonate rocks plunge generally northward in the range, so Cambrian and Precambrian siliciclastic rocks and the Tertiary intrusive rocks form the core of the southern Grant Range.

The Quinn Canyon Range, south of the Grant Range, is bordered by Garden Valley to the east, the southern end of Railroad Valley to the north and northwest, and Penoyer Valley (Sand Spring Valley) to the south. Garden Valley is a narrow graben several hundred meters deep, between the Quinn Canyon and Golden Gate ranges ([plate 3](#), cross sections T–T' and Q–Q'). The Quinn Canyon Range is almost entirely underlain by all or parts of several eastern calderas of the newly discovered Monotony Valley caldera complex (Ekren et al., 2012), the source of the Monotony Tuff (27 Ma) and Shingle Pass Tuff (26 Ma). It is the eastern part of a cluster of calderas that continues west and northwest (Dixon et al., 1972; Ekren et al., 1972, 1973a and b, 1974; Snyder et al., 1972; Quinlivan et al., 1974). This cluster of calderas is what Best et al. (1993, 2013b) and Scott et al. (1995a) called the central Nevada caldera complex. This feature is not, however, a true caldera complex because not all of it has subsided as a caldera; instead, individual calderas are separated by pre-caldera rocks, so it might better be considered a cluster of adjacent calderas. The southeastern end of the Quinn Canyon Range and the southern edge of the Monotony Valley caldera complex is in Lincoln County. The caldera complex underlies Penoyer Valley (Sand Spring Valley), which makes up the single-basin Penoyer Valley flow system (Harrill et al., 1988).

Gravity surveys on the eastern side of White River Valley (Scheirer, 2005) suggest that the valley consists of thick basin-fill sediments and volcanic and carbonate rocks. We interpret that the White River Valley contains at least 1500 m of valley fill (Dixon et al., 2007a and c) ([plate 3](#), cross sections Q–Q' and U–U'). The valley narrows southward east of the Seaman Range (here called Pahroc Valley) as the ephemeral White River was incised into Pleistocene basin-fill sediments during canyon cutting following drainage integration with the Colorado River (Dixon, 2007) ([plate 3](#), cross section T–T').

Springs are abundant in White River Valley, especially in the center of the valley and near Nevada Highway 318, which is just west of the eastern side of the valley. Those in the center of the valley are warm and hot springs, some of which supply lakes that together were grouped and set aside as the Wayne Kirch Wildlife Management Area, managed by the Nevada Department of Wildlife. As far as we can tell, virtually all springs in White River Valley come up along north-trending normal faults, many of them with Quaternary displacement. Hydrologic data and geologic cross sections of most springs in White River Valley are discussed in Volume 3 of Southern Nevada Water Authority (2008), including Hot Creek Spring in the Wayne Kirch Wildlife Management Area.

WORTHINGTON MOUNTAINS AND TIMPAHUTE RANGE

The northern end of the narrow, 25 km-long, north-trending Worthington Mountains is just southeast of the Quinn Canyon Range. The Worthington Mountains define the northeastern side of Penoyer Valley and the western side of southern Garden Valley. The Worthington Mountains consists mostly of west-dipping Ordovician through Mississippian rocks that are uplifted along a north-striking fault on the eastern side of the range. The range contains the east-verging Freiburg thrust, which placed Ordovician rocks on Ordovician and Devonian rocks during Sevier deformation (Taylor et al., 2000). The thrust is part of the central Nevada thrust belt (Greene, 2014).

The Worthington Mountains extend southward into the east-trending Timpahute Range, which separates the southeastern side of Penoyer Valley from northern Tikaboo Valley. The Timpahute Range is underlain by Upper Cambrian through Permian sedimentary rocks, unconformably overlain by Tertiary volcanic rocks. The Paleozoic rocks are cut by several Sevier thrusts, the lowest of which places Devonian rocks over Devonian through Permian rocks. The uppermost thrust places Cambrian through Ordovician rocks above younger rocks (Taylor et al., 1994). The western end of the range includes the Tempiute mining district of tungsten and silver, associated with two Tertiary granite stocks. The range is heavily broken by north-south normal faults and synchronous east-west faults. The east-west faults, which define the southern margin of the range, are part of the Timpahute transverse zone, which also controls the northern side of the Caliente caldera complex.

Garden Valley, east of the Worthington Mountains, terminates southward against the eastern Timpahute Range. Garden Valley is a graben containing about 1000 m of basin-fill sediment ([plate 3](#), cross section T–T'). Penoyer Valley is bounded on the east by a range-front fault and on the south by the east-west Timpahute transverse zone. Penoyer Valley probably contains about 1000 m meters of basin-fill sediments.

GOLDEN GATE RANGE, MOUNT IRISH, AND PAHRANAGAT RANGE

The north-trending Golden Gate Range is 60 km long and consists of low faulted hills that pass southward into the Mount Irish Range, a 15-km by 15-km range bounded by east-striking faults. The Mount Irish Range is the northernmost part of the larger, 60-km-long Pahrnagat Range, which continues southward into the 80-km-long Sheep Range. The northern end of the Golden Gate Range, located in Nye County, Nevada, forms the western side of White River Valley and the eastern side of Garden Valley. The main part of this range forms the boundary between Garden and Coal valleys in Nye and Lincoln counties. In Nye County, the Golden Gate Range consists of Devonian through Pennsylvanian rocks overlain by

Tertiary volcanic rocks. Here and farther south, the range is a west-tilted horst; the main controlling normal fault is on the eastern side. In Lincoln County, the rocks of the Golden Gate Range are Devonian to Pennsylvanian sedimentary deposits, of which Ordovician through Devonian rocks are thrust over Devonian to Mississippian rocks (Armstrong, 1991) ([plate 3](#), cross section T–T').

The Mount Irish Range is a stubby, east-trending block that is the eastern continuation of the Timpahute Range and is controlled by east-striking, oblique-slip faults of the Timpahute transverse zone. The Mount Irish Range is made up of Ordovician through Mississippian rocks containing the same thrusts, including the Gass Peak thrust, that occur in the Timpahute Range ([plate 3](#), cross sections O–O' and S–S') (Taylor et al., 1994 and 2000). The Mount Irish block closes the southern end of Coal Valley.

The Pahrnatag Range, including a separate parallel structural block along the eastern side that is called the East Pahrnatag Range, is bounded by deep (thick basin-fill sediments) Tikaboo Valley on the west and shallow Pahrnatag Valley (Tingley et al., 2010) on the east. The Pahrnatag Range (Page et al., 2005a; Jayko, 1990 and 2007) is a horst bounded on both sides by major normal faults ([plate 3](#), cross sections M–M' and N–N'). In the north, the range dips gently west but in the south it is a syncline. The east-verging Sevier-related Gass Peak thrust strikes the length of the range, placing Middle Cambrian to Devonian rocks on Devonian to Mississippian rocks. The East Pahrnatag Range locally consists of an overturned fold of Devonian to Pennsylvanian rocks. Tertiary volcanic rocks unconformably overlie the folded and thrust-faulted Paleozoic rocks and are thickest where downfaulted into a graben between the Pahrnatag Range and East Pahrnatag Range. At their southern ends, the Pahrnatag and East Pahrnatag Ranges are separated from the northern Sheep Range by a series of east-northeast-striking splays of the predominantly left-lateral Pahrnatag shear zone (PSZ) (Ekren et al., 1977; Johnson, M. 2007a). The southern splay of the PSZ is the Maynard Lake fault zone ([plate 4](#), cross section A–A') (Tschanz and Pampeyan, 1970; Jayko, 1990 and 2007). The western part of this fault is interpreted to join the main north-south normal fault that

defines the western side of the Sheep Range, and the eastern part of the fault is interpreted to join the main north-south normal fault that defines the western side of the Delamar Mountains. In this interpretation, the Maynard Lake zone—like the others of the PSZ—is a transfer fault that transfers east-west extension (pulling apart) into left-lateral shear. In this scenario, in those places where faults strike north, all east-west extension is taken up by normal movement down the dip of the fault plane, and where faults strike northeast, east-west pulling apart is taken up by mostly left-lateral movement.

Pahrnatag Valley (see also [North Pahrnatag, South Pahrnatag, and Hiko Ranges](#)), between the East Pahrnatag Range on the west and the Hiko Range on the east, is a remarkably well-watered valley containing the agricultural communities of Hiko and Alamo, Nevada, and two large lakes that are the home of the Pahrnatag National Wildlife Refuge (U.S. Fish and Wildlife Service). Structurally, the valley is a shallow graben ([plate 3](#), cross sections S–S', O–O', N–N', and M–M'). Several large regional springs, including Hiko and Crystal springs and Ash Spring, are controlled by normal faults (Dixon and Van Liew, 2007; Volume 3 of Southern Nevada Water Authority, 2008).

SHEEP RANGE, LAS VEGAS RANGE, AND ELBOW RANGE

The northern Sheep Range is a narrow and high mountain range that consists of Cambrian and Ordovician sedimentary rocks forming the leading edge of the Gass Peak thrust fault of the main Sevier frontal thrust belt ([plate 4](#), cross section L–L'; Page et al., 2005a; see also Greene, 2014). The southern Sheep Range consists of mostly Cambrian and Ordovician carbonate rocks that dip eastward ([plate 4](#), cross sections E–E', F–F', G–G', and H–H') (Guth, 1980). The entire range is a large tilt block uplifted along major north-striking, normal faults on its western side. The thrust transported Neoproterozoic to Cambrian quartzite and Cambrian to Devonian carbonate rocks eastward over Cambrian to Mississippian rocks. Within the Sheep Range, north-striking normal faults are abundant, but some cross-faults

that strike east to east-northeast also have been mapped.

Quaternary normal faults define much of the eastern side of the range (Dohrenwend et al., 1996). Pleistocene basalt has locally been injected into some of these eastern faults.

A small, north-trending range lies east of the northwestern arm of Coyote Spring Valley and west of Pahranaagat Wash, U.S. Highway 93, and northeastern Coyote Spring Valley. The small range is considered part of the northern Sheep Range but is separated from the high Sheep Range to the west by northwestern Coyote Spring Valley. The northern end of this small range terminates against the Maynard Lake fault zone of the PSZ. This small Basin and Range tilt block consists largely of east-dipping volcanic rocks (Jayko, 1990 and 2007) that rest unconformably on Pennsylvanian and Permian carbonate rocks. North-striking normal faults within, west, and east of the small range pass into the Maynard Lake fault zone and transfer their normal slip to oblique slip. The buried north-striking trace of the Gass Peak thrust fault passes beneath the normal faults near the western side of the small range.

The Las Vegas Range northwest of Apex is defined by the Gass Peak thrust, which transported rocks as old as the Cambrian Wood Canyon Formation eastward over Mississippian, Pennsylvanian, and Permian carbonate rocks of the Bird Spring Formation ([plate 4](#), cross sections F–F', G–G', H–H', and I–I') (Maldonado and Schmidt, 1991). Most of the range is made up of folded Bird Spring limestone, with the Gass Peak thrust exposed along its western side (Maldonado and Schmidt, 1991; Page, 1998). The small Elbow Range, which bounds the Las Vegas Range on the northeast, is made up of thrust and folded Bird Spring Formation (Page and Pampeyan, 1996) that has been uplifted as a horst ([plate 4](#), cross sections E–E' and F–F'). The southern ends of the Sheep Range and Las Vegas Range, and continuing east, of the Arrow Canyon Range (see [Arrow Canyon Range](#)), Dry Lake Range, and Muddy Mountains (see [North Muddy Mountains](#), [Muddy Mountains](#), and [Dry Lake Range](#)) terminate against the west-northwest-striking, oblique-slip (right-lateral and normal) Las Vegas Valley Shear Zone (LVVSZ), which defines the northern side of the Las Vegas

basin (Workman et al., 2002a and b; Page et al., 2005a and b; Beard et al., 2007; Anderson and Beard, 2010).

CHERRY CREEK RANGE

The high Cherry Creek Range is in northern White Pine and southern Elko counties. The range is a large horst of gently to moderately west-dipping Precambrian through Permian sedimentary rocks. Normal faults separate it from Butte Valley on the west and from Steptoe Valley on the east; the bigger fault is on the east. A thin sliver of bedrock cored by a Tertiary intrusion connects the Cherry Creek Range with the northern Egan Range. A northeast-striking oblique-slip fault, left-lateral and down-to-the-west, cuts through the southern end of this sliver.

NORTHERN EGAN RANGE

Like the Cherry Creek Range to the north, the Egan Range is a high, north-trending west-tilted horst of Precambrian through Permian rocks, unconformably overlain by Tertiary volcanic rocks. The major normal fault zone that uplifted the Egan Range is along the eastern side. The vertical displacement along this fault is at least 3000 m. The range continues southward for 110 km in White Pine County, then another 60 km in Lincoln County. In the northern end of the range, the rocks dip westward and are intruded by Tertiary stocks. The Snake Range décollement is present here as a thin skin of Paleozoic rocks at the crest of the range and along its western slope ([plate 3](#), cross section X–X'). The décollement is a Tertiary denudation/attenuation fault that transported rocks as old as Middle Cambrian eastward and placed them on top of older rocks. Butte Valley is to the west and Steptoe Valley is to the east of the northern Egan Range.

About 30 km south of the northern end of the Egan Range, the range becomes considerably wider and lower as the Butte Mountains join it from the west and Butte Valley closes. Here, the range is broken into a series of horsts and grabens ([plate 3](#), cross section W–W'). The downthrown areas on the western side of the Egan Range are underlain by Tertiary volcanic rocks that form low ridges and

hills that connect with the southeastern Butte Mountains. The towns of Ely and Ruth, Nevada, are located in this broad, low, heavily faulted part of the Egan Range, in areas called Copper Flat and Smith Valley. A major mining district, the Robinson district, was developed on a series of east-trending ore deposits of copper, molybdenum, lead, zinc, silver, and gold associated with a middle Cretaceous pluton. Barren Eocene rhyolite plutons and volcanic rocks also are present in the area and extend to Ely on the eastern side of the Egan Range adjacent to Steptoe Valley (Brokaw and Shawe, 1965; Brokaw and Heidrick, 1966; Brokaw and Barosh, 1968; Brokaw, 1967, Brokaw et al., 1973; Jones, 1996; Gans et al., 2001; Tingley et al., 2010). Southwest of the mining district, a series of low hills extends southwest to the White River caldera of the White Pine Range. These hills provide the southeastern margin of Jakes Valley and the north-northwestern margin of White River Valley ([figure 2](#)).

South of the Robinson mining district, the Egan Range continues southward for almost 50 km to the latitude of Lund as a single, high horst of east-dipping Cambrian through Permian rocks that together are more than 10 km thick ([plate 3](#), cross section V–V') (Kellogg, 1963 and 1964; Taylor et al., 1991). Patches of volcanic rocks overlie the Paleozoic rocks on the eastern edge of the range. Several small plutons also are exposed. Major faults of the horst separate the Egan Range from the White River Valley to the west and southern Steptoe Valley to the east. Steptoe Valley is a deep graben containing as much as 2500 m of basin-fill sediments. Thus, it is one of the deepest grabens in the central Great Basin.

SOUTHERN EGAN RANGE

At the latitude of Lund, Nevada, a narrow ridge of Cambrian to Permian rocks extends southeastward from the main part of the Egan Range to the Schell Creek Range. This ridge, at Bullwhack Summit, forms the southern end of Steptoe Valley and the northern end of Cave Valley. The Egan and Schell Creek Ranges continue southward, with Cave Valley between them. Along the western side of Cave Valley ([plate 3](#), cross section U–U'), the Egan Range is a complexly

faulted horst of east-dipping Cambrian to Permian rocks, overlain by Tertiary volcanic rocks. White River Valley is west of the Egan Range. Southward, halfway down Cave Valley, at a latitude about 30 km south of Lund, a northeast-striking oblique-slip fault passes through the Egan Range at Shingle Pass ([plate 3](#), cross section R–R') then crosses Cave Valley to join the western range-front fault of the Schell Creek Range. Farther south, the Egan Range remains an east-tilted horst of Cambrian through Tertiary rocks, then bends southeast to join the southern end of the Schell Creek Range. Prominent springs occur along the western range-front fault of the entire Egan Range, as well as along many faults in eastern White River Valley. Cave Valley terminates where the Egan and Schell Creek ranges join each other in a complex of north-northeast- and north-northwest-striking normal and oblique-slip faults. Farther south, the combined Egan and Schell Creek ranges become a low, narrow, north-northwest-striking horst of faulted Paleozoic sedimentary rocks and Tertiary volcanic rocks ([plate 3](#), cross section Q–Q') that topographically continues southward to the northern end of the North Pahroc Range.

Cave Valley consists of two distinct but connected portions, separated by the oblique-slip fault at Shingle Pass. One of these portions, northern Cave Valley, is a narrow graben containing mostly east-dipping Cambrian rocks at shallow depth overlain by relatively thin volcanic rocks and in turn basin-fill sediments ([plate 3](#), cross section U–U'). Gravity data (Scheirer, 2005) and oil test well logs (Hess, 2004) indicate that the base of the combined basin-fill sediments and volcanic rocks is about 1000 m below the valley floor of northern Cave Valley.

Shingle Pass is formed by the intersection of several major faults, but primarily it is defined by the northeast-striking, oblique-slip (left lateral and normal) fault zone. At the western end of Shingle Pass, this fault zone cuts through upper Paleozoic limestone on its northern side and lower Paleozoic limestone on its southern side.

Southern Cave Valley, in Lincoln County, is as narrow as about 3 km wide at its northern end. The narrowing is due to a northeast-trending tilt block bounded on the northwest by the fault at Shingle

Pass and striking northeast across most of Cave Valley. The block is buried but continues in the subsurface to the northeast to the large north-trending range-front fault zone that uplifts the Schell Creek Range ([plate 3](#), cross section R–R'). To the southwest, the tilt block swings into the main north-trending part of the Egan Range, which continues to the south. The tilt block consists of southeast-dipping Cambrian through Mississippian rocks that includes the Mississippian Chainman Shale, which is buried along the southeastern edge of the block. These relationships are supported by oil-test-well drilling, gravity surveys, seismic surveys and AMT profiles (Hess, 2004; McPhee et al., 2005, 2006a and b; Mankinen et al., 2006; Scheirer, 2005). Southern Cave Valley generally contains less than 1000 m of basin-fill sediments and volcanic rocks. In a narrow, central, north-trending axial part of the valley, however, these Cenozoic rocks are 2000 m or more thick. McPhee et al. (2005 and 2007) provided information on faults on the eastern side of the basin based on AMT profiles.

At the southern end of Cave Valley, a series of north-northwest-striking right-lateral oblique-slip faults and north-northeast-striking, left-lateral oblique-slip faults forms the boundary between southern Cave Valley, northern Pahroc Valley, and northern Dry Lake Valley. The range-front, oblique-slip fault (left-lateral and normal) zone that defines the western side of the southern Schell Creek Range juxtaposes Devonian dolomite against intrusive rocks. Two other north-northeast-striking faults west of the range-front fault cut through upper Paleozoic limestone, largely overlain by a relatively thin veneer of Tertiary ash-flow tuffs, in the block that defines the southern end of Cave Valley east of the eastern range-front fault of the Egan Range.

SEAMAN RANGE

The 55-km-long, intensely faulted Seaman Range, located in Nye and Lincoln counties, is a horst that trends north and northwest and joins the Golden Gate Range at the northern end of both ranges (see [Golden Gate Range, Mount Irish, and Pahrangat Range](#)). Coal Valley, between the two ranges, is a graben containing about 1000 m

of basin-fill sediments ([plate 3](#), cross section T–T'). The valley is bounded on the south by the Timpahute Range. At its northern end, the Seaman Range is low and bounds the southern end of the White River Valley. In Nye County, the Seaman Range is made up of Devonian to Pennsylvanian sedimentary rocks, overlain unconformably by Tertiary volcanic rocks (du Bray and Hurtubise, 1994). In Lincoln County, the Seaman Range is made up of gently west-dipping Ordovician to Pennsylvanian rocks that are unconformably overlain by Tertiary volcanic rocks. The Tertiary volcanic rocks include the dacitic to rhyolitic Seaman volcanic center of flows, subordinate tuffs, and a central plug (Ekren et al., 1977; Hurtubise and du Bray, 1992; du Bray, 1993; du Bray and Hurtubise, 1994).

NORTH PAHROC, SOUTH PAHROC, AND HIKO RANGES

The North Pahroc Range extends south for 60 km from the junction with the southern Egan and Schell Creek ranges. It is separated from the smaller South Pahroc Range by an east-trending belt of faulted rocks of low relief formed by the east-striking Timpahute transverse zone. This zone of faulted rocks is also the boundary between Dry Lake Valley to the north and Delamar Valley to the south. The Seaman (see [Seaman Range](#)) and the North Pahroc ranges are separated by Pahroc Valley but the ranges join together at their southern ends. The Hiko Range continues south of this intersection. The Hiko Range is a small range parallel to and west of the South Pahroc Range and east of northern Pahrangat Valley. The South Pahroc Range is south of the North Pahroc Range and forms the western boundary of Delamar Valley. The South Pahroc Range connects with the Hiko Range at their southern ends to form the eastern boundary of southern Pahrangat Valley. The ephemeral channel of the White River is present along the western side of the North Pahroc Range. The channel is deeply incised through Tertiary volcanic rocks at White River Narrows (Cook, 1965; du Bray, 1995; Dixon, 2007) then enters the Pahrangat Valley north of the town of Hiko, where the ephemeral channel is called Pahrangat Wash. Pahrangat Valley (see [Golden Gate Range](#),

[Mount Irish, and Pahrnagat Range](#)) is a shallow graben west of the Hiko Range that contains volcanic and Paleozoic bedrock ([plate 3](#), cross sections S–S', O–O', and N–N'). The large springs, including Crystal Spring (Dixon and Van Liew, 2007; Johnson, M., 2007b), in eastern Pahrnagat Valley, are controlled by the range-front faults that define the western side of the Hiko Range.

The North Pahroc, South Pahroc, and Hiko ranges are complex horsts. The North Pahroc Range consists of upper Paleozoic rocks overlain by Tertiary volcanic rocks. These rocks dip west off major faults along the eastern and western sides of the range (Scott et al., 1994 and 1995b; Scott and Swadley, 1992; Swadley et al., 1994a). The South Pahroc Range is a series of west-tilted blocks of volcanic rocks. The main faults are on the eastern side of the range (Swadley and Scott, 1991; Scott et al., 1993). The Hiko Range consists of Devonian rocks and overlying volcanic rocks that dip east off the normal fault that separates the range from the floor of Pahrnagat Valley. The South Pahroc and Pahrnagat ranges terminate to the south against the east-northeast-trending PSZ, which also truncates Pahrnagat and Delamar valleys.

Dry Lake Valley is a deep graben ([plate 3](#), cross sections T–T', P–P', and S–S'), bounded in part by Quaternary faults and located east of the southern Schell Creek Range and North Pahroc Range. The valley contains, in most places, 1000–1500 m of basin-fill sediments (Swadley, 1995; Mankinen et al., 2006; Dixon and Rowley, 2007b) but locally along the axis of the graben as much as 3000 m of sediments and underlying downfaulted volcanic rocks (Scheirer, 2005). Delamar Valley, just south of Dry Lake Valley, is a southward-deepening graben with a general maximum thickness of more than 1000 m of basin-fill sediments east of the South Pahroc Range (Mankinen et al., 2006; Dixon and Rowley, 2007b) but locally as much as 1500 m of sediments and underlying downfaulted volcanic rocks (Scheirer, 2005). AMT profiles show some details of the faults in Dry Lake and Delamar valleys.

The basin boundary between Dry Lake Valley and Delamar Valley is so low as to be imperceptible to a person standing on the ground. Here US 93 runs east-west along the boundary, traversing what appears to be a continuous north-trending

valley. Bedrock made up of east-striking fault blocks of Tertiary ash-flow tuffs and lava flows are exposed along the basin boundary both west (Scott and Swadley, 1992; Scott et al., 1995b; Swadley et al., 1994a) and east (Swadley and Rowley, 1994) of the valley, and regional tectonic studies (Rowley, 1998; Rowley and Dixon, 2001) indicate that the buried Timpahute transverse zone passes beneath the valley at US 93 and is exposed to the east and west of the valley. A depth-to-basement map shows that the thickness of basin-fill sediments and volcanic rocks along the basin boundary is from 750 to 2000 m thick. This thickness at the basin boundary, as well as continuation through the basin boundary between Dry Lake Valley and Delamar Valley of north-striking normal faults that bound the ranges on either side of the combined valleys, indicate that any basin boundary is indeed superficial.

The southern end of Delamar Valley is structurally complicated. It is defined by the northeast-trending PSZ (Ekren et al., 1977; Scott et al., 1993; Johnson, M., 2007b), which has at least 5 parallel, left-lateral faults, spread across a width of about 16 km. Three of these faults enter southern Delamar Valley, where they pass into a north-striking normal fault. In addition, other north-striking normal faults, some feeding into faults of the shear zone, define the east and west sides of Delamar Valley; some continue southward into Coyote Spring Valley. Two of the fault zones of the PSZ that enter southern Delamar Valley are the Delamar Lake fault to the north and the Maynard Lake fault to the south. The Maynard Lake fault continues southwestward to define the southern end of Pahrnagat Valley and the Pahrnagat Range and the northern end of the Sheep Range, then the fault enters Tikaboo Valley. AMT profiles made across both faults in southern Delamar Valley show that both are large subvertical faults. Near Maynard Lake, some of the fractures in the fault zone served as vents for late Cenozoic basalt lava flows. The fault creates a natural dam that impounds southern Pahrnagat Lake, in the southern end of Pahrnagat Valley. The lake is fed by springs that issue from the western range-front fault of the southern Hiko Range.

SHELL CREEK RANGE

The northern end of the Schell Creek Range is just south of the northern border of White Pine County. The range continues south for 190 km, mostly as a high, narrow, north-striking horst. Steptoe and Cave valleys are on the west, and Spring Valley, northern Lake Valley, and northern Dry Lake Valley (Muleshoe Valley) are on the east. The northern part of the Schell Creek Range is made up of a west-dipping sequence of Neoproterozoic through Permian rocks (Lumsden et al., 2002), with overlying Tertiary volcanic rocks along the faulted western flank of the range ([plate 3](#), cross section X–X'). Small Tertiary intrusions are exposed locally along the range. The main bounding normal fault, likely with thousands of meters of vertical throw, is on the eastern side of the range. The Snake Range décollement is locally exposed at the crest of the Schell Creek Range. This denudation/attenuation fault transported Middle Cambrian and younger rocks both westward and eastward over Lower Cambrian and older rock. About 15 km northeast of Ely, two north-northeast-striking, high-angle normal faults form a graben, Duck Creek Valley, within the range ([plate 3](#), cross section W–W'). The southern half of the Schell Creek Range along Cave Valley contains a narrow, heavily faulted sequence of Neoproterozoic through Tertiary rocks that dips east. Here the dominant fault is on the western flank of the range. West of the Geyser Ranch (Johnson, M., 2007a) ([plate 3](#), cross section U–U'), the rocks are mostly Neoproterozoic and Cambrian quartzite (Van Loenen, 1987), but farther south the rocks are dropped down along an east-trending fault at Patterson Pass and are mostly of middle to upper Paleozoic and Tertiary age ([plate 3](#), cross section R–R'). Where the Schell Creek Range joins the Egan Range, a Tertiary pluton has mineralized adjacent carbonate rocks at the Silver King Mine ([plate 3](#), cross section Q–Q').

Spring Valley, discussed in [Snake Range and Limestone Hills](#), is a broad, deep graben. On the southwestern side of Spring Valley, a thin ridge of gently northeast-dipping Pennsylvanian and Permian carbonate rocks extends southeast from the central Schell Creek Range to the Fortification

Range. Here, the low pass traversed by US 93 is called Lake Valley Summit. Spring Valley continues southeast on the eastern side of the Fortification Range. South of the thin carbonate ridge is Lake Valley (Johnson, M., 2007a), between the Schell Creek Range and the Fortification Range. Lake Valley contains at least 600 m of basin-fill sediments throughout its 90 km length but locally the sediments may be much thicker ([plate 3](#), cross sections U–U', R–R', and Q–Q') (Scheirer, 2005). The Schell Creek Range forms the northwestern boundary of Lake Valley for about 30 km southward until it bends south-southwest to join the Egan Range.

Northern Dry Lake Valley, also known as Muleshoe Valley, lies east of the southern Schell Creek Range. This valley contains about 1000 m of basin-fill sediments ([plate 3](#), cross section Q–Q'), and gravity surveys (Scheirer, 2005) indicate that locally more than 2000 m of basin-fill sediments plus underlying downfaulted volcanic rocks underlie the valley. A seismic profile crosses the valley.

FAIRVIEW, BRISTOL, WEST, ELY SPRINGS, HIGHLAND, BLACK CANYON, BURNT SPRING, AND CHIEF RANGES, AND PIOCHE HILLS

From north to south, the Fairview, Bristol, Highland, and Chief ranges are a 90-km-long group of north-trending, heavily faulted ranges of mostly east-dipping rocks. These in-line horsts and tilt blocks lie west of Lake and Panaca (Meadow) valleys. From north to south, the West, Ely Springs, Black Canyon, and Burnt Spring ranges are small horsts along the western side of the Bristol, Highland, and Chief ranges. Northern Dry Lake (Muleshoe) Valley is west of the Fairview Range, and the rest of Dry Lake Valley is west of the West, Ely Springs, Black Canyon, and Burnt Spring ranges. The Pioche Hills, which extend southeast from the eastern side of the southern Bristol Range, separates Lake Valley on the north from Panaca (Meadow) Valley on the south. All the ranges are uplifted along normal and oblique-slip (left-lateral and right-lateral, normal) faults.

The Fairview Range touches the Schell Creek Range across Muleshoe Pass, through which runs

the range-front faults for both the Schell Creek and Fairview Ranges. The Fairview Range is a horst made up of Devonian to Pennsylvanian rocks at both the northern and southern ends of the range (Best et al., 1998). The central part of the range consists of the western lobe of the Indian Peak caldera complex. The low passes between the Fairview Range and the Bristol Range and between Muleshoe Valley and the main part of Dry Lake Valley are cut by numerous east-striking faults of the Blue Ribbon transverse zone (Ekren and Page, 1995; Page and Ekren, 1995), which crosses the entire Great Basin at about this latitude (Rowley, 1998; Rowley and Dixon, 2001).

The Bristol Range is a horst that consists mostly of an east-dipping sequence of Cambrian carbonate rocks. The range is cored by a Tertiary pluton on the northern end that is associated with silver deposits of the Jackrabbit and Bristol districts. A low angle, west-dipping denudation or gravity-slide fault that placed Devonian rocks on Cambrian rocks is exposed in the northwestern part of the range (Page and Ekren, 1995). The Highland Range, which is the southward continuation of the Bristol Range, consists of east-dipping Cambrian carbonate rocks, underlain by Neoproterozoic and Cambrian quartzite. A moderately west-dipping, down-to-the-west fault on the western side of the range, apparently the breakaway part of the Highland detachment fault, placed the younger carbonate rocks on the apparently older quartzite. The Chief Range, south of the Highland Range, is made up of east-dipping Neoproterozoic and Cambrian quartzite that is unconformably overlain by Tertiary volcanic rocks and cut by a Tertiary pluton that controls the small Chief gold district (Rowley et al., 1992, 1994). The faults that lift the range on the western side consist of an oblique-slip fault (right lateral and normal) and the west-dipping Highland detachment fault.

The small West Range, to the west of the northern Bristol Range, consists of Devonian sedimentary rocks and Tertiary volcanic rocks on which Devonian rocks are emplaced along a low-angle fault that can be interpreted as a denudation fault or a gravity-slide plane (plate 3, cross section T–T') (Page and Ekren, 1995). The Ely Springs Range, south of the West Range and northwest of the Highland Range, consists of Cambrian through

Silurian rocks, overlain by Tertiary volcanic rocks. The Black Canyon Range, south of the Ely Springs Range and southwest of the Highland Range, consists of Cambrian sedimentary rocks and Tertiary volcanic rocks (plate 3, cross section P–P'). The Burnt Springs Range, southwest of the Black Canyon Range, is made up of Cambrian sedimentary rocks unconformably overlain by Tertiary volcanic rocks (plate 3, cross section S–S').

The Pioche Hills consists of Cambrian sedimentary rocks unconformably overlain to the northeast by Tertiary volcanic rocks (Dixon and Rowley, 2007c). The hills contain the major Pioche lead-zinc-silver mining district, which is controlled by its proximity to the margin of the Indian Peak caldera complex (Best et al., 1989a and b). The margin includes caldera-collapse megabreccia and caldera ring dikes. Panaca (Meadow) Valley, south of the Pioche Hills, is probably at least 1500 m deep (plate 3, cross section P–P') and is filled with Pliocene to upper Miocene basin-fill sediments of the Panaca Formation (Rowley and Shroba, 1991).

DELAMAR MOUNTAINS

The Delamar Mountains extend southward for 60 km from the Burnt Springs Range, forming the western side of Delamar Valley and continuing to Coyote Spring Valley. The boundary between the Delamar and Burnt Spring ranges is the northern caldera wall of the Caliente caldera complex, here controlled by the east-trending Timpahute transverse zone (Ekren et al., 1976; Swadley and Rowley, 1994; Rowley, 1998). The eastern side of the northern Delamar Mountains is bounded by perennial, south-flowing Meadow Valley Wash, which drains Panaca (Meadow) Valley, passes south through Caliente, Nevada, and then creates Rainbow Canyon that separates the Delamar Mountains from the Clover Mountains to the east (Dixon and Rowley, 2007a and c; Tingley et al., 2010). The stream becomes ephemeral at the southern end of Rainbow Canyon, but in the Pleistocene it was part of through-flowing drainage that joined the Muddy River at Glendale, Nevada, and from there to the Colorado River. The eastern side of the southern Delamar Mountains is

Kane Springs Valley, to the east of which are the Meadow Valley Mountains.

The Delamar Mountains consist of east-dipping Neoproterozoic to Cambrian rocks and Tertiary volcanic rocks. The range, however, is dominated by Tertiary caldera complexes. The western end of the 24 to 12 Ma Caliente caldera complex is in the northern part of the range, and the 16 to 14 Ma Kane Springs Wash caldera complex is in the central part of the range ([plate 3](#), cross sections N–N', D–D', and C–C') (Scott et al., 1990a and b, 1991a and b, 1995a, and 1996; Swadley et al., 1994b; Harding et al., 1995; Rowley et al., 1995; Rowley and Dixon, 2001; Dixon et al., 2007b). The main bounding fault of the Delamar Mountains is the down-to-the-west normal fault on the western side (Page et al., 1990; Scott et al., 1990b), and this is joined from the southwest by several splays of the left-lateral and normal PSZ (Ekren et al., 1977). In Kane Springs Valley, the bounding fault is the oblique (left-lateral and normal down-to-the-west) Kane Springs Wash fault zone (Scott et al., 1991a; Swadley et al., 1994b).

MEADOW VALLEY MOUNTAINS

The Meadow Valley Mountains constitutes a narrow, generally low, north-northeast-trending range about 60 km long. The northern 50 km of the range consists mostly of outflow ash-flow tuffs and part of the Kane Springs Wash caldera complex ([plate 3](#), cross section C–C') (Scott et al., 1991a; Scott and Harding, 2006). The southern end of the Meadow Valley Mountains, just east of Coyote Spring Valley, is made up of mostly thrust-faulted and normally faulted Paleozoic rocks ([plate 3](#), cross sections C–C'; [plate 4](#), cross sections B–B', E–E', and F–F') (Pampeyan, 1993; Las Vegas Valley Water District, 2001). The Meadow Valley Mountains are separated from the Delamar Mountains on the west by Kane Springs Valley, a shallow valley underlain along the eastern side by the oblique-slip (normal, left-lateral) Kane Springs Wash fault zone (Swadley et al., 1994b; Harding et al., 1995; Scott et al., 1996). The broad, deep valley of Meadow Valley Wash lies east of the Meadow Valley Mountains and west of the

Mormon Mountains (Schmidt, 1994; Dixon and Rowley, 2007a).

ARROW CANYON RANGE

The Arrow Canyon Range is a sharp, narrow, north-trending range consisting of a syncline of Cambrian to Mississippian carbonate rocks. It is uplifted along its western side by normal faults of the Arrow Canyon Range fault zone ([plate 4](#), cross section I–I') (Schmidt and Dixon, 1995; Page and Pampeyan, 1996; Page, 1992, 1998). The trace of the north-striking Dry Lake thrust, which carries Cambrian rocks over Silurian through Permian carbonate rocks, is exposed and projected north just east of the range (Page and Dixon, 1992; Schmidt and Dixon, 1995; Las Vegas Valley Water District, 2001). East of the Dry Lake thrust, the Silurian through Permian rocks form a series of low, unnamed, north-trending hills. These hills are controlled by north-striking normal faults, along some of which are Pleistocene carbonate spring-mound deposits that indicate that the faults formerly carried significant groundwater (Schmidt and Dixon, 1995).

Coyote Spring Valley is west of the Arrow Canyon Range and Meadow Valley Mountains. A gravity survey by Phelps et al. (2000), as discussed by Dixon et al. (2007a), indicates that most of the valley is underlain by thin basin-fill sediments, generally less than 300 m thick ([plate 4](#), cross sections E–E', F–F', G–G', and L–L'), but that two deep (maximum depth at least 1000 m), north-trending sub-basins occur just west of the southern Meadow Valley Mountains and northern Arrow Canyon Range. The generally shallow (maximum depth about 500 m) Table Mountain basin lies just east of the northern Arrow Canyon Range (Page, 1992).

Pahrnagat Wash drains Coyote Spring Valley, then continues between the Arrow Canyon Range and the Meadow Valley Mountains to join the Muddy River near Muddy River Springs. Pahrnagat Wash is currently an intermittent stream but was perennial after White River Valley was integrated with the Colorado River, at least ten thousand years ago. It is well known that southeast-flowing groundwater beneath Pahrnagat Wash is the principal source of the many large springs in

the Muddy River Springs area, which currently create the surface flow in the perennial part of the Muddy River below the springs (Schmidt and Dixon, 1995; Donovan et al., 2004; Buqo, 2007; Donovan, 2007; Johnson, J., 2007). The details of the groundwater flow to Muddy River Springs were determined in part from the geologic mapping by Page (1992), Page and Pampeyan (1996), Schmidt et al. (1996), Williams et al. (1997c), and Donovan et al. (2004), and the geophysics of Scheirer et al. (2006). The mapping recognized that, following stream integration during the late Pleistocene, ancestral Pahrnagat Wash flowed southeast—as it does now—through Table Mountain basin, which contains well exposed basin-fill sediments of the Muddy Creek Formation and younger Holocene to late Miocene deposits. Many of these younger sediments were deposited by spring discharge. From Table Mountain basin, the ancestral river continued southeast, parallel to and south of Nevada Highway 168, through an unnamed ridge of north-trending, east-dipping, Paleozoic carbonates. The ridge is the southward continuation of the southeastern prong of the Meadow Valley Mountains. Among other southeastern tributaries, the ancestral stream cut spectacular Arrow Canyon (Page, 1992), which is currently dry. At Muddy River Springs, the dry Pahrnagat Wash becomes the Muddy River.

Additional geologic mapping by the USGS and SNWA showed that the bedrock ridge continues, although locally buried, for 30 km south of Arrow Canyon to become the Dry Lake Range (plates [2](#) and [4](#), cross sections F–F', G–G', H–H', and I–I'). The bedrock ridge is uplifted on both sides by north-trending basin and range faults, the largest being on the western side. These faults, plus others that parallel them on the east, served as groundwater conduits that carried groundwater southward, forming several upper Pleistocene spring mounds north of I-15 and west of the railway stop of Ute. Calcite veins as wide as 2 m, exposed in Wildcat Wash in the unnamed bedrock ridge, represent feeders for groundwater discharge along faults and fractures of the ancestral White River groundwater flow system (Page and Pampeyan, 1996). Within the bedrock ridge, east-trending faults are abundant, including some that

control Arrow Canyon and Battleship Wash just to the south. In addition, mapping suggests that a west- northwest-striking fault zone, probably with right-lateral motion, formed a broad canyon now followed by Highway 168 that was probably the result of another large ancestral stream that carried surface water, with groundwater beneath it. Virtually all springs in the Muddy River springs complex are controlled by fault intersections of east-, north-, and northwest-trending faults. Locally the faults created abrupt Pleistocene scarps, some of which failed as landslides (Donovan et al., 2004). White, post-Muddy Creek Formation (Pliocene) sediments were deposited by spring discharge east-southeast of Muddy River springs, in upper Moapa Valley. The new mapping indicated that west- to northwest-striking faults appear to control nearly the entire course of the Muddy River between Muddy River Springs and Logandale, including the course of the river through the North Muddy Mountains (at Jackman Narrows). As described in [North Muddy Mountains, Muddy Mountains, and Dry Lake Range](#), north-northwest-striking faults probably controlled the course of the Muddy River from Logandale to Overton, as well as the Overton Arm of Lake Mead. Some of the faults suggested by new mapping between Table Mountain basin and Lake Mead are buried by surficial sediments. To test the likelihood of faults in these areas, Scheirer and Andreasen (2008) interpreted gravity data that they collected along traverses oriented perpendicular to buried parts of some of the possible faults. The gravity data supported faults beneath Pahrnagat Wash in Table Mountain basin (gravity line 2 of Scheirer and Andreasen, 2008), along Nevada 168 in Table Mountain basin (gravity lines 1 and 2) and perhaps north of Muddy River springs (gravity line 3), perhaps at Muddy River springs (gravity line 3), beneath the Muddy River south of Moapa (gravity line 4se), and perhaps in three places near Overton (gravity line 12).

FORTIFICATION RANGE, WILSON CREEK RANGE, AND WHITE ROCK MOUNTAINS

The Fortification Range is a narrow, locally high, north-northwest-trending range about 30 km

long. The range is a horst bounded on both sides by normal faults. Northern Lake Valley is on the west, and the southern end of Spring Valley is on the east. The northern half of the Fortification Range is a series of faulted, upper Paleozoic carbonate rocks including, at the northern end, a narrow, low, north-northwest-trending, northeast-dipping cuesta that joins the eastern side of the Schell Creek Range. The northern Fortification Range is complexly faulted and contains repeated sections of the Chainman Shale beneath the surface.

The southern half of the Fortification Range consists of east-dipping volcanic rocks (Loucks et al., 1989), part of which we interpret to be intracaldera rocks of the Indian Peak caldera complex. The Fortification Range connects at its southern end with the broad Wilson Creek Range beyond a low pass. This pass, at the mining town of Atlanta, Nevada, is partly underlain by an east-striking normal fault.

The Wilson Creek Range is a complexly faulted, north-northwest-trending range that forks southward, with the continuation of the Wilson Creek Range on the west and with the White Rock Mountains on the east. A small central valley (graben), named Spring Valley, separates the two ranges. This valley is called “little” Spring Valley in this report to distinguish it from the much larger Spring Valley to the north. The Wilson Creek Range and White Rock Mountains are each about 55 km long and consist entirely of intracaldera volcanic rocks, probably floored by an unexposed intracaldera (resurgent) intrusion of the Indian Peak caldera complex (Willis et al., 1987; Best et al., 1989c). The western side of the Wilson Creek Range is bounded by its main normal fault. The valleys to the west of the range are northern Lake and Patterson (southern Lake) valleys. The southern half of northern Lake Valley and all of Patterson Valley are within the Indian Peak caldera. The White Rock Mountains are a horst, with its main fault on the eastern side. The southern ends of the Wilson Creek Range and White Rock Mountains pass into a series of mostly unnamed, generally low fault blocks of intracaldera volcanic rocks (Best, 1987; Keith et al., 1994; Best and Williams, 1997; Williams et al., 1997a). These fault blocks continue southward for 15 km to the southern wall of the Indian Peak caldera. The fault

blocks of the southern end of the White Rock Mountains extend eastward to join the southern Needle Range (Indian Peak Range) (Best et al., 1987a, b, and c), thereby closing off Hamlin Valley east of the White Rock Mountains. More fault blocks extend southward another 25 km as outflow volcanic rocks to the Clover Mountains, which is underlain by the Caliente caldera complex. Panaca Summit, traversed by Nevada State Route (SR) 319 and 15 km east of Panaca, is a pass through these hills of outflow volcanic rocks.

CLOVER MOUNTAINS AND BULL VALLEY MOUNTAINS

The Clover Mountains, Bull Valley Mountains, and northern Delamar Mountains represent a poorly defined, broad, east-trending, 100 km-long series of low mountains made up of heavily faulted volcanic rocks. North-south Rainbow Canyon, at the western edge of the mountain mass, is a narrow erosional cut made by Meadow Valley Wash. The northern part of the Delamar Mountains is west of Rainbow Canyon. The Clover Mountains extends from Rainbow Canyon for about 50 km to the Utah/Nevada border on the east, and from the Panaca (Meadow) Valley on the north about 40 km to the Tule Desert on the south. The Bull Valley Mountains extends another 30 km eastward from the Utah/Nevada border and is about 30 km north to south. The entire east-trending mountain mass passes into north-trending ranges on all sides. The mountain mass gets its unusual easterly trend partly because it is cored by the 80-km by 30-km Caliente caldera complex (Ekren et al., 1977; Rowley et al., 1992, 1995), mostly in Nevada but partly in Utah, and one of the largest calderas in the United States. The caldera complex is floored by an inferred intracaldera intrusion of batholithic dimensions, but it is exposed in few places ([plate 3](#), cross sections N–N' and D–D'). The caldera complex is unusually long lived, from 24 to 12 Ma.

Another reason for the easterly trend of the mountain mass is that the east-elongated Caliente caldera complex is bounded on the north and south by east-trending transverse zones, the Timpahute on the north and the Helene on the south (Rowley, 1998). The zones here consist of oblique-slip

(normal and left-lateral) faults. Locally, the transverse zones are caldera margins. These transverse zones facilitated differential east-west growth (spreading) of the caldera, driven by east-west extension and caldera eruptions. Rowley and Anderson (1996) referred to the complex as a syntectonic caldera. Hudson et al. (1998) called the mountain mass the Caliente-Enterprise zone. They found from paleomagnetic data that Tertiary calc-alkaline igneous rocks within this belt have undergone vertical-axis counterclockwise rotation due to the mass being bounded by left-lateral shears that were active largely during Basin and Range extension. The northern of these shears corresponds to the Timpahute transverse zone, and the southern corresponds to the Helene transverse zone. Petronis et al. (2014) provided additional data in Utah that confirmed most of the conclusions of Hudson et al. Petronis et al. found that the zone extends eastward to the Colorado Plateau, where the rocks are not rotated. Furthermore, the northern side of the zone represents, and owes its rotation to, a place where the generally north-south Colorado Plateau–Great Basin boundary swings abruptly to trend west, so that east-west extension is pulling on an east-west boundary. South of the caldera complex, the Clover Mountains is underlain by Paleozoic carbonate rocks cut by a Sevier thrust fault and many high-angle normal faults, but these rocks are blanketed by a thick cover of outflow ash-flow tuff, and the area is remote and poorly studied and mapped.

Anderson et al. (2013) interpreted that the Caliente-Enterprise zone formed from southerly ductile flow of middle- to lower-crustal material, and they questioned whether plate tectonics is the most logical driving force for such flow. However, in the latest of many analyses of GPS data in the Great Basin, Hammond et al. (2014) confirmed generally east-west extension and resulting shear across the central Great Basin, with maximum strain rates at the eastern and western margins of the Great Basin, all consistent with known Pacific/North American relative plate motions.

MORMON MOUNTAINS

The Mormon Mountains are a nearly circular range, about 30 km across, east of lower Meadow

Valley Wash. The Mormon Mountains represent a dome of mostly Cambrian to Permian rocks, underlain by Paleoproterozoic crystalline metamorphic rocks. East-verging Sevier thrust faults placed Cambrian rocks above Cambrian to Mississippian rocks. The range subsequently underwent major uplift, and it now is underlain by prominent positive aeromagnetic and gravity anomalies. Wernicke et al. (1985) interpreted the range to contain west-verging detachment faults that resulted from late Tertiary extension above a metamorphic core complex. Wernicke et al. (1985) suggested that these detachment faults followed thrust faults within the mountains. Anderson and Barnhard (1993) disputed the detachment hypothesis, and they instead emphasized footwall deformation along normal and oblique-slip, generally high-angle faults that flatten upward and formed during the major domal uplift. Carpenter and Carpenter (1994a) also disputed the detachment hypothesis, partly on seismic data unavailable to Wernicke and colleagues. Carpenter and Carpenter (1994a and b) argued for Tertiary extension along high-angle normal faults and explained Wernicke's low-angle structures as representing gravity slides. Walker et al. (2007) discussed data that supported the gravity-slide concept. These interpretations based on the findings since 1985 have been largely adopted by Page et al. (2005a), Scheirer et al. (2006), Anderson et al. (2010), and this report.

The broad valley of Meadow Valley Wash, to the west and northwest of the Mormon Mountains, is underlain by three geophysical sub-basins, the northern two of which contain basin-fill sediments and underlying volcanic rocks as thick as 2000 m, whereas the southern geophysical basin contains basin-fill and volcanic rocks as thick as 3000 m (Scheirer et al., 2006). Well logs suggest that the component of basin-fill sediments in these sub-basins is as much as 900 m ([plate 4](#), cross section E–E'). Northwest of the Mormon Mountains, two buried thrust faults have been hypothesized ([plate 3](#), cross section C–C'). Southwest of the Mormon Mountains, buried Paleozoic carbonate rocks may be present beneath Meadow Valley Wash ([plate 4](#), cross section B–B'). A band of hills continuing southward from the Mormon Mountains is underlain by Paleozoic

sedimentary rocks that are cut by Sevier thrust faults, including the Glendale/Muddy Mountains thrust ([plate 4](#), cross sections E–E' and F–F').

NORTH MUDDY MOUNTAINS, MUDDY MOUNTAINS, AND DRY LAKE RANGE

The southeastern corner of the study area contains the North Muddy Mountains and, to the south, the Muddy Mountains ([plate 4](#), cross sections H–H', I–I', and K–K') (Bohannon, 1983). The North Muddy Mountains separates the California Wash area on the west from the Mesquite basin (Virgin River Valley) on the east. The Muddy Mountains occupy the northern side of Lake Mead. West of the Muddy Mountains, the study area includes the small Dry Lake Range east of Apex. This range is made up mostly of Bird Spring carbonate rocks. A narrow arm of bedrock extending west from Apex connects with the southern Arrow Canyon Range/Las Vegas Range. A thin finger of Quaternary sediments at Apex, just west of the Dry Lake Range, most probably was a pathway for Tertiary and Quaternary basin-fill sediments entering the Las Vegas Valley in the southwestern corner of the study area. The finger also is along the trace of the north-northeast-striking Dry Lake thrust (Page and Dixon, 1992). Basin-fill sediments to the northeast along the I-15 corridor (California Wash area) belong to an east-tilted half graben that reaches depths of 3000 to 4000 m (Langenheim et al., 2001, 2010; Scheirer et al., 2006). The California Wash area does not appear to have been connected with the Las Vegas basin because, based on limited mapping in the area, the basin sediments are not correlated with those in the Las Vegas Valley.

In the Muddy Mountains and North Muddy Mountains, high-angle normal faults strike north-northeast (Bohannon, 1983; Beard et al., 2007), and the east-west gap between the two ranges, now occupied by Tertiary and Quaternary basin-fill sediments, is also likely underlain by fractures of the same strike. The northern Muddy Mountains and North Muddy Mountains contain significant Jurassic sedimentary rocks (Bohannon, 1983; Beard et al., 2007), including the Aztec Formation. The northwestern side of the North Muddy Mountains is made up of upper Paleozoic

carbonate rocks (Eichhubl et al., 2004; dePolo and Taylor, 2012). East-striking faults define the northern Muddy Mountains. These faults include the northeast-verging Glendale/Muddy Mountains thrust (Bohannon, 1983; Carpenter and Carpenter, 1994b; Beard et al., 2007). Bohannon interpreted this structure as the northern continuation of the Keystone thrust zone, which has been displaced approximately 60 km right laterally by the LVVSZ (see [Sheep Range, Las Vegas Range, and Elbow Range](#)). As with the Keystone/Glendale/Muddy Mountains thrust zone, the Dry Lake thrust just west of the Keystone/Glendale/Muddy Mountains thrust has been displaced the same amount by the same shear zone; its southern equivalent is the Deer Creek thrust in the Spring Mountains. Farther east in the North Muddy Mountains, the Summit/Willow Tank thrust is exposed ([plate 4](#), cross section J–J') (Bohannon, 1983, 1984, and 1992; Carpenter and Carpenter, 1994b; Beard et al., 2007). At the southeastern end of the Muddy Mountains and northern side of Lake Mead, the LVVSZ passes eastward into the northeast-striking, oblique-slip (left-lateral and normal) Lake Mead fault zone, both part of Quaternary and late Tertiary east-west extension in the area (Anderson and Barnhard, 1993; Castor et al., 2000; Workman et al., 2002a and b; Anderson, 2003; Duebendorfer, 2003; Page et al., 2005a and b; Beard et al., 2007, 2010; Langenheim et al., 2010; Anderson, 2013).

Lower Moapa Valley, in the southeastern edge of the study area and northwest of where the Muddy and Virgin rivers enter the Overton Arm of Lake Mead, is clearly an area of groundwater discharge (Harrill et al., 1988). Surficial sediments, dominated by Quaternary and Pliocene river deposits of the ancestral and present Virgin and Muddy rivers, and resistant calcretes underlie the valley and Mormon Mesa (Williams, 1996 and 1997; Williams et al., 1997b and c). The surficial deposits are underlain by Pliocene and upper Miocene basin-fill deposits making up the southwestern end of Mesquite basin (Billingsley and Workman, 2000; Dixon and Katzer, 2002; Johnson et al., 2002). Surficial and basin-fill sediments are lumped as the QTa unit in [plates 2](#) and [4](#), respectively, but in this area most basin-fill sediments are represented by the Horse Spring and

Muddy Creek Formations, which are exposed as low hills west of the river lowlands at Logandale and Overton. The Black Mountains and Gold Butte areas, respectively southwest and east of Lake Mead, contain Proterozoic metamorphic rocks that extend northeastward to the southwestern Virgin Mountains. Numerous fault zones have been mapped here and in the north Muddy Mountains (Beard et al., 2007; Anderson, 2003). These faults include northeast-striking faults of the Lake Mead fault zone (e.g., Anderson and Beard, 2010) that are discharge points for Rogers and Blue Point springs in the Lake Mead National Recreation Area.

Although not distinguished on the maps from Tertiary basin-fill deposits, deposits of the ancestral and present-day Virgin and Muddy rivers are likely to be many tens of meters thick, inasmuch as both rivers have been carrying and depositing sediments since at least the Pliocene. Permeability in the deposits is probably considerably greater than in the underlying finer-grained Muddy Creek Formation but probably not in the coarser Horse Springs Formation. A large northwest-striking, down-to-the-northeast, normal fault is interpreted to partly control the axis of the basin and the linear nature of Overton arm of Lake Mead. Gravity line 12 (Scheirer and Andreasen, 2008) imaged three density contrasts that might represent splays of the fault, even though density contrasts would be expected to be small between different beds in the underlying basin sediments. This fault downthrows river deposits on the northeast against Muddy Creek Formation on the southwest. Southwest of that fault, the poorly exposed Muddy Creek Formation may be dropped down against the Horse Spring Formation by a queried normal fault. These rock units, as well as underlying Mesozoic rocks west of them, dip northeast into the basin.

ANTELOPE RANGE

The Antelope Range, in northeastern White Pine County, Nevada, is a relatively small, low range of faulted, Tertiary volcanic rocks that unconformably overlie west-dipping Silurian to Permian sedimentary rocks, dominantly carbonate rocks. It is a horst between the narrow, northern part of Spring Valley on the west, and Tippet Valley (Antelope Valley) on the east. At its

northern end, Spring Valley contains about 600 m of basin-fill sediments. Tippet Valley contains at least 300 m of basin-fill sediments, with thick volcanic rocks beneath these sediments. Geophysical data, however, indicate that the depth to the pre-volcanic rocks locally is as much as 5500 m.

Gans et al. (1989) and Sweetkind et al. (2007a) speculatively showed the caldera source of the largest ash-flow tuff in the area, the 35 Ma Kalamazoo tuff, to be buried beneath northern Spring Valley just south of the Antelope Range and southwest of the Red Hills. Detailed gravity data were collected and analyzed by Mankinen and McKee (2011) of the USGS, through a cooperative agreement with SNWA. The gravity anomalies and depth-to-basement data do not support a caldera there, but suggest alternative caldera sites within Tippet Valley (see [Kern Mountains and Adjacent Small Ranges](#)).

DEEP CREEK RANGE

The Deep Creek Range is a high (about 3650 m altitude), north-trending range about 60 km long just east of the Nevada-Utah border and northeast of the Kern Mountains. The Deep Creek Range is a horst bounded by north-striking normal faults on either side that separate it from Deep Creek Valley to the west and northern Snake Valley and the Great Salt Lake Desert to the east. The fault on the eastern side of the Deep Creek Range appears to be the main normal fault controlling the range, and has vertical displacement of at least 3000 m, based on the height of the range and the Precambrian and plutonic rocks on its crest. Some of that displacement is Holocene (Black et al., 2003). The normal fault on the western side is also significant, for it drops Deep Creek Valley, which contains as much as 1500 m of basin-fill sediments.

Geologic mapping of the Deep Creek Range began with Nolan's (1935) classic report on the Gold Hill mining district at the northern end of the range. Here, Jurassic, Eocene, and Miocene plutons formed gold, tungsten, arsenic, silver, lead, copper, and zinc deposits in limestone of mostly Pennsylvanian and Mississippian age (Nolan, 1935; Robinson, 1993). Nolan mapped many east-striking faults that he called "transverse faults" and

recognized that they cut the range in many places. Rocks in the northern part of the mountains dip east and range from Neoproterozoic to Cambrian quartzite on the east to Devonian dolomite on the west. In the central part of the range, another Tertiary pluton, the Ibapah granite of 39 Ma (Rodgers, 1987; Miller et al., 1999a) spans the width of the range. The southern part of the range consists of highly deformed Neoproterozoic quartzite and schist of the McCoy Creek and Trout Creek groups. These Precambrian units have a combined thickness estimated at 6000 m (Nutt et al., 1990; Hintze and Kowallis, 2009). West of the southern part of the range, Paleozoic sedimentary rocks dip westward. These rocks range from Neoproterozoic and Cambrian quartzite through Cambrian and Devonian carbonate rocks and Mississippian Chainman Shale. They are cut by many low- to high-angle faults subparallel to the north-northeast-striking beds. The faults include low-angle faults (Miller et al., 1999a) that probably represent attenuation deroofing of the Deep Creek Range during its uplift.

KERN MOUNTAINS AND ADJACENT SMALL RANGES

The Kern Mountains is a 27-km-long, east-trending range that was structurally controlled by the Sand Pass transverse zone. East-striking faults occur on both the northern and southern sides of the range (Rowley, 1998; Rowley and Dixon, 2001). The granite core of the Kern Mountains is made up of three separate plutons. These plutons are all biotite-bearing. The largest pluton also contains primary muscovite. The plutons range in age from 75 to 35 Ma (Best et al., 1974; Ahlborn, 1977; Miller et al., 1999a). A separate, shallow Tertiary pluton erupted lava flows on the southeastern side of the range (Gans et al., 1989). The batholith that underlies the Kern Mountains is considered by Miller et al. (1999a) to represent part of an underlying core complex that formed the Snake and Deep Creek ranges and their attenuation/denudation faults. The Red Hills, a small north-trending range south of the western end of the Kern Mountains, consists mostly of complexly faulted and mineralized Paleozoic rocks. A narrow east-draining valley, Pleasant

Valley, separates the Kern Mountains and the Deep Creek Range to the north. This valley may have as much as 1000 m of valley fill ([plate 3](#), cross section X–X'). A broad unnamed valley between the Kern Mountains and the Snake Range contains white, coarse-grained, basin-fill sediments at its eastern end but these rocks appear to be relatively thin.

SNAKE RANGE AND LIMESTONE HILLS

The Snake Range is a broad, high, north-trending range. It contains Wheeler Peak, within Great Basin National Park (GBNP). The range is about 100 km long, nearly all of it in White Pine County, but with the low southern end in Lincoln County. The range is a complexly faulted horst, bounded on both sides by major high-angle normal fault zones. South of the Snake Range, the Limestone Hills are a narrow, low, heavily-faulted east-tilted low horst of mostly Devonian carbonate rocks about 30 km long.

Except for the southern end, the Snake Range is cored by Neoproterozoic to Cambrian quartzite that is intruded by a massive composite batholith formed apparently by multiple episodes of intrusion in Middle and Late Jurassic and Tertiary time (Whitebread, 1969; Miller et al., 1994, 1995, 1999a and b; Gans et al., 1999a and b; Lee et al., 1999a, b, and c; Miller and Gans, 1999; Gans, 2000b). The range was uplifted along its high-angle faults and the roof stretched apart so that its rocks failed along bedding planes in the Pioche Shale and moved in opposite directions down the flanks of the range as a non-rooted, gravity-driven structure best known as the Snake Range décollement (see [Basin and Range Extension](#)). The décollement places complexly faulted Middle Cambrian carbonate and younger rocks over a lower plate of Middle Cambrian carbonate rocks, Lower Cambrian clastic rocks, and older rocks. Most development of the décollement was synchronous with Basin and Range extension (Miller et al., 1999a; Gans, 2000a). The décollement is exposed on the top and both sides of the northern half of the range (Tingley et al., 2010; Ruksznis and Miller, 2014) ([plate 3](#), cross section W–W'). East of the range, the décollement has been interpreted to have been imaged by

seismic profiles (Allmendinger et al., 1983 and 1985; Hauser et al., 1987; Miller et al., 1999a) as it passes eastward beneath the surface of Snake Valley. Allmendinger et al. (1983) and Kirby and Hurlow (2005) suggested that the eastern frontal fault of the Snake Range, separating the range from Snake Valley, is the low-angle Snake Range décollement itself. Geophysics (Mankinen and McKee, 2009; McPhee et al., 2009) and the straight range front argue instead for our interpretation of a high-angle normal fault that bounds the eastern side of the range (plates 1 and 6). Rodgers (1987), Alam (1990), Smith et al. (1991), Alam and Pilger (1991), McGrew (1993), and Miller et al. (1999a, figure 10) also showed such a high-angle normal fault that is younger than, and thus cuts, the décollement ([plate 3](#), cross section W–W'). They considered, however, that this fault had “minor” displacement (Miller et al., 1999a, p. 891). Geophysics and well data argue otherwise.

The central part of the Snake Range is narrower and becomes progressively lower southward, and décollement faults are not exposed. Where U.S. Highway 6/U.S. Highway 50 crosses the range at Sacramento Pass, north-striking, east-dipping listric normal faults drop down to the east Miocene basin-fill sediments that are about 2000 m thick (Gans et al., 1989; Miller et al., 1994, 1995, and 1999a). The area south of Sacramento Pass includes GBNP (Sweetkind, 2007a and b), the centerpiece of which is Wheeler Peak, which at 13,065 ft (3982 m) is the second highest mountain peak in Nevada. The northern part of the Park was geologically mapped by Whitebread (1969) at 1:48,000 scale. In his mapping, he recognized the Snake Range décollement, which he left unnamed but referred to it not as a thrust but as a low-angle fault that placed younger rocks on older rocks. He considered all faults in the area to be of low angle and of the same structural event, although it is not clear whether he considered them of Sevier or Tertiary age. This mapping was compiled at 1:250,000 scale by Hose and Blake (1976). Following comprehensive detailed mapping in mostly the northern Snake Range (Miller et al., 1994, 1995, and 1999b; Gans et al., 1999a and b; Lee et al., 1999a, b, and c; Miller and Gans, 1999), Miller et al. (1999a) summarized the geology of the Snake Range décollement. Miller and her

colleagues continued their mapping southward to include the entire Park, resulting in an unpublished, unauthored, and unreviewed digital 1:24,000-scale draft geologic map of the park, on file in 2008 with the National Park Service (NPS). It compiled—with some modifications—and expanded the mapping of Whitebread. Because the emphasis of their project was the Snake Range décollement, their mapping—as with Whitebread (1969)—of surficial (Quaternary) and basin-fill (Quaternary to Miocene) deposits was cursory and inadequate, and large-displacement, high-angle, basin and range normal faults that define both sides of the range and uplift the range, and also are abundant within the range, were not recognized. Updating the geology of the Snake Range on [plate 1](#) required examination of 1:40,000-scale aerial photos and Google Earth images as well as limited field work and a review of more recent publications, including those on young and active high-angle faults in the area (Black et al., 2003; dePolo et al., 2009). Many previously unrecognized high-angle, generally north-trending, normal faults, some cutting Quaternary and Pliocene surficial and basin-fill deposits, were added to the maps. The two broad, north-striking range-front fault zones that define the western and eastern sides of the Snake Range include many of these Quaternary faults. Cumulative vertical displacement along these two great fault zones was thousands of meters. These two fault zones led to the deroofing (denudation) of the range along faults of the Snake Range décollement.

The southern end of the Snake Range is a low series of tilt-block cuestas of Devonian and Mississippian sedimentary rocks faulted against Tertiary volcanic rocks ([plate 3](#), cross section U–U'). These tilt blocks become progressively lower in elevation to the south, and the eastern tilt blocks plunge beneath the valley fill. The western tilt blocks continue southward to become the Limestone Hills, which consists mostly of east-dipping Devonian carbonate rocks bounded by normal faults on the western and eastern sides. The Limestone Hills continues southward into the Wilson Creek Range (see [Fortification Range, Wilson Creek Range, and White Rock Mountains](#)). The southern end of the Limestone Hills forms part of the northern wall of the Indian Peak caldera

complex. Here the Atlanta silver-gold mining district is in Silurian to Ordovician carbonate rocks along the east-striking caldera margin.

Spring Valley, west of the Snake Range, is a 160-km-long, broad, deep graben containing about 2000 m of basin-fill sediments and defined by normal faults of at least 3000 m of vertical displacement (McPhee et al., 2005, 2006a and b; Mankinen et al., 2006; Dixon and Rowley, 2007d; Mankinen, 2007; MCPhee, 2007) ([plate 3](#), cross sections X–X', W–W', V–V', and U–U'). Details on the faults bounding and within the valley are given by isostatic residual gravity and maxspots and depth to pre-Cenozoic basement. About 25 AMT profiles in the valley locate range-front and subsidiary faults and provide estimates of depth to bedrock (Pari and Baird, 2011).

Spring Valley is made up of at least two geophysical sub-basins, as indicated by gravity data. The northern of these is about 145 km long. It is structurally deepest at its northern end, west of the Antelope Range, where it is a separate small basin. The southern end of the northern geophysical sub-basin is near the northeastern end of the Fortification Range, where depth-to-basement data show a shallow buried east-west bedrock ridge connecting the northern Fortification Range with the southern Snake Range. Near the central part of this northern geophysical sub-basin, just south of where US 6/50 crosses Spring Valley, Rattlesnake Knoll protrudes above the valley. This Knoll, investigated by Mankinen et al. (2006), may be the surface expression of another, narrower, buried east-west ridge. The southern geophysical sub-basin is about 30 km long, between the Fortification Range and the Limestone Hills. It is part of the same surface-drainage basin as the northern geophysical sub-basin, with surface flow northward into the low part of the northern sub-basin.

Snake Valley, east of the Snake Range, is a 150 km-long, broad, deep graben that passes southward into Hamlin Valley (Rowley et al., 2009, [plate 1](#)). The main graben-bounding faults, which also define the ranges on either side of Snake Valley, are interpreted to be high-angle normal faults (cross sections in our [plate 1](#)). These faults locally (cross section W–W') drop down the Snake Range

décollement, which cut the Cambrian units beneath the basin fill of Snake Valley and perhaps from there pass beneath the western part of the Confusion Range.

As noted above, not all previous workers subscribed to the view that Snake Valley is a graben. In fact, even fewer workers interpreted a high-angle normal fault on the eastern side of Snake Valley as on the western side. Allmendinger et al. (1983), Miller et al. (1983, 1999a), Hauser et al. (1987), Smith et al. (1991), McGrew (1993), and Kirby and Hurlow (2005) suggested that the Confusion and related ranges represent the hanging wall of the Snake Range décollement, with no range-front normal fault defining the western side of Snake Valley. One possible reason for this misinterpretation is because Consortium for Continental Reflection Profiling (COCORP) data did not image any fault here. Yet, as Derik Howard (Southern Nevada Water Authority, personal commun., 2009) and A.G. Green (Swiss Federal Institute of Technology, 2009 "Pitfalls in high-resolution seismic methods," online at http://www.aug.geophys.ethz.ch/methods/seismic/seismic_pitfalls.html) noted that high-angle faults are notorious for not being imaged or poorly imaged by seismic data.

By itself, the presence of linear range fronts on both sides of Snake Valley argues for high-angle faults. The only place where the linear front is interrupted is east of where Sacramento Pass crosses the Snake Range. Here a westward embayment in the range front is underlain by a small basin containing deformed, west-dipping Miocene basin-fill sediments at least 2000 m thick (Miller et al., 1995 and 1999a). These sediments are cut by listric normal faults (Miller et al., 1995). A suggestion that these listric faults feed into the décollement at depth (Miller et al., 1995 and 1999a) does not explain the origin of the basin itself. Instead, a basin containing a great thickness of sediments requires a graben created by high-angle listric faults with significant vertical displacement, as elsewhere along the eastern flank of the Snake Range. Abundant northwest-striking Quaternary faults and a parallel youthful range front on the southwestern side of the Miocene basin argue that these northwest-striking faults control one side of the graben and continue across

the range through Sacramento Pass. Other Quaternary faults, most of them trending northerly, have been mapped throughout the length and width of Snake Valley ([plate 1](#)). Clearly Snake Valley is a deep, complex graben bounded by mostly high-angle faults, and that the interior part of the valley itself and its basin-fill sediments are cut by innumerable smaller faults of the same age and origin. Gravity data (Mankinen and McKee, 2009), including max spots that locally define some faults, and AMT profiles that image faults themselves (McPhee et al., 2009; Asch and Sweetkind, 2010, 2011), support this picture.

Basin-fill sediments beneath Snake Valley are locally more than 2000 m thick, with local holes in the basin containing thicker (3000 m) basin-fill and volcanic rocks ([plate 3](#), cross sections X–X', W–W', and V–V') (Allmendinger et al., 1983; Saltus and Jachens, 1995; Davis, 2005; Kirby and Hurlow, 2005). Seismic sections (Alam, 1990; Alam and Pilger, 1991) and logs of oil wells in Snake Valley support these thicknesses (Herring et al., 1998). Logs of five test wells are particularly instructive: (1) Baker Creek no. 12-1 (TD=1459 m), 5 km east-northeast of Baker, indicated that basin-fill sediments and presumed Tertiary volcanic rocks extend to 1400 m depth (Hess, 2004); (2) Shell Oil Baker Creek Unit 1 (TD=1286 m), 10 km northeast of Baker, encountered basin-fill deposits that extend to a depth of more than 1100 m, if not 1250 m (Utah Division of Oil, Gas, and Mining, 2006, 2011); (3) Balcron Cobra State no. 12-36 (TD=1148 m), 50 km north-northeast of Baker, penetrated 562 m of basin-fill sediments, then 245 m of possible basal Tertiary sedimentary rocks (but more likely older basin-fill sedimentary rocks) (Herring, 1998a); (4) EREC Mamba Federal no. 31-22 (TD=993 m), 45 km north-northeast of Baker, penetrated 853 m of basin-fill sediments, underlain by Chainman Shale (Herring, 1998b); and (5) Amarada-Hess Federal no. 1-28 (TD=2372 m), 35 km north-northeast of Baker, penetrated at least 300 m of basin-fill sediments (the rocks between 300 and 1394 m below the surface were considered "undetermined") (Schalla, 1998; Hintze and Davis, 2002b). Additional information on thicknesses is given from gravity data and AMT profiles.

As with Spring Valley west of Snake Valley and other valleys east of Snake Valley, surficial sediments in northern Snake Valley are dominated by deposits of late Pleistocene lakes, notably Lake Bonneville (Currey, 1982; Reheis et al., 2014). Bonneville shorelines reach as far south as the Baker area, with an elevation of about 1560 m, and the older Provo shorelines reach as far south as the Gandy area, with an elevation of about 1462 m (Currey, 1982).

Hamlin Valley, southeast of the Snake Range and south of, and tributary to, Snake Valley is about 90 km long. Like Snake Valley, it is a deep graben bounded by high-angle normal faults ([plate 1](#), cross sections Q–Q', U–U'; see also Rowley et al., 2009, [plate 1](#)). Gravity data indicate that the maximum thickness of basin-fill deposits and underlying volcanic rocks beneath Hamlin Valley is about 3000 m (Mankinen and McKee, 2009). The Valley in most places contains at least 1200 m of basin-fill sediments. Five east-west and one north-south, oil company seismic profiles in southern Snake Valley and northern Hamlin Valley (Alam, 1990; Alam and Pilger, 1991) support this conclusion. Of these profiles, the northern east-west profile, which crosses the valley about 19 km south of Baker, found a thickness of basin-fill sediments of about 1000 m. The southern east-west profile, which crosses the valley east of the southern Limestone Hills, found a thickness of basin-fill sediments of about 2000 m. Both profiles discriminated volcanic rocks beneath the sediments.

The five profiles are tied to two oil-test boreholes, the Outlaw Federal no. 1 and the Fletcher no. 1. These and two other wells provide additional information on thicknesses: (1) Outlaw Federal no. 1 (TD=3962 m), near the eastern side of Snake Valley and the northern end of the Mountain Home Range, about 27 km south-southeast of Baker, spudded in, then went through, about 400 m of Arcturus Formation (Alam, 1990, figure 8); (2) Fletcher no. 1 (TD=2280 m), near the center of Hamlin Valley 54 km south of Baker, went through 1950 m of basin-fill sediments underlain by volcanic rocks to its total depth (Alam, 1990, figure 9; Hess, 2004); (3) Hamlin Wash no. 18-1 (TD=1216 m), located 3 km north of the

Fletcher well, penetrated 790 m of basin-fill sediments, then 180 m of volcanic rocks (Hess, 2004); and (4) Hamlin Wash no. 19-1 (TD=2127 m), located near Hamlin Wash no. 18-1, penetrated 1070 m of basin-fill sediments, then about 180 m of volcanic rocks (Hess, 2004). About 15 km south of the Fletcher well, the buried northern margin of the Indian Peak caldera complex is projected across Hamlin Valley. The southern half of Hamlin Valley contains a presumed similar thickness of basin-fill sediments as shown by the Fletcher and Hamlin Wash wells, but these sediments are underlain instead by intracaldera volcanic and intrusive rocks.

Many springs in Snake and Hamlin valleys (USGS, 2008) owe their presence to normal faults, which allow groundwater to move to the surface from the underlying water table. Big Springs occurs on the southeastern flank of the Snake Range at the edge of northwestern Hamlin Valley.

CONFUSION RANGE, CONGER RANGE, BURBANK HILLS, AND TUNNEL SPRING MOUNTAINS

The Confusion Range and small ranges of similar rocks form the entire eastern (Utah) side of Snake Valley. The area includes hills (Middle Range) connected to and east of the northern end of the Confusion Range. The Confusion Range proper is 95 km long, with a general northerly trend. The Conger Range is a 25-km-long, southwest-diverging fork in the southern Confusion Range and is located northeast of the small communities of Baker, Nevada, and Garrison, Utah. The Burbank Hills is a 25-km-long range south of the Conger Range and southeast of Baker and Garrison. The Burbank Hills is separated from the Conger Range by a northwest-trending valley known as the Ferguson Desert. The Tunnel Spring Mountains is a narrow, 30-km-long range southeast of the Burbank Hills and east of northern Pine Valley. Tule Valley is east of the Confusion Range. Northern Pine Valley connects with the southeastern end of the Ferguson Desert.

All of these ranges consist almost entirely of north-striking, folded, thrust, and attenuated, middle to upper Paleozoic rocks and Triassic rocks that together form a synclinorium, in other

words a combination of synclines and anticlines that overall appear as a broad syncline (plates 1 and 3, cross sections W–W' and V–V') (Hose, 1977; Hintze and Davis, 2002a and b, and 2003). The Mississippian Chainman Shale, 300 to 600 m thick in the area, is repeated and thus exposed on both sides of and beneath all these ranges because it is deformed into north-striking folds (Hintze and Davis, 2002a and b, and 2003). Tertiary regional ash-flow tuffs formerly covered most of the area to a thickness of as much as 150 m, but erosion has left only patches of these tuffs, notably the Oligocene Needles Range Group, derived from the Indian Peak caldera complex (Best et al., 1989a and b). Normal faults cut all these ranges, but most are of small displacement so individual stratigraphic units are remarkably coherent and continuous over this large area. The most significant normal fault is the northerly-trending fault zone that defines the eastern side of Snake Valley. Normal faults that separate the Confusion Range from Tule Valley have moderate vertical offset.

Greene and Herring (2013) and Greene (2014) suggested that Sevier thrusting in the Confusion Range is much more significant than previously reported, yet they agreed that exposed thrusts are in general correct as portrayed by previous mappers. Therefore, their proposed new thrusts, as shown in their new cross sections, exist only in the subsurface and have no support by existing drilling or seismic sections. Some of their proposed thrusts are beneath the depth of our cross sections. Greene (2014) called the thrusts in the Confusion Range the western Utah thrust belt, which he considered to be one of several small belts in the Sevier hinterland west of the large frontal Sevier thrust belt.

Tule Valley is an internally drained, north-trending valley that is about 100 km long. It joins the Great Salt Lake Desert to the north and the Wah Wah Valley to the south over low passes of about 1525 m elevation. The Valley is a graben, with a maximum thickness of basin fill suggested by Davis (2005) to be 2000 m based on a seismic profile published by Allmendinger et al. (1985). Gravity data, however, indicate that the maximum thickness of basin-fill deposits and volcanic rocks beneath Tule Valley are about 1200 m (Mankinen

and McKee, 2009). The surface of Tule Valley is dominated by deposits of Pleistocene pluvial Lake Bonneville (Sack, 1990), including Bonneville shorelines (elevation 1564 to 1583 m) and Provo shorelines (elevation 1460 to 1470 m) (Currey, 1982). Tule Valley contains several warm springs (Stephens, 1977), with temperatures between 75°F and 88°F (24°C and 31°C; Blackett and Wakefield, 2004), that are aligned along north-south normal faults (Stephens, 1977; Sack, 1990).

The Ferguson Desert, about 30 km long, connects Snake Valley with Pine Valley. Gravity data indicate that the Ferguson Desert is shallow, and as much as 1000 m of basin-fill deposits is shown on [plate 3](#), cross section V–V'. A water well in the center of the upper Ferguson Desert penetrated only 158 m of basin-fill sediments before intersecting limestone bedrock (Hood and Rush, 1965, p. 19). The western part of the Ferguson Desert is cut by many north-northeast-trending normal faults and is underlain at shallow depth by the Chainman Shale. Pine Valley is an internally drained, north-trending valley about 80 km long. The basin is a graben underlain by basin-fill sediments and underlying volcanic rocks that have a maximum thickness of about 3000 m (Mankinen and McKee, 2009).

NEEDLE RANGE AND WAH WAH MOUNTAINS

The Needle Range, just east of the Nevada-Utah state line, is about 80 km long and consists of two subranges, the Mountain Home Range to the north and the Indian Peak Range to the south. The Mountain Home Range merges with the Burbank Hills to the north. Hamlin Valley, to the west, separates the Needle Range from the southern Snake Range, Limestone Hills, and White Rock Mountains to the west. To the east of the Needle Range is Pine Valley and to the south is the Escalante Desert. The Wah Wah Mountains are a parallel tilt block of similar length to, and located east of, the Needle Range, east of the study area. The Wah Wah Mountains are the southward continuation of the Confusion Range. Wah Wah Valley is east of the Wah Wah Mountains and west of the San Francisco Mountains.

The northern part of the Needle Range consists of folded, middle to upper Paleozoic rocks (Hintze and Davis, 2002b). Locally, lower Paleozoic carbonate rocks are thrust over upper Paleozoic carbonate rocks (Best et al., 1987a and b). Most of the Needle Range, however, consists of east-dipping outflow ash-flow tuffs derived primarily from the Indian Peak caldera complex. The southeastern caldera margin passes through much of the southern part of the range (Williams et al., 1997a). The Needle Range is a faulted horst, with the main normal fault separating Hamlin Valley from the Needle Range ([plate 1](#), cross sections U–U' and Q–Q'). The basin-fill sediments in the southern half of Hamlin Valley are underlain by the Indian Peak caldera complex ([plate 3](#), cross section Q–Q'). A significant normal fault separates the eastern side of the Needle Range from Pine Valley.

The northern Wah Wah Mountains, like the southern Confusion Range just to the north, consist of gently folded and locally thrust, lower to middle Paleozoic carbonate rocks. These structures and those in the Needle Range are part of Greene's (2014) western Utah thrust belt. Farther south, east-dipping Neoproterozoic to Cambrian quartzite and overlying Cambrian carbonate rocks form most of the range (Hintze and Davis, 2002b; Rowley et al., 2009, plate 1). An oil well drilled by Hunt Oil Company in the southern Wah Wah Mountains was spudded in the Prospect Mountain Quartzite and penetrated 3800 m of rocks, including several thrust zones (Erskine, 2001). Other thrust faults that place lower Paleozoic rocks over middle and upper Paleozoic rocks are well exposed and unconformably overlain by east-dipping, Tertiary ash-flow tuffs (Abbott et al., 1983). Near the southern end of the range, other Sevier thrusts place Cambrian rocks above the Jurassic Navajo Sandstone (Best et al., 1987c; Hintze et al., 1994b). The thrusts in the southern Wah Wah Mountains are part of the main Sevier frontal thrust belt. The southeastern part of the Indian Peak caldera complex cuts the southwestern end of the Wah Wah Mountains (Williams et al., 1997a). As with the Needle Range, the dominant structure controlling the range is a normal fault zone on the western margin, beneath Pine Valley. The southern ends of both the Needle Range and

the Wah Wah Mountains merge with each other (Best et al., 1987c) and, still farther southwest, merge with the White Rock Mountains. These southern range margins form the northern margin of the Escalante Desert and the southern margin of the Indian Peak caldera complex (Best, 1987).

Wah Wah Valley is an internally drained valley about 50 km long. At its southern end, a low pass at an elevation of about 1700 m separates the valley from the Escalante Desert to the south. At the northern end of Wah Wah Valley, an even lower pass separates the valley from the Sevier Desert to the north. The thickness of basin-fill sediments in Wah Wah Valley is not well known. From comparison of gravity data with well logs in and near the valley, Stephens (1977) estimated the maximum thickness of basin-fill sediments to be 730 m. Mankinen and McKee (2009) applied a modern gravity survey to calculate a more likely maximum thickness of basin-fill and volcanic deposits beneath the valley to be about 2000 m. Bonneville and Provo shorelines are mapped in the northern half of Wah Wah Valley (Currey, 1982).

FISH SPRINGS AND HOUSE RANGES

The 30-km-long Fish Springs Range extends south from the Great Salt Lake Desert. The southward continuation of the Fish Springs Range is the 100-km-long House Range. The two ranges form the eastern boundary of Tule Valley. The Fish Springs Range is a highly faulted but generally gently west-dipping horst consisting of Middle Cambrian to Middle Devonian carbonate rocks that rest on Lower Cambrian siliciclastic rocks ([plate 3](#), cross section X–X') (Kepper, 1960; Hintze, 1980a and b; Morris, 1987; Hintze et al., 2000; Hintze and Kowallis, 2009). The range is bounded by large normal faults on its western and eastern sides, with the main fault being the one on the eastern side. This fault is still active and has components of Holocene and Pleistocene movement (Oviatt, 1991; Black et al., 2003). East-striking, oblique-slip faults have been mapped throughout the range (Hintze, 1980a and b). Some of them partly control the Fish Springs zinc-lead-silver-tungsten mining district on the northwestern side of the range (Oliveira, 1975; Christiansen,

1977). A newly discovered, buried Eocene quartz monzonite pluton also controls this district (Puchlik, 2009). A concentrated series of east-striking faults occurs at Sand Pass, which separates the southern end of the Fish Springs Range from the northern end of the House Range. This east-trending fault zone is part of the Sand Pass transverse zone, which extends intermittently as far to the east as the Wasatch front and as far to the west as the Kern Mountains (Stoeser, 1993; Rowley, 1998; Rowley and Dixon, 2001). At Sand Pass, the transverse zone contains small intrusions (Chidsey, 1978) and causes profound structural differences (the rocks have opposite dips and the main fault is on opposite sides) between the two ranges north and south of it, as in some other transverse zones (Faulds and Varga, 1998).

The high House Range is a tilted horst, bounded on the western side by a major normal fault beneath eastern Tule Valley and on the eastern side by a fault of lesser displacement. The faults uplift the range and tilt it several degrees east (Hintze and Davis, 2002a; Rowley et al., 2009, plate 1). Like the main bounding fault zone of the Fish Springs Range, the main fault zone of the House Range is an active fault zone of large displacement that includes Holocene and Pleistocene movement (Sack, 1990; Black et al., 2003), but this fault zone is on the western side of the House Range. The range, famous among paleontologists for its trilobites, consists mostly of Cambrian strata, which include clastic sedimentary rocks at the western base of the range and carbonate rocks above. The central part of the range is intruded by the Notch Peak quartz monzonite pluton of Jurassic age.

Fish Springs Flat is a 50-km-long, north-trending valley east of the Fish Springs Range and northern House Range. It drains northward into the Dugway Proving Ground part of the Great Salt Lake Desert (Clark et al., 2007, 2008). The south end of Fish Springs Flat is marked by a low pass at about 1550 m that separates it from northern Whirlwind Valley. Whirlwind Valley drains southward into Sevier Lake. Fish Springs Flat is a complex graben bounded on the west by the major late Miocene to Pleistocene Fish Springs fault zone that was reactivated in the Holocene, and on the east by faults that raise the Black Rock Hills,

Thomas Range, Drum Mountains, and Little Drum Mountains. The northern end of Fish Springs Flat contains the large Fish Springs spring complex, managed by the USFWS as the Fish Springs National Wildlife Refuge. Although the groundwater that discharges from Fish Springs is part of the north-flowing Great Salt Lake Desert flow system, the source of this water is controversial, as discussed by Rowley and others (2009, 2016), Hurlow (2014), and Gardner and Heilweil (2014). All springs are controlled by the

Fish Springs fault zone. The thickness of basin-fill sediments and underlying volcanic rocks beneath Fish Springs Flat is about 1000 m (Mankinen and McKee, 2009) ([plate 3](#), cross section X–X'). At the surface of Fish Springs Flat and the flanks of its bounding ranges, deposits of late Pleistocene pluvial Lake Bonneville are well exposed, including the Bonneville shoreline (elevation 1583 to 1591 m) and Provo shoreline (elevation 1471 to 1476 m) (Currey, 1982; Oviatt, 1991).

CONCLUSIONS

This report describes the results of a long-term study of the three-dimensional geologic framework of a large part of the Great Basin of Nevada and Utah so as to identify and understand two regional groundwater flow systems as well as adjacent flow systems that might interact with the subject flow systems.

GEOLOGIC FRAMEWORK

In the Neoproterozoic and Early Cambrian, thick quartzite and other clastic rocks were deposited in Eastern Nevada and adjacent parts of Utah. These rocks represent the initial deposits of the Cordilleran miogeocline, and were deposited in shallow marine water along the western passive continental margin of North America. Middle Cambrian through Lower Permian rocks record a shift in deposition to mostly carbonate sedimentation. Predominately limestone and dolomite strata, with a thickness of 10,000 m or locally more, are known as the great carbonate aquifer. All these rocks can be grouped into two facies that are gradational over time and place: (1) a western facies of the Cordilleran miogeocline, now exposed over most of the study area, that represents a Neoproterozoic through Devonian offshore carbonate shelf and intertidal environment of deposition and an overlying Mississippian to Permian carbonate platform; and (2) a thinner eastern facies that includes cratonic platform rocks (Colorado Plateau) in the extreme southeastern part of the study area that are mostly shallow marine but locally are near-shore through continental sediments.

In Late Devonian to Late Mississippian time, thrust faults and folds of the Antler orogeny transported deeper-marine rocks eastward to approximately the longitude of Eureka, Nevada, and created a highland there. Clastic sediments, which included the Chainman Shale, were deposited in a marine foreland basin east of the Antler Highland. Carbonate deposition resumed by Late Mississippian time and continued through the Pennsylvanian and into the Permian.

Triassic, Jurassic, and Cretaceous rocks in the study area are mostly continental clastic units

deposited only in the eastern part of the area. In fact, the entire study area was characterized by erosion during and after deposition of these units. Thus, Jurassic, and Cretaceous strata are variably dispersed and have a collective thickness of less than several thousand meters, although thicker in the extreme southeastern part of the study area. From Middle Jurassic through the early Paleocene, thrust faults, folds, and intrusions of the Sevier orogenic belt were emplaced. The thrusts transported western facies rocks eastward onto thinner eastern, more cratonic facies. A series of large frontal thrusts are well exposed throughout the southern part of the area. Most thrusts strike north-northeast and therefore pass east of the northern part of the study area. The central and northern parts of the area are referred to as the hinterland of the thrusts, characterized by minor thrusting and folding. The deformation created a highland over most of the area that shed clastic sediment eastward.

During and following the waning stages of the Sevier deformation in the Paleocene, erosional stripping of the Sevier highland that included the northern two-thirds of the study area led to sedimentation east of the study area. Only the post-deformational Sheep Pass Formation in mostly White Pine County and the Claron Formation just southeast of the area remain as sediment patches unconformably deposited on the older thrust and folded structures. These sedimentary rocks, as well as the deeply eroded underlying Paleozoic and Mesozoic rocks, were then inundated by voluminous Eocene to Miocene calc-alkaline, subduction-related arc volcanic rocks. Most of these rocks are ash-flow tuff, derived from many scattered calderas in and near the area, but andesitic to dacitic lava flows and volcanic mudflow breccia from stratovolcanoes in the area were also deposited. Depositional thickness of overall outflow ash-flow tuffs and flows ranged from about 300 to 2000 m thick over most of the area, but intracaldera tuffs are thicker. Intrusions, the ultimate sources of the volcanic rocks, are abundant. The eruptive centers, including the intrusive sources, for these rocks formed three east-trending igneous belts, as

supported by aeromagnetic data. The belts become younger from north to south, so most depositional products from the northern belt have been removed by erosion. The locations and types of post-Sevier, pre-extension faults that deformed the lower to middle Tertiary sedimentary and volcanic rocks are uncertain but doubtless included oblique-slip, high-angle faults and were part of an upland remaining from Sevier times. East-trending transverse zones, which began to form in the Mesozoic, deformed the calc-alkaline rocks and continued active throughout the Cenozoic, including today.

By early Miocene, at roughly 20 Ma in and east of the study area, subduction ceased and east-west regional extension began. The Basin and Range extension was predominantly characterized by north-striking high-angle normal faults. The map pattern, however, demonstrates that additional structures also accommodated the deformation, namely low-angle attenuation/denudation normal faults of various strikes, mostly northwesterly-striking right-lateral and northeasterly-striking left-lateral oblique-slip transfer faults, and east-striking transverse zones. As the rocks were extended east-west, all these structures had their own part in the deformation and left their trademark features. The high-angle normal faults resulted in the north-trending ranges that were uplifted on one side as tilt blocks or more commonly on both sides as horsts, and adjacent north-trending basins went down as tilt blocks or grabens. Isostatic residual gravity data, in conjunction with horizontal gradients (maxspots) calculated from gravity and magnetic data provide evidence that all major basins and ranges are bounded by high-angle normal faults. The low-angle attenuation/denudation faults are non-rooted, gravity-driven structures that resulted from sliding of the flanks and tops of the rising ranges into the adjacent valley, generally along weak shale beds, notably the Pioche Shale and Chainman Shale. The northwest- and northeast-striking transfer faults, where strike-slip motion is greater the closer the strike of the fault is to east-west, in places pass along strike into north-striking high-angle normal faults, where the motion is largely dip slip. The transverse zones are a type of transform zone, by which broad east-trending masses of rock north

and south of each transverse zone moved at different amounts and rates or along different structures, with respect to the other side of the zone, in response to regional east-west compression (during the Sevier event) or east-west extension (during the Basin and Range event). Transverse zones are considered to be deep high-angle structures and so may not be always expressed at the surface in all places along the strike of the zone.

The basins and ranges that were produced early (20 to 10 Ma) during Basin and Range extension are not necessarily in the same places as the current basins and ranges. The current basins and ranges seemed to have started to form at about 10 Ma based on information from in and east of the study area. At this time, extensional deformation appears to have intensified and the present topography began to form. The rising ranges were stripped by erosion and the subsiding basins were again filled by erosional debris. The resulting basin-fill sediments accumulated to many kilometers thick. Bimodal (basalt and rhyolite) volcanic rocks, generally thin, are locally intertongued with the basin-fill sediments. The sedimentary basin fill is the primary current aquifer in the study area, as elsewhere in the Great Basin. Gravity geophysical data converted to depth-to-pre-Cenozoic basement by the gravity-inversion method provide accurate information on basin depths. Including thin calc-alkaline volcanic rocks that underlie the basin-fill sediments that cannot be geophysically separated from basin-fill sediments, thicknesses of Cenozoic rocks are locally more than 6 km thick in some basins. Most of this depth, relative to the pre-Cenozoic bedrock ("basement") in the adjacent ranges, can be ascribed to offset along multiple high-angle normal faults. All Basin and Range structures, whether high-angle normal faults, low-angle normal faults, transfer faults, or transverse zones, show Quaternary displacement in the study area or nearby.

Geologic maps at 1:250,000 scale cannot do justice to the actual fault complexity of the study area, for thousands of real faults cannot be shown. AMT profiles, as presented here, determined the fault architecture of parts of some basins and of their range-bounding faults, most of which were

buried by young basin-fill and surficial sediments. All of the AMT profiles shown in the geophysics chapter, and especially several of the longer profiles, demonstrate this detailed complexity. Examples are Profiles SVN10 West and East ([figure 24](#) and [figure 25](#)) across central Spring Valley, Profile SVNA ([figure 28](#)) across southern Spring Valley, and Profile SNK4 ([figure 34](#)) across southern Snake Valley. We consider these profiles to typify the level of fault complexity across most basins and ranges in the study area. The profiles also distinguish many regional from subsidiary (smaller) faults. These same AMT profiles provide information on the lithology of basin-fill sediments versus underlying bedrock and as such allow information on the size of these faults as well as their location.

Some of the transfer faults were crossed by AMT profiles, showing that many of these faults are comparable in size and extent of deformation to the regional range-front high-angle normal faults. Examples are Profile SVN13 ([figure 22](#)) at Sacramento Pass across the Snake Range, Profile DLV50 ([figure 36](#)) in eastern Dry Lake Valley, and Profiles DELA5 and DELA1 ([figure 41](#) and [figure 42](#)) that cross different strands of the PSZ in southern Delamar Valley. AMT profiles across some of the Quaternary faults show that some of these faults have large displacements, perhaps a conclusion not anticipated considering that the scarps in Pleistocene and Holocene sediments are rarely higher than 3 m. Examples of large faults that have Quaternary displacement are Profiles DLV3 ([figure 37](#)) and DLV8 ([figure 40](#)) in Dry Lake Valley. Clearly these faults have been active for a longer time than just Quaternary.

HYDROGEOLOGIC IMPLICATIONS

Understanding the regional hydrology of areas making up many thousands of square kilometers and in complex geologic terrains requires major investments in time and finances. SNWA's investment in time has been almost 30 years. The first step in this major investigation was to accumulate geologic information, leading next to putting together the three-dimensional geologic and geophysical framework of the area of interest. This framework is the subject of the present report.

Such a framework allowed synchronous and later hydrologic and biologic investigations to proceed. Of these, the hydrologic studies enabled predictions of amounts and quality of groundwater, directions of groundwater flow, sources of recharge of groundwater, and best sites for extraction of groundwater. Data and conclusions on these topics, however, are found in unpublished reports by SNWA that were intended for presentations at public hearings of the Nevada State Engineer. Yet published hydrologic studies in much the same area, using their own geologic frameworks, were done independently during the last decade by the UGS (e.g., Hurlow, 2014; Hurlow and Inkenbrandt, 2016) and the USGS (e.g., Welch et al., 2007; Heilweil and Brooks, 2011; Masbruch et al., 2014, 2016). Perhaps not unexpectedly, the major hydrologic conclusions from the studies of all three organizations are remarkably similar, with some exceptions noted by Rowley et al. (2016). Regardless of the relatively small differences in the major conclusions, their similarity demonstrates the value of different groups independently working on the same complex problem by applying similar long-term efforts. The investigations by the three organizations is continuing. For example, hydrologists and biologists at the SNWA, UGS, and USGS continue their monitoring, and the UGS and USGS periodically issue new published hydrologic reports.

Major hydrologic conclusions given in many SNWA reports are not covered here because they require the supporting data, including maps of water levels, monitoring of water levels, precipitation values, recorded annual well discharges, water chemistry, cross sections and analyses of the controls and discharges of major springs, water budgets, aquifer tests such as pumped volumes and other hydraulic data, etc. However, speaking only of hydrogeologic conclusions resulting from our framework study, several items stand out, although the discovery of many of these must be credited also to previous work, especially on the Death Valley regional groundwater flow system and other work on the NTS that all current authors participated in. First, as documented in the Introduction, the governing concept in determining groundwater flow through

regional flow systems in the Great Basin is fracture flow along normal faults and their parallel fault-caused joints. It seems undeniable that the flow of the main volumes of groundwater is along these faults and their related joints. Therefore the geologic mapping of faulted terranes provides the first approximation of groundwater flow directions and locations.

Many of the hydrographic areas (basins) in the study area are closed basins. The first approximation as to whether groundwater moves beneath topographic divides to another basin, therefore determination of what basins make up a groundwater flow system (e.g., Harrill et al., 1988), and what the likely groundwater pathways are, derives largely from the topography, maps of water levels, and hydraulic heads observed. However, geologic mapping of the faults and the relative positions of aquifers and confining units making up the boundaries of basins will allow a more accurate interpretation of whether flow paths are likely, unlikely, or permissible across any particular part of basin boundaries. Such an exercise was part of the overall study (Dixon et al., 2007a; Rowley et al., 2011, 2016) and those by the UGS and USGS. Accurate geologic maps are essential in making assessments of flow paths beneath basin boundaries.

Each succeeding episode of deposition of rocks and their deformation had increasingly greater effects on the hydrogeology of the study area. Most of the hydrogeologic effects for Paleozoic events, including the Antler orogeny in the Devonian and Mississippian, resulted from deposition of the various sedimentary units that would become important aquifers and aquitards in the study area. The greatest of these bedrock aquifers is the Cambrian to Permian carbonate aquifer. In these rocks, groundwater dissolution resulted in even larger and more interconnected conduits. And an interruption in this carbonate deposition by Antler clastic sedimentation resulted in perhaps the most important confining unit in the northern part of the study area, the Chainman Shale. After the Permian, deposition of clastic continental sedimentary rocks dominated throughout the Mesozoic, resulting primarily in confining units or low-permeability sedimentary rocks. Yet most of these Mesozoic rocks were stripped away during Sevier

deformation, so such Mesozoic rocks have little bearing on water resources over most parts of the study area. Although Sevier thrust faults are large and relatively abundant in the south, they are relatively small and sparse elsewhere in the study area. Either way, individual thrusts seem to have had negligible effects to groundwater flow, and they created barriers when the thrusts carried confining units onto the carbonate sequences.

During the Eocene, Oligocene, and early Miocene, emplacement of calderas, with associated caldera ring-fault walls and intracaldera intrusions, created areas of low permeability. Aeromagnetic data help to define calderas and plutons, which formed east-trending highlands that erupted thick sequences of volcanic rocks. Yet the calc-alkaline ash-flow tuffs derived from the calderas--whether filling the calderas or spread outside their source calderas--formed significant although thin aquifers in many places. Some other calc-alkaline volcanic rocks, such as mudflows that tend to be confining units and may be sandwiched between valley fill above and carbonate rocks below, may reduce the interconnection between the carbonate aquifer and the valley fill in some basins. Such relationships would explain some carbonate aquifers that are under artesian pressure or at least have a piezometric head higher than that of basin fill. Some springs may result from this. During Mesozoic to late Cenozoic, east-west transverse zones developed. These zones may provide potential conduits or barriers to groundwater flow, although their hydraulic significance is generally unknown.

From middle Miocene to the present time, extensional tectonics resulted in the dominant north-south high-angle faults of the Great Basin. This deformational regime and the rocks deposited as a result of it had by far the greatest effect on groundwater resources and their movement. The north-striking structures are excellent conduits to north or south groundwater flow. Gouge in the core zone of these faults acted as partial to complete barriers, however, to east or west flow. There is significant evidence, as well as simple logic, that indicates that large faults have a greater influence on flow than smaller faults, and therefore plates [1](#) and [2](#) show both sizes, with the clear suggestion that the bigger ones are more important in

hydrologic assessments. During Basin and Range tectonism, all rocks became fractured, but brittle units such as carbonate rocks, ash-flow tuffs, basalt and rhyolite flows, and locally some quartzite units became shattered throughout and thus are local or regional aquifers. The most important and most extensive aquifer in the study area is the basin-fill aquifer. Depth-to-basement calculations based on gravity data provide the information needed to assess the size of this aquifer in any one place.

Concealed normal faults, whether defining the edges of most basins or within basins, can be located by gravity (maxspots) and AMT data. Upward-continued gravity and aeromagnetic maxspots and some AMT profiles can determine which way the fault or caldera wall dips. Of the two types of geophysics, AMT profiles also provide information on depths to groundwater in some parts of basins. AMT profiles are sufficiently detailed to allow siting of wells on faults, which are the best places to locate production and monitoring wells. Ideally, the best location would be a range-front fault of a large range with abundant recharge, near the mouth of a perennial creek that carries some of that recharge. The objective to site a well is to drill the downthrown side of a high-angle

normal fault, the larger the better, to intersect the fault beneath the water table. If the dip of this fault is not known but the direction of throw (and the depth to the water table) is, one can assume an average dip of 60 degrees, then position the drill rig with respect to the fault accordingly.

Virtually all significant springs in the study area arise along faults. That includes warm and hot springs, most of which represent rapid vertical rise along faulted "channels" of water heated by the geothermal gradient. Springs provide the surface expression of fracture flow, and mapping of springs gives valuable information on water tables, local permeability, and availability of groundwater. Fault and fracture pathways for groundwater commonly leave behind calcite growths, in places expressed as spring mounds or, where older and more deeply eroded, as calcite veins.

This long-term study combined simultaneous and closely coordinated studies of cutting-edge geology, geophysics, and hydrology. We suggest that it is a model for future hydrological analyses elsewhere in the increasingly thirsty western United States.

ACKNOWLEDGMENTS

This report is the culmination of more than two decades of work by the authors, including several interim reports. Nearly all reports were funded by the Southern Nevada Water Authority. Our work involved, with our grateful appreciation, collaboration with many colleagues, only some of whom are mentioned below. We received hydrologic, geologic, and geophysical data, expertise, and advice from Ken Albright, Zane Marshall, Casey Collins, Jim Prieur, Gavin Kistinger, Frank Baird, Steve Acheampong, and Dave Donovan of SNWA, from Jim Faulds of NBMG, from private consultants Terry Katzer of Reno, Farrel Lytle of Pioche, and Frank D'Agnese of Tucson, from Hugh Hurlow, Lucy Jordan, and Paul Inkenbrandt of the Utah Geological Survey, from Ric Page, Randy Lacznia, Mel Kuntz, Jim

Harrill, Vicki Langenheim, Tom Hildenbrand, Bob Jachens, Rick Blakely, Marith Reheis, Vic Heilweil, Phil Gardner, Bruce Chuchel, Louise Pellerin, Jonathan Caine, Jeremy Workman, Dave Prudic, and Don Sweetkind of the USGS, from Dan Netcher, Mark Henderson, and Dawna Ferris of the Bureau of Land Management, and from Bill Van Liew of the National Park Service. Word processing was accomplished through the help of Yvonne Honore, Donna Lewis, and Cheri Walker. Mel Kuntz, Emeritus Geologist of the USGS, Denver, did a thorough technical review of the entire text and plates. We thank Andrew Zuza, Jim Faulds, Rachel Micander, Jennifer Vican, and Jack Hursh of NBMG for their detailed and valuable technical reviews of, and editorial comments on, the text, sections, and maps.

DESCRIPTION OF MAP UNITS

QTa – Surficial and basin-fill deposits (Holocene to lower Miocene) — Unconsolidated to moderately consolidated, locally tuffaceous beds of sand, gravel, silt, and minor limestone deposited mostly by streams and small playa lakes. Generally thin, but where unit fills basin-range-fault-bounded basins, may be significantly more than 1500 meters thick and forms the upper valley-fill aquifer. Some basin-fill deposits bear local names, including the Muddy Creek Formation (southern part of [plate 2](#)), Panaca Formation (southern part of [plate 1](#)), Horse Camp Formation (northwestern part of plate 1), and Salt Lake Formation (northeastern part of plate 1).

QTb – Basalt lava flows (Holocene to lower Miocene) — Resistant, thin basalt lava flows and cinder cones. The mafic end of the bimodal volcanic sequence that is synchronous with basin-range extensional faulting.

Ts4 – Sedimentary rocks, unit 4 (Miocene) — Moderately to well consolidated, mostly fluvial sandstone, conglomerate, and minor lacustrine limestone. Primarily the Horse Spring Formation (11 to 20 Ma), a basal basin-fill sedimentary unit that is locally thick (1000+ meters) in the southern part of [plate 2](#).

Ts3 – Sedimentary rocks, unit 3 (Miocene and Oligocene) — Moderately to well consolidated, thin, mostly fluvial, tuffaceous sandstone and bedded ash-fall tuff.

Ts2 – Sedimentary rocks, unit 2 (Oligocene) — Moderately to well consolidated, thin, mostly fluvial, tuffaceous sandstone and conglomerate. Includes the Gilmore Gulch Formation, with an age of about 30 Ma, in the northwestern part of [plate 1](#).

Ts1 – Sedimentary rocks, unit 1 (Oligocene to Upper Cretaceous?) — Moderately to well consolidated, mostly fluvial sandstone, conglomerate, and minor lacustrine limestone. Primarily the Sheep Pass Formation, but just southeast of [plate 1](#), includes the Paleocene and Upper Cretaceous(?) Grapevine Wash Formation and the Eocene and Paleocene Claron Formation.

Includes the Fowkes Formation and White Sage Formation in the northeastern part of [plate 1](#). In most places, unit is overlain by volcanic rocks.

Tv – Volcanic rocks, undivided (Miocene to Eocene) — Unit shown only in cross sections. May be several thousand meters thick in many places. In calderas and near other source vents, unit may be many thousands of meters thick. On plates [1](#) and [2](#), unit is separated into several rock types based on age, following the mapping strategy of Ekren et al. (1977). Locally includes QTb where too thin to show.

Tt4 – Ash-flow tuff and interbedded ash-fall tuff, unit 4 (Miocene) — Poorly to densely welded, bimodal high-silica rhyolite and locally peralkaline ash-flow tuff and related ash-fall tuffs. Includes the tuff of Honeycomb Rock (12.0 Ma), Ox Valley Tuff (14.0 Ma), tuff of Etna (14.0 Ma), tuff of Rainbow Canyon (15.6 Ma), tuff of Acklin Canyon (17.1 Ma), and tuff of Dow Mountain (17.4 Ma), derived from the Caliente caldera complex. Includes the Kane Wash Tuff (14.4 to 14.7 Ma), the tuff of Boulder Canyon (15.1 Ma), and the tuff of Narrow Canyon (15.8 Ma), derived from the Kane Springs Wash caldera complex.

Tt3 – Ash-flow tuff and interbedded ash-fall tuff, unit 3 (Miocene to Oligocene) — Poorly to densely welded, calc-alkaline, low-silica rhyolite to dacite ash-flow tuff and related ash-fall tuffs. Includes the tuff of Teepee Rocks (17.8 Ma), Hiko Tuff (18.3 Ma), Racer Canyon Tuff (18.7 Ma), and both Bauers Tuff Member (22.8 Ma) and Swett Tuff Member (23.7 Ma) of the Condor Canyon Formation, all derived from the Caliente caldera complex. Also includes the Harmony Hills Tuff (22.0 Ma), probably derived from the eastern Bull Valley Mountains; the Leach Canyon Formation (23.8 Ma), probably derived from the Caliente caldera complex; the Bates Mountain Tuff (22.8 Ma), derived from Lander County, Nevada; and the tuff of Saulsbury Wash (21.6 Ma), the Pahranaagat Formation (22.6 Ma), the tuff of White Blotch Spring (24 to 25 Ma), the tuff of Kiln Canyon (24.1 to 25.1 Ma), the tuff of Lunar Cuesta (24.6 Ma), the

tuff of the Quinn Canyon Range, and the Shingle Pass Tuff (26.4), all derived from central Nevada, including the Monotony Valley caldera complex; and the tuff of Bald Mountain (about 25 Ma), derived from the Bald Mountain caldera in the Groom Range.

Tt₂ – Ash-flow tuff and interbedded ash-fall tuff, unit 2 (Oligocene) — poorly to densely welded, calc-alkaline, low-silica rhyolite to dacite and trachydacite ash-flow tuff and related ash-fall tuffs. Includes the Isom Formation (about 27 Ma), probably derived from the Indian Peak caldera complex; the outflow Monotony Tuff (27.3 Ma), the intra caldera tuff of Goblin Knobs (27.3 Ma), and the tuff of Hot Creek Canyon (30.0 Ma), all probably derived from the Monotony Valley caldera complex; the outflow Windous Butte Formation (31.4 Ma) and intracaldera tuff of Williams Ridge and Morey Peak (31.3 Ma), derived from the Williams Ridge caldera of central Nevada; and the Needles Range Group (27 to 32 Ma), derived from the Indian Peak caldera complex.

Tt₁ – Ash-flow tuff and interbedded ash-fall tuff, unit 1 (Oligocene to Eocene) — Poorly to densely welded, calc-alkaline, low-silica rhyolite to dacite and trachydacite ash-flow tuff and related ash-fall tuffs. Deposited in the northern part of [plate 1](#). Includes the Pancake Summit Tuff (33.7 Ma), derived from the Broken Back caldera west of Eureka; the Stone Cabin Formation (35.4 Ma), derived from an unknown caldera in or near northern Railroad Valley; and the Kalamazoo tuff (35 Ma), derived from an unknown caldera source probably in the northern Schell Creek Range or beneath adjacent northern Spring Valley or Antelope Valley. In Utah, includes the Tunnel Spring Tuff (35.4 Ma).

Tr₄ – Rhyolite lava flows, unit 4 (Miocene) — High-silica rhyolite lava flows and volcanic domes, mostly in and near the Caliente and Kane Springs Wash caldera complexes.

Tr₃ – Rhyolite lava flows, unit 3 (Miocene to Oligocene) — Low-silica rhyolite lava flows and

volcanic domes, mostly in and near the Indian Peak, Caliente, and other caldera complexes.

Tr₂ – Rhyolite lava flows, unit 2 (Oligocene) — Low-silica rhyolite lava flows and volcanic domes, mostly in central Nevada and the Indian Peak caldera complex.

Tr₁ – Rhyolite lava flows, unit 1 (Oligocene to Eocene) — Low-silica rhyolite lava flows and volcanic domes, exposed in the northern part of [plate 1](#).

Ta₄ – Intermediate-composition lava flows, unit 4 (Miocene) — Andesitic and locally dacitic lava flows, flow breccia, and mudflow breccia. Includes andesite of the Hamblin-Cleopatra volcano (11.5 to 14.2 Ma) in the Lake Mead area.

Ta₃ – Intermediate-composition lava flows, unit 3 (Miocene to Oligocene) — Andesitic and locally dacitic lava flows, flow breccia, and mudflow breccia. Includes andesite between the Racer Canyon Tuff and Condor Canyon Formation just southeast of [plate 2](#), between the Caliente and Kane Springs Wash caldera complexes, and in and near the Indian Peak caldera complex.

Ta₂ – Intermediate-composition lava flows, unit 2 (Oligocene) — Andesitic and locally dacitic lava flows, flow breccia, and mudflow breccia. Includes andesite in and near the Indian Peak caldera complex and in the southern Egan Range.

Ta₁ – Intermediate-composition lava flows, unit 1 (Oligocene to Eocene) — Andesitic and locally dacitic lava flows, flow breccia, and mudflow breccia. Exposed in the northern part of [plate 1](#). In the northeastern part of plate 1 includes thin ash-flow tuffs, notably the Kalamazoo tuff. In Utah, includes the Horn Silver Andesite.

Tmb – Megabreccia (Miocene to Oligocene) — Masses of mostly Paleozoic sedimentary rocks and intertongued volcanic breccia deposited within calderas from landsliding of the oversteepened caldera margins following caldera subsidence as a result of rapid eruptions of ash-flow tuff. Includes rocks in the Indian Peak caldera complex, Caliente

caldera complex, and calderas in central Nevada. Also includes gravity slides west of the Sheep Range and Beaver Dam Mountains.

Ti – Intrusive rocks (Miocene to Paleocene) — Mostly silicic, calc-alkaline plutons.

TKi – Intrusive rocks (Miocene to Cretaceous) — Mostly silicic, calc-alkaline plutons.

Ki – Intrusive rocks (Upper Cretaceous) — Mostly silicic, calc-alkaline plutons that accompanied Sevier deformation.

Ks – Sedimentary rocks, undivided (Upper and Lower Cretaceous) — Sevier-age, mostly thin, fluvial synorogenic clastic deposits, including the Baseline Sandstone (Upper and Lower Cretaceous) and Willow Tank Formation (Upper Cretaceous) in the southern part of [plate 2](#); the Iron Springs Formation (Upper Cretaceous), Cedar Mountain Formation (Upper Cretaceous), and Dakota Sandstone (Upper Cretaceous) east of plate 2; and the Newark Canyon Formation (Paleocene? to Lower Cretaceous?) in the northern part of [plate 1](#).

Ji – Intrusive rocks (Jurassic) — Mostly silicic, calc-alkaline plutons that accompanied Sevier deformation.

Js – Sedimentary rocks, undivided (Jurassic) — Includes, in the southeastern part of [plate 2](#), the mostly marine Carmel and underlying Temple Cap Formations (Middle Jurassic). Also in the southeastern part of plate 2, includes the eolian Navajo Sandstone and mostly fluvial Kayenta and Moenave Formations, all Lower Jurassic. Mostly clastic units. In the southern part of plate 2, the Aztec Sandstone is the equivalent of the Navajo Sandstone. Includes the Dunlap Formation (Lower Jurassic) in the northwestern part of [plate 1](#).

Ts – Sedimentary rocks, undivided (Triassic) — Includes, in the southeastern part of [plate 2](#), the mostly fluvial Chinle Formation (Upper Triassic) and mostly fluvial Moenkopi Formation (Middle? and Lower Triassic). Includes the Luning Formation (Upper Triassic) in the northwestern part of [plate 1](#). In the northeastern part of plate 1,

includes the Thaynes Formation (Lower Triassic). The majority of these rocks are clastic.

Pzu – Sedimentary rocks, undivided (Paleozoic) — Shown on [plate 3](#), where rocks in the hanging wall of the Snake Range decollement are buried by younger rocks.

Pp – Park City Group, undivided (Upper and Lower Permian) — From top to base, consists of the Gerster Limestone (Upper Permian), Plympton Formation (Upper and Lower Permian), Kaibab Limestone (Lower Permian), and Toroweap Formation (Lower Permian). These make up the top of the upper carbonate aquifer.

Par – Arcturus Formation and Rib Hill Sandstone, undivided (Lower Permian) — Included within the upper carbonate aquifer. Includes the Pequop Formation in Elko County, a redbed unit in the southern part of [plate 2](#), and the Queantoweap Sandstone in the southeastern part of plate 2.

Pa – Arcturus Formation (Lower Permian) — Predominantly carbonate rocks in the northern part of [plate 1](#), thickening eastward.

Pr – Rib Hill Sandstone (Lower Permian) — Nonresistant sandstone and dolomite only in the northwestern part of [plate 1](#).

PIP – Riepe Spring Limestone and Ely Limestone, undivided (Lower Permian to Pennsylvanian) — Mapped only in the northern part of [plate 1](#). The Riepe Spring Limestone (Lower Permian) is exposed in the northwestern part of plate 1. Includes the Brock Canyon Formation (Permian and/or Pennsylvanian) in the northwestern part of plate 1; the Oquirrh Group (Lower Permian and Pennsylvanian) in the northeastern part of plate 1; and the Bird Spring Formation (Lower Permian to Upper Mississippian) in Clark County, Nevada, and the Pakoon formation (Lower Permian) in Utah.

IP – Ely Limestone (Pennsylvanian) — May include Mississippian rocks at its base. Mapped mostly in the central and northern part of [plate 1](#).

thickening eastward. Includes the Wildcat Peak Formation in the northwestern part of plate 1 and the Callville Limestone in the southern and eastern part of [plate 2](#).

MDd – Diamond Peak Formation, Chainman Shale, Joana Limestone, and Pilot Shale, undivided (Upper Mississippian to Upper Devonian).

Md – Diamond Peak Formation (Upper Mississippian) — Only in the northwestern part of [plate 1](#). This is a clastic unit derived from erosion of the Antler highland, including the Roberts Mountain thrust formed during the Antler deformational event. Includes the Scotty Wash Quartzite in the southwestern part of [plate 2](#).

Mc – Chainman Shale (Upper Mississippian) — A clastic confining unit that has a similar origin to the Diamond Peak Formation. The two make up the upper aquitard in the northern half of [plate 1](#). Thus for this part of the map area, it separates the upper from the lower carbonate aquifer; in the area of [plate 2](#), the Chainman Shale is thin and does not constitute a significant regional aquitard.

MD – Joana Limestone and Pilot Shale, undivided (Lower Mississippian to Upper Devonian) — The Joana Limestone (Lower Mississippian) and Pilot Shale (Lower Mississippian and Upper Devonian) make up the top of the lower carbonate aquifer in the northern half of [plate 1](#). Includes local Lower Mississippian units Mercury Limestone and Bristol Pass Limestone. Includes the Rogers Spring Limestone (Lower Mississippian) and Monte Cristo Limestone (Upper and Lower Mississippian) in the southern part of [plate 2](#); the Eleana Formation (Mississippian and Upper Devonian) in the western part of plate 2; the Webb Formation (Lower Mississippian) in Elko County; the Ochre Mountain Limestone and underlying Woodman Formation (Lower Mississippian) in the eastern part of plate 1; and the West Range Limestone (Upper Devonian) in northern Lincoln County. May include, at the top, thin deposits of the Chainman Shale.

Dc – Carbonate and clastic rocks, undivided (Devonian to Upper Cambrian).

DS – Sedimentary rocks, undivided (Devonian to Silurian).

Du – Carbonate sedimentary rocks, undivided (Devonian) — Includes the Woodruff Formation (Upper and Middle Devonian) in Elko County; and the Muddy Peak Limestone (Upper and Middle? Devonian) in the southern part of [plate 2](#).

Dd – Devils Gate Formation (Upper to Middle Devonian) — The western equivalent of the Guilmette Formation.

Dg – Guilmette Formation (Upper to Middle Devonian) — Mapped throughout, except in the western part of [plate 1](#). Includes the Sultan Limestone in Clark County.

Dn – Nevada formation (Middle to Lower Devonian) — The western equivalent of the Simonson and Sevy Dolomites. Includes the Cockalorum Wash formation, also in the western part of [plate 1](#).

Ds – Simonson Dolomite (Middle to Lower Devonian) and Sevy Dolomite, undivided (Lower Devonian) — Mapped in all but the western part of [plate 1](#).

SO – Sedimentary rocks, undivided (Silurian to Ordovician) — Unit shown only on the cross sections.

SOU – Dolomite, upper part, undivided (Silurian to Upper Ordovician) — Includes the Laketown Dolomite (Silurian), Fish Haven Dolomite (Upper Ordovician), Ely Springs Dolomite (Upper Ordovician), and Hanson Creek Formation (Upper Ordovician). Includes the Roberts Mountains Formation and the Lone Mountain Dolomite in the northwestern part of [plate 1](#).

Ol – Dolomite, lower part, undivided (Middle to Lower Ordovician) — Mostly the Eureka Quartzite (Middle Ordovician) and the Pogonip Group (Middle and Lower Ordovician). Includes

the Vinini Formation and Valmy Formation in the northwestern part of [plate 1](#). Includes the Laketown Dolomite and Ely Springs Dolomite where thin in Clark and Lincoln counties. In Utah, includes the Crystal Peak Dolomite, Watson Ranch Quartzite, and Fillmore formations and the House Limestone.

€c – Carbonate sedimentary rocks, undivided (Cambrian) — Unit shown only on the cross sections.

€u – Limestone and shale, upper part, undivided (Lower Ordovician? to Upper Cambrian) — Includes the Notch Peak Formation, Orr Formation, Windfall Formation, Nopah Formation, Dunderberg Shale, and Corset Spring Shale. In the extreme southwestern part of [plate 2](#), includes the Emigrant Formation (Upper and Middle Cambrian).

€m – Limestone and shale, middle part, undivided (Upper to Middle Cambrian) — Mostly the Highland Peak Formation and its southwestern equivalent, the Bonanza King Formation. In Nevada, includes local units known as the Pole Canyon Limestone, Lincoln Peak Formation, Patterson Pass Shale, Hamburg formation, Secret Canyon Shale, Geddes Limestone, and Eldorado formation. Includes the Muav Limestone in eastern Clark County. In Utah, includes the Wah Wah Summit Formation, Trippe Limestone, Pierson Cove Formation, Eye of

Needle Limestone, Swasey Limestone, Whirlwind Formation, Dome Limestone, Chisholm Shale, and Howell Limestone. This unit is a thick limestone sequence that marks the base of the lower carbonate aquifer.

€p€s – Lower part (Middle Cambrian to Neoproterozoic) — Chisholm Shale (Middle Cambrian), Lyndon Limestone (Middle Cambrian), Pioche Shale (Middle and Lower Cambrian), Carrara Formation (Middle and Lower Cambrian), Stella Lake Quartzite (Lower Cambrian), Prospect Mountain Quartzite (Lower Cambrian and Neoproterozoic), and Johnnie Formation (Neoproterozoic). The Prospect Mountain Quartzite, in turn, has been subdivided into the Zabriskie Quartzite (Lower Cambrian), Wood Canyon Formation (Lower Cambrian), and Stirling Quartzite (Lower Cambrian and Neoproterozoic). Locally includes the Reed Dolomite (Lower Cambrian) and underlying Wyman formation (Lower Cambrian?) in the southwestern part of [plate 2](#).

p€ – Metamorphosed and crystalline basement rocks (Neoproterozoic to Paleoproterozoic) — Throughout most of plates [1](#) and [2](#), consists of metamorphosed quartzite of Neoproterozoic age, namely the McCoy Creek Group and, in Utah, also the underlying Trout Creek group. Locally, in the southern part of [plate 2](#), includes crystalline basement rocks.

REFERENCES

- Abbott, J.T., Best, M.G., and Morris, H.T., 1983, Geologic map of the Pine Grove-Blawn Mountain area, Beaver County, Utah: U.S. Geological Survey Miscellaneous Investigations Series Map I-1479, scale 1:24,000.
- Acheampong, S.Y., Farnham, I.M., and Watrus, J.M., 2009, Geochemical characterization of ground water and surface water of Snake Valley and the surrounding areas in Utah, *in* Tripp, B.T., Krahulec, K., and Jordan, J.L., editors, *Geology and geologic resources and issues of western Utah*: Utah Geological Association Publication 38, p. 325–344.
- Ahlborn, R.C., 1977, Mesozoic-Cenozoic structural development of the Kern Mountains, eastern Nevada-western Utah [M.S. thesis]: Brigham Young University Geology Studies, v. 24, Pt. 2, p. 117–131.
- Alam, A.H.M.S., 1990, Crustal extension in the southern Snake Range and vicinity, Nevada-Utah: An integrated geological and geophysical study [Ph.D. dissertation]: Louisiana State University, 126 p.
- Alam, A.H.M.S., and Pilger, Jr., R.H., 1991, An integrated geologic and geophysical study of the structure and stratigraphy of the Cenozoic extensional Hamlin Valley, Nevada-Utah, *in* Raines, G.L., Lisle, R.E., Schafer, R.W., and Wilkinson, W.H., editors, *Geology and ore deposits of the Great Basin*: Geological Society of Nevada, Symposium Proceedings, April 1–5, 1990, v. 1, p. 93–100.
- Allmendinger, R.W., Sharp, J., VonTish, D., Oliver, J., and Kaufman, S., 1985, A COCORP crustal-scale seismic profile of the Cordilleran hingeline, eastern Basin and Range province, *in* Gries, R.R., and Dyer, R.C., editors, *Seismic exploration of the Rocky Mountain region*: Denver, Rocky Mountain Association of Geologists and Denver Geophysical Society, p. 23–30.
- Allmendinger, R.W., Sharp, J.W., Von Tish, D., Serpa, L., Brown, L., Kaufman, S., Oliver, J., and Smith, R.B., 1983, Cenozoic and Mesozoic structure of the eastern Basin and Range province, Utah, from COCORP seismic-reflection data: *Geology*, v. 11, no. 9, p. 532–536.
- Anderson, R.E., 1981, Structural ties between the Great Basin and Sonoran Desert sections of the Basin and Range province, *in* Howard, K.A., Carr, M.D., and Miller, D.M., editors, *Tectonic framework of the Mohave Sonoran Desert, California and Arizona*: U.S. Geological Survey Open-File Report 81-503, p. 4–6.
- Anderson, R.E., 1983, Cenozoic structural history of selected areas in the eastern Great Basin, Nevada-Utah: U.S. Geological Survey Open-File Report 83-504, 47 p.
- Anderson, R.E., 1989, Tectonic evolution of the Intermontane System, Basin and Range, Colorado Plateau, and High Lava Plains, *in* Pakiser, L.C., and Mooney, W.D., editors, *Geophysical framework of the continental United States*: Geological Society of America Memoir 172, p. 163–176.
- Anderson, R.E., 2003, Geologic map of the Callville Bay quadrangle, Clark County, Nevada and Mohave County, Arizona: Nevada Bureau of Mines and Geology Map 139, scale 1:24,000.
- Anderson, R.E., 2013, On the importance of non-uniform tilt, strike slip, and hydrogeology in shaping the Neogene tectonics of the eastern Lake Mead area, *in* Anderson, R.E., editor, *Neogene deformation between central Utah and the Mojave Desert*: Geological Society of America Special Paper 499, p. 69–94.
- Anderson, R.E., and Barnhard, T.P., 1993, Aspects of three-dimensional strain at the margin of the extensional orogen, Virgin River depression area, Nevada, Utah, and Arizona: *Geological Society of America Bulletin*, v. 105, p. 1019–1052.
- Anderson, R.E., and Beard, L.S., 2010, Geology of the Lake Mead region—an overview, *in* Umhoefer, P.J., Beard, L.S., and Lamb, M.A., editors, *Miocene tectonics of the Lake Mead region, central Basin and Range*: Geological Society of America Special Paper 463, p. 1–28.
- Anderson, R.E., Beard, L.S., Mankinen, E.A., and Hillhouse, J.W., 2013, Analysis of Neogene deformation between Beaver, Utah, and Barstow, California—suggestions for altering the extensional paradigm, *in* Anderson, R.E., editor, *Neogene deformation between central Utah and the Mojave Desert*: Geological Society of America Special Paper 499, p. 1–67.
- Anderson, R.E., Felger, T.J., Diehl, S.F., Page, W.R., and Workman, J.B., 2010, Integration of tectonic, sedimentary, and geohydrologic processes leading to a small-scale extension model for the Mormon Mountains area north of Lake Mead, Lincoln County, Nevada, *in* Umhoefer, P.J., Beard, L.S., and Lamb, M.A., editors, *Miocene tectonics of the Lake Mead region, central Basin and Range*:

- Geological Society of America Special Paper 463, p. 395–426.
- Armstrong, P.A., 1991, Displacement and deformation associated with lateral thrust propagation—an example from the Golden Gate Range, southern Nevada [M.S. thesis]: University of Utah, Salt Lake City, 162 p.
- Armstrong, R.L., 1963, Geochronology and geology of the eastern Great Basin in Nevada and Utah: New Haven, Connecticut, unpublished Ph.D. thesis, Yale University, 202 p + illustrations.
- Armstrong, R.L., 1968, Sevier orogenic belt in Nevada and Utah: Geological Society of America Bulletin, v. 79, no. 4, p. 429–458.
- Armstrong, R.L., 1970, Geochronology of Tertiary igneous rocks, eastern Basin and Range province, western Utah, eastern Nevada, and vicinity, U.S.A.: *Geochimica et Cosmochimica Acta*, v. 34, no. 2, p. 203–232.
- Armstrong, R.L., 1972, Low-angle (denudation) faults, hinterland of the Sevier orogenic belt, eastern Nevada and western Utah: Geological Society of America Bulletin, v. 83, no. 6, p. 1729–1754.
- Asch, T.H., and Sweetkind, D.S., 2010, Geophysical characterization of range-front faults, Snake Valley, Nevada: U.S. Geological Survey Open-File Report 2010-1016, 39 p.
- Asch, T.H., and Sweetkind, D.S., 2011, Audiomagnetotelluric characterization of range-front faults, Snake Range, Nevada: *Geophysics*, v. 76, p. B1–B7.
- Bankey, V., Grauch, V.J.S., and Kucks, R.P., 1998, Utah aeromagnetic and gravity maps and data, a web site for distribution of data: U.S. Geological Survey Open-File Report 98-761. [<http://pubs.usgs.gov/of/1998/ofr-98-0761/>]
- Baranov, V., 1957, A new method for interpretation of aeromagnetic maps—Pseudo-gravimetric anomalies: *Geophysics*, v. 22, p. 359–383.
- Bartley, J.M., and Gleason, Gayle, 1990, Tertiary normal faults superimposed on Mesozoic thrusts, Quinn Canyon and Grant ranges, Nye County, Nevada, in Wernicke, B.P., editor, Basin and Range extensional tectonics near the latitude of Las Vegas, Nevada: Geological Society of America Memoir 176, p. 195–212.
- Bartley, J.M., and Wernicke, B.P., 1984, The Snake Range décollement interpreted as a major extensional shear zone: *Tectonics*, v. 3, no. 6, p. 647–657.
- Bartley, J.M., Axen, G.J., Taylor, W.J., and Fryxell, J.E., 1988, Cenozoic tectonics of a transect through eastern Nevada near 38° N latitude, in Weide, D.L., and Faber, M.L., editors, This extended land—geological journeys in the southern Basin and Range: Geological Society of America, Cordilleran Section, Field trip guidebook, p. 1–20.
- Beard, L.S., Anderson, R.E., Block, D.L., Bohannon, R.G., Brady, R.J., Castor, S.B., Duebendorfer, E.M., Faulds, J.E., Felger, T.J., Howard, K.A., Kuntz, M.A., and Williams, V.S., 2007, Preliminary geologic map of the Lake Mead 30'×60' quadrangle, Clark County, Nevada, and Mohave County, Arizona: U.S. Geological Survey Open-File-Report 2007-1010, 109 p., 3 plates, scale 1:100,000. [<http://pubs.usgs.gov/of/2007/1010/>].
- Beard, L.S., Campagna, D.J., and Anderson, R.E., 2010, Geometry and kinematics of the eastern Lake Mead fault system in the Virgin Mountains, Nevada and Arizona, in Umhoefer, P.J., Beard, L.S., and Lamb, M.A., editors, Miocene tectonics of the Lake Mead region, central Basin and Range: Geological Society of America Special Paper 463, p. 243–274.
- Belcher, W.R., editor, 2004, Death Valley regional ground-water flow system, Nevada and California—hydrogeologic framework and transient ground-water flow model: U.S. Geological Survey Scientific Investigations Report 2004–5205, 408 p.
- Berger, D.L., Kilroy, K.C., and Schaefer, D.H., 1987, Geophysical logs and hydrologic data for eight wells in Coyote Spring Valley area, Clark and Lincoln Counties, Nevada: U.S. Geological Survey Open-File Report 87-679, 59 p.
- Best, M.G., 1987, Geologic map and sections of the area between Hamlin Valley and Escalante Desert, Iron County, Utah: U.S. Geological Survey Miscellaneous Investigations Series Map I-1774, scale 1:50,000.
- Best, M.G., and Williams, V.S., 1997, Geologic map of the Rose Valley quadrangle, Lincoln County, Nevada: U.S. Geological Survey Geologic Quadrangle Map GQ-1765, scale 1:24,000.
- Best, M.G., Armstrong, R.L., Graustein, W.C., Embree, G.F., and Ahlborn, R.C., 1974, Mica granites of the Kern Mountains pluton, eastern White Pine County, Nevada: Remobilized basement of the Cordilleran miogeosyncline?: Geological Society of America Bulletin, v. 85, p. 1277–1286.
- Best, M.G., Barr, D.L., Christiansen, E.H., Gromme, S., Deino, A.L., and Tingey, D.G., 2009, The Great Basin aliplano during the middle Cenozoic ignimbrite flareup—insights from volcanic rocks:

- International Geology Review, v. 51, p. 589–633.
- Best, M.G., Christiansen, E.H., and Blank, Jr., R.H., 1989a, Oligocene caldera complex and calc-alkaline tuffs and lavas of the Indian Peak volcanic field, Nevada and Utah: Geological Society of America Bulletin, v. 101, p. 1076–1090.
- Best, M.G., Christiansen, E.H., Deino, A.L., Grommé, C.S., McKee, E.H., and Noble, D.C., 1989b, Eocene through Miocene volcanism in the Great Basin of the western United States, *in* Chapin, C.E., and Zidek, J., editors, Field excursions to volcanic terranes in the western United States, Volume II: Cascades and Intermountain West: New Mexico Bureau of Mines and Mineral Resources Memoir 47, p. 91–133.
- Best, M.G., Christiansen, E.H., Deino, A.L., Gromme, C.S., Hart, G.L., and Tingey, D.G., 2013a, The 31–18 Ma Indian Peak-Caliente ignimbrite field and calderas, southwestern Great Basin, U.S.A.—Multicyclic super-eruptions: *Geosphere*, v. 9, p. 1–87.
- Best, M.G., Grant, S.K., Hintze, L.F., Cleary, J.G., Hutsinpillar, A., and Saunders, D.M., 1987a, Geologic map of the Indian Peak (southern Needle) Range, Beaver and Iron Counties, Utah: U.S. Geological Survey Miscellaneous Investigations Series Map I-1795, scale 1:50,000.
- Best, M.G., Gromme, Sherman, Deino, A.L., Christiansen, E.H., Hart, G.L., and Tingey, D.G., 2013b, The 36–18 Ma central Nevada ignimbrite field and calderas, Great Basin, USA—Multicyclic super-eruptions: *Geosphere*, v. 9, p. 1–75.
- Best, M.G., Hintze, L.F., Deino, A.L., and Maughan, L.L., 1998, Geologic map of the Fairview Range and Grassy Mountain, Lincoln County, Nevada: Nevada Bureau of Mines and Geology Map 114, scale 1:24,000, 2 sheets.
- Best, M.G., Hintze, L.F., and Holmes, R.D., 1987b, Geologic map of the southern Mountain Home and northern Indian Peak Ranges (central Needle Range), Beaver County, Utah: U.S. Geological Survey Miscellaneous Investigations Series Map I-1796, scale 1:50,000.
- Best, M.G., Morris, H.T., Kopf, R.W., and Keith, J.D., 1987c, Geologic map of the southern Pine Valley area, Beaver and Iron Counties, Utah: U.S. Geological Survey Miscellaneous Investigations Series Map I-1794, scale 1:50,000.
- Best, M.G., Scott, R.B., Rowley, P.D., Swadley, W.C., Anderson, R.E., Grommé, C.S., Harding, A.E., Deino, A.L., Christiansen, E.H., Tingey, D.G., and Sullivan, K.R., 1993, Oligocene-Miocene caldera complexes, ash-flow sheets, and tectonism in the central and southeastern Great Basin, *in* Lahren, M.M., Texler, Jr., J.H., and Spinosa, C., editors, Crustal evolution of the Great Basin and Sierra Nevada—Field trip guidebook: Geological Society of America, Cordilleran and Rocky Mountain sections meeting, p. 285–311.
- Best, M.G., Toth, M.I., Kowallis, J.B., Willis, J.B., and Best, V.C., 1989c, Geologic map of the northern White Rock Mountains-Hamlin Valley area, Beaver County, Utah, and Lincoln County, Nevada: U.S. Geological Survey Miscellaneous Investigations Series Map I-1881, scale 1:50,000.
- Bhark, E., Kelly, V., Pickens, J., Ruskau, G., Gable, C., Reimus, P., and Vesselinov, V., 2006, Well ER-6-1 tracer test analysis: Yucca Flat, Nevada Test Site, Nye County, Nevada: Stoller-Navarro, 177 p.
- Biek, R.F., Hacker, D.B., and Rowley, P.D., 2014, New constraints on the extent, age, and emplacement history of the early Miocene Markagunt Megabreccia, southwest Utah—one of the World's largest subaerial gravity slides, *in* MacLean, J.S., Biek, R.F., and Huntoon, J.E., editors, Geology of Utah's far south: Utah Geological Association Publication 43, CD, p. 565–598.
- Biek, R.F., Rowley, P.D., Anderson, J.J., Maldonado, Florian, Moore, D.W., Eaton, J.G., Hereford, Richard, and Matyjasik, Basia, 2015, Geologic map of the Panguitch 30'x60' quadrangle, Garfield, Iron, and Kane Counties, Utah: Utah Geological Survey Map 270, CD, scale 1:65,000.
- Biek, R.F., Rowley, P.D., Hayden, J.M., Hacker, D.B., Willis, G.C., Hintze, L.F., Anderson, R.E., and Brown, K.D., 2009, Geologic map of the St. George and east part of the Clover Mountains 30'x60' quadrangles, Washington and Iron Counties, Utah: Utah Geological Survey Map 242, 109 p.
- Billingsley, G.H., and Workman, J.B., 2000, Geologic map of the Littlefield 30'x60' quadrangle, Mohave County, northwestern Arizona: U.S. Geological Survey Geologic Investigations Series Map I-2628, scale 1:100,000.
- Black, B.D., Hecker, S., Hylland, M.D., Christenson, G.L., and McDonald, G.N., 2003, Quaternary fault and fold database and map of Utah: Utah Geological Survey Map 193DM, scale 1:500,000. (CD-ROM).
- Blackett, R.E., and Wakefield, S., 2004, Geothermal resources of Utah—2004: Utah Geological Survey Open-File Report 431DM, CD-ROM.
- Blakely, R.J., 1995, Potential theory in gravity and magnetic applications: Cambridge, U.K., Cambridge University Press, 441 p.

- Blakely, R.J., Langenheim, V.E., Ponce, D.A., and Dixon, G.L., 2000, Aeromagnetic survey of the Amargosa Desert, Nevada and California—a tool for understanding near-surface geology and hydrology: U.S. Geological Survey Open-File Report 00-188, 35 p.
- Blakely, R.J., Morin, R.L., McKee, E.H., Schmidt, K.M., Langenheim, V.E., and Dixon, G.L., 1998, Three-dimensional model of Paleozoic basement beneath Amargosa Desert and Pahrump Valley, California and Nevada—implications for tectonic evolution and water resources: U.S. Geological Survey Open-File Report 98-496, 27 p.
- Blakely, R.J., and Simpson, R.W., 1986, Approximating edges of source bodies from magnetic or gravity anomalies: *Geophysics*, v. 51, p. 1494–1498.
- Blank, H.R., 1993, Basement structure in the Railroad Valley—Grant Range region, east-central Nevada, from interpretation of potential-field anomalies, *in* Scott, R.W., Jr., Detra, P.S., and Berger, B.R., editors, *Advances related to United States and international frameworks and exploration technologies*: U.S. Geological Survey Bulletin 2039, p. 25–30.
- Bohannon, R.G., 1983, Geologic map, tectonic map and structure sections of the Muddy and Northern Black Mountains, Clark County, Nevada: U.S. Geological Survey Miscellaneous Investigations Series Map I-1406, scale 1:62,500.
- Bohannon, R.G., 1984, Nonmarine sedimentary rocks of Tertiary age in the Lake Mead region, southeastern Nevada and northwestern Arizona: U.S. Geological Survey Professional Paper 1259, 72 p.
- Bohannon, R.G., 1992, Geologic map of the Weiser Ridge quadrangle, Clark County, Nevada: U.S. Geological Survey Geologic Quadrangle Map GQ-1714, scale 1:24,000.
- Brokaw, A.L., 1967, Geologic map and sections of the Ely quadrangle, White Pine County, Nevada: U.S. Geological Survey Geologic Quadrangle Map GQ-697, scale 1:24,000.
- Brokaw, A.L., and Barosh, P.J., 1968, Geologic map and sections of the Riepetown quadrangle, White Pine County, Nevada: U.S. Geological Survey Geologic Quadrangle Map GQ-758, scale 1:24,000.
- Brokaw, A.L., and Heidrick, T., 1966, Geologic map and sections of the Giroux Wash quadrangle, White Pine County, Nevada: U.S. Geological Survey Geologic Quadrangle Map GQ-476, scale 1:24,000.
- Brokaw, A.L., and Shawe, D.R., 1965, Geologic map and sections of the Ely 3 SW quadrangle, White Pine County, Nevada: U.S. Geological Survey Miscellaneous Geological Investigations Map I-449, scale 1:24,000.
- Brokaw, A.L., Bauer, H.L., and Breitrick, R.A., 1973, Geologic map of the Ruth quadrangle, White Pine County, Nevada: U.S. Geological Survey Geologic Quadrangle Map GQ-1085, scale 1:24,000.
- Brown, C.L., and Schmitt, J.G., 1991, Horse Camp Formation: Record of Miocene-Pliocene extensional basin development, northern Grant Range, Nevada, *in* Flanigan, Donna M.H., Mike Hansen and T. Edward Flanigan, editors, *Geology of White River Valley, the Grant Range, Eastern Railroad Valley and Western Egan Range, Nevada: 1991 Fieldtrip Guidebook*, Nevada Petroleum Society, Reno, p. 7–13.
- Bureau of Land Management, 2012, Clark, Lincoln, and White Pine Counties Groundwater Development Project Final Environmental Impact Statement, FES 12-33.
- Buqo, T., 2007, Carbonate development in the Muddy Springs area, *in* Coache, R., ed., *Regional tour of the carbonate system guidebook: Nevada Water Resources Association*, Clark County, Nevada, June 18–20, 2007, p. 5–6.
- Burbey, T.J., 1997, Hydrogeology and potential for ground-water development, carbonate-rock aquifers, southern Nevada and southeastern California: U.S. Geological Survey Water-Resources Investigations 95–4168, 65 p.
- Burchfiel, B.C., Fleck, R.J., Secor, D.T., Vincelette, R.R., and Davis, G.A., 1974, Geology of the Spring Mountains, Nevada: *Geological Society of America Bulletin*, v. 85, no. 7, p. 1013–1022.
- Burns, A.G., and Drici, W., 2011, Hydrology and water resources of Spring, Cave, Dry Lake, and Delamar valleys, Nevada and vicinity: Presentation to the Office of the Nevada State Engineer: Southern Nevada Water Authority, Las Vegas, Nevada.
- Caine, J.S., Evans, J.P., and Forster, C.B., 1996, Fault zone architecture and permeability structure: *Geology*, v. 24, no. 11, p. 1025–1028.
- Caine, J.S., and Forster, C.B., 1999, Fault zone architecture and fluid flow: Insights from field data and numerical modeling, *in* Haneberg, W.C., Mozley, P.S., Moore, J.C., and Goodwin, L.B., editors, *Faults and subsurface fluid flow in the shallow crust*: American Geophysical Union Geophysical Monograph 113, p. 101–127.

- Caine, J.S., Manning, A.H., Berger, B.R., Kremer, Y., Guzman, M.A., Eberl, D.D., and Schuller, K., 2010, Characterization of geologic structures and host rock properties relevant to the hydrogeology of the Standard Mine in Elk Basin, Gunnison County, Colorado: U.S. Geological Survey Open-File Report 2010–1008, 56 p.
- Carpenter, J.A., and Carpenter, D.G., 1994a, Analysis of Basin-Range and Fold-Thrust Structure, and Reinterpretation of the Mormon Peak Detachment and Similar Features as Gravity Slide Systems: Southern Nevada, Southwest Utah, and Northwest Arizona, *in* Dobbs, S.W., and W.J. Taylor, editors, Structural and Stratigraphic Investigations and Petroleum Potential of Nevada, with Special Emphasis South of the Railroad Valley Producing Trend: Nevada Petroleum Society Conference Volume II, p. 15–52.
- Carpenter, J.A., and Carpenter, D.G., 1994b, Fold-Thrust Structure, Synorogenic Rocks, and Structural Analysis of the North Muddy and Muddy Mountains, Clark County Nevada, *in* Dobbs, S.W., and W.J. Taylor, editors, Structural and Stratigraphic Investigations and Petroleum Potential of Nevada, with Special Emphasis South of the Railroad Valley Producing Trend: Nevada Petroleum Society Conference Volume II, p. 65–94.
- Carpenter, J.A., Carpenter, D.G., and Dobbs, S.W., 1994, Antler Orogeny: Paleostuctural Analysis and Constraints on Plate Tectonic Models with a Global Analogue in Southeast Asia, *in* Dobbs, S.W., and W.J. Taylor, editors, Structural and Stratigraphic Investigations and Petroleum Potential of Nevada, with Special Emphasis South of the Railroad Valley Producing Trend: Nevada Petroleum Society Conference Volume II, p. 187–240.
- Castor, S.B., Faulds, J.E., Rowland, S.M., and dePolo, C.M., 2000, Geologic map of the Frenchman Mountain quadrangle, Clark County, Nevada: Nevada Bureau of Mines and Geology Map 127, scale 1:24,000.
- Chidsey, Jr., T.C., 1978, Intrusions, alteration, and economic implications in the northern House Range, Utah: Brigham Young University Geology Studies, v. 25, pt. 3, p. 47–65.
- Christiansen, W.J., 1977, Geology of the Fish Springs mining district, Juab County, Utah [M.S. thesis]: Salt Lake City, University of Utah, 66 p.
- Christiansen, R.L., and Lipman, P.W., 1972, Cenozoic volcanism and plate-tectonic evolution of the western United States: II. Late Cenozoic: Royal Society of London Philosophical Transactions A, v. 271, no. 1213, p. 249–284.
- Christiansen, R.L., and Yeats, R.S., 1992, Post-Laramide geology of the U.S. Cordilleran region, *in* Burchfiel, B.C., Lipman, P.W., and Zoback, M.L., editors, The Cordilleran Orogen: Conterminous U.S.: Boulder, Colorado, Geological Society of America, The Geology of North America, v. G-3, p. 261–406.
- Clark, D.L., Oviatt, C.G., and Page, David, 2007, Progress Report geologic map of Dugway Proving Ground and adjacent areas, parts of the Wildcat Mountain, Rush Valley, and Fish Springs 30'x60' quadrangles, Tooele County, Utah (Year 1 of 2): Utah Geological Survey Open-File Report 501, scale 1:62,5000.
- Clark, D.L., Oviatt, C.G., and Page, David, 2008, Interim geologic map of Dugway Proving Ground and adjacent areas, parts of the Wildcat Mountain, Rush Valley, and Fish Springs 30'x60' quadrangles, Tooele County, Utah (Year 2 of 2): Utah Geological Survey Open-File Report 532, scale 1:75,000.
- Coats, R.R., 1987, Geology of Elko County, Nevada: Nevada Bureau of Mines and Geology Bulletin 101, 112 p.
- Coney, P.J., 1974, Structural analysis of the Snake Range décollement, east-central Nevada: Geological Society of America Bulletin, v. 85, no. 6, p. 973–978.
- Coney, P.J., and Harms, T., 1984, Cordilleran metamorphic core complexes—Cenozoic extensional relics of Mesozoic compression: Geology, v. 12, p. 550–554.
- Cook, E.F., 1965, Stratigraphy of Tertiary volcanic rocks in eastern Nevada: Nevada Bureau of Mines and Geology Report 11, 61 p.
- Cook, K.L., Bankey, V., Mabey, D.R., and DePangher, M., 1989, Complete Bouguer gravity anomaly map of Utah: Utah Geological and Mineral Survey Map 122, scale 1:500,000.
- Cordell, L., 1979, Gravimetric expression of graben faulting in Santa Fe County and the Espanola Basin, *in* Ingersoll, R.V., editor, Guidebook to Santa Fe County, 30th Field Conference: New Mexico Geological Society, p. 59–64.
- Cordell, L., and Grauch, V.J.S., 1985, Mapping basement magnetization zones from aeromagnetic data in the San Juan Basin, New Mexico, *in* Hinze, W.J., editor, The utility of regional gravity and magnetic anomaly maps: Society of Exploration Geophysicists, Tulsa, Oklahoma, p. 181–197.
- Cornwall, H.R., 1972, Geology and mineral deposits

- of southern Nye County, Nevada: Nevada Bureau of Mines and Geology Bulletin 77, 49 p.
- Crafford, A.E.J., 2007, Geologic Map of Nevada: U.S. Geological Survey Data Series 249, 1 CD-ROM, 46 p., 1 plate.
- Currey, D.R., 1982, Lake Bonneville: Selected features of relevance to neotectonic analysis: U.S. Geological Survey Open-File Report 82-1070, 30 p.
- Currey, D.R., Atwood, G., and Mabey, D.R., 1984, Major levels of Great Salt Lake and Lake Bonneville: Utah Geological Survey Map 73, scale 1:750,000.
- D'Agnese, F.A., O'Brien, G.M., Faunt, C.C., Belcher, W.R., and San Juan, C., 2002, A three-dimensional numerical model of predevelopment conditions in the Death Valley regional ground-water flow system, Nevada and California: U.S. Geological Survey Water-Resources Investigations Report 02-4102, 114 p.
- Davis, F.D., 2005, Water resources of Millard County, Utah: Utah Geological Survey Open-File Report 447, 27 p.
- DeCelles, P.G., 2004, Late Jurassic to Eocene evolution of the Cordilleran thrust belt and foreland basin systems, western U.S.A.: *American Journal of Science*, v. 304, p. 105–168.
- DeCelles, P.G., and Coogan, J.C., 2006, Regional structure and kinematic history of the Sevier fold-and-thrust belt, central Utah: *Geological Society of America Bulletin*, v. 118, p. 841–864.
- dePolo, C.M., and Taylor, W.J., 2012, Geologic map of the Ute quadrangle, Clark County, Nevada: Nevada Bureau of Mines and Geology Map 177, scale 1:24,000.
- dePolo, C.M., Johnson, G.L., Price, J.G., and Mauldin, J.M., 2009, Quaternary faults in Nevada—Online interactive map: Nevada Bureau of Mines and Geology Open-File Report 09-9, scale 1:1,000,000.
- Dettinger, M.D., 1992, Geohydrology of areas being considered for exploratory drilling and development of the carbonate-rock aquifers in southern Nevada—preliminary assessment: U.S. Geological Survey Water-Resources Investigations Report 90-4077, 35 p.
- Dettinger, M.D., Harrill, J.R., Schmidt, D.L., and Hess, J.W., 1995, Distribution of carbonate-rock aquifers and the potential for their development, southern Nevada and adjacent parts of California, Arizona, and Utah: U.S. Geological Survey Water-Resources Investigations Report 91-4146, 100 p.
- Dickinson, W.R., 2006, Geotectonic evolution of the Great Basin: *Geosphere*, v. 2, p. 353–368.
- Dickinson, W.R., 2009, Anatomy and global context of the North American cordillera, *in* Kay, S.M., Ramos, V.A., and Dickinson, W.R., editors, *Backbone of the Americas—shallow subduction, plateau uplift, and ridge and terrane collision*: Geological Society of America Memoir 204, p.1–29.
- Dickinson, W.R., 2013, Phanerozoic palinspastic reconstruction of Great Basin geotectonics (Nevada-Utah, USA): *Geosphere*, v. 9, p. 1384–1396.
- Dilek, Y., and Moores, E.M., 1999, A Tibetan model for the early Tertiary western United States: *Journal of the Geological Society, London*, v. 156, p. 929–941.
- Dixon, G., 2007, Geology of White River Narrows and Pahroc Valley, *in* Coache, R., editor, *Regional tour of the carbonate system guidebook*: Nevada Water Resources Association, Clark County, Nevada, June 18-20, 2007, p. 17–18.
- Dixon, G.L., and Katzer, T., 2002, Geology and hydrology of the lower Virgin River Valley in Nevada, Arizona, and Utah: Virgin Valley Water District, Mesquite, Nevada, Report VVWD-01, 126 p.
- Dixon, G., and Rowley, P., 2007a, Hydrogeology of Caliente and lower Meadow Valley Wash, *in* Coache, R., editor, *Regional tour of the carbonate system guidebook*: Nevada Water Resources Association, Clark County, Nevada, June 18–20, 2007, p. 65–66.
- Dixon, G.L., and Rowley, P.D., 2007b, Hydrogeology of Dry Lake and Delamar valleys, *in* Coache, R., editor, *Regional tour of the carbonate system guidebook*: Nevada Water Resources Association, Clark County, Nevada, June 18-20, 2007, p. 69–70.
- Dixon, G.L., and Rowley, P.D., 2007c, Hydrogeology of Pioche, Panaca and Caliente areas, *in* Coache, R., editor, *Regional tour of the carbonate system guidebook*: Nevada Water Resources Association, Clark County, Nevada, June 18–20, 2007, p. 63–64.
- Dixon, G.L., and Rowley, P.D., 2007d, Hydrogeology of Spring Valley, *in* Coache, R., editor, *Regional tour of the carbonate system guidebook*: Nevada Water Resources Association, Clark County, Nevada, June 18–20, 2007, p. 35–36.
- Dixon, G.L., Donovan, D.J., and Rowley, P.D., 2007b, Geology of Oak Springs Summit, *in* Coache, R., editor, *Regional tour of the carbonate system guidebook*: Nevada Water Resources Association, Clark County, Nevada, June 18–20, 2007, p. 71–72.
- Dixon, G.L., Donovan, D.J., and Rowley, P.D., 2007c,

- Hydrogeology of White River Valley, *in* Coache, R., editor, Regional tour of the carbonate system guidebook: Nevada Water Resources Association, Clark County, Nevada, June 18–20, 2007, p. 21–22.
- Dixon, G.L., Hedlund, D.C., and Ekren, E.B., 1972, Geologic map of the Pritchards Station quadrangle, Nye County, Nevada: U.S. Geological Survey Miscellaneous Geologic Investigations Map I-728, scale 1:48,000.
- Dixon, G.L., Rowley, P.D., Burns, A.G., Watrus, J.M., Donovan, D.J., and Ekren, E.B., 2007a, Geology of White Pine and Lincoln counties and adjacent areas, Nevada and Utah: The geologic framework of regional groundwater flow systems: Southern Nevada Water Authority, Las Vegas, Nevada, Doc. No. HAM-ED-0001, 157 p.
- Dixon, G.L., and Van Liew, B., 2007, Hydrogeology of Crystal Springs, *in* Coache, R., editor, Regional tour of the carbonate system guidebook: Nevada Water Resources Association Clark County, Nevada, June 18–20, 2007, p. 13–14.
- Dobbs, S.W., Garbee, Jr., J.J., Stuart, C.K., and Nelson, S.L., 1994, Integrated [sic] Geological and Geophysical Interpretation in the Newark Valley Area, Eureka Fold-and-Thrust Belt, East-Central Nevada, *in* Dobbs, S.W., and Taylor, W.J. editors, Structural and Stratigraphic Investigations and Petroleum Potential of Nevada, with Special Emphasis South of the Railroad Valley Producing Trend: Nevada Petroleum Society Conference Volume II, p. 241–253.
- Dohrenwend, J.C., Schell, B.A., Menges, C.M., Moring, B.C., and McKittrick, M.A., 1996, Reconnaissance photogeologic map of young (Quaternary and late Tertiary) faults in Nevada, *in* Singer, D.A., editor, An analysis of Nevada's metal-bearing mineral resources: Nevada Bureau of Mines and Geology Open-File Report 96–2, p. 9-1–9-12.
- Donovan, D.J., 2007, Geology of Muddy River Springs, *in* Coache, R., editor, Regional tour of the carbonate system guidebook: Nevada Water Resources Association, Clark County, Nevada, June 18-20, 2007, p. 1–2.
- Donovan, D.J., Dixon, G.L., and Rowley, P.D., 2004, Detailed geologic mapping in the Muddy Springs area, Clark County, Nevada [abs.]: Nevada Water Resources Association Annual Conference, Mesquite, Nevada, February 24–26, 2004, p. 23.
- Douglass, W. B., Jr., 1960, Geology of the southern Butte Mountains, White Pine County, Nevada, *in* Geology of east central Nevada: Intermountain Association Petroleum Geologists Guidebook, 11th Annual Field Conference, 1960, p. 181–185.
- Drewes, Harald, 1967, Geology of the Connors Pass quadrangle, Schell Creek Range, east-central Nevada: U.S. Geological Survey Professional Paper 557, 94 p., scale 1:24,000.
- Druschke, P., Hanson, A.D., Wells, M.L., Rasbury, T., Stockli, D.F., and Gehrels, G., 2009, Synconvergent surface-breaking normal faults of Late Cretaceous age within the Sevier hinterland, east-central Nevada: *Geology*, v. 37, no. 5, p. 447–450.
- du Bray, E.A., 1993, The Seaman volcanic center—a rare middle Tertiary stratovolcano in southern Nevada: U.S. Geological Survey Bulletin 2052, 19 p.
- du Bray, E.A., 1995, Chemistry and petrology of Oligocene and Miocene ash-flow tuffs of the southeastern Great Basin, Nevada: U.S. Geological Survey Professional Paper 1559, 38 p.
- du Bray, E.A., and Hurtubise, D.O., 1994, Geologic map of the Seaman Range, Lincoln and Nye counties, Nevada: U.S. Geological Survey Miscellaneous Investigations Series Map I-2282, scale 1:50,000.
- Duebendorfer, E.M., 2003, Geologic map of the Government Wash quadrangle, Clark County, Nevada: Nevada Bureau of Mines and Geology Map 140, scale 1:24,000.
- Eakin, T.E., 1966, A regional interbasin groundwater system in the White River area, southeastern Nevada: *Water Resources Research*, v. 2, no. 2, p. 251–271.
- Eberhart-Phillips, D., Stanley, W.D., Rodriguez, B.D., and Lutter, W.J., 1995, Surface seismic and electrical methods to detect fluids related to faulting: *Journal of Geophysical Research*, v. 100, no. B7, p. 12919–12936.
- Ehni, W., and Faults, J., editors, 2002, Detachment and attenuation in eastern Nevada and its application to petroleum exploration: Nevada Petroleum Society 2002 Field Trip Guidebook, 163 p.
- Eichhubl, P., Taylor, W.L., Pollard, D.D., and Aydin, A., 2004, Paleo-fluid flow and deformation in the Aztec Sandstone at the Valley of Fire, Nevada—evidence for the coupling of hydrogeologic, diagenetic, and tectonic processes: *Geological Society of America Bulletin*, v. 116, p. 1120–1136.
- Ekren, E.B., and Page, W.R., 1995, Preliminary geologic map of the Coyote Spring quadrangle, Lincoln County, Nevada: U.S. Geological Survey Open-File Report 95–550, scale 1:24,000.
- Ekren, E.B., Bucknam, R.C., Carr, W.J., Dixon, G.L.,

- and Quinlivan, W.D., 1976, East-trending structural lineaments in central Nevada: U.S. Geological Survey Professional Paper 986, 16 p.
- Ekren, E.B., Hinrichs, E.N., and Dixon, G.L., 1972, Geologic map of The Wall quadrangle, Nye County, Nevada: U.S. Geological Survey Miscellaneous Geologic Investigations Map I-719, scale 1:48,000.
- Ekren, E.B., Hinrichs, E.N., Quinlivan, W.D., and Hoover, D.L., 1973a, Geologic map of the Moores Station quadrangle, Nye County, Nevada: U.S. Geological Survey Miscellaneous Geologic Investigations Map I-756, scale 1:48,000.
- Ekren, E.B., Orkild, P.P., Sargent, K.A., and Dixon, G.L., 1977, Geologic map of Tertiary rocks, Lincoln County, Nevada: U.S. Geological Survey Miscellaneous Investigations Series Map I-1041, scale 1:250,000.
- Ekren, E.B., Quinlivan, W.D., Snyder, R.P., and Kleinhampl, F.J., 1974, Stratigraphy, structure, and geologic history of the Lunar Lake caldera of northern Nye County, Nevada: U.S. Geological Survey Journal of Research, v. 2, no. 5, p. 599–608.
- Ekren, E.B., Rogers, C.L., and Dixon, G.L., 1973b, Geologic and bouguer gravity map of the Reveille quadrangle, Nye County, Nevada: U.S. Geological Survey Miscellaneous Geologic Investigations Map I-806, scale 1:48,000.
- Ekren, E.B., Rowley, P.D., Dixon, G.L., Page, W.R., Kleinhampl, F.J., Ziony, J.I., Brandt, J.M., and Patrick, B.G. 2012, Geology of the Quinn Canyon Range and vicinity, Nye and Lincoln Counties, Nevada: Southern Nevada Water Authority, Las Vegas, Nevada, Doc. No. HAM-ED-0004, 46 p., scale 1:250,000.
- Erskine, M.C., 2001, Structural overlap of passive continental margin stratigraphic packages onto the Colorado Plateau cratonic package in southwestern Utah, *in* Erskine, M.C., Faulds, J.E., Bartley, J.M., and Rowley, P.D., editors, The geologic transition, High Plateaus to Great Basin—a symposium and field guide: The Mackin Volume: Utah Geological Association Publication 30, and American Association of Petroleum Geologists Publication GB78, September 20–22, 2001, p. 365–377.
- Faulds, J.E., and Varga, R.J., 1998, The role of accommodation zones and transfer zones in the regional segmentation of extended terranes, *in* Faulds, J.E., and Stewart, J.H., editors, Accommodation zones and transfer zones—the regional segmentation of the Basin and Range province: Geological Society of America Special Paper 323, p. 1–45.
- Fenneman, N.M., 1931, Physiography of western United States: New York, McGraw-Hill Book Company, Inc., 534 p.
- Fouch, T.D., Lund, K., Schmitt, J.G., Good, S.C., and Hanley, J.H., 1991, Late Cretaceous(?) and Paleogene sedimentary rocks and extensional(?) basins in the region of the Egan and Grant ranges, and White River and Railroad valleys, Nevada: Their relation to Sevier and Laramide contractional basins in the southern Rocky Mountains and Colorado Plateau, *in* Flanigan, Donna M.H., Mike Hansen and T. Edward Flanigan, editors, Geology of White River Valley, the Grant Range, Eastern Railroad Valley and Western Egan Range, Nevada: 1991 Fieldtrip Guidebook, Nevada Petroleum Society Inc., p. 15–28.
- Francis, R.D., and Walker, C.T., 2002, Cenozoic detachments and attenuation in east-central Nevada, *in* Ehni, William, and Faulds, James, editors, Detachment and attenuation in eastern Nevada and its application to petroleum exploration: Nevada Petroleum Society 2002 Field Trip Guidebook, p. 73–95.
- French, Don E., and Schalla, Robert A., editors, 1998, Hydrocarbon habitat and special geologic problems of the Great Basin: 1998 Field Trip Guidebook, Nevada Petroleum Society, 109 p.
- Fryxell, J.E., 1988, Geologic map and descriptions of stratigraphy and structure of the west-central Grant Range, Nye County, Nevada: Geological Society of America Map and Chart Series MCH064, 15 p., scale 1:24,000.
- Gans, P.B., 2000a, The northern White Pine Range, *in* Gans, P.B., and Seedorff, E., editors, Geology and ore deposits 2000: The Great Basin and beyond: Geological Society of Nevada, Symposium Proceedings, May 15–18, 2000, p. 83–95.
- Gans, P.B., 2000b, The Snake Range metamorphic core complex—Geologic overview of the northern Snake Range, *in* Gans, P.B., and Seedorff, E., editors, Geology and ore deposits 2000: The Great Basin and beyond: Geological Society of Nevada, Symposium Proceedings, May 15–18, 2000, p. 99–117.
- Gans, P.B., and Miller, E.L., 1985, Comment on “The Snake Range décollement interpreted as a major extensional shear zone” by John M. Bartley and Brian P. Wernicke: Tectonics, v. 4, no. 4, p. 411–415.
- Gans, P.B., Mahood, G.A., and Schermer, E., 1989, Synextensional magmatism in the Basin and Range province: A case study from the eastern

- Great Basin: Geological Society of America Special Paper, v. 233, 53 p.
- Gans, P.B., Miller, E.L., Huggins, C.C., and Lee, J., 1999b, Geologic map of the Little Horse Canyon quadrangle, Nevada and Utah: Nevada Bureau of Mines and Geology Field Studies Map 20, scale 1:24,000.
- Gans, P.B., Miller, E.L., and Lee, J., 1999a, Geologic map of the Spring Mountain quadrangle, Nevada and Utah: Nevada Bureau of Mines and Geology Field Studies Map 18, scale 1:24,000.
- Gans, P.B., Miller, E.L., McCarthy, J., and Ouldcott, M.L., 1985, Tertiary extensional faulting and evolving ductile-brittle transition zones in the northern Snake Range and vicinity: New insights from seismic data: *Geology*, v. 13, p. 189–193.
- Gans, P.B., Seedorff, E., Fahey, P.L., Hasler, R.W., Maher, D.J., Jeanne, R.A., and Shaver, S.A., 2001, Rapid Eocene extension in the Robinson district, White Pine County, Nevada: Constraints from $^{40}\text{Ar}/^{39}\text{Ar}$ dating: *Geology*, v. 29, no. 6, p. 475–478.
- Gardner, P.M., and Heilweil, V.M., 2014, A multiple-tracer approach to understanding regional groundwater flow in the Snake Valley area of the eastern Great Basin, U.S.A.: *Applied Geochemistry*, v. 45, p. 33–49.
- Garside, L.J., Hess, R.H., Fleming, K.L., and Weimer, B.S., 1988, Oil and gas developments in Nevada: Nevada Bureau of Mines and Geology Bulletin 104, 136 p.
- Gebelin, A., Teyssier, C., Heizler, M.T., and Mulch, A., 2015, Meteoric water circulation in a rolling-hinge detachment system (northern Snake Range core complex, Nevada): *Geological Society of America Bulletin*, v. 127, p. 149–161.
- Grauch, V.J.S., Blakely, R.J., Blank, H.R., Oliver, H.W., Plouff, D., and Ponce, D.A., 1988, Geophysical delineation of granitic plutons in Nevada: U.S. Geological Survey Open-File Report 88-11, scale 1:1,000,000.
- Greene, D.C., 2014, The Confusion Range, west-central Utah—fold-thrust deformation and a western Utah thrust belt in the Sevier hinterland: *Geosphere*, v. 10, p. 148–169.
- Greene, D.C., and Herring, D.M., 2013, Structural architecture of the Confusion Range, west-central Utah—a Sevier fold-thrust belt and frontier petroleum province: Utah Geological Survey Open-File Report 613, CD.
- Guth, P.L., 1980, Geology of the Sheep Range, Clark County, Nevada [Ph.D. dissertation]: Massachusetts Institute of Technology, Cambridge, Massachusetts, 189 p.
- Hacker, D.B., 1998, Catastrophic gravity sliding and volcanism associated with the growth of laccoliths—examples from early Miocene hypabyssal intrusions of the Iron Axis magmatic province, Pine Valley Mountains, southwest Utah: Kent, Ohio, unpublished Ph.D. thesis, Kent State University, 258 p.
- Hacker, D.B., Biek, R.F., and Rowley, P.D., 2014, Catastrophic emplacement of the gigantic Markagunt gravity slide, southwest Utah (USA)—implications for hazards associated with sector collapse of volcanic fields: *Geology*, v. 42, no. 11, p. 943–946.
- Hacker, D.B., Holm, D.K., Rowley, P.D., and Blank, H.R., 2002, Associated Miocene laccoliths, gravity slides, and volcanic rocks, Pine Valley Mountains and Iron Axis region, southwestern Utah, in Lund, W.R., editor, Field guide to geologic excursions in southwestern Utah and adjacent areas of Arizona and Nevada, prepared for the Geological Society of America, Rocky Mountain Section Meeting in Cedar City, Utah, May 7–9, 2002: U.S. Geological Survey Open-File Report 02-172, p. 236–283.
- Hagstrum, J.T., and Gans, P.B., 1989, Paleomagnetism of the Oligocene Kalamazoo Tuff—Implications for middle Tertiary extension in east-central Nevada: *Journal of Geophysical Research*, v. 94, p. 1827–1842.
- Hamilton, W.B., 1995, Subduction systems and magmatism, in Smellie, J.L., editor, *Volcanism Associated with Extension at Consuming Plate Margins*: Geological Society Special Publication No. 81, p. 3–28.
- Hamilton, Warren, and Myers, W.B., 1966, Cenozoic tectonics of the western United States: *Reviews of Geophysics*, v. 4, p. 509–549.
- Hammond, W.C., Blewitt, G., and Kreemer, C., 2014, Steady contemporary deformation of the central Basin and Range province, United States: *Journal of Geophysical Research*, v. 119, doi:10.1002/2014JB011145, 19 p. (online).
- Harding, A.E., Scott, R.B., Mehnert, H.H., and Snee, L.W., 1995, Evidence of the Kane Springs Wash caldera in the Meadow Valley Mountains, southeastern Nevada, in Scott, R.B., and Swadley, W.C., editors, *Geologic studies in the Basin and Range—Colorado Plateau transition in southeastern Nevada, southwestern Utah, and northwestern Arizona*, 1992: U.S. Geological Survey Bulletin 2056, p. 135–180.
- Harrill, J.R., Gates, J.S., and Thomas, J.M., 1988, Major ground-water flow systems in the Great

- Basin region of Nevada, Utah, and adjacent states: U.S. Geological Survey Hydrologic Investigations Atlas HA-694-C, scale 1:1,000,000, 2 sheets.
- Harrill, J.R., and Prudic, D.E., 1998, Aquifer systems in the Great Basin region of Nevada, Utah, and adjacent states—summary report: U.S. Geological Survey Professional Paper 1409-A, 66 p.
- Hauser, E., Potter, C., Hauge, T., Burgess, S., Burtch, S., Mutschler, J., Allmendinger, R., Brown, L., Kaufman, S., and Oliver, J., 1987, Crustal structure of eastern Nevada from COCORP deep seismic reflection data: Geological Society of America Bulletin, v. 99, p. 833–844.
- Hazzard, J.C., and Turner, E.F., 1957, Décollement-type overthrusting in south-central Idaho, northwestern Utah, and northeastern Nevada [abs.]: Geological Society of America Bulletin, v. 68, no. 12, p. 1829.
- Heilweil, V.M., and Brooks, L.E., editors, 2011, Conceptual model of the Great Basin carbonate and alluvial aquifer system: U.S. Geological Survey Scientific Investigations Report 2010-5193, 191 p.
- Heiskanen, W.A., and Vening Meinesz, F.A., 1958, The earth and its gravity field: New York, McGraw-Hill, 470 p.
- Henry, C.D., 2008, Ash-flow tuffs and paleovalleys in northeastern Nevada—Implications for Eocene paleogeography and extension in the Sevier hinterland, northern Great Basin: *Geosphere*, v. 4, p. 1–35.
- Henry, C.D., Hinz, N.H., Faulds, J.E., Colgan, J.P., John, D.A., Brooks, E.R., Cassel, E.J., Garside, L.J., Davis, D.A., and Castor, S.B., 2012, Eocene-early Miocene paleotopography of the Sierra Nevada—Great Basin—Nevadaplano based on widespread ash-flow tuffs and paleovalleys: *Geosphere*, v. 8, p. 1–27.
- Herring, D.M., 1998a, Drilling results for the Balcron Oil #12-36 Cobra State dry hole, Millard County, Utah, *in* French, D.E., and Schalla, R.A., editors, Hydrocarbon habitat and special geologic problems of the Great Basin: 1998 Field Trip Guidebook, Nevada Petroleum Society, p. 88–89.
- Herring, D.M., 1998b, Drilling results of the EREC #31-22 Mamba Federal dry hole, Millard County, Utah, *in* French, D.E., and Schalla, R.A., editors, Hydrocarbon habitat and special geologic problems of the Great Basin: 1998 Field Trip Guidebook, Nevada Petroleum Society, p. 85–86.
- Herring, D.M., Greene, D.C., French, D.E., Schalla, R.A., and Taylor, W.J., 1998, 1998 Nevada Petroleum Society Field Trip—Day 3: Ely to Snake Valley, *in* French, D.E., and Schalla, R.A., editors, Hydrocarbon habitat and special geologic problems of the Great Basin: 1998 Field Trip Guidebook, Nevada Petroleum Society, p. 81–101.
- Hess, R., 2001, Nevada oil and gas well map: Nevada Bureau of Mines and Geology Open-File Report 2001–07.
- Hess, R., 2004, Nevada oil and gas well database (NVOILWEL): Nevada Bureau of Mines and Geology Open-File Report 04–01, 240 p.
- Hess, R.H., Henson, M.A., Davis, D.A., Limerick, S.H., Siewe, S.S., and Niles, M., 2011, Oil and gas well information for Nevada—2011 update: Nevada Bureau of Mines and Geology Open-File Report 11-6, 9643 digital files.
- Hess, R.H., and Johnson, G.L., 1997, Nevada Bureau of Mines and Geology county digital mapping project: Nevada Bureau of Mines and Geology Open-File Report 97–1, scale 1:250,000.
- Hildenbrand, T.G., 1983, FFTFIL—A filtering program based on two-dimensional Fourier analysis: U.S. Geological Survey Open-File Report 83-237, 61 p.
- Hildenbrand, T.G., and Kucks, R.P., 1988a, Filtered magnetic anomaly maps of Nevada: Nevada Bureau of Mines and Geology Map 93B, scale 1:1,000,000, 5 sheets.
- Hildenbrand, T.G., and Kucks, R.P., 1988b, Total intensity magnetic anomaly map of Nevada: Nevada Bureau of Mines and Geology Map 93A, scale 1:750,000.
- Hildenbrand, T.G., Kucks, R.P., and Sweeney, R.E., 1983, Digital colored magnetic-anomaly map of the Basin and Range province: U.S. Geological Survey Open-File Report 83-189, 11 p.
- Hildenbrand, T.G., Phelps, G., and Mankinen, E.A., 2006, Inversion of gravity data to define the pre-Cenozoic surface and regional structures possibly influencing groundwater flow in the Rainier Mesa region, Nye County, Nevada: U.S. Geological Survey Open-File Report 2006-1299, 28 p.
- Hintze, L.F., 1980a, Geologic map of Utah: Utah Geological and Mineralogical Survey, scale 1:500,000.
- Hintze, L.F., 1980b, Preliminary geologic map of the Sand Pass NW quadrangle, Juab County, Utah: U.S. Geological Survey Miscellaneous Field Studies Map MF-1149, scale 1:24,000.
- Hintze, L.F., 1988, A field guide to Utah's rocks: Geologic history of Utah: Brigham Young University Geology Studies, Special Publication 7, 202 p.

- Hintze, L.F., 2005, Utah's spectacular geology: How it came to be. Provo, Utah, Brigham Young University.
- Hintze, L.F., Anderson, R.E., and Embree, G.F., 1994a, Geologic map of the Motoqua and Gunlock quadrangles, Washington County, Utah: U.S. Geological Survey Miscellaneous Investigations Series Map I-2427, scale 1:24,000.
- Hintze, L.F., and Davis, F.D., 2002a, Geologic map of the Tule Valley 30'×60' quadrangle and parts of the Ely, Fish Springs, and Kern Mountains 30'×60' quadrangles, northwest Millard County, Utah: Utah Geological Survey Map 186, scale 1:100,000, 2 sheets.
- Hintze, L.F., and Davis, F.D., 2002b, Geologic map of the Wah Wah Mountains North 30'×60' quadrangle and part of the Garrison 30'×60' quadrangle, southwest Millard County and part of Beaver County, Utah: Utah Geological Survey Map 182, scale 1:100,000, 2 sheets.
- Hintze, L.F., and Davis, F.D., 2003, Geology of Millard County, Utah: Utah Geological Survey Bulletin 133, 305 p.
- Hintze, L.F., Grant, S.K., Weaver, C.L., and Best, M.G., 1994b, Geologic map of the Blue Mountain-Lund area, Beaver and Iron counties, Utah: U.S. Geological Survey Miscellaneous Investigations Map I-2361, scale 1:50,000.
- Hintze, L.F., and Kowallis, B.J., 2009, Geologic history of Utah. Provo, Utah, Brigham Young University Geology Studies Special Publication 9, 225 p.
- Hintze, L.F., Willis, G.C., Laes, D.Y.M., Sprinkel, D.A., and Brown, K.D., 2000, Digital geologic map of Utah: Utah Geological Survey Map 179DM, scale 1:500,000, 2 sheets.
- Hitchborn, A.D., Arbonies, D.G., Peters, S.G., Connors, K.A., Noble, D.C., Larson, L.T., Beebe, J.S., and McKee, E.H., 1996, Geology and gold deposits of the Bald Mountain mining district, White Pine County, Nevada, *in* Coyner, A.R., and Fahey, P.L., editors, Geology and Ore Deposits of the American Cordillera: Geological Society of Nevada Symposium Proceedings, Reno/Sparks, Nevada, April 1995, p. 505–546.
- Hood, J.W., and Rush, F.E., 1965, Water-resources appraisal of the Snake Valley area, Utah and Nevada: Nevada Department of Conservation and Natural Resources Water Resources—Reconnaissance Series Report 34, 40 p.
- Hose, R.K., 1977, Structural geology of the Confusion Range, west-central Utah: U.S. Geological Survey Professional Paper 971, 9 p.
- Hose, R.K., and Blake, Jr., M.C., 1976, Geology and mineral resources of White Pine County, Nevada Part I, Geology: Nevada Bureau of Mines and Geology Bulletin 85, p. 1–35.
- Howard, E.L., 1978, Geologic map of the eastern Great Basin, Nevada and Utah: Terrascan Group, Inc., Lakewood, Colorado, scale 1:250,000.
- Howard, K.A., Kistler, R.W., Snoke, A.W., and Willden, R., 1979, Geologic map of the Ruby Mountains, Nevada: U.S. Geological Survey Miscellaneous Investigations Series Map I-1136, scale 1:125,000.
- Howard, K.A., Wooden, J.L., Barnes, C.G., Premo, W.R., Snoke, A.W., and Lee, S.-Y., 2011, Episodic growth of a Late Cretaceous and Paleogene intrusive complex of pegmatitic leucogranite, Ruby Mountains core complex, Nevada, USA: *Geosphere*, v. 7, p. 1220–1248.
- Hudson, M.R., and Geissman, J.W., 1982, Dispersed paleomagnetic data from the Kern Mountains metamorphic core complex, northeastern Nevada: *Eos, Transactions of the American Geophysical Union*, v. 63, no. 45, p. 919.
- Hudson, M.R., Rosenbaum, J.G., Gromme, C.S., Scott, R.B., and Rowley, P.D., 1998, Paleomagnetic evidence for counterclockwise rotation in a broad sinistral shear zone, Basin and Range province, southeastern Nevada and southwestern Utah, *in* Faulds, J.E., and Stewart, J.H., editors, Accommodation zones and transfer zones—the regional segmentation of the Basin and Range province: Geological Society of America Special Paper 323, p. 149–180.
- Humphreys, E.D., 1995, Post-Laramide removal of the Farallon slab, western United States: *Geology*, v. 23, p. 987–990.
- Humphreys, E., 2009, Relation of flat subduction to magmatism and deformation in the western United States, *in* Kay, S.M., Ramos, V.A., and Dickinson, W.R., editors, Backbone of the Americas—shallow subduction, plateau uplift, and ridge and terrane collision: Geological Society of America Memoir 204, p. 85–98.
- Hurlow, H., editor, 2014, Hydrogeologic studies and groundwater monitoring in Snake Valley and adjacent hydrographic areas, west-central Utah and east-central Nevada: Utah Geological Survey Bulletin 135, 294 p. (DVD).
- Hurlow, H.A., and Inkenbrandt, P.C., 2016, Analysis (sic) of groundwater-level records from Snake Valley, western Millard County, Utah, *in* Comer, J.B., Inkenbrandt, P.C., Krahulec, K.A., and Pinnell, M.L., editors, Resources and geology of Utah's West Desert: Utah Geological Association Publication 45, p. 221–246.

- Hurtubise, D.O., and du Bray, E.A., 1992, Stratigraphy and structure of the Seaman Range and Fox Mountain, Lincoln, and Nye Counties, Nevada: U.S. Geological Survey Bulletin 1988-B, 31 p.
- Jachens, R.C., and Moring, B.C., 1990, Maps of the thickness of Cenozoic deposits and the isostatic residual gravity over basement for Nevada: U.S. Geological Survey Open-File Report 90-404, 15 p.
- Jachens, R.C., and Roberts, C.W., 1981, Documentation of program, ISOCIETYOMP, for computing isostatic residual gravity: U.S. Geological Survey Open-File Report 81-574, 26 p.
- Jayko, A.S., 1990, Shallow crustal deformation in the Pahrnatag area, southern Nevada, *in* Wernicke, B.P., ed., Basin and Range extensional tectonics near the latitude of Las Vegas, Nevada: Boulder, Colorado, Geological Society of America Memoir 176, p. 213–236.
- Jayko, A.S., 2007, Geologic map of the Pahrnatag Range 30'×60' quadrangle, Lincoln and Nye Counties, Nevada: U.S. Geological Survey Scientific Investigations Map 2904, scale 1:100,000. [<http://pubs.usgs.gov/sim/2007/2904/>].
- Johnson, J.A., 2007, Hydrology of Muddy River Springs, *in* Coache, R., editor, Regional tour of the carbonate system guidebook: Nevada Water Resources Association, Clark County, Nevada, June 18–20, 2007, p. 3–4.
- Johnson, M., 2007a, Geyser Spring complex hydrology and Lake Valley activities, *in* Coache, R., editor, Regional tour of the carbonate system guidebook: Nevada Water Resources Association, Clark County, Nevada, June 18–20, 2007, p. 59–60.
- Johnson, M., 2007b, Hydrogeology of Pahrnatag shear zone and surrounding area, *in* Coache, R., editor, Regional tour of the carbonate system guidebook: Nevada Water Resources Association, Reno, Nevada, p. 11–12.
- Johnson, M., Dixon, G.L., Rowley, P.D., Katzer, T.C., and Winters, M., 2002, Hydrology and ground-water conditions of the Tertiary Muddy Creek Formation in the lower Virgin River basin of southeastern Nevada and adjacent Arizona and Utah, *in* Lund, W.R., editor, Field guide to geologic excursions in southwestern Utah and adjacent areas of Arizona and Nevada: Utah Geological Survey Open-File Report 02-172, p. 284–315.
- Jones, A.E., ed., 1996, Geology and gold deposits of eastern Nevada—1996 Spring Field Trip Guidebook: Geological Society of Nevada Special Publication No. 23, Reno, Nevada, May 3–5, 1996, 166 p.
- Keith, J.D., Tingey, D.G., and Best, M.G., 1994, Geologic map of the Rice Mountain quadrangle, Nevada and Utah: Nevada Bureau of Mines and Geology Field Studies Map 7, scale 1:24,000.
- Keller, G.V., 1987, Rock and mineral properties, *in* Nabighian, M.N., editor, Electromagnetic methods in applied geophysics: Volume 1, Theory, Tulsa, Oklahoma, Society of Exploration Geophysicists, Investigations in Geophysics no. 3, p. 13–51.
- Kellogg, H.E., 1963, Paleozoic stratigraphy of the southern Egan Range, Nevada: Geological Society of America Bulletin, v. 74, p. 685–708.
- Kellogg, H.E., 1964, Cenozoic stratigraphy and structure of the southern Egan Range, Nevada: Geological Society of America Bulletin, v. 75, p. 949–968.
- Kepper, J.C., 1960, Stratigraphy and structure of the southern half of the Fish Springs Range, Juab County, Utah [M.S. thesis]: University of Washington, Seattle, 92 p.
- Kirby, S., and Hurlow, H., 2005, Hydrogeologic setting of the Snake Valley hydrologic basin, Millard County, Utah, and White Pine and Lincoln Counties, Nevada—implications for possible effects of proposed water wells: Utah Geological Survey Report of Investigation 254, 39 p.
- Kistinger, G.M., Prieur, J.P., Rowley, P.D., and Dixon, G.L., 2009, Characterization of streams and springs in the Snake Valley area, Utah and Nevada, *in* Tripp, B.T., Krahulec, K., and Jordan, J.L., editors, Geology and geologic resources and issues of western Utah: Utah Geological Association Publication 38, p. 299–323.
- Kleinhampl, F.J., and Ziony, J.I., 1985, Geology of northern Nye County, Nevada: Nevada Bureau of Mines and Geology Bulletin 99A, 172 p.
- Kucks, R.P., Hill, P.L., and Ponce, D.A., 2006, Nevada magnetic and gravity maps and data—a website for the distribution of data: U.S. Geological Survey Data Series 234 [<http://pubs.er.usgs.gov/usgspubs/ds/ds234/>].
- Laczniak, R.J., Cole, J.C., Sawyer, D.A., and Trudeau, D.A., 1996, Summary of hydrogeologic controls on ground-water flow at the Nevada Test Site, Nye County, Nevada: U.S. Geological Survey Water-Resources Investigations Report 96-4109, 59 p.
- Langenheim, V.E., Beard, L.S., and Faulds, J.E., 2010, Implications of geophysical analysis on basin geometry and fault offsets in the northern Colorado River extensional corridor and adjoining Lake Mead region, Nevada and Arizona, *in* Umhoefer, P.J., Beard, L.S., and

- Lamb, M.A., editors, Miocene tectonics of the Lake Mead region, central Basin and Range: Geological Society of America Special Paper 463, p. 39–59.
- Langenheim, V.E., Glen, J.M., Jachens, R.C., Dixon, G.L., Katzer, T.C., and Morin, R.L., 2000, Geophysical constraints on the Virgin River depression, Nevada, Utah, and Arizona: U.S. Geological Survey Open-File Report 2000-407, 26 p.
- Langenheim, V.E., Miller, J.J., Page, W.R., and Grow, J.A., 2001, Thickness and geometry of Cenozoic deposits in California Wash area, Nevada, based on gravity and seismic-reflection data: U.S. Geological Survey Open-File Report 01-393, 26 p.
- Larson, E.R., and Langenheim, Jr., R.L., 1979, The Mississippian and Pennsylvanian (Carboniferous) systems in the United States—Nevada: U.S. Geological Survey Professional Paper 1110-BB, p. BB1–BB19.
- Las Vegas Valley Water District, 2001, Water resources and ground-water modeling in the White River and Meadow Valley flow systems, Clark, Lincoln, Nye and White Pine counties, Nevada: Las Vegas Valley Water District, Las Vegas, Nevada, 297 p.
- Layne Geosciences, 2009, Status report audiomagnetotelluric surveys Spring and Snake valleys, Nevada: Layne Geosciences, Fontana, California, 274 p.
- Leahy, P.P., and Lyttle, P.T., 1998, The re-emerging and critical role of geologic understanding in hydrology, *in* Brahana, J.V., Eckstein, Y., Ongley, L.K., Schneider, R., and Moore, J.E., editors, Gambling with groundwater—physical, chemical, and biological aspects of aquifer-stream relations: Proceedings International Association of Hydrogeologists and the American Institute of Hydrologists, Las Vegas, Nevada, September 28–October 2, 1998: The American Institute of Hydrology, p. 19–24.
- Lee, J., 1995, Rapid uplift and rotation of mylonitic rocks from beneath a detachment fault—Insights from potassium feldspar $^{40}\text{Ar}/^{39}\text{Ar}$ thermochronology, northern Snake Range, Nevada: *Tectonics*, v. 14, p. 54–77.
- Lee, J., Gans, P.B., and Miller, E.L., 1999a, Geologic map of the Mormon Jack Pass quadrangle, Nevada: Nevada Bureau of Mines and Geology Field Studies Map 17, scale 1:24,000.
- Lee, J., Gans, P.B., and Miller, E.L., 1999b, Geologic map of the Third Butte East quadrangle, Nevada: Nevada Bureau of Mines and Geology Field Studies Map 16, scale 1:24,000.
- Lee, J., Miller, E.L., Gans, P.B., and Huggins, C.C., 1999c, Geologic map of the Mount Moriah quadrangle, Nevada: Nevada Bureau of Mines and Geology Field Studies Map 19, scale 1:24,000.
- Lewis, C.J., Wernicke, B.P., Selverstone, Jane, and Bartley, J.M., 1999, Deep burial of the footwall of the northern Snake Range décollement, Nevada: *Geological Society of America Bulletin*, v. 111, p. 39–51.
- Liberty, L.M., Heller, P.L., and Smithson, S.B., 1994, Seismic reflection evidence for two-phase development of Tertiary basins from east-central Nevada: *Geological Society of America Bulletin*, v. 106, p. 1621–1633.
- Link, P.K., Christie-Blick, N., Devlin, W.J., Elston, D.P., Horodyski, R.J., Levy, M., Miller, J.M.G., Pearson, R.C., Prave, A., Stewart, J.H., et al., 1993, Middle and Late Proterozoic stratified rocks of the western U.S. Cordillera, Colorado Plateau, and Basin and Range province, *in* Reed, Jr., J.C., editor, Precambrian: Conterminous U.S.: Geological Society of America, The Geology of North America, v. C-2, p. 463–595.
- Lipman, P.W., Prostka, H.J., and Christiansen, R.L., 1972, Cenozoic volcanism and plate-tectonic evolution of the western United States. I. Early and middle Cenozoic: *Royal Society of London Philosophical Transactions A*, v. 271, no. 1213, p. 217–248.
- Long, S.P., 2012, Magnitudes and spatial patterns of erosional exhumation in the Sevier hinterland, eastern Nevada and western Utah, USA—Insight from a Paleogene paleogeologic map: *Geosphere*, v. 8, p. 881–901.
- Long, S.P., 2014, Preliminary geologic map of Heath Canyon, central Grant Range, Nye County, Nevada: Nevada Bureau of Mines and Geology Open-File Report 14-6, scale 1:24,000, 4 p.
- Long, S.P., and Walker, J.P., 2015, Geometry and kinematics of the Grant Range brittle detachment system, eastern Nevada, U.S.A.: an end-member style of upper-crustal extension: *Tectonics*, v. 34, TC003918, 26 p., doi: 10.1002/2015TC003918
- Long, S.P., Henry, C.D., Muntean, J.L., Edmondo, G.P., and Casel, E.V., 2014, Early Cretaceous construction of a structural culmination, Eureka, Nevada, U.S.A.—implications for out-of-sequence deformation in the Sevier hinterland: *Geosphere*, v. 10, p. 564–584.
- Long, S.P., Thomson, S.N., Reiners, P.W., and Di Fiori, R.V., 2015, Synorogenic extension localized by upper-crustal thickening—an example from the

- Late Cretaceous Nevadaplano: *Geology*, v. 43, p. 351–354.
- Longwell, C.R., Pampeyan, E.H., Bowyer, B., and Roberts, R.J., 1965, *Geology and mineral deposits of Clark County, Nevada*: Nevada Bureau of Mines and Geology Bulletin 62, 218 p.
- Loucks, M.D., Tingey, D.G., Best, M.G., Christiansen, E.H., and Hintze, L.F., 1989, *Geologic map of the Fortification Range, Lincoln and White Pine Counties, Nevada*: U.S. Geological Survey Miscellaneous Investigations Series Map I-1866, scale 1:50,000.
- Lumsden, W.W., Walker, C.T., and Francis, R.D., 2002, The Precambrian and Paleozoic stratigraphy of the White Pine, Grant and Schell Creek Ranges in eastern Nevada—The key to interpreting structures formed by extension and attenuation, *in* Ehni, W., and Faulds, J., editors, *Detachment and attenuation in eastern Nevada and its application to petroleum exploration*: Nevada Petroleum Society 2002 Field Trip Guidebook, p. 33–72.
- Lund, Karen, and Beard, L.S., 1992, Extensional geometry in the northern Grant Range, east central Nevada—implications for oil deposits in Railroad Valley, *in* Thorman, C.H., editor, *Application of structural geology to mineral and energy resources of the central and western United States*: U.S. Geological Survey Bulletin 1212, p. I1–I9.
- Lund, K., Beard, L.S., and Perry, Jr., W.J., 1991, Structures of the northern Grant Range and Railroad Valley, Nye County, Nevada: Implications for oil occurrences, *in* Flanigan, D.M.H., Hansen M., and Flanigan, T.E., editors, *Geology of White River Valley, the Grant Range, Eastern Railroad Valley and Western Egan Range, Nevada*: 1991 Fieldtrip Guidebook, Nevada Petroleum Society Inc., Reno, p. 1–6.
- Mabey, D.R., Zietz, I., Eaton, G.P., and Kleinkopf, M.D., 1978, Regional magnetic patterns in part of the Cordillera in the western United States, *in* Smith, R.B., and Eaton, G.P., editors, *Cenozoic tectonics and regional geophysics of the western Cordillera*: Geological Society of America Memoir 152, p. 93–106.
- Maldonado, F., and Schmidt, D.L., 1991, *Geologic map of the southern Sheep Range, Fossil Ridge, and Castle Rock area, Clark County, Nevada*: U.S. Geological Survey Miscellaneous Investigations Series Map I-2086, scale 1:24,000.
- Maldonado, F., Spengler, R.W., Hanna, W.F., and Dixon, G.L., 1988, Index of granitic rock masses in the State of Nevada: U.S. Geological Survey Bulletin 1831, 81 p.
- Mankinen, E.A., 2007, Gravity and magnetic studies of the Spring Valley region, *in* Coache, R., editor, *Regional tour of the carbonate system guidebook*: Nevada Water Resources Association, Clark County, Nevada, June 18–20, 2007, p. 37–38.
- Mankinen, E.A., and McKee, E.H., 2007, Gravity data from Newark Valley, White Pine County, Nevada: U.S. Geological Survey Open-File Report 2007-1306, 18 p.
- Mankinen, E.A., and McKee, E.H., 2009, Geophysical setting of western Utah and eastern Nevada between latitudes 37°45' and 40°N, *in* Tripp, B.T., Krahulec, K., and Jordan, J.L., editors, *Geology and geologic resources and issues of western Utah*: Utah Geological Association Publication 38, p. 271–286.
- Mankinen, E.A., and McKee, E.H., 2011, Principle facts for gravity stations collected in 2010 from White Pine and Lincoln Counties, east-central Nevada: U.S. Geological Survey Open-File Report 2011-1084, 24 p.
- Mankinen, E.A., Roberts, C.W., McKee, E.H., Chuchel, B.A., and Moring, B.C., 2006, *Geophysical Data from the Spring and Snake valleys area, Nevada and Utah*: U.S. Geological Survey Open-File Report 2006-1160, 36 p.
- Mankinen, E.A., Roberts, C.W., McKee, E.H., Chuchel, B.A., and Moring, R.L., 2007, *Geophysical data from Spring Valley to Delamar Valley, east-central Nevada*: U.S. Geological Survey Open-File Report 2007-1190, 42 p.
- Mankinen, E.A., Rowley, P.D., Dixon, G.L., and McKee, E.H., 2016, Regional geophysics of western Utah and eastern Nevada, with emphasis on the Confusion Range, *in* Comer, J.B., Inkenbrandt, P.C., Krahulec, K.A., and Pinnell, M.L., editors, *Resources and geology of Utah's West Desert*: Utah Geological Association Publication 45, p. 147–166.
- Mankinen, E.A., Chuchel, B.A., and Moring, B.C., 2008, Gravity data from Dry Lake and Delamar Valleys, east-central Nevada: U.S. Geological Survey Open-File Report 2008-1299, 30 p. [<http://pubs.usgs.gov/of/2008-1299/>].
- Masbruch, M.D., Gardner, P.M., and Brooks, L.E., 2014, Hydrology and numerical simulation of groundwater movement and heat transport in Snake Valley and surrounding areas, Juab, Millard, and Beaver counties, Utah, and White Pine and Lincoln counties, Nevada: U.S. Geological Survey Scientific Investigations Report 2014-5103, 108 p.
- Masbruch, M.D., Gardner, P.M., and Brooks, L.E., 2016, Numerical simulation of groundwater movement and heat transport in Snake Valley and

- surrounding areas, Juab, Millard, and Beaver counties, Utah, and White Pine and Lincoln counties, Nevada, *in* Comer, J.B., Inkenbrandt, P.C., Krahulec, K.A., and Pinnell, M.L., editors, *Resources and geology of Utah's West Desert*: Utah Geological Association Publication 45, p. 201–220.
- Mason, J.L., Atwood, J.W., and Buettner, P.S., 1985, Selected test-well data from the MX-missile siting study, Tooele, Juab, Millard, Beaver, and Iron Counties, Utah: Utah Hydrologic-Data Report 43, U.S. Geological Survey Open-File Report 85-374, 15 p.
- McGrew, A.J., 1993, The origin and evolution of the southern Snake Range décollement, east central Nevada: *Tectonics*, v. 12, no. 1, p. 21–34.
- McPhee, D.K., 2007, Audiomagnetotelluric imaging of the Spring Valley region, *in* Coache, R., editor, *Regional tour of the carbonate system guidebook*: Nevada Water Resources Association, Clark County, Nevada, June 18–20, 2007, p. 39–40.
- McPhee, D.K., Chuchel, B.A., and Pellerin, L., 2006b, Audiomagnetotelluric data from Spring, Cave, and Coyote Spring valleys, Nevada: U.S. Geological Survey Open-File Report 2006-1164, 43 p.
- McPhee, D.K., Chuchel, B.A., and Pellerin, L., 2007, Audiomagnetotelluric data and two-dimensional models from Spring, Snake, and Three Lakes Valleys, Nevada: U.S. Geological Survey Open-File Report 2007-1181, 47 p. [<http://pubs.usgs.gov/of/2007/1181/>].
- McPhee, D.K., Chuchel, B.A., and Pellerin, L., 2008, Audiomagnetotelluric data and preliminary two-dimensional models from Spring, Dry Lake, and Delamar Valleys, Nevada: U.S. Geological Survey Open-File Report 2008-1301, 59 p.
- McPhee, D.K., Pari, K., and Baird, F., 2009, Audiomagnetotelluric investigation of Snake Valley, eastern Nevada and western Utah, *in* Tripp, B.T., Krahulec, K., and Jordan, J.L., editors, *Geology and geologic resources and issues of western Utah*: Utah Geological Association Publication 38, p. 287–298.
- McPhee, D.K., Pellerin, L., Chuchel, B.A., and Dixon, G.L., 2005, Resistivity imaging of Spring Valley, Nevada, using the audiomagnetotelluric method, *EOS, Transactions American Geophysical Union*, 86(18), Joint Assembly Supplement, Abstract NS23B-06.
- McPhee, D.K., Pellerin, L., Chuchel, B.A., Tilden, J.E., and Dixon, G.L., 2006a, Resistivity imaging in eastern Nevada using the audiomagnetotelluric method for hydrogeologic framework studies, *in* *Proceedings of the 19th Annual Symposium on the Application of Geophysics to Engineering and Environmental Problems (SAGEEP)*, Seattle, Washington, April 2–6, 2006, p. 712–718.
- Mifflin, M.D., and Wheat, M.M., 1979, Pluvial lakes and estimated pluvial climates of Nevada: Nevada Bureau of Mines and Geology Bulletin 94, 57 p.
- Miller, E.L., and Gans, P.B., 1989, Cretaceous crustal structure and metamorphism in the hinterland of the Sevier thrust belt, western U.S. Cordillera: *Geology*, v. 17, p. 59–62.
- Miller, E.L., and Gans, P.B., 1999, Geologic map of The Cove quadrangle, Nevada and Utah: Nevada Bureau of Mines and Geology Field Studies Map 22, scale 1:24,000.
- Miller, E.L., Gans, P.B., and Garing, J., 1983, The Snake Range décollement—an exhumed mid-Tertiary ductile-brittle transition: *Tectonics*, v. 2, no. 3, p. 239–263.
- Miller, E.L., Dumitru, T.A., Brown, R.W., and Gans, P.B., 1999a, Rapid Miocene slip on the Snake Range—Deep Creek Range fault system, east-central Nevada: *Geological Society of America Bulletin*, v. 111, no. 6, p. 886–905.
- Miller, E.L., Gans, P.B., and Grier, S.P., 1994, Geologic map of Windy Peak 7.5' quadrangle, White Pine County, Nevada: U.S. Geological Survey Open-File Report 94-687, scale 1:24,000.
- Miller, E.L., Gans, P.B., Grier, S.P., Huggins, C.C., and Lee, J., 1999b, Geologic map of the Old Mans Canyon quadrangle, Nevada: Nevada Bureau of Mines and Geology Field Studies Map 21, scale 1:24,000.
- Miller, E.L., Grier, S.P., and Brown, J.L., 1995, Geologic map of the Lehman Caves quadrangle, White Pine County, Nevada: U.S. Geological Survey Geologic Quadrangle Map GQ-1758, scale 1:24,000.
- Misch, P., 1960, Regional structural reconnaissance in central-northeast Nevada and some adjacent areas—observations and interpretations, *in* Boettcher, J.W., and Sloan, Jr., W.W., editors, *Guidebook to the geology of east central Nevada*: Intermountain Association of Petroleum Geologists and Eastern Nevada Geological Society, 11th Annual Field Conference, Salt Lake City, Utah, September 8–10, 1960, p. 17–42.
- Moores, E.M., Scott, R.B., and Lumsden, W.W., 1968, Tertiary tectonics of White Pine-Grant Range region, east-central Nevada, and some regional implications: *Geological Society of America Bulletin*, v. 79, no. 12, p. 1703–1726.
- Morelli, C., editor, 1974, *The international gravity standardization net 1971*: International Association

- of Geodesy Special Publication 4, 194 p.
- Morris, H.T., 1987, Preliminary geologic map of the Delta 2° quadrangle, Tooele, Juab, Millard, and Utah Counties, Utah: U.S. Geological Survey Open-File Report 87-185, scale 1:250,000, 3 sheets.
- Nelson, R.B., 1966, Structural development of northernmost Snake Range, Kern Mountains, and Deep Creek Range, Nevada and Utah: American Association of Petroleum Geologists Bulletin, v. 50, no. 5, p. 921-951.
- Nolan, T.B., 1935, The Gold Hill mining district, Utah: U.S. Geological Survey Professional Paper 177, 172 p.
- Norman, B.W., and Gans, P.B., 2014, Polyphase (Eocene and Miocene) extensional faulting of the central Schell Creek Range, White Pine County, Nevada (abs.): Geological Society of America 2014 Abstracts with Programs, v. 46, no. 6, p. 171.
- North American Magnetic Anomaly Group (NAMAG), 2002, Digital data grids for the magnetic anomaly map of North America: U.S. Geological Survey Open-File Report 02-414, 4 p.
- Nutt, C.J., 2000, Geologic map of the Alligator Ridge area, including the Buck Mountain East and Mooney Basin Summit quadrangles and parts of the Sunshine Well NE and Long Valley Slough quadrangles, White Pine County, Nevada: U.S. Geological Survey Geologic Investigations Series Map I-2691, scale 1:24,000.
- Nutt, C.J., and Hart, K.S., 2004, Geologic map of the Big Bald Mountain quadrangle and part of the Tognini Spring quadrangle, White Pine County, Nevada: Nevada Bureau of Mines and Geology Map 145, scale 1:24,000.
- Nutt, C.J., Zimbelman, D.R., Campbell, D.L., Duval, J.S., and Hannigan, B.J., 1990, Chapter C: Mineral resources of the Deep Creek Mountains wilderness study area, Juab and Tooele counties, Utah: U.S. Geological Survey Bulletin 1745-C, 40 p.
- Oliveira, M.E., 1975, Geology of the Fish Springs mining district, Fish Springs Range, Utah: Brigham Young University Geology Studies, v. 22, pt. 1, p. 69-104.
- Otto, B.R., 2008, Geologic map of the central Butte Range, White Pine County, Nevada: Nevada Bureau of Mines and Geology Map 160, scale 1:48,000.
- Oviatt, C.G., 1991, Quaternary geology of Fish Springs Flat, Juab County, Utah: Utah Geological Survey Special Study 77, 16 p.
- Page, W.R., 1992, Preliminary geologic map of the Paleozoic rocks in the Arrow Canyon quadrangle, Clark County, Nevada: U.S. Geological Survey Open-File Report 92-681, scale 1:24,000.
- Page, W.R., 1998, Geologic map of the Arrow Canyon NW quadrangle, Clark County, Nevada: U.S. Geological Survey Geologic Quadrangle Map GQ-1776, scale 1:24,000.
- Page, W.R., and Dixon, G.L., 1992, Northern terminus of Mesozoic Dry Lake thrust fault, Arrow Canyon Range, southeastern Nevada [abs]: Geological Society of America Abstracts with Programs, v. 24, no. 6, p. 56.
- Page, W.R., and Ekren, E.B., 1995, Preliminary geologic map of the Bristol Well quadrangle, Lincoln County, Nevada: U.S. Geological Survey Open-File Report 95-580, scale 1:24,000.
- Page, W.R., and Pampeyan, E.H., 1996, Preliminary geologic map of the Paleozoic rocks in the Wildcat Wash SE and Wildcat Wash SW quadrangles, Lincoln and Clark Counties, Nevada: U.S. Geological Survey Open-File Report 96-26, scale 1:24,000, 2 sheets.
- Page, W.R., Dixon, G.L., Rowley, P.D., and Brickey, D.W., 2005a, Geologic map of parts of the Colorado, White River, and Death Valley groundwater flow systems, Nevada, Utah, and Arizona: Nevada Bureau of Mines and Geology Map 150, scale 1:250,000.
- Page, W.R., Lundstrom, S.C., Harris, A.G., Langenheim, V.E., Workman, J.B., Mahan, S.A., Paces, J.B., Dixon, G.L., Rowley, P.D., Burchfiel, B.C., Bell, J.W., and Smith, E.I., 2005b, Geologic and geophysical maps of the Las Vegas 30'x60' quadrangle, Clark and Nye Counties, Nevada, and Inyo County, California: U.S. Geological Survey Scientific Investigations Map 2814, scale 1:100,000, 2 sheets.
- Page, W.R., Scheirer, D.S., and Langenheim, V.E., 2006, Geologic cross sections of parts of the Colorado, White River, and Death Valley regional ground-water flow systems, Nevada, Utah, and Arizona: U.S. Geological Survey Open-File Report 2006-1040, Denver, CO, 80225.
- Page, W.R., Swadley, W.C., and Scott, R.B., 1990, Preliminary geologic map of the Delamar 3 SW quadrangle, Lincoln County, Nevada: U.S. Geological Survey Open-File Report 90-336, scale 1:24,000.
- Palacky, G.J., 1987, Resistivity characteristics of geologic targets, in Nabighian, M.N., editor, Electromagnetic methods in applied geophysics, Volume 1, Theory: Society of Exploration Geophysics, Tulsa, Oklahoma, Investigations in

- Geophysics, no. 3, p. 53–129.
- Pampeyan, E.H., 1993, Geologic map of the Meadow Valley Mountains, Lincoln and Clark Counties, Nevada: U.S. Geological Survey Miscellaneous Investigations Series Map I-2173, scale 1:50,000, 2 sheets.
- Pari, K.T., and Baird, F.A., 2011, Audiomagnetotellurics investigations in selected basins in White Pine and Lincoln Counties, East-Central Nevada: Southern Nevada Water Authority, Las Vegas, Nevada, Doc. No. RDS-ED-0022, 81 p.
- Pekarek, A.H., 1988, Structural geology and petroleum potential of Long Valley, White Pine County, Nevada: *Mountain Geologist*, v. 25, no. 4, p. 141–180.
- Petronis, M.S., Holm, D.K., Geissman, J.W., Hacker, D.B., and Arnold, B.J., 2014, Paleomagnetic results from the eastern Caliente-Enterprise zone, southwestern Utah—implications for initiation of a major Miocene transfer zone: *Geosphere*, v. 10, p. 534–563.
- Phelps, G.A., Jewel, E.B., Langenheim, V.E., and Jachens, R.C., 2000, Principal facts for gravity stations in the vicinity of Coyote Spring Valley, Nevada, with initial gravity modeling results: U.S. Geological Survey Open-File Report 00–420, 22 p.
- Ponce, D.A., 1992, Complete Bouguer gravity map of Nevada, Ely sheet: Nevada Bureau of Mines and Geology Map 99, scale 1:250,000.
- Ponce, D.A., 1997, Gravity data of Nevada: U.S. Geological Survey Digital Data Series DDS-42, 27 p., CD-ROM.
- Ponce, D.A., Morin, R.L., and Robbins, S.L., 1996, Bouguer gravity map of Nevada, Elko sheet: Nevada Bureau of Mines and Geology Map 107, scale 1:250,000.
- Poole, F.G., and Sandberg, C.A., 1977, Mississippian paleogeography and tectonics of the western United States, *in* Stewart, J.H., Stevens, C.H., and Fritsche, A.E., editors, *Paleozoic paleogeography of the western United States*: Society of Economic Paleontologists and Mineralogists, Pacific Section, Pacific Coast Paleogeography Symposium 1, April 22, 1977, p. 67–85.
- Poole, F.G., and Sandberg, C.A., 1991, Mississippian paleogeography and conodont biostratigraphy of the western United States, *in* Cooper, J.D., and Stevens, C.H., editors, *Paleozoic paleogeography of the western United States—II*: Society of Economic Paleontologists and Mineralogists, Pacific Section, Pacific Coast Paleogeography, p. 107–136.
- Puchlik, K., 2009, The crypto zinc-indium-copper-molybdenum skarn deposit, western Juab County, Utah: *Utah Geological Association Newsletter*, v. 41, no. 6, p. 1–2.
- Quinlivan, W.D., Rogers, C.L., and Dodge, Jr., H.W., 1974, Geologic map of the Portuguese Mountain quadrangle, Nye County, Nevada: U.S. Geological Survey Miscellaneous Investigations Series Map I-804, scale 1:48,000.
- Raines, G.L., Connors, K.A., Moyer, L.A., and Miller, R.J., 2003, Spatial digital database for the geologic map of Nevada. Digital database, Version 3.0: U.S. Geological Survey Open-File Report 03–66.
- Reheis, M.C., Adams, K.D., Oviatt, C.G., and Bacon, S.N., 2014, Pluvial lakes in the Great Basin of the western United States—a view from the outcrop: *Quaternary Science Reviews*, v. 97, p. 1–25.
- Roberts, R.J., Montgomery, K.M., and Lehner, R.E., 1967, Geology and mineral resources of Eureka County, Nevada: Nevada Bureau of Mines and Geology Bulletin 64, 152 p., scale 1:250,000, 12 sheets.
- Robinson, J.P., 1993, Provisional geologic map of the Gold Hill quadrangle, Tooele County, Utah: Utah Geological Survey Map 140, scale 1:24,000, 3 sheets.
- Rodgers, D.W., 1987, Thermal and structural evolution of the southern Deep Creek Range, west central Utah and east central Nevada [Ph.D. dissertation]: Stanford University, California, 149 p.
- Rowley, P.D., 1998, Cenozoic transverse zones and igneous belts in the Great Basin, western United States: Their tectonic and economic implications, *in* Faulds, J.E., and Stewart, J.H., editors, *Accommodation zones and transfer zones—the regional segmentation of the Basin and Range Province*: Geological Society of America Special Paper 323, p. 195–228.
- Rowley, P.D., and Anderson, R.E., 1996, The syntectonic caldera—a new caldera type bounded by synchronous linear faults [abs.]: Geological Society of America Abstracts with Programs, v. 28, no. 7, p. A-449.
- Rowley, P.D., and Dixon, G.L., 2001, The Cenozoic evolution of the Great Basin area, U.S.A.—new interpretations based on regional geologic mapping, *in* Erskine, M.C., Faulds, J.E., Bartley, J.M., and Rowley, P.D., editors, *The geologic transition, High Plateaus to Great Basin—A symposium and field guide: The Mackin Volume*: Utah Geological Association Publication 30 and

- American Association of Petroleum Geologists Publication GB78, September, 20–22, 2001, p. 169–188.
- Rowley, P.D., and Dixon, G.L., 2004, The role of geology in increasing Utah's ground-water resources from faulted terranes—lessons from the Navajo Sandstone, Utah, and the Death Valley flow system, Nevada-California, *in* Spangler, L.E., editor, Ground water in Utah—Resource, protection, and remediation—Field Symposium: Utah Geological Association, Salt Lake City, Utah, September 24–25, 2004, Publication 31, p. 27–41.
- Rowley, P.D., and Shroba, R.R., 1991, Geologic map of the Indian Cove quadrangle, Lincoln County, Nevada: U.S. Geological Survey Geologic Quadrangle Map GQ-1701, scale 1:24,000.
- Rowley, P.D., Christensen, E.F., Dixon, G.L., Burns, A.G., Watrus, J.M., and Collins, C.A., 2012, Fault derived conduit and barrier groundwater flow at Sawyer Spring, eastern margin of the Pine Valley Mountains, Washington County, Utah, *in* Hylland, M.D., and Harty, K.M., editors, Selected topics in engineering and environmental geology in Utah: Utah Geological Association Publication 41, CD, p. 99–114.
- Rowley, P.D., Dixon, G.L., Burns, A.G., and Collins, C.A., 2009, Geology and hydrogeology of the Snake Valley area, western Utah and eastern Nevada, *in* Tripp, B.T., Krahulec, K., and Jordan, J.L., editors, Geology and geologic resources and issues of western Utah: Utah Geological Association Publication 38, p. 251–269.
- Rowley, P.D., Dixon, G.L., Burns, A.G., Pari, K.T., Watrus, J.M., and Ekren, E.B., 2011, Geology and geophysics of Spring, Cave, Dry Lake, and Delamar valleys, White Pine and Lincoln counties and adjacent areas, Nevada and Utah: The geologic framework of regional groundwater flow systems: Presentation to the Office of the Nevada State Engineer: Southern Nevada Water Authority, Las Vegas, Nevada.
- Rowley, P.D., Dixon, G.L., D'Agnese, F.A., O'Brien, G.M., and Brickey, D.W., 2004, Geology and hydrology of the Sand Hollow reservoir and well field area, Washington County, Utah: Washington County Water Conservancy District Report WCWCD-01, 14 p.
- Rowley, P.D., Dixon, G.L., Watrus, J.M., Burns, A.G., Mankinen, E.A., McKee, E.H., Pari, K.T., Ekren, E.B., and Patrick, W.G., 2016, Geology, selected geophysics, and hydrogeology of the White River and parts of the Great Salt Lake Desert regional groundwater flow systems, Utah and Nevada, *in* Comer, J.B., Inkenbrandt, P.C., Krahulec, K.A., and Pinnell, M.L., editors, Resources and geology of Utah's West Desert: Utah Geological Association Publication 45, p. 167–200.
- Rowley, P.D., Hacker, D.B., Maxwell, D.J., Maxwell, J.D., and Boswell, J.T., 2008, Interim geologic map of the Utah part of the Deer Lodge Canyon, Prohibition Flat, Uvada, and Pine Park quadrangles (east part of the Caliente 30'×60' quadrangle), Iron and Washington counties, Utah: Utah Geological Survey Open-File Report 530, scale 1:24,000.
- Rowley, P.D., Lipman, P.W., Mehnert, H.H., Lindsey, D.A., and Anderson, J.J., 1978, Blue Ribbon lineament, an east-trending structural zone within the Pioche mineral belt of southwestern Utah and eastern Nevada: U.S. Geological Survey Journal of Research, v. 6, no. 2, p. 175–192.
- Rowley, P.D., Nealey, L.D., Unruh, D.M., Snee, L.W., Mehnert, H.H., Anderson, R.E., and Grommé, C.S., 1995, Stratigraphy of Miocene ash-flow tuffs in and near the Caliente caldera complex, southeastern Nevada and southwestern Utah, *in* Scott, R.B., and Swadley, W.C., editors, Geologic studies in the Basin and Range—Colorado Plateau transition in southeastern Nevada, southwestern Utah, and northwestern Arizona, 1992: U.S. Geological Survey Bulletin 2056, p. 43–88.
- Rowley, P.D., Shroba, R.R., Simonds, F.W., Burke, K.J., Axen, G.J., and Olmore, S.D., 1994, Geologic map of the Chief Mountain quadrangle, Lincoln County, Nevada: U.S. Geological Survey Geologic Quadrangle Map GQ-1731, scale 1:24,000.
- Rowley, P.D., Snee, L.W., Anderson, R.E., Nealey, L.D., Unruh, D.M., and Ferris, D.E., 2001, Field trip to the Caliente caldera complex, east-striking transverse zones, and nearby mining districts in Nevada-Utah—Implications for petroleum, ground-water, and mineral resources, *in* Erskine, M.C., Faulds, J.E., Bartley, J.M., and Rowley, P.D., editors, The geologic transition, High Plateaus to Great Basin—a symposium and field guide: The Mackin Volume: Utah Geological Association Publication 30 and American Association of Petroleum Geologists Publication GB78, September 20–22, 2001, p. 401–418.
- Rowley, P.D., Snee, L.W., Mehnert, H.H., Anderson, R.E., Axen, G.J., Burke, K.J., Simonds, F.W., Shroba, R.R., and Olmore, S.D., 1992, Structural setting of the Chief mining district, eastern Chief Range, Lincoln County, Nevada, *in* Thorman, C.H.,

- editor, Application of structural geology to mineral and energy resources of the central and western United States: U.S. Geological Survey Bulletin 2012, p. H1–H17.
- Rowley, P.D., Steven, T.A., and Mehnert, H.H., 1981, Origin and structural implications of upper Miocene rhyolites in Kingston Canyon, Piute County, Utah: Geological Society of America Bulletin, Part I, v. 92, p. 590–602.
- Rowley, P.D., Williams, V.S., Vice, G.S., Maxwell, D.J., Hacker, D.B., Snee, L.W., and Mackin, J.H., 2006, Interim geologic map of the Cedar City 30'x60' quadrangle, Iron and Washington counties, Utah: Utah Geological Survey Open-File Report 476DM, scale 1:100,000.
- Ruksznis, A., and Miller, E.L., 2014, Stratigraphy and age of Cenozoic syn-extensional sedimentary basins, east-central Nevada (abs.): Geological Society of America 2014 Abstracts with Programs, v. 46, no. 5, p. 24.
- Sack, D., 1990, Quaternary geologic map of Tule Valley, west-central Utah: Utah Geological and Mineral Survey Map 124, scale 1:100,000.
- Saltus, R.W., 1988a, Bouguer gravity anomaly map of Nevada: Nevada Bureau of Mines and Geology Map 94A, scale 1:750,000.
- Saltus, R.W., 1988b, Regional, residual, and derivative gravity maps of Nevada: Nevada Bureau of Mines and Geology Map 94B, scale 1:000,000, 4 sheets.
- Saltus, R.W., and Jachens, R.C., 1995, Gravity and basin-depth maps of the Basin and Range province, western United States: U.S. Geological Survey Geophysical Investigations Map GP-1012, scale 1:2,500,000.
- Sandberg, C.A., Morrow, J.R., and Warme, J.E., 1997, Late Devonian Alamo impact event, global Kellwasser Events, and major eustatic events, eastern Great Basin, Nevada and Utah: Brigham Young University Geology Studies, v. 42, pt. 1, p. 129–160.
- Sargent, K.A., and Roggensack, K., 1984, Map showing outcrops of pre-Quaternary ash-flow tuffs and volcanoclastic rocks, Basin and Range province, Nevada: U.S. Geological Survey Water-Resources Investigations Report 83-4119-E, scale 1:500,000, 2 sheets.
- Saucier, A.E., 1997, The Antler Thrust System in Northern Nevada, *in* Perry, A.J., and Abbott, E.W., editors, The Roberts Mountains Thrust, Elko and Eureka counties, Nevada: Nevada Petroleum Society, 1997 Field Trip Guidebook, Reno, Nevada, p. 1–16.
- Schaefer, D.H., Morris, T.M., and Dettinger, M.D., 1989, Hydrogeologic and geophysical data for selected wells and springs in the Sheep Range, Clark and Lincoln counties, Nevada: U.S. Geological Survey Open-File Report 89-425, 36 p.
- Schalla, R.A., 1998, History of recent exploration activity in Snake Valley, *in* French, D.E., and Schalla, R.A., editors, Hydrocarbon habitat and special geologic problems of the Great Basin: 1998 Field Trip Guidebook, Nevada Petroleum Society p. 84–85.
- Schalla, R.A., and Johnson, E.H., editors, 1994, Oil fields of the Great Basin: Nevada Petroleum Society, Reno, Nevada, 380 p.
- Scheirer, D.S., 2005, Gravity studies of Cave, Dry Lake, and Delamar valleys, east-central Nevada: U.S. Geological Survey Open-File Report 2005-1339, 27 p.
- Scheirer, D.S., Page, W.R., and Miller, J.J., 2006, Geophysical studies based on gravity and seismic data of Tule Desert, Meadow Valley Wash, and California Wash basins, southern Nevada: U.S. Geological Survey Open-File Report 2006-1396, 42 p.
- Scheirer, D.S., and Andreasen, A.D., 2008, Results of gravity fieldwork conducted in March 2008 in the Moapa Valley region of Clark County, Nevada: U.S. Geological Survey Open-File Report 2008-1300, 35 p. [<http://pubs.usgs.gov/of/2008/1300/>].
- Schellart, W.P., Stegman, D.R., Farrington, R.J., Freeman, J., and Moresi, L., 2010, Cenozoic tectonics of western North America controlled by evolving width of Farallon slab: Science, v. 329, no. 5989, p. 316–319.
- Schmidt, D.L., 1994, Preliminary geologic map of the Farrier quadrangle, Clark and Lincoln counties, Nevada: U.S. Geological Survey Open-File Report 94-625, scale 1:24,000.
- Schmidt, D.L. and Dixon, G.L., 1995, Geology and aquifer system of the Coyote Spring Valley area, southeastern Nevada: U.S. Geological Survey Open-File Report 95-579, 47 p.
- Schmidt, D.L., Page, W.R., and Workman, J.B., 1996, Preliminary geologic map of the Moapa West quadrangle, Clark County, Nevada: U.S. Geological Survey Open-File Report 96-521, scale 1:24,000.
- Scott, R.B., 1965, The Tertiary geology and ignimbrite petrology of the Grant Range, east-central Nevada: Houston, Texas, unpublished Rice University Ph.D. thesis, 116 p.
- Scott, R.B., and Harding, A.E., 2006, Geologic map of the Vigo NE quadrangle, Lincoln County, Nevada:

- U.S. Geological Survey Scientific Investigations Map 2892, 18 p., scale 1:24,000.
- Scott, R.B., and Swadley, WC, 1992, Preliminary geologic map of the Pahroc Summit Pass quadrangle and part of the Hiko SE quadrangle, Lincoln County, Nevada: U.S. Geological Survey Open-File Report 92-613, scale 1:24,000.
- Scott, R.B., and Swadley, WC, editors, 1995, Geologic studies in the Basin and Range—Colorado Plateau transition in southeastern Nevada, southwestern Utah, and northwestern Arizona, 1992: U.S. Geological Survey Bulletin 2056, 275 p.
- Scott, R.B., Grommé, C.S., Best, M.G., Rosenbaum, J.G., and Hudson, M.R., 1995a, Stratigraphic relationships of Tertiary volcanic rocks in central Lincoln County, southeastern Nevada, *in* Scott, R.B., and Swadley, WC, editors, Geologic studies in the Basin and Range—Colorado Plateau transition in southeastern Nevada, southwestern Utah, and northwestern Arizona, 1992: U.S. Geological Survey Bulletin 2056, p. 7–41.
- Scott, R.B., Harding, A.E., Swadley, WC, and Pampeyan, E.H., 1991a, Preliminary geologic map of the Vigo NW quadrangle, Lincoln County, Nevada: U.S. Geological Survey Open-File Report 91-389, scale 1:24,000.
- Scott, R.B., Novak, S.W., and Swadley, WC, 1990a, Preliminary geologic map of the Delamar 3 NE quadrangle, Lincoln County, Nevada: U.S. Geological Survey Open-File Report 90-33, scale 1:24,000.
- Scott, R.B., Page, W.R., and Swadley, WC, 1990b, Preliminary geologic map of the Delamar 3 NW quadrangle, Lincoln County, Nevada: U.S. Geological Survey Open-File Report 90-405, scale 1:24,000.
- Scott, R.B., Rowley, P.D., Snee, L.W., Anderson, R.E., Harding, A.E., Unruh, D.M., Nealey, L.D., Hudson, M.R., Swadley, WC, and Ferris, D.E., 1996, Synchronous Oligocene and Miocene extension and magmatism in the vicinity of caldera complexes in southeastern Nevada: Colorado Geological Survey Open-File Report 96-4, 36 p.
- Scott, R.B., Swadley, WC, and Novak, S.W., 1993, Geologic map of the Delamar Lake quadrangle, Lincoln County, Nevada: U.S. Geological Survey Geologic Quadrangle Map GQ-1730, scale 1:24,000.
- Scott, R.B., Swadley, WC, Page, W.R., and Novak, S.W., 1991b, Preliminary geologic map of the Gregerson Basin quadrangle, Lincoln County, Nevada: U.S. Geological Survey Open-File Report 90-646, scale 1:24,000.
- Scott, R.B., Swadley, WC, and Taylor, W.J., 1994, Preliminary geologic map of the Wheatgrass Spring quadrangle, Lincoln County, Nevada: U.S. Geological Survey Open-File Report 94-175, scale 1:24,000.
- Scott, R.B., Swadley, WC, Taylor, W.J., and Harding, A.E., 1995b, Preliminary geologic map of the Deadman Spring quadrangle, Lincoln County, Nevada: U.S. Geological Survey Open-File Report 95-94, scale 1:24,000.
- Shawe, D.R., 1972, Reconnaissance geology and mineral potential of Thomas, Keg, and Desert calderas, central Juab Count, Utah: U.S. Geological Survey Professional Paper 800-B, p. B67–B77.
- Sibson, R.H., 1996, Structural permeability of fluid-driven fault-fracture meshes: *Journal of Structural Geology*, v. 18, Issue 8, p. 1031–1042.
- Simpson, R.W., Jachens, R.C., Blakely, R.J., and Saltus, R.W., 1986, A new isostatic residual gravity map of the conterminous United States with a discussion on the significance of isostatic residual anomalies: *Journal of Geophysical Research*, v. 91, p. 8348–8372.
- Slate, J.L., Berry, M.E., Rowley, P.D., Fridrich, C.J., Williams, V.S., Morgan, K.S., Workman, J.B., Young, O.D., Dixon, G.L., Williams, V.S., et al., 1999, Digital geologic map of the Nevada Test Site and vicinity, Nye, Lincoln, and Clark counties, Nevada, and Inyo County, California: U.S. Geological Survey Open-File Report 99-554-A, 53 p.
- Smith, D.L., Gans, P.B., and Miller, E.L., 1991, Palinspastic restoration of Cenozoic extension in the central and eastern Basin and Range province at latitude 39–40°N, *in* Raines, G.L., Lisle, R.E., Schafer, R.W., and Wilkinson, W.H., editors, *Geology and ore deposits of the Great Basin*, Geological Society of Nevada, Symposium Proceedings, April 1–5, 1990, v. 1, p. 75–86.
- Snee, L.W., and Rowley, P.D., 2000, New $^{40}\text{Ar}/^{39}\text{Ar}$ dates from the Caliente caldera complex, Nevada-Utah—at least 10 million years of Tertiary volcanism in one of the World's largest caldera complexes: *Geological Society of America Abstracts with Programs*, v. 32, no. 7, p. A-461.
- Snyder, R.P., Ekren, E.B., and Dixon, G.L., 1972, Geologic map of the Lunar Crater quadrangle, Nye County, Nevada: U.S. Geological Survey Miscellaneous Geologic Investigations Map I-700, scale 1:48,000.
- Southern Nevada Water Authority, 2006, Documentation of the physical settings of selected

- springs in White Pine, Lincoln and Clark counties, Nevada: Technical Report 3, Spring documentation and evaluation, Southern Nevada Water Authority, Las Vegas, Nevada, 156 p + appendices.
- Southern Nevada Water Authority, 2008, Baseline characterization report for Clark, Lincoln, and White Pine counties groundwater development project: Southern Nevada Water Authority, Las Vegas, Nevada, 1146 p.
- Southern Nevada Water Authority, 2011, Southern Nevada Water Authority Clark, Lincoln, and White Pine counties groundwater development project conceptual plan of development: Southern Nevada Water Authority, Las Vegas, Nevada, 152 p.
- Staargard, C.F., 2009, Geology and exploration at the Crypto zinc-indium-copper-molybdenum skarn, in Tripp, B.T., Krahulec, K., and Jordan, J.L., editors, Geology and geologic resources and issues of western Utah: Utah Geological Association Publication 38, p. 143–156.
- Stephens, J.C., 1977, Hydrologic reconnaissance of the Tule Valley drainage basin, Juab and Millard counties, Utah: Utah Department of Natural Resources Technical Publication, no. 56, 37 p.
- Steven, T.A., Morris, H.T., and Rowley, P.D., 1990, Geologic map of the Richfield 1°×2° quadrangle, west-central Utah: U.S. Geological Survey Miscellaneous Investigations Series Map I-1901, scale 1:250,000.
- Steven, T.A., Rowley, P.D., and Cunningham, C.G., 1984, Calderas of the Marysvale volcanic field, west central Utah: *Journal of Geophysical Research*, v. 89, p. 8751–8764.
- Stewart, J.H., 1970, Upper Precambrian and Lower Cambrian strata in the southern Great Basin, California and Nevada: U.S. Geological Survey Professional Paper 620, 206 p.
- Stewart, J.H., 1971, Basin and Range structure—a system of horsts and grabens produced by deep-seated extension: *Geological Society of America Bulletin*, v. 82, p. 1019–1044.
- Stewart, J.H., 1974, Correlation of uppermost Precambrian and lower Cambrian strata from southern to east-central Nevada: *U.S. Geological Survey Journal of Research*, v. 2, p. 609–618.
- Stewart, J.H., 1976, Late Precambrian evolution of North America: Plate tectonics implication: *Geology*, v. 4, p. 11–15.
- Stewart, J.H., 1980a, Regional tilt patterns of late Cenozoic basin-range fault blocks, western United States: *Geological Society of America Bulletin*, part I, v. 91, p. 460–464.
- Stewart, J.H., 1980b, Geology of Nevada—a discussion to accompany the *geologic map of Nevada*: Nevada Bureau of Mines and Geology Special Publication 4, 136 p.
- Stewart, J.H., 1984, Stratigraphic sections of lower Cambrian and upper Proterozoic rocks in Nye, Lander, and Lincoln counties, Nevada, and Sonora, Mexico: U.S. Geological Survey Open-File Report 84-691, 53 p.
- Stewart, J.H., and Carlson, J.E., 1976, Cenozoic rocks of Nevada—four maps and brief description of distribution, lithology, age, and centers of volcanism: Nevada Bureau of Mines and Geology Map 52, scale 1:1,000,000, 4 sheets.
- Stewart, J.H., and Carlson, J.E., 1978, Geologic map of Nevada: U.S. Geological Survey, scale 1:500,000.
- Stewart, J.H., Moore, W.J., and Zietz, I., 1977, East-west patterns of Cenozoic igneous rocks, aeromagnetic anomalies, and mineral deposits, Nevada and Utah: *Geological Society of America Bulletin*, v. 88, p. 67–77.
- Stewart, J.H., and Poole, F.G., 1974, Lower Paleozoic and uppermost Precambrian Cordilleran miogeocline, Great Basin, western United States, in Dickinson, W.R., editor, *Tectonics and sedimentation: Society of Economic Paleontologists and Mineralogists Special Publication No. 22*, p. 28–57.
- Stoeser, D.B., 1993, Tertiary calderas and regional extension of the east-central part of the Tintic-Deep Creek mineral belt, eastern Great Basin, Utah, in Scott, Jr., R.W., Detra, P.S., and Berger, B.R., editors, *Advances related to United States and International Mineral Resources: Developing frameworks and exploration technologies*: U.S. Geological Survey Bulletin 2039, p. 5–23.
- Swadley, WC, 1995, Maps showing modern fissures and quaternary faults in the Dry Lake Valley area, Lincoln County, Nevada: U.S. Geological Survey Miscellaneous Investigations Series Map I-2501, scale 1:50,000.
- Swadley, WC, Page, W.R., and Scott, R.B., 1994a, Preliminary geologic map of the Deadman Spring NE quadrangle, Lincoln County, Nevada: U.S. Geological Survey Open-File Report 94-283, scale 1:24,000.
- Swadley, WC, Page, W.R., Scott, R.B., and Pampeyan, E.H., 1994b, Geologic map of the Delamar 3 SE quadrangle, Lincoln County, Nevada: U.S. Geological Survey Geologic Quadrangle Map GQ-1754, scale 1:24,000.
- Swadley, WC, and Rowley, P.D., 1994, Geologic map

- of the Pahroc Spring SE quadrangle, Lincoln County, Nevada: U.S. Geological Survey Geologic Quadrangle Map GQ-1752, scale 1:24,000.
- Swadley, W.C., and Scott, R.B., 1991, Preliminary geologic map of the Delamar NW quadrangle, Lincoln County, Nevada: U.S. Geological Survey Open-File Report 90-622, scale 1:24,000.
- Sweetkind, D.S., 2007b, Geology of Great Basin National Park, *in* Coache, R., editor, Regional tour of the carbonate system guidebook: Nevada Water Resources Association, Clark County, Nevada, June 18–20, 2007, p. 47–48.
- Sweetkind, D.S., 2007a, Geology of Snake Range, *in* Coache, R., editor, Regional tour of the carbonate system guidebook: Nevada Water Resources Association, Clark County, Nevada, June 18–20, 2007, p. 43–44.
- Sweetkind, D.S., and duBray, E.A., 2008, Compilation of stratigraphic thicknesses for caldera-related tertiary volcanic rocks, east-central Nevada and west-central Utah: U.S. Geological Survey Data Series 271, 40 p.
- Sweetkind, D.S., Knochenmus, L.A., Ponce, D.A., Wallace, A.R., Scheirer, D.S., Watt, J.T., and Plume, R.W., 2007b, Hydrogeologic framework, *in* Welch, A.H., Bright, D.J., and Knochenmus, L.A., editors, Water resources of the Basin and Range carbonate-rock aquifer system, White Pine County, Nevada, and adjacent areas in Nevada and Utah: U.S. Geological Survey Scientific Investigations Report 2007-5261, p. 11–36.
- Sweetkind, D.S., Knochenmus, L.A., Ponce, D.A., Wallace, A.R., Scheirer, D.S., Watt, J.T., and Plume, R.W., 2007a, Hydrogeologic map and cross sections, White Pine County, Nevada, and adjacent areas in Nevada and Utah, *in* Welch, A.H., Bright, D.J., and Knochenmus, L.A., editors, Water resources of the Basin and Range carbonate-rock aquifer system, White Pine County, Nevada, and adjacent areas in Nevada and Utah: U.S. Geological Survey Scientific Investigations Report 2007-5261, Plate 1, scale 1:500,000.
- Taylor, M.E., Poole, F.G., and Cook, H.E., 1991, Summary of Paleozoic stratigraphy in the southern Egan and Schell Creek ranges, east-central Nevada, *in* Flanigan, D.M.H., Hansen, M., and Flanigan, T.E., editors, Geology of White River Valley, the Grant Range, Eastern Railroad Valley and Western Egan Range, Nevada: 1991 Fieldtrip Guidebook, Nevada Petroleum Society Inc., Reno, p. 29–35.
- Taylor, W.J., Bartley, J.M., Fryxell, J.E., Schmitt, J.G., and Vandervoort, D.S., 1993, Tectonic style and regional relations of the central Nevada thrust belt, *in* Lahren, M.M., Trexler, J.H., Jr., and Spinosa, C., editors, Crustal evolution of the Great Basin and Sierra Nevada: Geological Society of America Guidebook, Cordilleran/Rocky Mountain Section, Department of Geological Sciences, University of Nevada, Reno, p. 57–96.
- Taylor, W.J., Bartley, J.M., Martin, M.W., Geissman, J.W., Walker, J.D., Armstrong, P.A., and Fryxell, J.E., 2000, Relations between hinterland and foreland shortening: Sevier orogeny, central North American Cordillera: Tectonics, v. 19, no. 6, p. 1124–1143.
- Taylor, W.J., Dobbs, S.W., Nelson, S.L., and Armstrong, P.A., 1994, Generation of four-way closure through multiple tectonic events: Structures of the Timpahute Range, southern Nevada, *in* Dobbs, S.W., and Taylor, W.J., editors, Structural and stratigraphic investigations and petroleum potential of Nevada, with special emphasis south of the Railroad Valley producing trend: Nevada Petroleum Society Conference Volume II, p. 141–156.
- Telford, W.M., Geldart, L.P., and Sheriff, R.E., 1990, Applied geophysics. Second edition: New York, Cambridge University Press.
- Tilden, J.E., Ponce, D.A., Glen, J.M.G., Chuchel, B.A., Tushman, K., and Duvall, A., 2006, Gravity, magnetic, and physical property data in the Smoke Creek Desert area, northwest Nevada: U.S. Geological Survey Open-File Report 2006-1197, 33 p.
- Tingley, J.V., Pizarro, K.A., Ross, C. and Pearthree, P.A., 2010, A geologic and natural history tour through Nevada and Arizona along U.S. Highway 93, with GPS coordinates: Nevada Bureau of Mines and Geology Special Publication 35 and Arizona Geological Survey Down-to-Earth 19, 175 p.
- Tschanz, C.M., and Pampeyan, E.H., 1970, Geology and mineral deposits of Lincoln County, Nevada: Nevada Bureau of Mines and Geology Bulletin 73, 187 p.
- U.S. Geological Survey, 2008, A study of the connection among basin-fill aquifers, carbonate-rock aquifers, and surface-water resources in southern Snake Valley, Nevada: U.S. Geological Survey Fact Sheet 2008-3071, 2 p.
- Utah Division of Oil, Gas, and Mining, 2006, Online oil and gas information system, well logs, database [Internet], [accessed March 8, 2006], available from <http://utstnrogmsg/3.state.ut.us/UTAHRBDMSSWe>

- b/Logs.htm.
- Utah Division of Oil, Gas, and Mining, 2011, Online oil and gas information system, well logs database [Internet], [accessed on May 4, 2011], available from <http://oilgas.ogm.utah.gov>.
- Utah Division of Water Rights, 2006, Well drilling database [Internet], [accessed March 8, 2006], available from <http://nrwrt1.nr.state.ut.us/cgi/bin/wellview.exe>.
- Vandervoort, D.S., and Schmitt, J.G., 1990, Cretaceous to early Tertiary paleogeography in the hinterland of the Sevier thrust belt, east-central Nevada: *Geology*, v. 18, p. 567–570.
- Van Loenen, R.E., 1987, Geologic map of the Mount Grafton wilderness study area, Lincoln and White Pine counties, Nevada: U.S. Geological Survey Miscellaneous Field Studies Map MF-1938, scale 1:50,000.
- Vozoff, K., 1991, The magnetotelluric method, in Nabighian, M.N., editor, *Electromagnetic methods in applied geophysics: Volume 2, Application Parts A and B*: Society of Exploration Geophysicists, Tulsa, Oklahoma, Investigations in Geophysics, no. 3, p. 641–711.
- Walker, C.D., Anders, M.H., and Christie-Blick, N., 2007, Kinematic evidence for downdip movement on the Mormon Peak detachment: *Geology*, v. 35, no. 3, p. 259–262.
- Walker, C.T., and Francis, R.D., 2002, Tectonic styles associated with extension and attenuation in the Grant, Schell Creek, and White Pine Ranges, in Ehni, W., and Faulds, J., editors, *Detachment and attenuation in eastern Nevada and its application to petroleum exploration*: Nevada Petroleum Society 2002 Field Trip Guidebook, p. 97–127.
- Walker, J.D., Geissman, J.W., Bowring, S.A., and Babcock, L.E., 2013, The Geological Society of America geologic time scale: *Geological Society of America Bulletin*, v. 125, p. 259–272.
- Wallace, A.R., Watt, J.T., and Ponce, D.A., 2007, Geologic and geophysical basin-by-basin descriptions, in Watt, J.T., and Ponce, D.A., editors, *Geophysical framework investigations influencing ground-water resources in east-central Nevada and west-central Utah*: U.S. Geological Survey Open-File Report 2007-1163, p. 9–28.
- Warme, J.E., Morrow, J.R., and Sandberg, C.A., 2008, Devonian carbonate platform of eastern Nevada: Facies, surfaces, cycles, sequences, reefs, and cataclysmic Alamo impact breccia, in Duebendorfer, E.M., and Smith, E.I., editors, *Field guide to plutons, volcanoes, faults, reefs, dinosaurs, and possible glaciation in selected areas of Arizona, California, and Nevada*: Geological Society of America Field Guides, v. 11, p. 215–247.
- Watt, J.T., and Ponce, D.A., 2007, Geophysical framework investigations influencing ground-water resources in east-central Nevada and west-central Utah, with a section on geologic and geophysical basin-by-basin descriptions, by Wallace, A.R., Watt, J.T., and Ponce, D.A.: U.S. Geological Survey Open-File Report 2007-1163 [<http://pubs.usgs.gov/of/2007/1163/>].
- Webring, M., 1981, MINC-A gridding program based on minimum curvature: U.S. Geological Survey Open-File Report 81-1224, 43 p.
- Welch, A.H., Bright, D.J., and Knochenmus, L.A., editors, 2007, Water resources of the Basin and Range carbonate-rock aquifer system, White Pine County, Nevada, and adjacent areas in Nevada and Utah: U.S. Geological Survey Scientific Investigations Report 2007-5261, 96 p.
- Wernicke, B., Walker, J.D., and Beaufait, M.S., 1985, Structural discordance between Neogene detachments and frontal Sevier thrusts, central Mormon Mountains, southern Nevada: *Tectonics*, v. 4, no. 2, p. 213–246.
- Whitebread, D.H., 1969, Geologic map of the Wheeler Peak and Garrison quadrangles, Nevada and Utah: U.S. Geological Survey Miscellaneous Geologic Investigations Map I-578, scale 1:48,000.
- Whitney, D.L., Teyssier, C., Rey, P., and Buck, W.R., 2013, Continental and ocean core complexes: *Geological Society of America Bulletin*, v. 125, p. 273–298.
- Williams, N., and Taylor, W.J., 2002, Extensional oblique-slip barrier transfer fault—the Currant Summit fault, east-central Nevada, in Ehni, W. and Faulds, J., editors, *Detachment and attenuation in eastern Nevada and its application to petroleum exploration*: Nevada Petroleum Society 2002 Field Trip Guidebook, p. 149–163.
- Williams, V.S., 1996, Preliminary geologic map of the Mesquite quadrangle, Clark and Lincoln counties, Nevada, and Mohave County Arizona: U.S. Geological Survey Open-File Report 96-676, scale 1:24,000.
- Williams, V.S., 1997, Preliminary geologic map of the Flat Top Mesa quadrangle, Clark and Lincoln counties, Nevada: U.S. Geological Survey unpublished data, scale 1:24,000.
- Williams, V.S., Best, M.G., and Keith, J.D., 1997a, Geologic map of the Ursine-Panaca Summit-Deer Lodge area, Lincoln County, Nevada, and Iron

- County, Utah: U.S. Geological Survey Miscellaneous Investigations Series Map I-2479, scale 1:50,000.
- Williams, V.S., Bohannon, R.G., and Hoover, D.L., 1997b, Geologic map of the Riverside quadrangle, Clark County, Nevada: U.S. Geological Survey Geologic Quadrangle Map GQ-1770, scale 1:24,000.
- Williams, V.S., Schmidt, D.L., and Bohannon, R.G., 1997c, Preliminary geologic map of the Moapa East quadrangle, Clark County, Nevada: U.S. Geological Survey Open-File Report 97-449, scale 1:24,000.
- Willis, J.B., Best, M.G., Kowallis, B.J., and Best, V.C., 1987, Preliminary geologic map of the northern Wilson Creek Range, Lincoln County, Nevada: U.S. Geological Survey Miscellaneous Field Studies Map MF-1971, scale 1:50,000.
- Winograd, I.J., and Thordarson, W., 1968, Structural control of ground-water movement in miogeosynclinal rocks of south-central Nevada, *in* Eckel, E.B., editor, Nevada Test Site: Geological Society of America Memoir 110, p. 35–48.
- Winograd, I.J., and Thordarson, W., 1975, Hydrogeologic and hydrochemical framework, south-central Great Basin, Nevada-California, with special reference to the Nevada Test Site: U.S. Geological Survey Professional Paper 712-C, 126 p.
- Workman, J.B., Menges, C.M., Page, W.R., Ekren, E.B., Rowley, P.D., and Dixon, G.L., 2002a, Tectonic map of the Death Valley ground-water model area, Nevada and California: U.S. Geological Survey Miscellaneous Field Studies Map MF-2381-B, 58 p., scale 1:250,000.
- Workman, J.B., Menges, C.M., Page, W.R., Taylor, E.M., Ekren, E.B., Rowley, P.D., Dixon, G.L., Thompson, R.A., and Wright, L.A., 2002b, Geologic map of the Death Valley ground-water model area, Nevada and California: U.S. Geological Survey Miscellaneous Field Studies MF-2381-A, 26 p., 1:250,000 scale, 2 sheets.
- Wright, J.E., and Snoke, A.W., 1993, Tertiary magmatism and mylonitization in the Ruby-East Humboldt metamorphic core complex, northeastern Nevada: U-Pb geochronology and Sr, Nd, and Pb isotope geochemistry: Geological Society of America Bulletin, v. 105, no. 7, p. 935–952.
- Zietz, I., Shuey, R., and Kirby, J.R., Jr., 1976, Aeromagnetic map of Utah: U.S. Geological Survey Geophysical Investigations Map GP-907, scale 1:1,000,000.
- Zietz, I., Gilbert, F.P., and Kirby, J.R., Jr., 1978, Aeromagnetic map of Nevada: U.S. Geological Survey Geophysical Investigations Map GP-922, scale 1:1,000,000.
- Zonge, K.L., and Hughes, L.J., 1991, Controlled source audio-frequency magnetotellurics, *in* Nabighian, M.N., editor, Electromagnetic methods in applied geophysics, Volume 2, Application Parts A and B: Society of Exploration Geophysicists, Tulsa, Oklahoma, Investigations in Geophysics, no. 3, p. 713–809.

Suggested Citation:

Rowley, P.D., Dixon, G. L., Mankinen, E.A., Pari, K.T., McPhee, D.K., McKee, E.H., Burns, A.G., Watrus, J.M., Ekren, E.B., Patrick, W.G., and Brandt, J.M., 2017, Geology and geophysics of White Pine and Lincoln counties, Nevada, and adjacent parts of Nevada and Utah: the geologic framework of regional groundwater flow systems: Nevada Bureau of Mines and Geology Report 56, scale 1:250,000, 4 plates, 146 p.

© Copyright 2017 The University of Nevada, Reno.
All Rights Reserved.